

## INFORMATION TO USERS

This manuscript has been reproduced from the microfilm master. UMI films the text directly from the original or copy submitted. Thus, some thesis and dissertation copies are in typewriter face, while others may be from any type of computer printer.

**The quality of this reproduction is dependent upon the quality of the copy submitted.** Broken or indistinct print, colored or poor quality illustrations and photographs, print bleedthrough, substandard margins, and improper alignment can adversely affect reproduction.

In the unlikely event that the author did not send UMI a complete manuscript and there are missing pages, these will be noted. Also, if unauthorized copyright material had to be removed, a note will indicate the deletion.

Oversize materials (e.g., maps, drawings, charts) are reproduced by sectioning the original, beginning at the upper left-hand corner and continuing from left to right in equal sections with small overlaps.

Photographs included in the original manuscript have been reproduced xerographically in this copy. Higher quality 6" x 9" black and white photographic prints are available for any photographs or illustrations appearing in this copy for an additional charge. Contact UMI directly to order.

ProQuest Information and Learning  
300 North Zeeb Road, Ann Arbor, MI 48106-1346 USA  
800-521-0600

UMI<sup>®</sup>



**THERMOCHEMICAL AND MECHANISTIC INVESTIGATION  
OF  
CARBOCATION ISOMERIZATIONS**

**By  
NICHOLAS A.D. BURKE**

**A Thesis**

**Submitted to the School of Graduate Studies**

**in Partial Fulfilment of the Requirements**

**for the Degree**

**Doctor of Science**

**McMaster University**

## CARBOCATION ISOMERIZATIONS

**Doctor of Science (1999)**

**McMaster University**

**(Chemistry)**

**Hamilton, Ontario**

**TITLE: Thermochemical and Mechanistic Investigation of Carbocation Isomerizations**

**AUTHOR: Nicholas Alexander Despard Burke, B.Sc. (McMaster University)**

**SUPERVISOR: Professor R.F. Childs**

**NUMBER OF PAGES: xxiv, 266**

## Abstract

This thesis describes experiments focussed on the isomerizations of carbocations, in particular, hydroxy-substituted carbocations produced by the protonation of ketones or phenols. Three classes of isomerization were investigated with the goal of determining the effect of substituents on the energetics of isomerization (carbocation stability, activation energy) and to probe the mechanisms of these reactions. It was proposed that differential scanning calorimetry (DSC) could be used to measure heats of isomerization to determine the effect of substituents on the energies of carbocations. Results presented in chapters 2, 3 and 4 demonstrate that DSC is a reliable technique for the determination of accurate and reproducible heats of isomerization of carbocations in superacid solution.

As described in chapter 2, methyl migrations in cyclohexadienyl, cyclohexenyl and cyclopentenyl cations were investigated and the effect of moving methyl groups on to charge bearing positions of the carbocations was quantified. In addition, the energetic advantage of having a hydroxy group on the central 3-position rather than the terminal 1-position of the pentadienyl cation  $\pi$ -system was determined.

Methyl substitution has pronounced effects upon the energetics of the isomerization of protonated bicyclo[3.1.0]hexenones to protonated phenols or cyclohexadienones and these results are described in chapter 3. These effects are consistent with the known charge distributions in the product and reactant cations. In addition, it was shown that the improved charge stabilization in the cyclohexadienyl cation product is a driving force for the isomerization, in contrast to the conclusions of an earlier study.

A series of protonated cyclopropyl ketones in triflic acid were found to undergo

ring expansion to oxolanylium ions except for two bicyclic ketones where steric constraints prevented ring expansion and ring opening to protonated enones occurred instead. The course of each reaction was determined and the reactant and product cations were characterized by  $^1\text{H}$  and  $^{13}\text{C}$  NMR spectroscopy. For use in later mechanistic studies, the stereochemistry of a set of dimethyl substituted cyclopropyl and oxolanylium compounds were established. The heats of isomerization of protonated cyclopropyl ketones were measured and found to fall in a narrow range which indicated that substituent effects were similar in the reactant and product cations.

The substituents on the cyclopropyl ring and on the carbonyl carbon affected the rates of ring expansion of protonated cyclopropyl ketones which, provided information about the charge distribution in the reactant and the transition state, and the charge stabilizing abilities of the substituents. The list of possible mechanistic pathways was narrowed with a combination of information (product studies, substituent effects, entropies of activation). Finally, evidence is provided for the occurrence of a concerted 1,3-sigmatropic migration during the ring expansion of protonated cyclopropyl ketones in triflic acid. However, other reaction pathways can be made competitive with minor changes in reactant structure or reaction medium.

## **Acknowledgements**

First and foremost I wish to thank my supervisor Ron Childs for his guidance, support and patience (or perhaps endurance is a better term). I also wish to acknowledge the assistance of my advisory committee, Professors Russell Bell and John Greedan. Financial assistance from NSERC and McMaster University was greatly appreciated.

In the rather lengthy life of this project I have had the good fortune to work with a number of exceptional people. Labmates Steve, Gary, Marianne P., Richard, John, George and Marianne K. made for an enjoyable time in the Childs' laboratory. A special thanks goes to Dr. Mailvaganam Mahendran for his guidance and for teaching me some of the intricacies of organic synthesis.

I would like to acknowledge the technical assistance of Dr. Don Hughes, Mr. Mike Malott and Dr. Chris Frampton.

It has been my great pleasure to work in the laboratories of Professors Jim Guillet and Harald Stöver. I wish to thank them for their support and to thank Professor Guillet for proofreading an earlier version of this thesis. Thank you also to Suzy and Maria.

My years at McMaster are highly treasured because of the friendships that were established or cemented during this time. Special thanks to Paul, Howard, Lesley, Steve, Carol, Brad, Chris and Karen.

Finally, I would like to thank my family. My parents, Sandy and Vella, my brother Toby and my sister Val helped me to get started on this journey. My wife Karen and my children Aidan and Elizabeth saw me through to the end. A special thanks to Karen, my wife and best friend. Without her unflinching encouragement, support and love I couldn't have made it to the end.



To my family

Sandy, Vella, Toby and Val

Karen, Aidan and Elizabeth

## **Table of Contents**

Descriptive Note	ii
Abstract	iii
Acknowledgement	v
Table of Contents	vii
List of Tables	xii
List of Figures	xiv
<b>Chapter 1: Introduction</b>	<b>1</b>
1.1 Superacids	2
1.2 Methods of Carbocation Generation	4
1.3 Structure of Carbocations	7
1.4 Isomerizations of Carbocations	14
1.5 Stability of Carbocations	16
1.5.1 Kinetic Measures of Carbocation Stability	17
1.5.2 Thermodynamic Measures of Carbocation Stability	19
1.6 Scanning Calorimetry	24
1.7 Thesis Outline	26
1.8 References	28
<b>Chapter 2: Methyl Migrations in Protonated Phenols and Related Carbocations</b>	<b>34</b>
2.1 Introduction	34
2.2 Experimental	37
2.3 Results and Discussion	41

2.3.1 Protonation	44
2.3.2 Isomerizations	48
2.3.3 Rates of Isomerization	51
2.4 Measurement of Heats of Isomerization by DSC	54
2.4.1 Validation of DSC Technique	54
2.4.2 Heats of Isomerization	58
2.4.3 Catalyzed Isomerization: Energy Difference Between Neutral Isomers	65
2.5 Conclusion	69
2.6 References	71
<b>Chapter 3: Isomerization of Protonated Bicyclo[3.1.0]hex-3-en-2-ones to Protonated Phenols</b>	<b>75</b>
3.1 Introduction	75
3.1.1 Charge Delocalization in the Bicyclo[3.1.0]hex-3-en-2-yl Cation	77
3.1.2 Photochemical Formation of Bicyclo[3.1.0]hex-3-en-2-one	80
3.1.3 Thermal Reactions of Protonated Bicyclo[3.1.0]hex-3-en-2-ones	83
3.1.4 Thermochemistry	91
3.1.5 Goals	95
3.2 Experimental	96
3.3 Results and Discussion	98
3.3.1 Isomerization of Protonated Bicyclo[3.1.0]hex-3-en-2-ones	98
3.3.2 Heats of Isomerization	103

3.3.3 Effect upon $\Delta H_R$ of Methyl Substitution at C6	104
3.3.4 Effect upon $\Delta H_R$ of Methyl Substitution on the Five-Membered Ring of the Bicyclo[3.1.0]hexenyl Cation	108
3.3.5 The Bicyclo[3.1.0]hexenyl/Cyclohexadienyl Energy Difference	111
3.3.6 Catalyzed Isomerization: Energy Difference Between a Bicyclo[3.1.0]hexenone and a Phenol	115
3.3.7 Energy Diagrams for Isomeric Carbocations	117
3.4 Conclusion	121
3.5 References	124
<b>Chapter 4: Isomerization of Protonated Cyclopropyl Ketones to Oxolanylium Ions</b>	<b>129</b>
4.1 Introduction	129
4.1.1 Cyclopropylcarbinyl Cations	130
4.1.2 Ring Expansion Reactions of Cyclopropyl Compounds	134
4.1.3 Goals	138
4.2 Experimental	139
4.3 Results and Discussion	145
4.3.1 Protonated Cyclopropyl Ketones	148
4.3.2 Comparison of NMR Data for Neutral and Protonated Cyclopropyl Ketones	151
4.3.3 Rearrangement of Protonated Cyclopropyl Ketones	155
4.3.4 Characterization of Oxolanylium Ions: $^1\text{H}$ and $^{13}\text{C}$ NMR	166
4.3.5 Stereochemistry of Dimethyl Substituted Cyclopropyl Ketones and Oxolanylium Ions	170
4.3.6 Products Other Than Oxolanylium Ions	175

4.3.7 Attempted Photoisomerization of Protonated Cyclopropyl Ketones	178
4.3.8 Heats of Isomerization of Protonated Cyclopropyl Ketones	180
4.4 Summary and Conclusions	184
4.5 References	185
Chapter 5: Mechanism of the Protonated Cyclopropyl Ketone to Oxolanylium Ion Isomerization	194
5.1 Introduction	194
5.1.1 Reaction via a Protonated Cyclopropyl Ring	195
5.1.2 Reaction via an Alkyl Cation Intermediate	198
5.1.3 Double Nucleophilic Displacement	203
5.1.4 Concerted Ring Expansion	207
5.1.5 Stereochemical Studies	208
5.1.6 Goals	212
5.2 Experimental	214
5.3 Results and Discussion	215
5.3.1 Kinetics of Isomerization	215
5.3.2 The Effect of the Substituent at C(O).	223
5.3.3 Isomerization Mechanism(s) Leading to Oxolanylium Ions	227
5.3.4 Concerted Ring Expansion or Double Nucleophilic Displacement?	229
5.3.5 Isomerizations of Stereochemically Labelled Protonated Cyclopropyl Ketones	235
5.4 Conclusion	241
5.5 References	242

<b>Chapter 6: Concluding Remarks</b>	<b>249</b>
<b>Appendix: Crystallographic Data for 40-DNP, the 2,4-Dinitrophenylhydrazone Derivative of trans,trans-2,3-Dimethylcyclopropyl Methyl Ketone (40)</b>	<b>252</b>

## List of Tables

Table 1.1: Physical Properties of Common Superacids.	3
Table 1.2: $^{13}\text{C}$ NMR chemical shift of cation centre in several carbocations	8
Table 1.3: Rates of solvolysis of alkyl chlorides	18
Table 1.4: $\text{pK}_{\text{R}^+}$ values for several cations	20
Table 1.5: Dissociation energies for $\text{R-H} \rightarrow \text{R}^+ + \text{H}^-$ heterolysis	21
Table 1.6: Heats of ionization determined by solution calorimetry	22
Table 2.1: $^1\text{H}$ NMR data for carbocations in triflic acid	45
Table 2.2: $^1\text{H}$ NMR data for compounds for which protonation in triflic acid occurs at multiple sites	48
Table 2.3: First-order rate constants and activation barriers for isomerizations involving methyl migrations	52
Table 2.4: Comparison of $^1\text{H}$ NMR data at concentration used in DSC experiments with literature data	55
Table 2.5: Heats of isomerization ( $\Delta H_{\text{R}}$ ) measured for isomerizations of <b>4H</b> , <b>3H</b> and <b>12H</b> in triflic acid	57
Table 2.6: Heats of reaction for isomerizations involving methyl migrations	59
Table 3.1: $^1\text{H}$ NMR data for neutral and protonated bicyclo[3.1.0]hex-3-en-2-ones	100
Table 3.2: $^1\text{H}$ NMR data for protonated phenols	100
Table 3.3: Rate constants, activation barriers, and enthalpies of reaction for isomerization of protonated bicyclo[3.1.0]hex-3-en-2-ones to protonated phenols in triflic acid	102
Table 4.1: $^1\text{H}$ NMR of protonated cyclopropyl ketones	150
Table 4.2: $^{13}\text{C}$ NMR data: neutral and protonated cyclopropylketones	152
Table 4.3: $^1\text{H}$ and $^{13}\text{C}$ NMR Data for neutral and protonated bicyclo[3.1.0]alkan-2-ones, <b>41</b> , <b>41H</b> , <b>42</b> and <b>42H</b>	153

Table 4.4: <sup>1</sup> H NMR of oxolanylium ions	161
Table 4.5: <sup>13</sup> C NMR data for oxolanylium ions	163
Table 4.6: <sup>1</sup> H NMR data for protonated enones produced by the isomerization of <b>41H</b> and <b>42H</b>	164
Table 4.7: <sup>1</sup> H NMR data for the 2,3-dimethylcyclopropyl methyl ketones, <b>38-40</b>	171
Table 4.8: Heats of reaction ( $\Delta H_p$ ) for the isomerization of protonated cyclopropyl ketones as determined by DSC	180
Table 5.1. Kinetic results for the isomerization of protonated cyclopropyl ketones to oxolanylium ions	218
Table 5.2: Kinetic results for the isomerization of protonated bicyclo[n.1.0]alkanones <b>41H</b> and <b>42H</b>	219
Table 5.3: The effect of acid strength on the rate of isomerization of <b>27H</b> to <b>44</b>	231
Table 5.4: Ratio of cis- to trans-4,5-dimethyloxolanylium ions produced during the isomerization of the protonated 2,3-dimethylcyclopropyl methyl ketones, <b>38H-40H</b>	237
Table A1: Crystal data and structure refinement for <b>40-DNP</b>	252
Table A2: Atomic coordinates ( $\times 10^4$ ) and equivalent isotropic displacement parameters ( $\text{\AA}^2 \times 10^3$ ) for <b>40-DNP</b> . $U(\text{eq})$ is defined as one third of the trace of the orthogonalized $U_{ij}$ tensor	254
Table A3: Selected bond lengths ( $\text{\AA}$ ) and angles ( $^\circ$ ) for <b>40-DNP</b>	255
Table A4: Bond lengths ( $\text{\AA}$ ) and angles ( $^\circ$ ) for <b>40-DNP</b>	256
Table A5: Anisotropic displacement parameters ( $\text{\AA}^2 \times 10^3$ ) for <b>40-DNP</b> . The anisotropic displacement factor exponent takes the form: $-2\pi^2 [(h\hat{a})^2 U_{11} + \dots + 2hka^*b^*U_{12}]$	258
Table A6: Hydrogen coordinates ( $\times 10^4$ ) and isotropic displacement parameters ( $\text{\AA}^2 \times 10^3$ ) for <b>40-DNP</b>	259
Table A7: Observed and calculated structure factors for <b>40-DNP</b>	260



## List of Figures

Figure 1.1: Formation of carbocations by heterolysis	5
Figure 1.2: Formation of carbocations by protonation	6
Figure 1.3: Conjugative interactions of $\pi$ -systems, lone pairs and $\sigma$ -bonds with the cation centre	10
Figure 1.4: $^{13}\text{C}$ chemical shifts in cyclohexadienyl, triphenylmethyl, pentenyl and 1-phenylbutenyl cations	11
Figure 1.5: Rotation about the $\text{C}^+$ -cyclopropyl bond exchanges methyl groups <b>a</b> and <b>b</b>	12
Figure 1.6: The crystal structure of protonated cyclopropyl phenyl ketone reveals that the phenyl group is planar with the cation centre while the cyclopropyl group forms a bisected geometry	13
Figure 1.7: The crystal structure of the 3,5,7-trimethyladamantyl cation shows structural changes consistent with the resonance structures shown	14
Figure 1.8: Sequential 1,2-shifts account for the isomerization of sec-butyl to t-butyl cation	15
Figure 1.9: Isomerization in bicyclo[3.1.0]hexenyl cations by 1,4-migrations	15
Figure 1.10: Ring closure by intramolecular addition to a $\text{C}=\text{O}$ group	16
Figure 1.11: Oxymercuration of 2-Me-butene yields only 2-Me-2-butanol	17
Figure 1.12: Heats of protonation ( $\Delta H_p$ in kcal/mol) of several ketones in $\text{FSO}_3\text{H}$ at $25^\circ\text{C}$	23
Figure 1.13: Resonance structures of protonated $\alpha,\beta$ -unsaturated ketones	24
Figure 1.14: Examples of isomerizations investigated with differential scanning calorimetry (DSC)	27
Figure 1.15: Examples of the three types of isomerization investigated in this work: a) methyl migrations in protonated cycloalkenones and cyclohexadienones, b) ring opening of protonated bicyclo[3.1.0.]hexenones to protonated phenols, and c) ring expansion of protonated cyclopropyl ketones to oxolanylium ions	28

Figure 2.1: Protonation of phenols or cyclohexadienones in superacids produces hydroxy-substituted cyclohexadienyl cations. Cyclohexenone yields the related hydroxycyclohexenyl cation.	35
Figure 2.2: C1, C3 and C5 bear the greatest charge in cyclohexadienyl cations; C1 and C3 in the cyclohexenyl cation.	35
Figure 2.3: 1,2 hydrogen/alkyl migrations are common for cations. The sec-butyl cation isomerizes by a series of 1,2 migrations.	36
Figure 2.4: Protonated bicyclo[3.1.0]hex-3-en-2-ones isomerize to protonated phenols.	37
Figure 2.5: Isomerization of cleanly protonated ions resulting in methyl migration only.	41
Figure 2.6: Isomerizations in which either the reactant or product is a mixture of protonated species.	42
Figure 2.7: Isomerization involving methyl migrations in which the hydroxy group is repositioned on the $\pi$ -system.	42
Figure 2.8: Dehydrogenation of 4,4-dimethylcyclohex-2-enone with DDQ yields 4,4-dimethylcyclohexa-2,5-dienone	43
Figure 2.9: Preparation of 6,6-dimethylcyclohexa-2,5-dienone, <b>10</b>	43
Figure 2.10: Preparation of hexamethylcyclohexa-2,4-dienone, <b>12</b>	44
Figure 2.11: Cations that are cleanly formed in triflic acid	44
Figure 2.12: Ions consisting of more than one species in triflic acid	47
Figure 2.13: 2,4-dimethylphenol gives three protonated species in fluorosulfuric acid	47
Figure 2.14: Mechanism for isomerization of <b>10H</b> to <b>11H</b> involves 1,2-methyl and hydrogen migrations. The hydroxy group is located at the centre of the $\pi$ -system following isomerization	48
Figure 2.15: $^1\text{H}$ NMR spectrum of protonated 4,4-dimethylcyclohex-2-enone, <b>4H</b> , in triflic acid before (top) and after (bottom) isomerization to protonated 3,4-dimethylcyclohex-2-enone, <b>5H</b> , by heating at 110° C for 100 minutes	53

Figure 2.16: Heats of isomerization for reactions which move a methyl group onto the $\pi$ -system	60
Figure 2.17: The differences in heats of protonation of the three ketones in $\text{FSO}_3\text{H}$ give a measure of the stabilization provided by a methyl group. The relative energies of the neutral and protonated analogs are shown.	62
Figure 2.18: Estimated charge density in cyclohexadienyl cation	63
Figure 2.19: Schematic illustration of the contributions to $\Delta H_R$ for <b>10H</b>	65
Figure 2.20: Mechanism of the acid-catalyzed isomerization of <b>8</b> to <b>9</b>	66
Figure 2.21: Estimate of $\Delta H_R$ for isomerization of <b>8</b> to <b>9</b> based on $\Delta H_f$ values measured for <b>9</b> and calculated for <b>8</b> . The relative contributions of aromatization and moving the methyl groups onto the $\pi$ -system are shown. Note: the calculated $\Delta H_f$ value is for 4,4-dichlorocyclohexadienone which should have $\Delta H_f$ identical to <b>8</b> .	68
Figure 3.1: Protonation of phenol yields a cyclohexadienyl cation. Irradiation transforms it to a protonated bicyclo[3.1.0]hexenone. Upon heating the protonated bicyclohexenone reverts to a cyclohexadienyl cation	76
Figure 3.2: $^1\text{H}$ NMR chemical shift difference ( $\Delta\delta$ ) between exo and endo protons and $^{13}\text{C}$ chemical shifts of the bridging and bridgehead carbons in the bicyclo[3.1.0]hexenyl and homotropylium ions	77
Figure 3.3: Resonance structures of bicyclo[3.1.0]hex-3-en-2-yl cation	78
Figure 3.4: Key bond lengths in 2-hydroxy-1,3,4,5-tetramethyl bicyclo[3.1.0]hex-3-en-2-yl cation	79
Figure 3.5: Proposed mechanism for the photochemical formation of the bicyclo[3.1.0]hexenyl framework from cyclohexadienones or cyclohexadienyl cations	81
Figure 3.6: The stereochemical outcome of thermal and photochemical ring closures of cyclopentadienyl cations	82
Figure 3.7: Ring closure produces the 3-hydroxybicyclo[3.1.0]hex-3-en-2-yl cation ( <b>A</b> ) which can isomerize to the more stable 2-hydroxybicyclo[3.1.0]hex-3-en-2-yl cation	82
Figure 3.8: Quantum yields for the photoisomerization of several methyl-substituted protonated phenols	84

Figure 3.9: Cyclopropyl migration in hexamethyl (R = H) or heptamethyl (R = CH <sub>3</sub> ) bicyclo[3.1.0]hexenyl cations causes methyl group bound to the five membered ring to be averaged. Note that the R group remains in an exo orientation	85
Figure 3.10: Scrambling of labelled methyl group shows that cyclopropyl migration (circumambulation) has occurred	86
Figure 3.11: Cyclopropyl migration precedes ring opening during the isomerization of protonated 1,3,4,6-exo-tetramethylbicyclo[3.1.0]hexenone	88
Figure 3.12: Examples of isomerizations in which cyclopropyl migration towards oxygen precedes ring opening	89
Figure 3.13: Examples of isomerizations in which cyclopropyl migration away oxygen precedes ring opening	89
Figure 3.14: Example of isomerization in which ring opening occurs without cyclopropyl migration	90
Figure 3.15: Rates of formation of protonated durenol from protonated 1,3,4,5-tetramethylbicyclo[3.1.0]hexenone and from protonated isodurenol	91
Figure 3.16: Reaction scheme for the storage of photochemical energy in a bicyclo[3.1.0]hexenyl compound	91
Figure 3.17: $\Delta H_p$ determined from heats of protonation measured at two different temperatures	93
Figure 3.18: $\Delta H_p$ determined from heats of protonation measured at two different temperatures	94
Figure 3.19: Relative energies (in kcal/mol) of neutral and protonated hexamethylbenzene and bicyclic isomers determined in FSO <sub>3</sub> H. Values in brackets are differences between measured heats of protonation ( $\Delta H_p$ ). Data from ref. 21	94
Figure 3.20: Relative energies (in kcal/mol) of neutral and protonated hexamethyl ketones in FSO <sub>3</sub> H. Values in brackets are differences in measured heats of protonation ( $\Delta H_p$ ). Data from ref. 21	95
Figure 3.21: Isomerizations of protonated bicyclo[3.1.0]hex-3-en-2-ones to protonated phenols or cyclohexadienones	99
Figure 3.22: <sup>1</sup> H NMR spectrum of protonated 1,3-dimethyl	

bicyclo[3.1.0]hex-3-en-2-one, <b>22H</b> , in triflic acid before (top) and after (bottom) isomerization to protonated 2,5-dimethylphenol, <b>15H</b> , by heating at 100 °C for 80 min. Note: after 80 min isomerization is incomplete and the solution contains ca. 7% of <b>22H</b>	101
Figure 3.23: DSC thermogram for the isomerization of protonated 1,3-dimethylbicyclo[3.1.0]hexenone, <b>22H</b> , to protonated 2,5-dimethylphenol, <b>15H</b> , in triflic acid. Scan rate = 1°C/min; sample size = 10.6 mg of <b>22</b>	104
Figure 3.24: Isomerizations of protonated bicyclo[3.1.0]hex-3-en-2-ones which differ in the degree of methyl substitution at C6. $\Delta H_R$ in kcal/mol are shown above the arrows	105
Figure 3.25: Isomerizations of bicyclo[3.1.0]hexenyl ions with different substitution patterns on the cyclopentyl ring	109
Figure 3.26: Relative energies (kcal/mol) of dimethyl isomers in triflic acid. Values in brackets are estimates	110
Figure 3.27: Comparison of energy difference between the two dimethylbicyclohexenyl isomers with $\Delta H_R$ for the isomerization of protonated 4,4-dimethylcyclohex-2-enone	110
Figure 3.28: Each pair of molecules give the same cation upon protonation. The difference in the heats of protonation ( $\Delta H_p$ ) reveals the relative energies of the molecules. The strain/bond energy contribution to the energy difference can be extracted by correcting for the contributions of resonance or conjugation	113
Figure 3.29: Acid catalyzed isomerization	114
Figure 3.30: Isomerization of <b>23</b> to <b>2</b> broken into two hypothetical steps; the first step driven by strain/bond energy changes and the second by aromatization of the cyclohexadienone	117
Figure 3.31: Relative energies (kcal/mol) of dimethyl isomers in triflic acid. Value in [ ] is the difference between measured $\Delta H_R$ values. Values in ( ) brackets are estimates	119
Figure 3.32: Relative energies (kcal/mol) of dimethyl isomers and transition states linking them. $\Delta G^\ddagger$ (denoted by *) and $\Delta H_R$ are in kcal/mol in triflic acid. Values in brackets are estimates	120
Figure 3.33: Relative energies (kcal/mol) of tetramethyl isomers in	

triflic acid. Values in brackets are differences between $\Delta H_R$ values	121
Figure 3.34: Relative energies (kcal/mol) of tetramethyl isomers and transition states linking them. $\Delta G^\ddagger$ (denoted with *) and $\Delta H_R$ were measured in $CF_3SO_3H$ . The value in brackets is $\Delta H_{tr}$ in $FSO_3H$	122
Figure 3.35: Relative energies (kcal/mol) of hexamethyl isomers and transition states linking them. $\Delta H_R$ were measured in $CF_3SO_3H$ . $\Delta G^\ddagger$ (marked with *) and $\Delta H_{tr}$ (in brackets) were measured in $FSO_3H$	123
Figure 4.1: Rates of solvolysis of isopropyl/cyclopropyl substituted compounds. X = p-nitrobenzoate except for last compound where X = benzoate	131
Figure 4.2: Rotation about C+-cyclopropyl bond exchanges methyl groups <b>a</b> and <b>b</b>	132
Figure 4.3: The geometry required for maximum orbital overlap in the cyclopropylcarbinyll and allyl systems	132
Figure 4.4: Resonance structures of a protonated cyclopropyl ketone	133
Figure 4.5: Ring expansion of a) cyclopropyl phenyl ketimine to 2-phenylpyrroline and b) vinylcyclopropane to cyclopentene	135
Figure 4.6: Reactions which involve ring expansion of cyclopropyl group and adjacent double bond to a five-membered ring	136
Figure 4.7: Reactions in strong acids of cyclopropyl ketones and cyclopropanecarboxylic acids	137
Figure 4.8: Cyclopropyl ketones studied in this work	146
Figure 4.9: Synthetic routes to cyclopropyl ketones	147
Figure 4.10: Synthesis of <b>37</b> by a) base catalyzed condensation of $\gamma$ -valerolactone and $\gamma$ -butyrolactone, and b) alkylation of 2-methylcyclopropanecarboxylic acid with cyclopropyl lithium	148
Figure 4.11: Synthesis of <b>38</b> by the route of Andrist et al	149
Figure 4.12: Synthesis of compounds <b>39</b> and <b>40</b> by route analogous to that for <b>38</b> (see Fig. 4.11) but with cis-2-butene as a starting material	149
Figure 4.13: Comparison of $^{13}C$ NMR data for protonated ketones with solvolysis rates found in the literature for cyclopropylcarbinyll	

3,5-dinitrobenzoates with the same substitution pattern on the ring. $\Delta\delta(\text{C}(\text{O}))$ is the difference in chemical shift of the carbonyl carbon in the protonated vs. neutral ketones	156
Figure 4.14: Comparison of $\Delta\delta$ , the change in the $^{13}\text{C}$ chemical shift of $\text{C}(\text{O})$ , of cyclopropyl ketones when protonated in triflic acid vs. rates of solvolysis found in the literature for similarly substituted cyclopropylcarbonyl 3,5-dinitrobenzoates	157
Figure 4.15: Oxolanylium ions produced by isomerization of protonated cyclopropyl ketones <b>26H-40H</b>	158
Figure 4.16: $^1\text{H}$ NMR spectra of protonated cyclopropyl methyl ketone, <b>27H</b> , before (top) and after (bottom) isomerization to 2-methyloxolanylium ion, <b>44</b> , by heating in triflic acid at 100 °C for 150 min	159
Figure 4.17: $^1\text{H}$ NMR spectra of protonated cyclopropyl phenyl ketone, <b>28H</b> , before (top) and after (bottom) isomerization to 2-phenyloxolanylium ion, <b>45</b> , by heating in triflic acid at 100 °C for 150 min	160
Figure 4.18: Isomerization of protonated bicyclo[3.1.0]hexanone, <b>41H</b> , and bicyclo[4.1.0]heptanone, <b>42H</b> , yields protonated enones	164
Figure 4.19: Oxolanylium ions result from a number of precursors: enones, cyclopropyl ketones, dihydrofuran, $\gamma$ -substituted ketones, and acylium ions/alkenes	166
Figure 4.20: Comparison of the $^{13}\text{C}$ chemical shifts (ppm) of oxolanylium ions with neutral and ionic model compounds	168
Figure 4.21: Resonance structures for the oxolanylium ion	169
Figure 4.22: cis and trans 2,4,5-trimethyloxolanylium ion isomers exist as an equilibrium mixture at 100 °C in triflic acid	170
Figure 4.23: Signal for H1 of <b>38H</b> shows cis and trans coupling constants	172
Figure 4.24: The 2,4-dinitrophenylhydrazone derivative of <b>40</b>	173
Figure 4.25: ORTEP diagram of the crystal structure of the 2,4-dinitrophenylhydrazone derivative of <b>40</b> . Note that both methyl groups are trans to the carbonyl (hydrazonyl) group	174
Figure 4.26: Two possible reaction paths for protonated cyclopropanecarboxaldehyde, <b>26H</b>	176

Figure 4.27: During a single isomerization of <b>35H</b> , protonated hexenone was formed in addition to the oxolanylium ion product <b>52</b> . Extended heating at 100 °C did not change the composition of the product mixture	176
Figure 4.28: Protonated dicyclopropyl ketone, <b>31H</b> , isomerizes to 2-cyclopropyloxolanylium ion, <b>48</b> , which isomerizes to 2-(1-propenyl)-oxolanylium ion, <b>57</b> . A second route may be partially responsible for the formation of <b>57</b>	177
Figure 4.29: Tetralones or indanones (via enones) could be formed from aryl cyclopropyl ketones in strong acids	178
Figure 4.30: Irradiation of <b>27H</b> at 254 nm or <b>28H</b> at 300 nm leads to the formation of the corresponding protonated enone	179
Figure 4.31: DSC thermogram for the isomerization of protonated cyclopropyl methyl ketone, <b>27H</b> , to 2-methyloxolanylium ion, <b>44</b> . Scan rate = 1°C/min; sample size = 18.4 mg of <b>27</b>	181
Figure 4.32: DSC thermogram for the isomerization of protonated cyclopropyl phenyl ketone, <b>28H</b> , to 2-phenyloxolanylium ion, <b>45</b> . Scan rate = 1°C/min; sample size = 13.4 mg of <b>28</b>	181
Figure 4.33: The principal ion-solvent interaction for protonated cyclopropyl ketone will be H-bonding to the proton on the carbonyl oxygen. With the oxolanylium ion, solvent will interact most strongly with the cation centre	183
Figure 5.1: Ring protonation mechanism: protonated cyclopropyl ring opens to alkyl cation or undergoes direct expansion to oxolanylium ion	196
Figure 5.2: Reactions of cyclopropanecarboxylic acids via protonated cyclopropyl ring. The ring protonated species may produce an alkyl cation	197
Figure 5.3: Evidence for cyclopropyl ring protonation: deuteration of all ring carbons and C2-C3 cleavage	197
Figure 5.4: Protonated cyclopropyl ketones give only C1-C2 cleavage and deuteration only at $\alpha$ -positions	198
Figure 5.5: Alkyl cation mechanism: ring opening to an alkyl cation precedes ring closure to oxolanylium ion	199
Figure 5.6: Isomerizations believed to occur via alkyl cation intermediates in strong acids	200



Figure 5.7: Aryl-substituted cyclopropyl ketones produce tetralones presumably via an alkyl cation intermediate	201
Figure 5.8: Enones should result from an alkyl cation intermediate. In the case of aryl substituted systems, indanones could be formed	201
Figure 5.9: Most simple alkyl-substituted cyclopropyl ketones yield oxolanylium ions in sulfuric acid but the 2,2-dimethyl analog gives a protonated enone in addition to the oxolanylium ion in FSO <sub>3</sub> H/SO <sub>2</sub> ClF at -50 °C	202
Figure 5.10: Thermal isomerization of azocyclopropane is thought to occur via biradical intermediates	203
Figure 5.11: Double nucleophilic displacement mechanism: a nucleophile opens the cyclopropyl ring and is subsequently displaced by the carbonyl oxygen during ring closure	203
Figure 5.12: Enhanced solvolysis of 4-chlorobutyrophenone is believed to be due to the formation of a stable oxolanylium ion intermediate. The intermediate can be isolated in the absence of nucleophiles	205
Figure 5.13: Ring expansion of 1,1-cyclopropanedicarboxylic acid in 0-98% sulfuric acid occurs by two pathways. Pathway A occurs at all acid strengths while pathway B occurs only in concentrated sulfuric acid	205
Figure 5.14: Cyclopropyl imine rearrangement requires protonation and the presence of a nucleophile	206
Figure 5.15: Concerted ring expansion mechanism: concerted ring expansion to an oxygen protonated dihydrofuran followed by deprotonation and reprotonation to produce the oxolanylium ion	207
Figure 5.16: Stereochemical outcome of the four pathways for a concerted [1,3]-sigmatropic rearrangement of a vinylcyclopropane	208
Figure 5.17: The trans dihydrofuran isomer predominates during thermal or photochemical isomerization. Free rotation in a biradical intermediate accounts for the observed stereochemistry	209
Figure 5.18: Rearrangement of 2-alkoxy-3-cyanocyclopropane carboxaldehydes produces the trans product preferentially	210
Figure 5.19: The cis and trans isomers of the methyl cyclopropanecarboxylate equilibrate via an acyclic allylic cation	210

Figure 5.20: Examples of ring expansions in which the stereochemistry of the starting material is retained	211
Figure 5.21: Isomerization of protonated cyclopropyl ketones <b>26-40</b> in triflic acid leads to oxolanylium ions <b>43-60</b>	215
Figure 5.22: Isomerization of protonated bicyclo[n.1.0] ketones <b>41H</b> and <b>42H</b> to protonated enones <b>61H-63H</b>	216
Figure 5.23: First order rate plots for isomerization in triflic acid of: a) protonated cyclopropyl methyl ketone, <b>27H</b> , at 99.3 °C; b) protonated cis,trans-2,3-dimethylcyclopropyl methyl ketone, <b>38H</b> , at 65.0 °C; c) protonated 2-methylcyclopropyl phenyl ketone, <b>36H</b> , at 56.2 °C	217
Figure 5.24: Isomerization of protonated 2,2-dimethylcyclopropyl methyl ketone	220
Figure 5.25: Comparison of the activation energy for ring expansion with the number of steric interactions between groups on the cyclopropyl ring	221
Figure 5.26: Comparison of activation barriers for isomerization of three similarly substituted cyclopropyl ketones in triflic acid	222
Figure 5.27: During isomerization by concerted, double nucleophilic displacement, or alkyl cation pathways, the charge at C(O) is reduced at the transition state	224
Figure 5.28: Methyl substitution at C(O) should lower the energy of the reactant but have little effect on the transition state energy and thus, the activation barrier should be larger for R = CH <sub>3</sub>	225
Figure 5.29: The activation barriers for the isomerization of the <b>26H-31H</b> series and the <b>35H-37H</b> series reveal the relative charge stabilizing abilities of the substituents at C(O)	226
Figure 5.30: Reactions for which a single methyl substitution causes a moderate rate acceleration but a second methyl group causes a large rate acceleration. The relative rates of ring expansion of protonated cyclopropyl ketones were calculated at 25 °C by assuming that $\Delta G^\ddagger$ was temperature independent (i.e. $\Delta S^\ddagger = 0$ )	230
Figure 5.31: Effect of acid strength on the activation barrier for isomerization of protonated cyclopropyl methyl ketone, <b>27H</b> , at 81-2 °C	232
Figure 5.32: Entropies of activation for the thermal ring expansions	

of several cyclopropyl compounds	233
Figure 5.33: Proposed ring-expansion mechanisms for 1,1-cyclopropane-dicarboxylic acids with 0, 1 or 2 methyl groups at the $\beta$ -position in water and aqueous sulfuric acid	234
Figure 5.34: Isomerization of protonated 2,3-dimethylcyclopropyl methyl ketones <b>38H-40H</b> produces the cis and trans 4,5-dimethyloxolanylium ions <b>55</b> and <b>56</b>	236
Figure 5.35: The <i>s-cis</i> conformer required for concerted ring expansion of <b>39H</b> is sterically crowded	237
Figure 5.36: Orbital interactions for thermally-allowed <i>si</i> pathway for ring expansion of protonated cis,trans-2,3-dimethylcyclopropyl methyl ketone	238
Figure 5.37: Inversion at the migrating centre rotates substituent <b>a</b> into the oxallyl framework in the transition state	239
Figure A.1: Crystal structure of <b>40-DNP</b> , the 2,4-dinitrophenylhydrazone derivative of trans,trans-2,3-dimethylcyclopropyl methyl ketone	265
Figure A.2: Unit cell for crystal of <b>40-DNP</b>	266

## **Chapter 1: Introduction**

Carbocations are positively charged organic species in which a large portion of the charge is borne by carbon. They have been implicated as intermediates in many reactions of organic molecules, including nucleophilic substitution, addition to alkenes, polymerizations, aromatic substitution and reactions of carbonyl compounds and carboxylic acids and their derivatives.[1] With the development of conditions under which carbocations are long lived, and because they have a rich chemistry of their own, they continue to be a popular topic for research.[2] The subject of study in this thesis is the rearrangements of carbocations and how changes in substitution affect the energetics of these rearrangements.

In the course of this work many new carbocations were prepared by the protonation of carbonyl or phenol precursors in superacids. The cations so formed were characterized by spectroscopic procedures and then the isomerizations of these cations were probed. Product analysis and rate studies provide information concerning the mechanisms of the isomerizations. In addition, differential scanning calorimetry was used to determine the heat of isomerization for many of the cations, thus providing a direct measure of the energy difference between isomeric cations.

## 1.1 Superacids

The term superacid was first used in 1927 to describe acid systems that could form salts with weak bases, such as carbonyl compounds, that did not form salts with aqueous solutions of the same acids.[3] In the 1950's and 1960's research accelerated in the use of superacid solutions to study of stable carbocations.[4] George Olah became a dominant force in the field of carbocation research and was awarded a Nobel Prize for his work in this area.

The study of carbocations in solution required highly acidic, non-aqueous systems. Superacids were arbitrarily defined by Gillespie as any acid system stronger than 100% sulfuric acid.[5] The Hammett acidity function ( $H_0$ ) is commonly used as a measure of the proton-donating ability of superacid media.  $H_0$  is defined as:

$$H_0 = -pK_B + \log \frac{[B]}{[BH^+]}$$

where **B** is a weak base such as 2,4-dinitroaniline, **BH<sup>+</sup>** is the protonated form of the base, and  $K_b$  is the dissociation constant of the base. The properties of some common superacids are shown in Table 1.1.

Table 1.1: Physical Properties of Common Superacids.[6]

Acid	mp(°C)	bp(°C)	-H <sub>0</sub>	comments
HF	-83	19.5	11	difficult to store, toxic
H <sub>2</sub> SO <sub>4</sub>	10	338(98%)	12	high mp, strong sulfonator, viscous
HClO <sub>4</sub>	-112	110	13	strong oxidizer, explosive
ClSO <sub>3</sub> H	-81	151	13.8	strong sulfonator
CF <sub>3</sub> SO <sub>3</sub> H	-34	162	14.1	solid at very low temps.
FSO <sub>3</sub> H	-89	163	15.1	difficult to store, toxic, strong sulfonator, low mp

While each of the acids listed in Table 1.1 are strongly acidic, they do have some drawbacks which prevent them being used routinely. Both HF and FSO<sub>3</sub>H, which produces HF upon hydrolysis, can dissolve glass and they cause severe, slow healing burns on contact with the skin. Perchloric acid in its anhydrous form is highly explosive so it is typically used as a ≤70% solution in water ( $-H_0 \leq 8$ ). Some of the acids react with potential substrates beyond simple protonation. Thus, H<sub>2</sub>SO<sub>4</sub>, HClO<sub>4</sub>, ClSO<sub>3</sub>H and FSO<sub>3</sub>H can cause oxidation or sulfonation of organic substrates leading to a variety of products.

Since many carbocations undergo decomposition or rearrangement at temperatures well below 0 °C, it is advantageous to have an acid which is a fairly low viscosity liquid at low temperatures. H<sub>2</sub>SO<sub>4</sub> (mp = 10 °C), and to a lesser extent CF<sub>3</sub>SO<sub>3</sub>H (mp = -34 °C) have some limitations as to which cations may be studied. The most commonly used simple acids for carbocation preparation are H<sub>2</sub>SO<sub>4</sub>, CF<sub>3</sub>SO<sub>3</sub>H and FSO<sub>3</sub>H. In this thesis CF<sub>3</sub>SO<sub>3</sub>H (trifluoromethanesulfonic acid, common name triflic

acid) was used almost exclusively because of its ease of handling, high acidity, high boiling point and the lack of undesirable side reactions. The carbocations investigated in this thesis were, in most cases, stable at temperatures above the freezing point of triflic acid.

The strength of Bronsted acids can be increased by the addition of a Lewis acid such as  $\text{SbF}_5$ . [6,7] For instance, the  $H_0$  value for  $\text{FSO}_3\text{H}$  is lowered from -15 to -19 by the addition of 10 mole%  $\text{SbF}_5$ . The 1:1 mixture of  $\text{FSO}_3\text{H}$  and  $\text{SbF}_5$ , known as Magic Acid, is perhaps the strongest protic acid known with  $H_0 = -22$ . [7] Some Lewis acids such as  $\text{SbF}_5$ ,  $\text{AsF}_5$ ,  $\text{NbF}_5$  and  $\text{TaF}_5$  are also considered superacids. Of these, antimony pentafluoride ( $\text{SbF}_5$ ) has been used most extensively in the preparation of carbocations.

## 1.2 Methods of Carbocation Generation

The formation of stable, long-lived carbocations in solution is generally accomplished in one of two manners: heterolytic fission of a C-X bond, or by the addition of a positively charged electrophile to a neutral precursor. During heterolytic fission a bond is broken such that both the bonding electrons remain on one fragment. Nucleophilic substitution by the  $\text{S}_{\text{N}}1$  mechanism yields a carbocation, and is an example of heterolytic fission. However, under the conditions typically used for nucleophilic substitution, the carbocation has a very short lifetime. To prepare stable, long-lived carbocations, the heterolysis is usually performed at low temperatures in a non-nucleophilic solvent ( $\text{SO}_2$ ,  $\text{SO}_2\text{ClF}$ ,  $\text{SO}_2\text{F}_2$ ,  $\text{CH}_2\text{Cl}_2$ ,  $\text{FSO}_3\text{H}$ ) and the heterolysis is often assisted by a Bronsted or Lewis acid. Examples of heterolytic fission leading to

carbocations are shown in Figure 1.1.[8-12] The fourth example in Figure 1.1 shows an ionization accompanied by isomerization, a common occurrence during carbocation preparation.

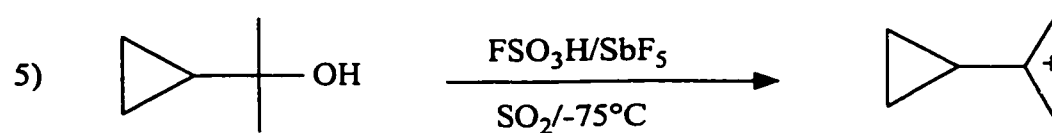
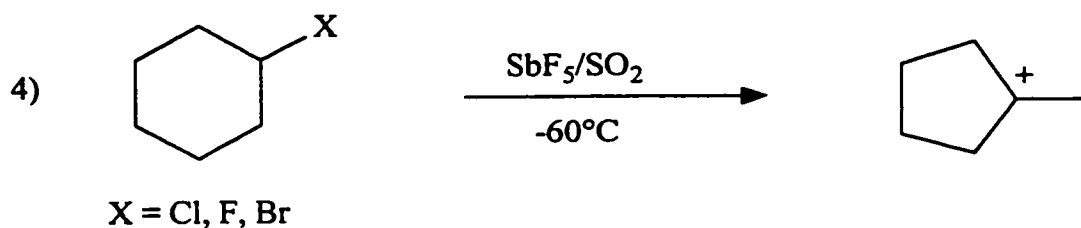
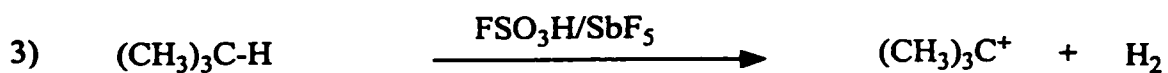
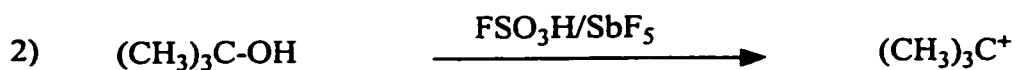


Figure 1.1: Formation of carbocations by heterolysis.



The production of carbocations by the addition of an electrophile typically involves addition to a  $\pi$ -system, although there are examples of addition to a  $\sigma$ -bond. These preparations are also normally performed at low temperatures in non-nucleophilic solvents. Examples of the addition of a proton are shown in Figure 1.2.[13-16] Similar reactions occur with other electrophiles. The carbocations studied in this thesis were prepared by the protonation of ketones and aromatic rings, the second and third examples, respectively, in Figure 1.2.

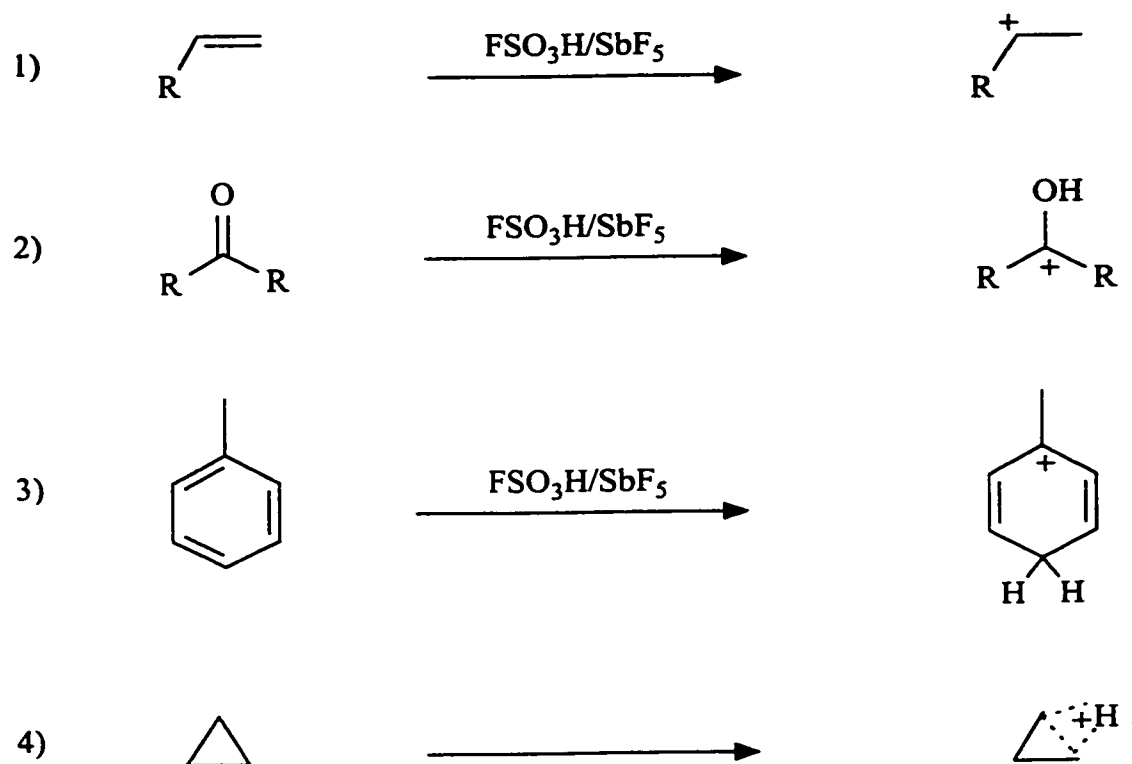


Figure 1.2: Formation of carbocations by protonation.

### 1.3 Structure of Carbocations

Information about carbocation structure (connectivity, geometry, charge distribution) comes from a variety of sources. VSEPR (valence shell electron-pair repulsion model) rules predict planar geometry about a 3-coordinate cation centre.[17] Vibrational spectroscopy (infrared and Raman) reveals that alkyl carbenium ions such as t-butyl cation ( $(\text{CH}_3)_3\text{C}^+$ ) have spectra similar to trivalent, planar boranes (i.e.  $(\text{CH}_3)_3\text{B}$ ), and that the ion adopts a  $C_3$  symmetry.[18] Heterolytic reactions of bridgehead compounds, which are constrained such that a planar cation centre cannot be achieved, are very slow.[19] The  $^{13}\text{C}$  NMR spectrum of the isopropyl cation shows that the central carbon bears considerable positive charge, and the direct  $^{13}\text{C}$ -H coupling constant of 169 Hz indicates that the central carbon is  $sp^2$  hybridized.[20] Atoms with  $sp^2$  hybridization, such as those in alkenes and aromatic compounds, are known to be planar. Finally, X-ray crystal structure determinations of carbocations such as t-butyl or trityl salts reveal a planar central carbon atom.[21,22]

Experimental information regarding the distribution of positive charge in carbocations comes principally from  $^1\text{H}$  and  $^{13}\text{C}$  NMR spectroscopy. The chemical shift of an atom is approximately proportional to the electron density surrounding that atom, however, chemical shifts can be influenced by other factors such as the presence of magnetically anisotropic groups. Thus, NMR spectroscopy is best used to investigate a series of closely related ions for changes in charge distribution.

The  $^1\text{H}$  NMR spectrum of the isopropyl cation consists of two signals.[20] The signal at 13 ppm is due to the hydrogen directly bonded to the cation centre while the

signal at 4.5 ppm is due to the two methyl groups. These signals are markedly downfield from those for similar groups in neutral molecules, suggesting that the molecule bears positive charge.  $^{13}\text{C}$  NMR spectroscopy can probe the cation centre directly. The isopropyl cation shows two signals, one at 52 ppm and the other at 320 ppm.[20] An alkene  $\text{sp}^2$  carbon resonates at about 120 ppm, while that in a carbonyl group is observed at 200-220 ppm. Thus the atom with a signal at 320 ppm is greatly deshielded, consistent with a large positive charge on the cation centre.

Replacing a methyl group of the t-butyl cation with a cyclopropyl, phenyl or hydroxy group causes the chemical shift of the cation centre to move upfield (Table 1.2).[20,23] This suggests that there is less positive charge on the central carbon and that these substituents are better electron donors than a methyl group. These conclusions are consistent with other measures of carbocation stability.

Table 1.2:  $^{13}\text{C}$  NMR chemical shift of cation centre in several carbocations.[20,23]

ion	$\delta$ (ppm)
$\text{Me}_3\text{C}^+$	328
(cyclopropyl) $\text{Me}_2\text{C}^+$	280
$\text{PhMe}_2\text{C}^+$	254
(OH) $\text{Me}_2\text{C}^+$	248

The ions in Table 1.2 provide good examples of the different ways in which charge is spread over carbocations. Electron density is supplied to the cation centre by

either induction or conjugation (delocalization). Inductive electron donation occurs through the bonds attached to the cation centre by bond polarization and the effect decreases with distance. The inductive effect is stabilizing for electropositive substituents, and destabilizing for those that are electronegative.

The conjugative effect involves electron donation from an adjacent bond or lone pair into the vacant p-orbital on the cation centre. It requires alignment of the donor and p-orbital, and results in an increased bond order between C<sup>+</sup> and the adjacent atom. Delocalization of charge by conjugation is often represented by two or more resonance structures. The resonance structures correspond to extremes in the electron distribution. The groups that can act as conjugative electron donors include double bonds, aromatic rings, heteroatoms (N, O, F, Cl, etc.) and  $\sigma$ -bonds, typically C-H or strained C-C bonds. When  $\sigma$ -bonds are involved the delocalization is termed hyperconjugation. Some examples of delocalization of charge are shown in Figure 1.3.

For most carbocations, both effects are operative, but often conjugative effects overwhelm inductive effects. Thus, sp<sup>2</sup> centres (aromatic rings or double bonds) and halogen atoms are inductively electron-withdrawing groups relative to hydrogen or alkyl groups, but they can conjugate to cation centres and lead to stabilization of the carbocation. If these groups are moved out of conjugation (i.e. one bond away or into an unfavourable geometry) then they will inductively destabilize the ion.[28]

When charge is delocalized as depicted in Figure 1.3, the atoms which bear charge in one of the resonance structures should be electron deficient, and the NMR signals due to these atoms should be shifted downfield. In Figure 1.4 the <sup>13</sup>C chemical shifts for

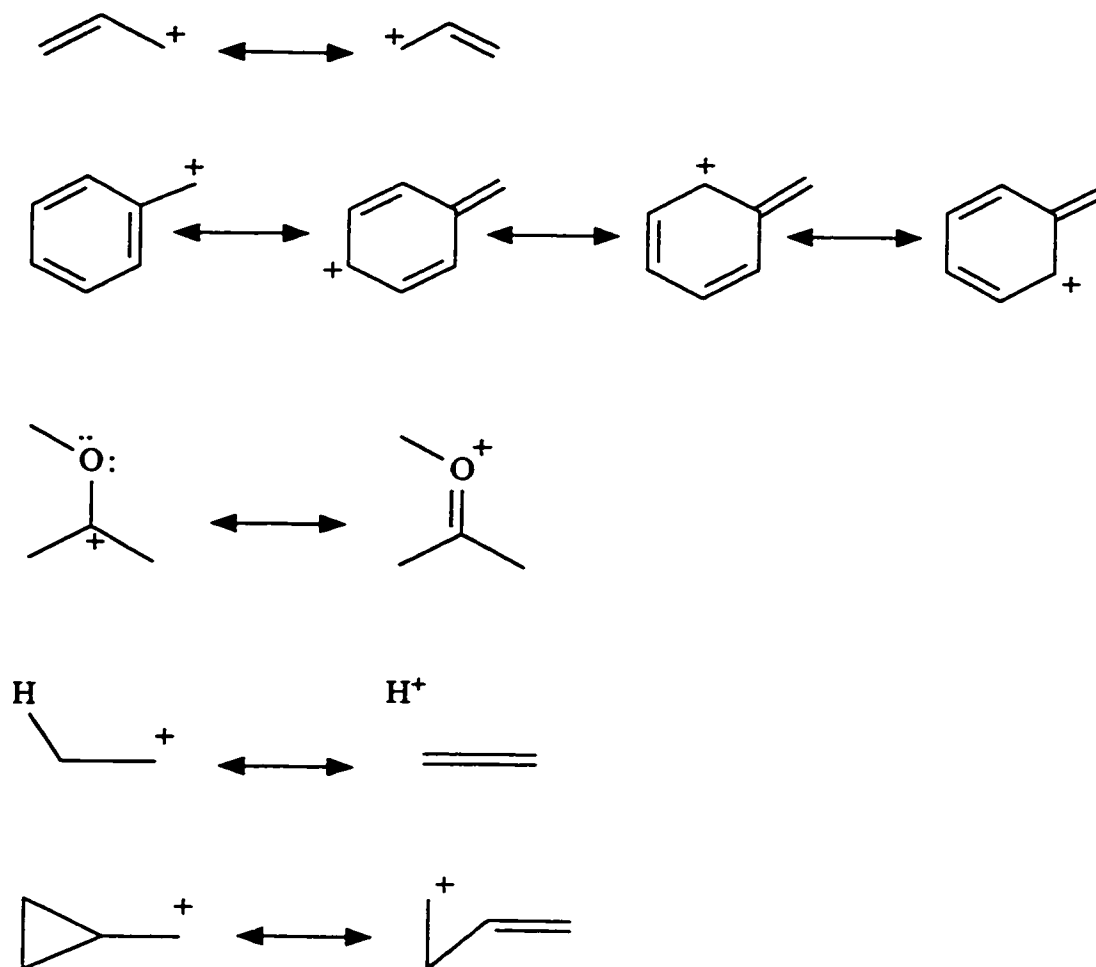


Figure 1.3: Conjugative interactions of  $\pi$ -systems, lone pairs and  $\sigma$ -bonds with the cation centre.

several delocalized cations are shown.[25-27] Three of the cations are of the allyl type; the cyclohexadienyl cation extends the conjugation by an additional double bond. The chemical shifts of C1 (and C5), and C3 are 40-80 ppm further downfield than the chemical shifts of C2 (and C4), consistent with the resonance picture of these cations. Similarly, two of the cations are of the benzylic cation type. The  $^{13}\text{C}$  chemical shifts of these ions are consistent with the resonance picture. The signals for the ortho and para

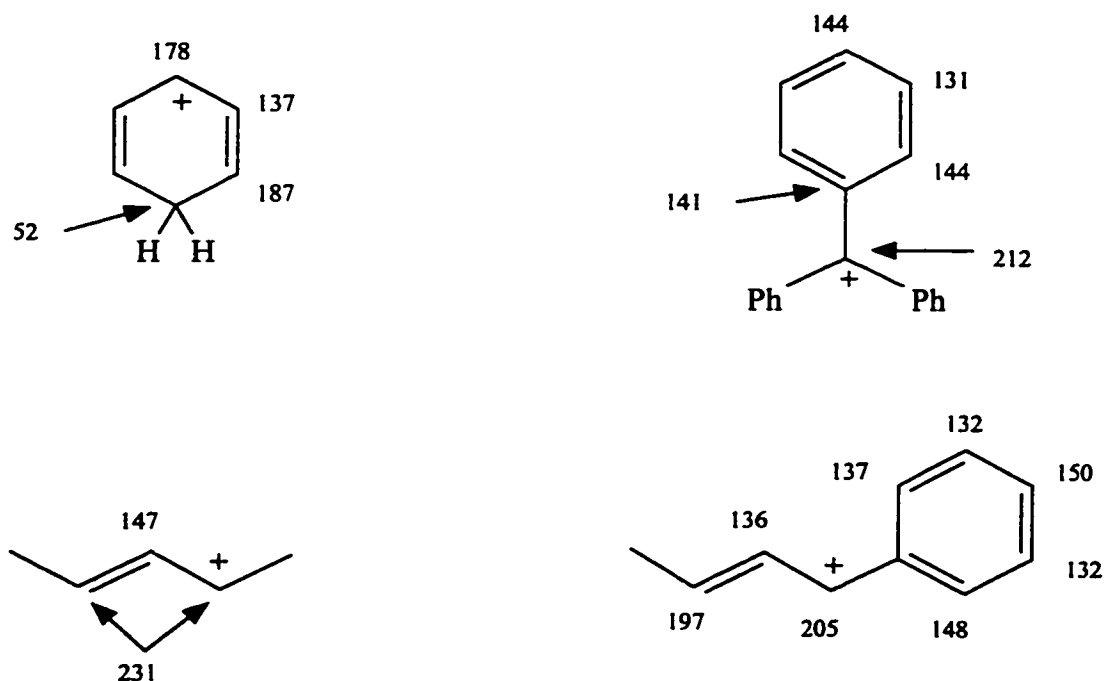


Figure 1.4:  $^{13}\text{C}$  chemical shifts in cyclohexadienyl, triphenylmethyl, pentenyl and 1-phenylbutenyl cations.

positions of the phenyl rings are further downfield than the meta positions.

As mentioned above, conjugative electron donation which requires an alignment of the vacant p-orbital and the donor orbital leads to an increase in the  $\text{C}^+\text{-R}$  bond order. Temperature dependent NMR spectroscopy provides evidence for conjugative interactions, as well as a quantitative measure of the strength of the interaction. Vinyl, phenyl, cyclopropyl and alkoxy substituted carbocations have NMR spectra consistent with restricted bond rotation between the cation centre and the substituent. The ions have a preferred geometry for maximum interaction between the cation centre and the donor. For example, the 1,1-dimethylcyclopropyl carbinyl cation displays two methyl signals in its low temperature NMR spectrum.[28] One methyl group is trans to the cyclopropyl

ring, while the other is located in the face of the three membered ring (Figure 1.5). The barrier to rotation about the bond joining the cyclopropyl ring and the cation centre was determined to be  $13.7 \pm 0.4$  kcal/mol.[29]

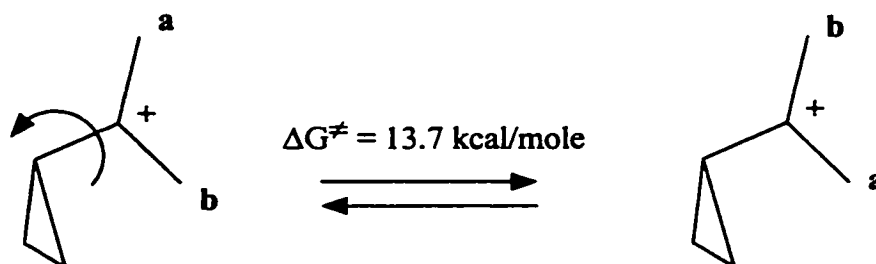


Figure 1.5: Rotation about C<sup>+</sup>-cyclopropyl bond exchanges methyl groups **a** and **b**.

Perhaps the most powerful technique for the experimental determination of carbocation structure is X-ray crystallography. In general, the atomic positions can be determined with high precision. Childs and coworkers [30] have determined the structure of a number of carbocation salts, almost all of which bear hydroxy or alkoxy groups in addition to other substituents. More recently, Laube and coworkers [31] have determined the structure of some simple alkyl carbocations.

Protonation of cyclopropyl phenyl ketone yields a carbocation bearing hydroxy, cyclopropyl and phenyl groups as shown in Figure 1.6. The crystal structure of this cation [30a] illustrates the geometry required for conjugation of each group with the cation centre; a bisected geometry with the cyclopropyl group, and planar with the phenyl ring. The bond lengths in the cation also show evidence of conjugation: the bonds joining C<sup>+</sup> to the cyclopropyl and phenyl groups are shortened, indicating the donation of electron

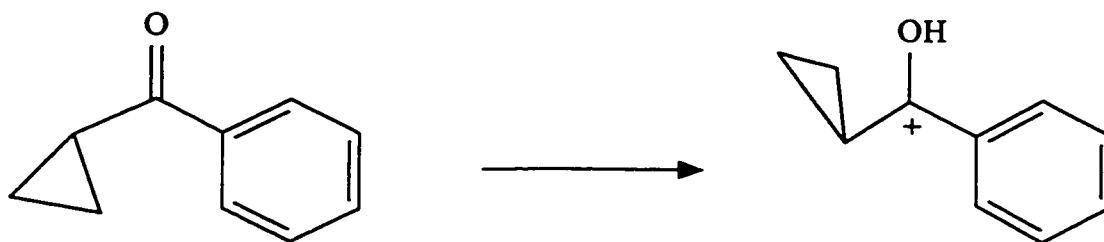


Figure 1.6: The crystal structure of protonated cyclopropyl phenyl ketone revealed that the phenyl group is planar with the cation centre while the cyclopropyl group forms a bisected geometry.

density to the cation centre.

Laube and coworkers[31] have determined the structure of a number of number of carbocations of fundamental importance including t-butyl,[31a] norbornyl,[31b] norbornenyl[31c], adamantyl[31d] and cumyl cations.[31e] The crystal structure of the 1-adamantyl cation (Figure 1.7) illustrates many of the features of carbocation structure. The cation centre is almost planar, in spite of the increased ring strain in this cage molecule. The bonds between  $C^+$  and the adjoining carbons are shortened, while the next bond,  $C_\alpha-C_\beta$ , is lengthened appreciably, consistent with donation of electron density from the  $C_\alpha-C_\beta$  bonds to the cation centre. This type of electron donation is an example of hyperconjugation.



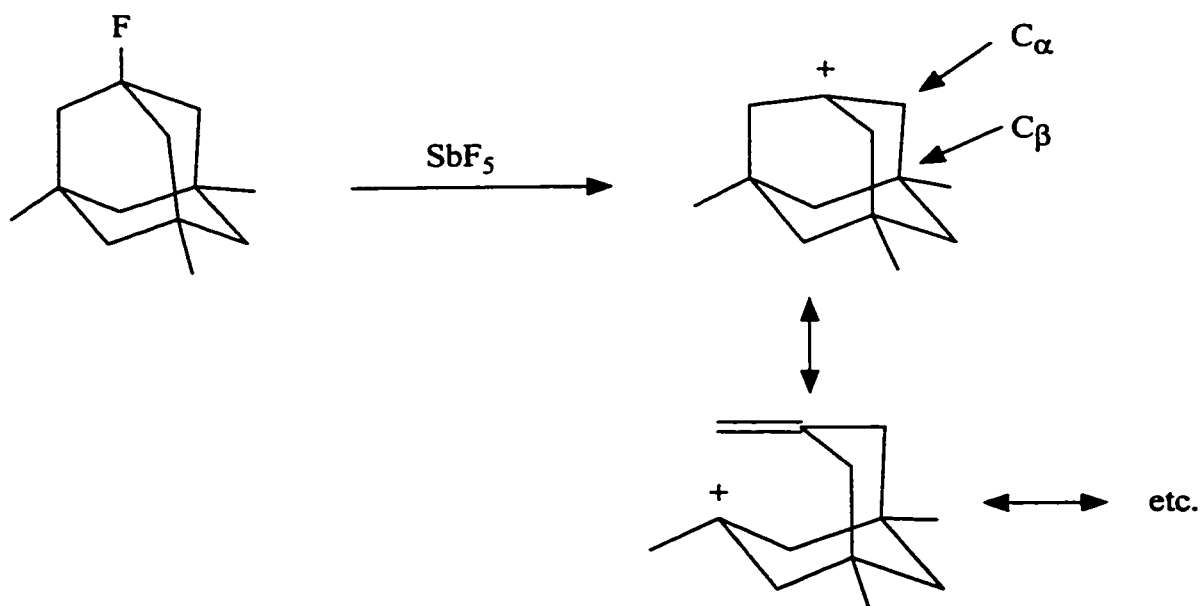


Figure 1.7: The crystal structure of the 3,5,7-trimethyladamantyl cation shows structural changes consistent with the resonance structures shown.

#### 1.4 Isomerizations of Carbocations

The conversion of a carbocation to another carbocation with the same number and type of atoms is termed an isomerization. Isomerizations (rearrangements) are so common for carbocations that this reaction serves as a hallmark of the carbocations.[32]

The most common isomerization is a 1,2-migration (or shift), in which an atom or group (along with its bonding electrons) migrates to an adjacent cation centre (see Figure 1.8).[32] Concerted suprafacial 1,2-shifts are allowed by orbital symmetry, while the corresponding reactions of carbanions and radicals are not.[33] In many cases, apparently complex rearrangements of carbocations may actually occur by a series of 1,2 shifts. Migrations over greater distances (i.e. 1,4 shifts) also occur. Cyclopropyl migration in the

bicyclo[3.1.0]hexenyl cations is known to occur via a 1,4 migration (Figure 1.9).[34]

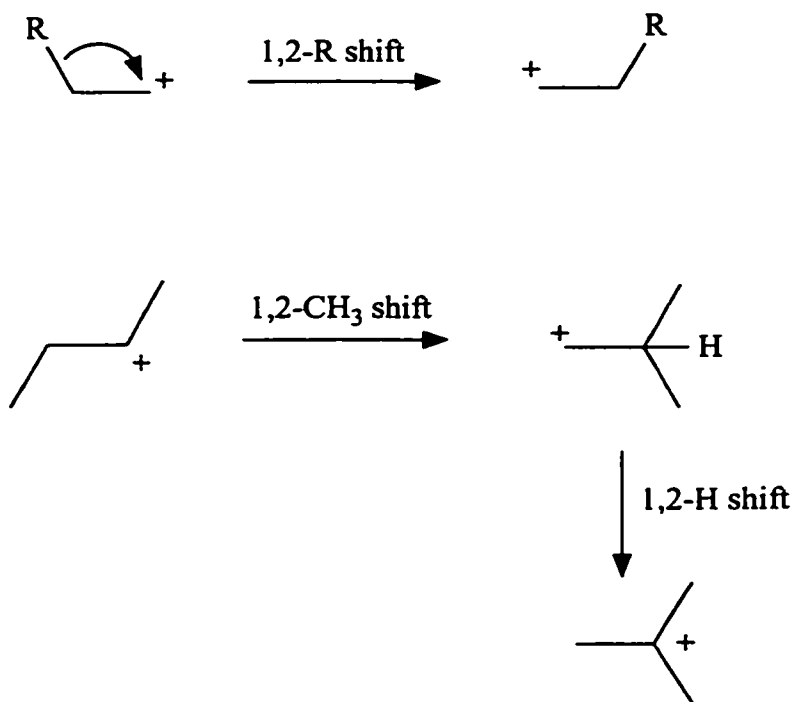


Figure 1.8: Sequential 1,2 shifts account for the isomerization of sec-butyl to t-butyl cation.

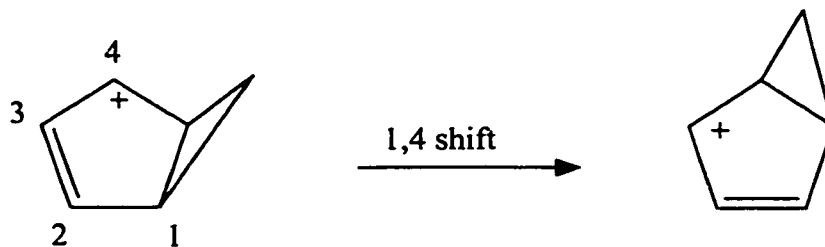


Figure 1.9: Isomerization in bicyclo[3.1.0]hexenyl cations by 1,4-migrations.

Reactions in which rings are formed or broken are also common for carbocations. One route for ring formation is by intramolecular addition of a carbocation to a  $\pi$ -system. An example of this type of reaction is shown in Figure 1.10.[35]

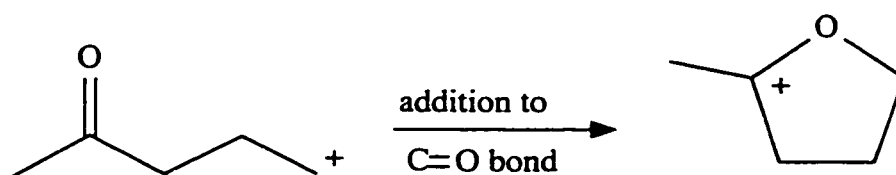


Figure 1.10: Ring closure by intramolecular addition to a C=O group.

### 1.5 Stability of Carbocations

The course of many reactions can be rationalized or even predicted if the factors affecting the stability of carbocations are known. Qualitative information about carbocation stability is obtained from the observation of long-lived ions, or determination of the regiochemistry of carbocation-mediated reactions. For example, oxymercuration of 2-methyl-2-butene yields only a tertiary alcohol (Figure 1.11), the result of addition of the electrophilic mercury to only one end of the double bond.[36] Addition to the other end would lead to a primary carbocation. This result indicates that a tertiary cation is more stable than a primary cation.

Quantitative measures of carbocation stability have been determined from a variety of experimental data including: 1) rates of reactions known to proceed via a carbocation, 2) persistence (lifetime), 3) the energy required to form carbocations, 4) the energy difference between two or more carbocations, 5) chemical shifts (NMR). The

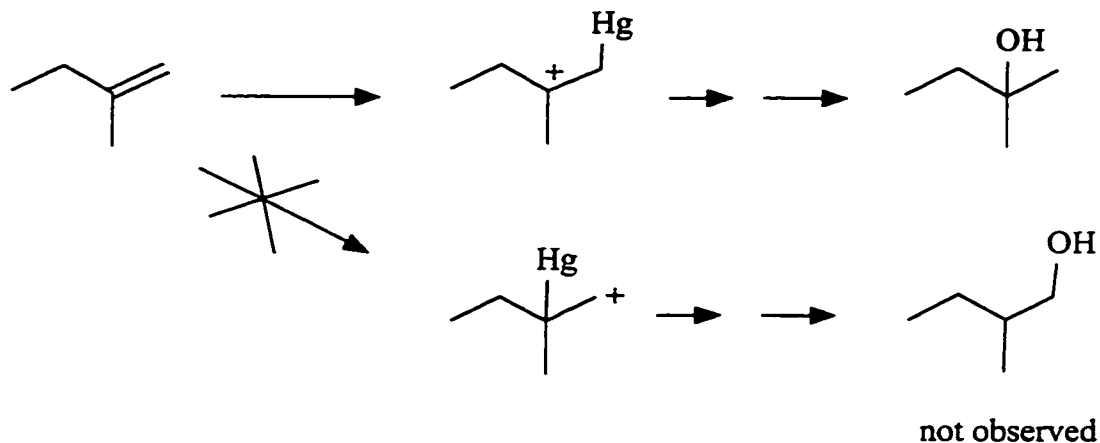


Figure 1.11: Oxymercuration of 2-Me-butene yields only 2-Me-2-butanol.

determination of rates or lifetimes are termed kinetic measures of stability since they depend, in part, on the energy of a transition state. When two ground state species (cation/neutral or cation/cation) are compared it is a thermodynamic measure of stability.

### 1.5.1 Kinetic Measures of Carbocation Stability

The comparison of solvolysis rates is the principal kinetic method used to rank carbocation stability. For solvolyses which are believed to occur via a carbocation, it is postulated that the transition state is similar in structure and energy to the carbocation intermediate (Hammond Postulate). A stable cation will be easier to form and thus its solvolysis should have a faster rate and lower activation barrier. In Table 1.3, the relative rates of solvolysis for three alkyl chlorides are presented.[37] When the hydrogen atom of isopropyl chloride is replaced with a methyl or phenyl group, the rate of solvolysis is accelerated, leading to the predicted carbocation stabilities of:  $\text{Me}_2\text{HC}^+$ ,  $\text{Me}_3\text{C}^+$ ,

$\text{Me}_2\text{PhC}^+$ . As the rate of solvolysis of other molecules are determined, the corresponding carbocations can be added to this series. For example, the rate of solvolysis of 1-adamantyl tosylate is about 1000 times slower than that for t-butyl tosylate.[38] Thus, the stability of the 1-adamantyl cation is predicted to rank between the isopropyl and t-butyl cations.

Table 1.3: Rates of solvolysis of alkyl chlorides.[37]

compound	relative rate
iPr-Cl	1
tBu-Cl	$5.5 \times 10^4$
cumyl-Cl	$2.5 \times 10^8$

While the comparison of solvolysis rates is a powerful means of determining relative carbocation stabilities and the effect of substituents, several cautions should be noted:

- 1) The structure and energy of the transition state for solvolysis may not be similar to the carbocation.
- 2) Some of the solvolysis may be due to bimolecular ( $\text{S}_{\text{N}}2$ ) processes, in which case, carbocation stability does not control the rate of reaction.
- 3) Other factors, such as the relief of strain, may account for accelerated rates of solvolysis.

### 1.5.2 Thermodynamic Measures of Carbocation Stability

Measurement of the free energy ( $\Delta G$ ) or enthalpy ( $\Delta H$ ) of carbocation formation is the basis for the determination of thermodynamic stability. Thermodynamic measures are also based on energy differences but the advantage of thermodynamic versus kinetic measures of stability is that the energy of the carbocation is one of those used to determine the magnitude of  $\Delta H$  or  $\Delta G$ . With kinetic measures, a transition state, which is assumed to be similar to the cation in energy and structure, determines the measured stability.

One common method for determining the stability of carbocations is based on the ionization of alcohols in acidic solution. The stability of the cation is given by  $pK_R^+$ , a function of the acidity of the medium and of the concentrations of the cation and alcohol. The equation relating these quantities is given below, where  $H_R$  is a measure of the acidity of the solution (e.g. pH or  $H_0$ ).



$$pK_R^+ = H_R + \log \frac{[R^+]}{[ROH]}$$

As cation stability increases the  $R^+/ROH$  ratio becomes larger and the  $pK_R^+$  value increases. The  $pK_R^+$  value is equal to the pH (or  $H_0$ ) at which the cation and alcohol exist at equal concentrations. The  $pK_R^+$  values for several cations are displayed in Table 1.4.[39] The tricyclopropylcyclopropenyl cation can be observed in alkaline aqueous

solution.

Table 1.4:  $pK_{R^+}$  values for several cations.[39]

carbocation ( $R^+$ )	$pK_{R^+}$
$Ph_2HC^+$	-13.3
$Ph_3C^+$	-6.63
$(cp)_3C^+$	-2.3
$(cp)_3\text{cyclopropenyl}^+$	9.7

a) cp = cyclopropyl

The stability of carbocations is also obtained from gas-phase measurements such as the determination of appearance potentials, dissociation energies or hydride affinities.[40] Gas-phase measurements have the advantage that the cation is produced in the absence of solvent or counterions. Thus, the measured heats of formation reflect the intrinsic stability of the ions, and the effect of substituents on ion stability is not attenuated by any other factors. The major disadvantage of these techniques is that they reveal very little about the structure of the ions. In Table 1.5, the dissociation energies for the heterolysis of some hydrocarbons to carbocations are displayed.[41] To form a t-butyl cation requires 83 kcal/mole less energy than a methyl cation, consistent with the much higher stability of the t-butyl cation. When a hydrogen atom of  $CH_3^+$  is replaced with a vinyl or phenyl group, the dissociation energy is drastically reduced.

A calorimetric method for determining the heats of carbocation formation by ionization has been developed by Arnett and coworkers.[42] In this technique, a neutral

Table 1.5: Dissociation energies for  $R-H \rightarrow R^+ + H^-$  heterolysis.[41]

carbocation ( $R^+$ )	dissociation energy (kcal/mol)
$CH_3^+$	315
$MeCH_2^+$	277
$Me_2CH^+$	249
$Me_3C^+$	232
$CH_2=CH-CH_2^+$	256
$PhCH_2^+$	238

precursor is introduced into the superacid solvent in the calorimeter and the heat released by carbocation formation ( $\Delta H_i$ ) is measured. The effect of substituents on carbocation stability is revealed by measuring the heat of carbocation formation for a series of ions. In general, substituent effects are more important in the carbocation than in the neutral precursors,[42,43] and thus differences in  $\Delta H_i$  should reflect differences in carbocation stability. Results obtained by Arnett and coworkers are given in Table 1.6.[42]

Secondary cation formation ( $iPr^+$ ,  $sBu^+$ ) is accompanied by lower heat release than the formation of a tertiary cation ( $tBu^+$ ). This is consistent with the greater stability of the tertiary cation. When sec-butyl chloride ( $sBuCl$ ) is ionized at  $-25\text{ }^\circ\text{C}$ , the t-butyl cation is formed. The  $\Delta H_i$  value for this process is 5 kcal/mol more exothermic than the ionization of t-butyl chloride. The 5 kcal/mole difference is the energy difference between the isomeric neutral precursors. In this case, structural change has a significant effect on the energies of both the neutral precursor and the cation.



Table 1.6: Heats of ionization determined by solution calorimetry.[42]

precursor	ion	$-\Delta H_i$ (kcal/mol)
iPr-Cl	iPr <sup>+</sup>	15.3
sBu-Cl	sBu <sup>+</sup>	15.9 (at -75 °C)
sBu-Cl	tBu <sup>+</sup>	30.0 (at -25 °C)
tBu-Cl	tBu <sup>+</sup>	24.8
tBu-OH	tBu <sup>+</sup>	35.5
Ph <sub>3</sub> C-OH	Ph <sub>3</sub> C <sup>+</sup>	49.0
cp <sub>3</sub> C-OH	cp <sub>3</sub> C <sup>+</sup>	59.2

- a) chlorides were ionized with SbF<sub>5</sub> in SO<sub>2</sub>ClF at -55 °C except where indicated.  
 b) alcohols were ionized with FSO<sub>3</sub>H/SbF<sub>5</sub> (1:1) in SO<sub>2</sub>ClF at -40 °C.  
 c) cp = cyclopropyl

Arnett and coworkers[42a] ionized sec-butyl chloride (sBuCl) at -75 and -25 °C, resulting in the formation of sec-butyl (sBu<sup>+</sup>) and t-butyl (tBu<sup>+</sup>) cations, respectively. The 14.1 kcal/mol difference between the two  $\Delta H_i$  values is the energy difference between the secondary and tertiary carbocations. The  $\Delta H$  difference corresponds closely to a value of 14.5 kcal/mol determined with a scanning calorimeter[44] and to values from gas-phase measurements.[45]

The final three entries in Table 1.6 list the energy released by ionization of alcohols bearing three methyl, phenyl, or cyclopropyl groups. The ionization is increasingly exothermic as the substituent changes from methyl to phenyl to cyclopropyl. On the basis of these results, the carbocation stabilizing abilities of these groups are ordered: methyl < phenyl < cyclopropyl. This relative ordering of stabilizing abilities has been observed in many, but not all, investigations.[42a,46]

There have been several calorimetric studies of carbocations produced by the protonation of  $\pi$ -systems such as alkenes, aromatic rings, ketones or esters.[43,47] The heats of protonation,  $\Delta H_{\text{p}}$ , for several ketones are displayed in Figure 1.12.[47a,47b]

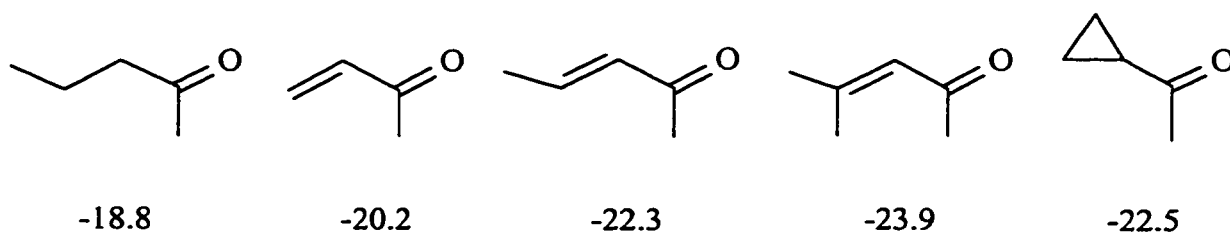


Figure 1.12: Heats of protonation ( $\Delta H_{\text{p}}$  in kcal/mol) of several ketones in  $\text{FSO}_3\text{H}$  at 25 °C.

Protonated ketones can be viewed as hydroxy-substituted carbocations (Figure 1.13). When the substituents on the carbonyl carbon are changed from an alkyl group to a vinyl group,  $\Delta H_{\text{p}}$  becomes more exothermic (Figure 1.12). As first one and then two methyl groups are added to the  $\beta$ -position of the double bond, the heat released by protonation increases. These observations are consistent with the resonance picture of the ions (Figure 1.13). The vinyl group bound to the cation centre delocalizes charge and thus stabilizes the ion. Since the  $\beta$ -carbon of the double bond bears charge, methyl substitution at this position causes  $\Delta H_{\text{p}}$  to be more exothermic, as observed. The final example in Figure 1.12 reveals that a cyclopropyl group is as effective as a double bond at stabilizing the carbocation.

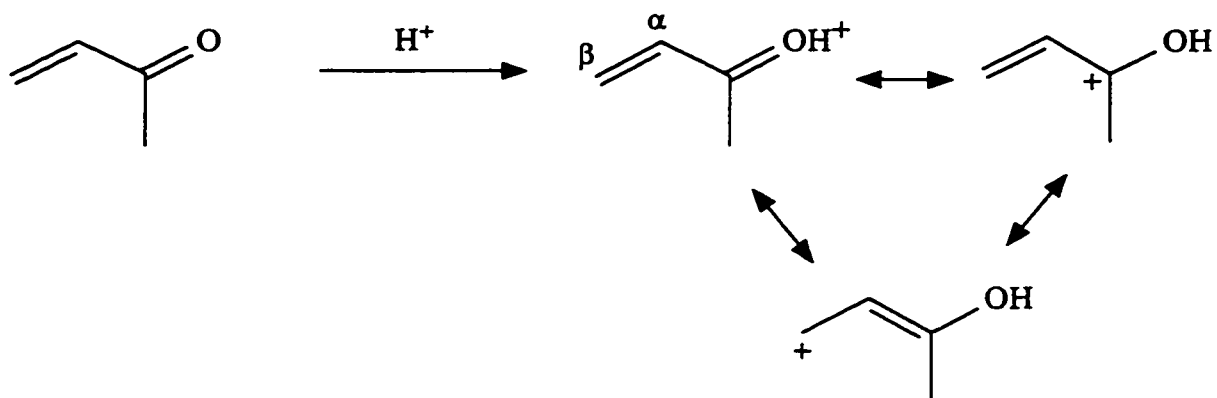


Figure 1.13: Resonance structures of a protonated  $\alpha,\beta$ -unsaturated ketone.

## 1.6 Scanning Calorimetry

During a scanning calorimetry experiment, the temperature of a sample is raised or lowered while the heat released or absorbed by the sample is measured. This technique is ideal for measuring the enthalpy of phase changes (melting or glass transitions). When scanning calorimetry is used to study a chemical reaction, the enthalpy of reaction ( $\Delta H_R$ ) can be determined. In the case of a carbocation isomerization, the enthalpy of reaction reveals the energy difference between the two ions. Thus, a direct comparison of structural or substituent effects on stability can be obtained. Unlike other measures of stability such as solvolysis rates or heats of ionization, the effect of substituents on the energies of neutral precursors need not be considered.

While this technique appears well suited to studying the isomerizations of carbocations, there is only one published example of scanning calorimetry monitoring a

carbocation isomerization. Bittner, Arnett and Saunders[44] measured the heat of isomerization of sec-butyl to t-butyl cation. sec-Butyl cation was prepared from sec-butyl chloride in  $\text{SbF}_5/\text{SO}_2\text{ClF}$  at  $-120\text{ }^\circ\text{C}$  in their "home-built", low-temperature calorimeter. Each experiment consisted of three separate scans: 1) the sec-butyl cation solution was heated from  $-80$  to  $-20\text{ }^\circ\text{C}$  producing the t-butyl cation, 2) the t-butyl cation solution was then heated from  $-80$  to  $-20\text{ }^\circ\text{C}$  to obtain a baseline, and 3) the solution was again heated from  $-80$  to  $-20\text{ }^\circ\text{C}$  while an electrical heater was used to reproduce the temperature rise observed during isomerization. The results of six separate experiments determined the heat of isomerization to be  $\Delta H_{\text{isom}} = -14.5 \pm 0.5\text{ kcal/mole}$ .

The measurement of the energy difference between these two carbocations was an experiment of fundamental importance. While other carbocation isomerizations could have been studied, the difficulties associated with operation of the low-temperature calorimeter may have dissuaded further investigation. In addition, the calorimeter was not particularly sensitive since a single experiment required 1.85 g of sec-butyl chloride. There are several ways to simplify this type of experiment: 1) use of a differential scanning calorimeter and/or 2) study of isomerizations which occur at higher temperatures (i.e.  $0\text{ }^\circ\text{C}$  or above).

The commercial development of low-temperature differential scanning calorimeters (DSC) has simplified the study of low-temperature isomerizations.[48] A DSC consists of a block which can be heated or cooled at a controlled rate. Inside the block are sample and reference cells. The difference in heat absorbed or released by the two cells is determined during each scan. Thus, in a single scan, the enthalpy of

isomerization can be determined. Many DSCs give easily measured signals with 10 mg samples.

DSC has been used to study the isomerizations of a number of neutral molecules.[49-56] Several examples are shown in Figure 1.14.[49-51] In the first two examples, the higher energy isomer (shown on the left) is produced photochemically from the other isomer. DSC reveals the amount of photochemical energy stored in the molecule, important information for solar energy storage studies. In addition, the effect of substituents on the energies of the isomers may be determined by studying a series of compounds. For instance, when the methyl groups of the Dewar benzene (bicyclo[2.2.0]hexa-2,5-diene) shown in the second example[50] of Figure 1.14 are replaced with trifluoromethyl groups, only about half as much energy is released (28.0 vs. 59.5 kcal/mole).[52]

One of the principal goals of this thesis was to establish whether DSC might be used to determine reliable thermochemical data for carbocation isomerizations.

## 1.7 Thesis Outline

This thesis focuses on three types of carbocation isomerizations and explores the use of DSC to determine the thermochemistry of these reactions. An example of each type of reaction is shown in Figure 1.15. The cations involved in the isomerizations are characterized by spectroscopic means, principally NMR. Rates and heats of isomerization were measured and used to determine the driving force for the rearrangements, the effect of substituents on cation stability, and to illuminate the

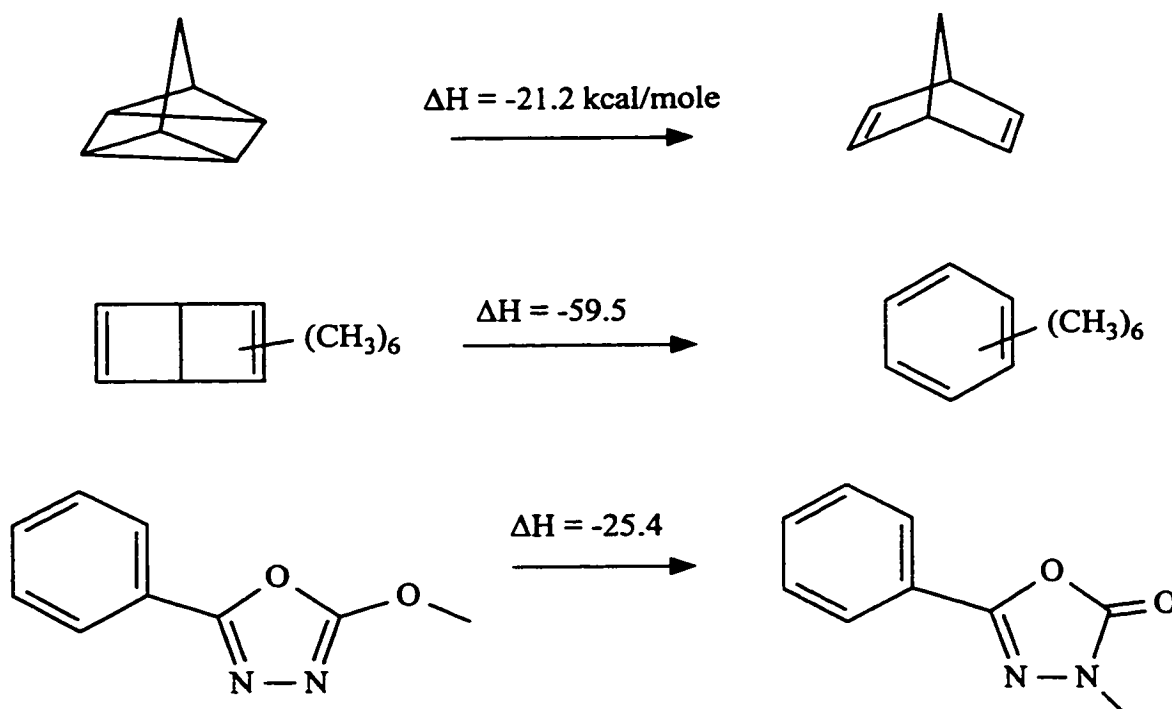


Figure 1.14: Examples of isomerizations investigated with differential scanning calorimetry (DSC).

mechanistic pathways involved. Methyl migrations about cyclohexadienyl and related cations are examined in chapter 2. Ring opening isomerizations of protonated bicyclo[3.1.0]hex-3-en-2-ones are discussed in chapter 3. The ring expansion rearrangement of protonated cyclopropyl ketones is the subject of the final two chapters. In chapter 4, the course of the isomerizations is established and the reactant and product cations are characterized, while chapter 5 concentrates on the mechanism of the ring expansion of protonated cyclopropyl ketones to oxolanylium ions. Each chapter contains a results and discussion section as well as introduction and experimental sections concerning the relevant isomerizations.

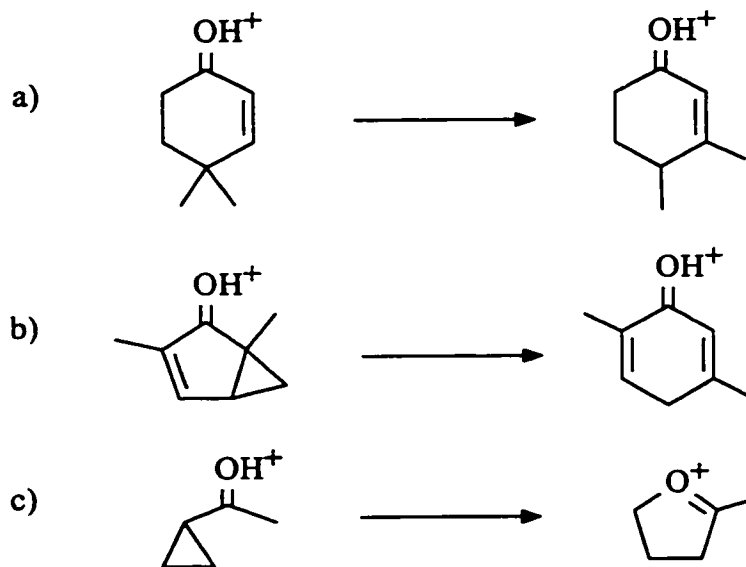


Figure 1.15: Examples of the three types of isomerization investigated in this work: a) methyl migrations in protonated cycloalkenones and cyclohexadienones, b) ring opening of protonated bicyclo[3.1.0]hexenones to protonated phenols, and c) ring expansion of protonated cyclopropyl ketones to oxolanylium ions.

## 1.8 References

1. J. March, *Advanced Organic Chemistry: Reactions, Mechanisms, and Structure*, 4th ed., Wiley, Toronto, 1992, chpts. 10, 11, 15, 16.
2. *Stable Carbocation Chemistry*, G.K.S. Prakash, P.v.R. Schleyer (eds.), Wiley, New York, 1997.
3. N.F. Hall, J.B. Conant, *J. Am. Chem. Soc.*, **1927**, *49*, 3047.
4. *Carbonium Ions*, G.A. Olah, P.v.R. Schleyer (eds.), Wiley, Toronto, vol. 1 (1968); vol. 2 (1970); vol. 3 (1972); vol. 4 (1973); vol. 5 (1976).
5. R.J. Gillespie, T.E. Peel, *Adv. Phys. Org. Chem.*, **1972**, *9*, 1; *J. Am. Chem. Soc.*, **1973**, *95*, 5173.

6. G.A Olah, G.K.S. Prakash, J. Sommer, *Superacids*, Wiley, Toronto, 1985, chpt. 2.
7. R. Jost, J. Sommer, *Rev. Chem. Intermed.*, **1988**, *9*, 171
8. G.A. Olah, E.B. Baker, J.C. Evans, W.S. Tolgyesi, J.S. McIntyre, I.J. Bastien, *J. Am. Chem. Soc.*, **1964**, *86*, 1360; G.A. Olah, W.S. Tolgyesi, S.J. Kuhn, M.E. Moffatt, I.J. Bastien, E.B. Baker, *J. Am. Chem. Soc.*, **1963**, *85*, 1328.
9. G.A. Olah, M.B. Comisarow, C.A. Cupas, C.U. Pittman, Jr., *J. Am. Chem. Soc.*, **1965**, *87*, 2997.
10. G.A. Olah, J. Lukas, *J. Am. Chem. Soc.*, **1967**, *89*, 2227; **1967**, *89*, 4739; **1968**, *90*, 933.
11. G.A. Olah, J.M. Bollinger, C.A. Cupas, J. Lukas, *J. Am. Chem. Soc.*, **1967**, *89*, 2692; G.A. Olah, J. Lukas, *J. Am. Chem. Soc.*, **1968**, *90*, 993.
12. C.U. Pittman, Jr., G.A. Olah, *J. Am. Chem. Soc.*, **1965**, *87*, 2998; N.C. Deno, J.S. Liu, J.O. Turner, D.N. Lincoln, R.E. Fruit, Jr., *J. Am. Chem. Soc.*, **1965**, *87*, 3000.
13. D.M. Brouwer, *Rec. Trav. Chim.*, **1968**, *87*, 210; G.A. Olah, Y. Halpern, *J. Org. Chem.*, **1971**, *36*, 2354.
14. G.A. Olah, A.M. White, D.H. O'Brien in *Carbonium Ions*, G.A. Olah, P.v.R. Schleyer (eds.), Wiley, Toronto, 1973, vol. 4, chpt. 31, p. 1697.
15. T. Birchall, R.J. Gillespie, *Can. J. Chem.*, **1964**, *42*, 502; D.M. Brouwer, E.L. Mackor, C. MacLean in *Carbonium Ions*, G.A. Olah, P.v.R. Schleyer (eds.), Wiley-Interscience, New York, 1970, vol. 2, chpt 20, p. 837; G.A. Olah, R.H. Schlosberg, R.D. Porter, Y.K. Mo, D.P. Kelly, G.D. Mateescu, *J. Am. Chem. Soc.*, **1972**, *94*, 2034.



16. G.A. Olah, J. Lukas, *J. Am. Chem. Soc.*, **1968**, *90*, 993.
17. R.J. Gillespie, *J. Chem. Educ.*, **1963**, *40*, 295 and *J. Chem. Educ.*, **1970**, *47*, 18.
18. G.A. Olah, A. Commeryas, J. DeMember, J.L. Bribes, *J. Am. Chem. Soc.*, **1971**, *93*, 459
19. P.D. Bartlett, L.H. Knox, *J. Am. Chem. Soc.*, **1939**, *61*, 3184; T.H. Lowry, K.S. Richardson, *Mechanism and Theory in Organic Chemistry*, 2nd ed., Harper and Row, New York, 1981, p. 357-60.
20. G.A. Olah, A.M. White, *J. Am. Chem. Soc.*, **1969**, *91*, 5801.
21. A.H. Gomes de Mesquita, C.H. MacGillavry, K. Eriks, *Acta Cryst.*, **1965**, *18*, 437.
22. S. Hollenstein, T. Laube, *J. Am. Chem. Soc.*, **1993**, *115*, 7240.
23. G.A. Olah, A.M. White, *J. Am. Chem. Soc.*, **1968**, *90*, 1884.
24. L.A. Paquette, M.K. Scott, *J. Am. Chem. Soc.*, **1972**, *94*, 6760; A. Streitwieser, Jr., *Solvolytic Displacement Reactions*, McGraw-Hill, New York, 1962, p. 102.
25. G.A. Olah, J.S. Staral, G. Asencio, G. Liang, D.A. Forsyth, G.D. Mateescu, *J. Am. Chem. Soc.*, **1978**, *100*, 6299.
26. G.A. Olah, P.W. Westerman, J. Nishimura, *J. Am. Chem. Soc.*, **1974**, *96*, 3548.
27. G.A. Olah, R.J. Spear, *J. Am. Chem. Soc.*, **1975**, *97*, 1539.
28. C.U. Pittman, Jr., G.A. Olah, *J. Am. Chem. Soc.*, **1965**, *87*, 2998, 5123; G.A. Olah, D.P. Kelly, C.L. Jeuell, R.D. Porter, *J. Am. Chem. Soc.*, **1970**, *92*, 2544.
29. D.S. Kabakoff, E. Namanworth, *J. Am. Chem. Soc.*, **1970**, *92*, 3234.
30. a) R.F. Childs, R. Faggiani, C.J.L. Lock, M. Mahendran, S.D. Zweep, *J. Am. Chem. Soc.*, **1986**, *108*, 1692; b) R.F. Childs, M.D. Kostyk, C.J.L. Lock, M. Mahendran, *J.*

- Am. Chem. Soc.*, 1990, 112, 8912; c) S.K. Chadda, R.F. Childs, R. Faggioli, C.J.L. Lock, *J. Am. Chem. Soc.*, 1986, 108, 1694; d) R.F. Childs, M.D. Kostyk, C.J.L. Lock, M. Mahendran, *Can. J. Chem.*, 1991, 69, 2024; e) R.F. Childs, R.M. Orgias, C.J.L. Lock, M. Mahendran, *Can. J. Chem.*, 1993, 71, 836; f) R.F. Childs, G.J. Kang, T.A. Wark, C.S. Frampton, *Can. J. Chem.*, 1994, 72, 2084; g) R.F. Childs, C.S. Frampton, G.J. Kang, T.A. Wark, *J. Am. Chem. Soc.*, 1994, 116, 8499.
31. a) T. Laube, *J. Am. Chem. Soc.*, 1993, 115, 7240; b) T. Laube, *Angew. Chem. Int. Ed. Engl.*, 1987, 26, 560; c) T. Laube, C. Lohse, *J. Am. Chem. Soc.*, 1994, 116, 9001; d) T. Laube, *Angew. Chem. Int. Ed. Engl.*, 1986, 25, 349; e) T. Laube, G.A. Olah, R. Bau, *J. Am. Chem. Soc.*, 1997, 119, 3087.
32. V.G. Shubin, *Top. Curr. Chem.*, 1984, 116/117, 267; J. March, *Advanced Organic Chemistry: Reactions, Mechanisms, and Structure*, 4th ed., Wiley, Toronto, 1992, p. 1052-62.
33. R.B. Woodward, R. Hoffmann, *The Conservation of Orbital Symmetry*, Academic Press, New York, 1970, p. 114; F.A. Carey, R.J. Sundberg, *Advanced Organic Chemistry*, Plenum Press, New York, 1990, part A, p. 609; T.H. Lowry, K.S. Richardson, *Mechanism and Theory in Organic Chemistry*, Harper & Row, New York, 1981, 2nd ed., p. 764, 868.
34. R.F. Childs, S. Winstein, *J. Am. Chem. Soc.*, 1974, 96, 6409.
35. H.R. Ward, P.D. Sherman, *J. Am. Chem. Soc.*, 1968, 90, 3812; J.P. Bégué, D. Bonnet-Delpon, *Org. Magn. Reson.*, 1980, 14, 349.
36. J. March, *Advanced Organic Chemistry: Reactions, Mechanisms, and Structure*,

- 4th ed., Wiley, Toronto, 1992, p.760.
37. H.C. Brown, M. Rei, *J. Am. Chem. Soc.*, **1964**, *86*, 5008
  38. T.H. Lowry, K.S. Richardson, *Mechanism and Theory in Organic Chemistry*, Harper & Row, New York, 1981, 2nd ed., p. 359; R.C. Bingham, P.v.R. Schleyer, *J. Am. Chem. Soc.*, **1971**, *93*, 3189.
  39. F.A. Carey, R.J. Sundberg, *Advanced Organic Chemistry*, Plenum Press, New York, 1990, part A, p. 272.
  40. D.H. Aue, M.T. Bowers in *Gas Phase Ion Chemistry*, M.T. Bowers (ed.), Academic Press, New York, 1979, vol. 2, p. 1; M.M. Bursey, F.W. McLafferty in *Carbonium Ions*, G.A. Olah, P.v.R Schleyer (eds.), Wiley, Toronto, 1968, vol. 1, p. 257.
  41. J.C. Schultz, F.A. Houle, J.L. Beauchamp, *J. Am. Chem. Soc.*, **1984**, *106*, 3917; F.P. Lossing, J.L. Holmes, *J. Am. Chem. Soc.*, **1984**, *106*, 6917.
  42. a) E.M. Arnett, T.C. Hofelich, *J. Am. Chem. Soc.*, **1983**, *105*, 2889; b) E.M. Arnett, N.J. Pienta, *J. Am. Chem. Soc.*, **1980**, *102*, 3329; c) E.M. Arnett, C. Petro, *J. Am. Chem. Soc.*, **1978**, *100*, 5408.
  43. J.W. Larsen, S. Ewing, *J. Am. Chem. Soc.*, **1971**, *93*, 5107; J.W. Larsen, S. Ewing, M. Wynn, *Tetrahed. Lett.*, **1970**, 539.
  44. E.W. Bittner, E.M. Arnett, M. Saunders, *J. Am. Chem. Soc.*, **1976**, *98*, 3734.
  45. F.P. Lossing, G.P. Semeluk, *Can. J. Chem.*, **1970**, *48*, 955; J.F. Wolf, R.H. Staley, I. Koppel, M. Taagepera, R.T. McIver, Jr., J.L. Beauchamp, R.W. Taft, *J. Am. Chem. Soc.*, **1977**, *99*, 5417; A. Goren, B. Munson, *J. Phys. Chem.*, **1976**, *80*, 2848.
  46. T.T. Tidwell in *The Chemistry of the Cyclopropyl Group*, Z. Rappoport (ed.),

- Wiley, Toronto, 1987, vol. 1, chpt. 10, p. 565.
47. a) E.M. Arnett, R.P. Quirk, J.W. Larsen, *J. Am. Chem. Soc.*, **1970**, *92*, 3977; b) R.F. Childs, D.L. Mulholland, A. Varadarajan, S. Yeroushalmi, *J. Org. Chem.*, **1983**, *48*, 1431; c) R.F. Childs, D.L. Mulholland, *J. Am. Chem. Soc.*, **1983**, *105*, 96.
48. J.L. McNaughton, C.T. Mortimer, *Int. Rev. Sci. Phys. Chem.*, **1975**, *10*, 1; H.K. Cammenga, M. Epple, *Angew. Chem. Int. Ed. Engl.*, **1995**, *34*, 1171.
49. D.S. Kabakoff, J.-C.G. Bünzli, J.F.M. Oth, W.B. Hammond, J.A. Berson, *J. Am. Chem. Soc.*, **1975**, *97*, 1510.
50. J.F.M. Oth, *Rec. Trav. Chim.*, **1968**, *87*, 1185; W. Adam, J.C. Chang, *Int. J. Chem. Kinet.*, **1969**, *1*, 487.
51. M. Dessolin, M. Golfier, A. Gonthier-Vassal, H. Szwarc, *Nouv. J. Chim.*, **1986**, *10*, 753.
52. D.H. Lemal, L.H. Dunlap, Jr., *J. Am. Chem. Soc.*, **1972**, *94*, 6562.
53. C. Bastianelli, V. Caia, G. Cum, R. Gallo, V. Mancini, *J. Chem. Soc. Perkin Trans. 2*, **1991**, 679.
54. J.F.M. Oth, J.-C. Bünzli, Y.J. Zelicourt, *Helv. Chim. Acta*, **1974**, *57*, 2276; K. Kusuda, R. West, V.N.M. Rao, *J. Am. Chem. Soc.*, **1971**, *93*, 3627; J.M. McBride, P.M. Keehn, H.H. Wasserman, *Tetrahed. Lett.*, **1969**, 4147.
55. H. Dreeskamp, S.M. Sarge, W. Tachtermann, *Tetrahedron*, **1995**, *51*, 3137.
56. P. Camps, M. Font-Bardia, F. Perez, L. Sola, X. Solans, S. Vazquez, *Tetrahed. Lett.*, **1996**, *37*, 8601.

## Chapter 2: Methyl Migrations in Protonated Phenols and Related Carbocations

### 2.1 Introduction

Dissolution of methyl-substituted phenols in superacids usually produces hydroxy-substituted cyclohexadienyl cations, the result of protonation at C4.[1] The same type of ion is obtained by O-protonation of cyclohexa-2,5-dienones (Figure 2.1).[2] Cyclohexenones and cyclopentenones yield the closely related cycloalkenyl ions when protonated. Cyclohexadienyl (or arenium) ions are well known[3] and the charge distribution in these and the related allyl ions is well understood (Figure 2.2). Resonance and molecular orbital descriptions[4], as well as experimental measures[5] indicate that the greatest charge is found at C1, C3 and C5 of the cyclohexadienyl cation and C1 and C3 of the cycloalkenyl cation. Thus, the ions which bear electron donors at C1 and C3 (and C5 in the cyclohexadienyl ions) are the most stable. If an energetically accessible pathway exists, isomerization would be expected to maximize the number of substituents on these positions.

Isomerization of carbocations is very common, most often occurring by 1,2-migrations of hydrogen and alkyl groups (Figure 2.3).[6] Indeed, the preparation of carbocations is often accompanied by rapid alkyl and/or hydrogen migrations which transform the initially formed cations into more stable isomers. In the case of protonated

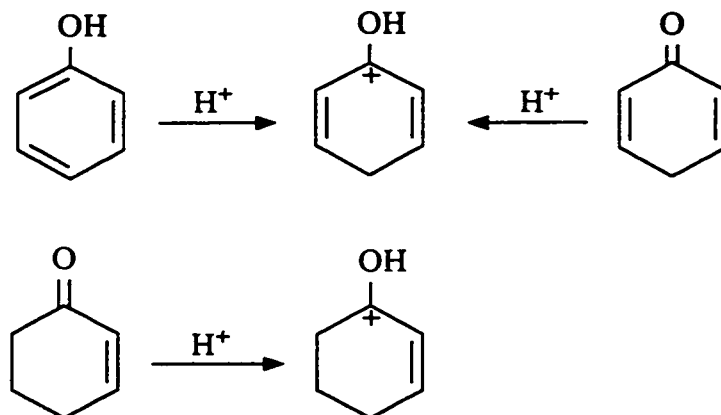


Figure 2.1: Protonation of phenols or cyclohexadienones in superacids produces hydroxy-substituted cyclohexadienyl cations. Cyclohexenone yields the related hydroxycyclohexenyl cation.

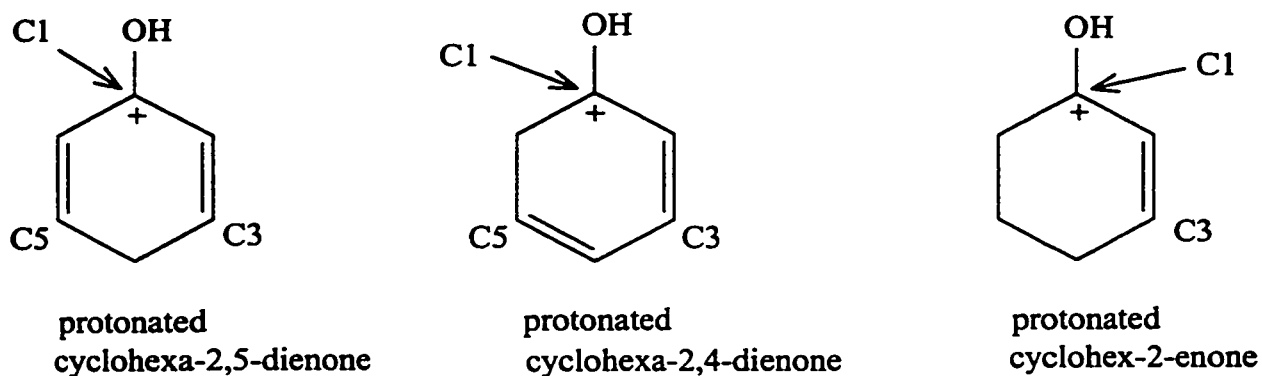


Figure 2.2: C1, C3 and C5 bear the greatest charge in cyclohexadienyl cations; C1 and C3 in the cyclohexenyl cation.

phenols, dienones and enones, the ions formed upon protonation are fairly stable, and isomerizations are more likely to occur at higher temperatures (room temperature or above).

In this work, the isomerizations of several methyl-substituted cyclohexadienyl (and cycloalkenyl) cations have been investigated, and in each case, methyl migrations were involved in the observed isomerization. In most instances, the reactant ions were

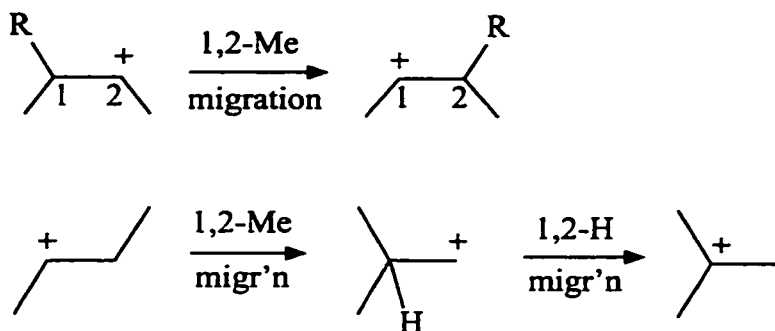


Figure 2.3: 1,2 hydrogen/alkyl migrations are common for cations. The sec-butyl cation isomerizes by a series of 1,2-migrations.

cleanly and quantitatively generated, isomerized by well known pathways, and the isomerizations proceeded cleanly and quantitatively from a single reactant to a single product. Therefore, these reactions were ideal candidates to be studied by differential scanning calorimetry (DSC).

Since little is known about the determination of thermochemical data for carbocation isomerizations by DSC, it was necessary to demonstrate that DSC can provide reliable and meaningful results. Towards this end, a number of control experiments were conducted, and the results of these experiments are presented in this chapter.

The heats of isomerization measured by DSC provides quantitative information about the effect of substituents on the stability of the ions. This information is essential for interpreting the effect of substituents on the stability of carbocations. The values determined in this chapter are particularly helpful in the analysis of the substituent effects upon the isomerization of 2-hydroxybicyclo[3.1.0]hex-3-en-2-yl cations to

hydroxycyclohexadienyl cations (Figure 2.4), the subject of chapter 3.

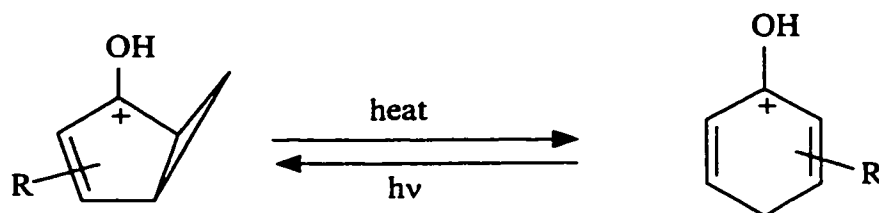


Figure 2.4: Protonated bicyclo[3.1.0]hex-3-en-ones isomerize to protonated phenols.

## 2.2 Experimental

$^1\text{H}$  NMR spectra were measured with Bruker AM200 (200 MHz) or Varian EM390 (90 MHz) spectrometers and chemical shifts are reported as  $\delta$  in ppm relative to tetramethylsilane and coupling constants in Hz. Triflic acid (Aldrich) was used as received. Compounds **2**, **4**, **6**, **9**, **11**, **14-18** were commercially available (Aldrich). Compounds **1** and **3** had been prepared in this laboratory previously.[7] Compounds **8**,**[8]** **10**,**[9]** and **12** [10] were prepared by procedures found in the literature. Compound **5** was prepared from **4** by isomerization in triflic acid.

*4,4-Dimethylcyclohexa-2,5-dienone*, **8** - Prepared by the procedure found in the literature.[8] **8** was obtained as a clear, colourless oil. Yield: 1.81 g (50%). NMR ( $\text{CCl}_4$ ): 1.29 (s, 6H, 4,4-( $\text{CH}_3$ )<sub>2</sub>), 6.05 (d(11), 2H, 2-H and 6-H), 6.75 (d(11), 2H, 3-H and 5-H).



*6,6-Dimethylcyclohexa-2,4-dienone, 10* - Prepared in three steps as described in the literature.[9] 6,6-Dimethylfulvene was obtained as an orange oil which solidified upon standing. NMR (CCl<sub>4</sub>): 2.15 (s, 6H, 6,6 -(CH<sub>3</sub>)<sub>2</sub>), 6.33 (s, 4H, =CH). 6,6-Dimethylfulvene-5,6-epoxide dimer was obtained as a white, crystalline solid. 6,6-Dimethylcyclohexa-2,4-dienone, **10**, was obtained as a yellow oil. NMR (CCl<sub>4</sub>): 1.15 (s, 6H, 6,6 -(CH<sub>3</sub>)<sub>2</sub>), 5.95 (d(10), 1H, 2-H), 6.05-6.35 (m, 0 2H, 4-H and 5-H), 6.95 (ddd(10, 6, 2), 1H, 3-H).

*2,3,4,5,6,6-Hexamethylcyclohexa-2,4-dienone, 12*

Prepared by the literature procedure.[10] **12** was a yellow oil which solidified upon storage in a refrigerator. GC analysis showed that **12** contained 1% of hexamethylbenzene. NMR (CCl<sub>4</sub>): 1.11 (s, 6H, 6,6-(CH<sub>3</sub>)<sub>2</sub>), 1.84 (bs, 9H, 2-CH<sub>3</sub>, 4-CH<sub>3</sub> and 5-CH<sub>3</sub>), 2.03 (s, 3H, 3-CH<sub>3</sub>).

*3,4-Dimethylcyclohex-2-enone, 5* - A mixture of 240 mg of 4,4-dimethylcyclohex-2-enone, **4**, and 1.5 mL of triflic acid was heated at 110 °C for 100 min, at which point <sup>1</sup>H NMR revealed that none of the starting material remained. The solution was cooled and then poured onto an ice/K<sub>2</sub>CO<sub>3</sub> slurry. Following extraction of the aqueous layer with ether, the organic extract was washed once with water and then dried over Na<sub>2</sub>SO<sub>4</sub>. Following solvent removal and distillation in a Kugelrohr apparatus (ca. 10 torr), a very pale yellow oil was obtained. Yield: 180 mg (75%). NMR (CCl<sub>4</sub>): 1.19 (d(7.1), 3H, 4-CH<sub>3</sub>), 1.65-2.55 (m, 5H, 4-CH, 5-CH<sub>2</sub> and 6-CH<sub>2</sub>), 1.93 (dd(1.2, 0.8), 3H, 3-CH<sub>3</sub>), 5.70

(q(1.2), 1H, 2-H). IR (neat,  $\text{cm}^{-1}$ ): 860 (m), 1624 (m), 1673 (s). MS (EI, m/z): 124 ( $\text{M}^+$ ), 109 ( $\text{M}^+ - \text{CH}_3$ ), 96 ( $\text{M}^+ - \text{CO}$ ), 81 ( $\text{M}^+ - \text{CO} - \text{CH}_3$ ).

*Protonation* - Samples for spectroscopic analysis were protonated by adding cooled triflic acid ( $\leq 0^\circ\text{C}$ ) to the phenols and ketones (15-30 mg) in medium wall NMR tubes cooled to ca.  $-60^\circ\text{C}$  (dry ice) or  $0^\circ\text{C}$  (ice bath). Dissolution occurred as the sample warmed to room temperature and the NMR tube was shaken.  $(\text{CH}_3)_4\text{N}^+ \text{BF}_4^-$  was added to the solutions as a chemical shift reference ( $\delta = 3.10$  ppm).

*Kinetic Measurements* - Measurement of isomerization rate-constants were conducted by heating samples in a constant temperature bath. For accurate rate determination, the constant temperature bath consisted of a solvent refluxing in a 3-necked flask equipped with a condenser and a thermometer (to continuously monitor the temperature). Protonated samples as triflic acid solutions were placed in NMR tubes and immersed in the refluxing solvent (eg. water at  $100^\circ\text{C}$ ). The tubes were removed at regular intervals, rapidly cooled in a water or ice bath, and the extent of isomerization was determined by  $^1\text{H}$  NMR. In some cases, rate estimates were obtained by heating in a steam bath ( $100^\circ\text{C}$ ) or oil bath.

*Heats of Isomerization* - Heats of isomerization were determined with a SETARAM DSC 111 differential scanning calorimetry (DSC). Stainless steel cells (approx. volume =  $150\ \mu\text{L}$ ) which could be sealed by compressing an aluminum O-ring into the gap between the

conical lid and the cell wall were used to hold the samples. Accurately weighed amounts (5-25 mg) of the unprotonated sample were placed into the steel cell, and then the cell was cooled to ca.  $-60^{\circ}\text{C}$  in an aluminum block resting in dry-ice. Triflic acid cooled to  $\leq 0^{\circ}\text{C}$  was added to the cell, and then the cell was sealed. The cell was then allowed to warm to room temperature (or lower for less stable samples) with vigorous shaking to insure proper mixing.

The block of the DSC was cooled to a temperature at which isomerization did not occur and then the sample cell and a reference cell (filled with triflic acid or empty) were placed inside the block. The cells were allowed to equilibrate before the block was heated at  $1^{\circ}\text{C}/\text{min}$  to a temperature at which isomerization was complete.

The DSC was calibrated by comparing the measured heats of melting/fusion of naphthalene, acetanilide, benzoic acid and indium standards with values found in the literature.[12]

#### *Catalyzed Isomerization of 4,4-Dimethylcyclohexa-2,5-dienone, 8 -*

4,4-Dimethylcyclohexadienone and 1.39 wt% (0.112 M) triflic acid/nitrobenzene were placed in an NMR tube for spectroscopic or kinetic studies, or in a DSC cell for measurement of the heat of isomerization.

## 2.3 Results and Discussion

The work described in this chapter focuses on the isomerizations shown in Figures 2.5-2.7, all of which involve methyl migrations. The reactants for each of these isomerizations were either commercially available or they were synthesized by known routes. Compounds **1** and **3** had been prepared in this laboratory previously[7] while **4**, **6**, **9**, **14** and **17** were commercially available. Compounds **8**,[8] **10**,[9] and **12**[10] were prepared by procedures found in the literature (Figures 2.8-2.10). In each case the product of synthesis had spectroscopic data consistent with the assigned structure and with data found in the literature.[8-10]

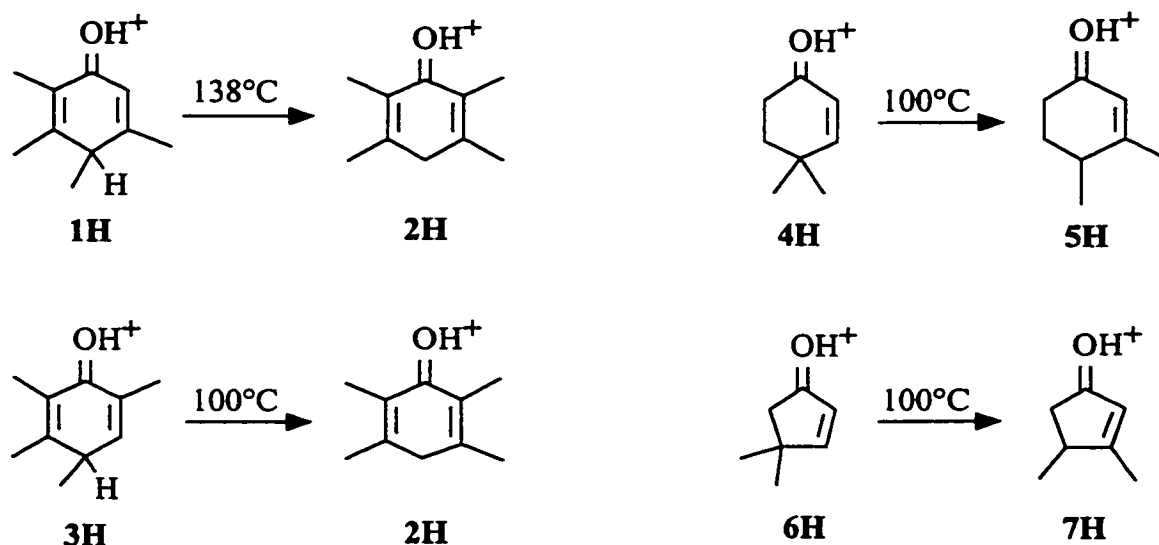


Figure 2.5: Isomerizations of cleanly protonated ions resulting in methyl migration only.

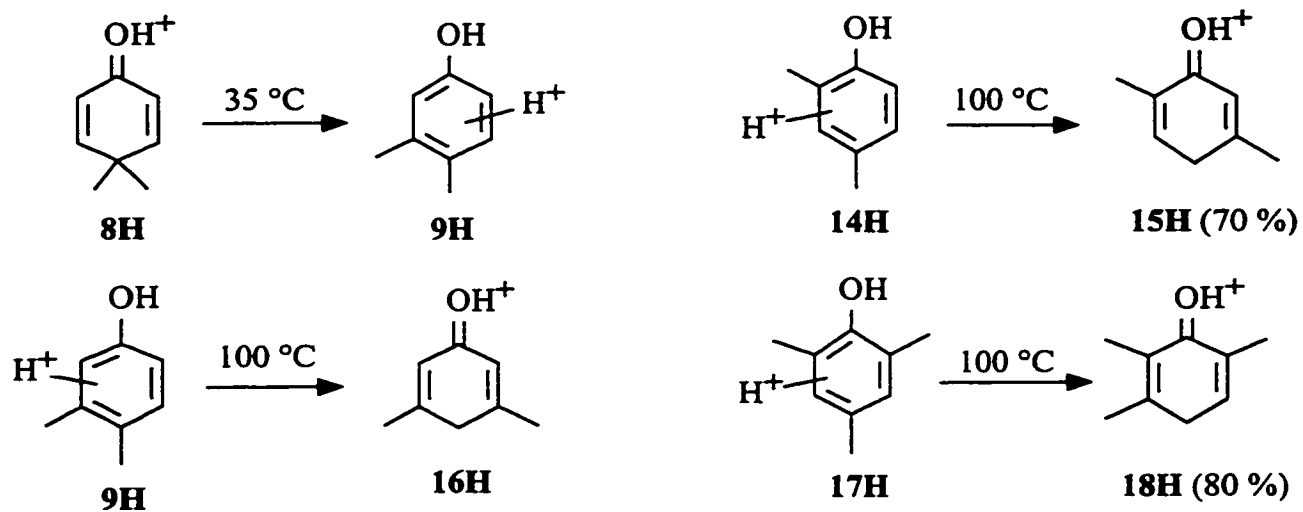


Figure 2.6: Isomerizations in which either the reactant or product is a mixture of protonated species.

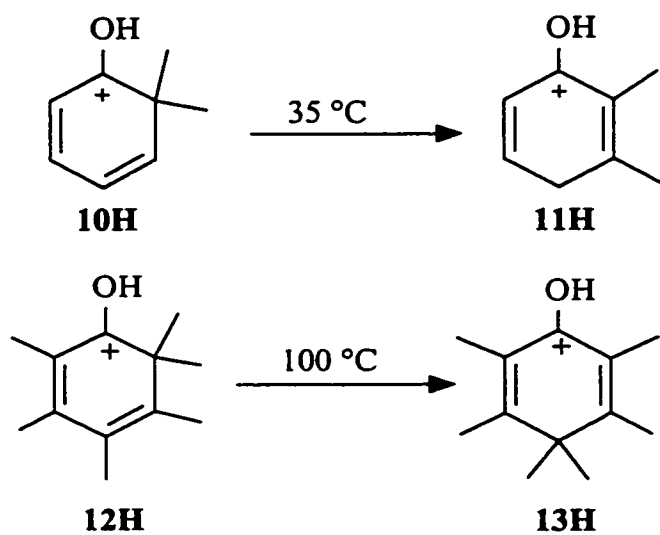


Figure 2.7: Isomerizations involving methyl migrations in which the hydroxy group is repositioned on the  $\pi$ -system.

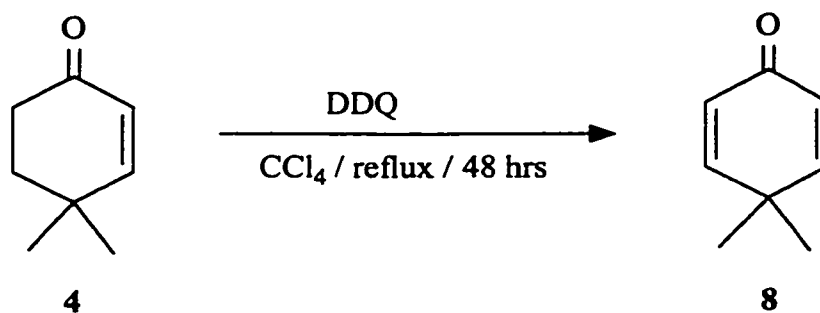


Figure 2.8: Dehydrogenation of 4,4-dimethylcyclohex-2-enone with DDQ yields 4,4-dimethylcyclohexa-2,5-dienone.

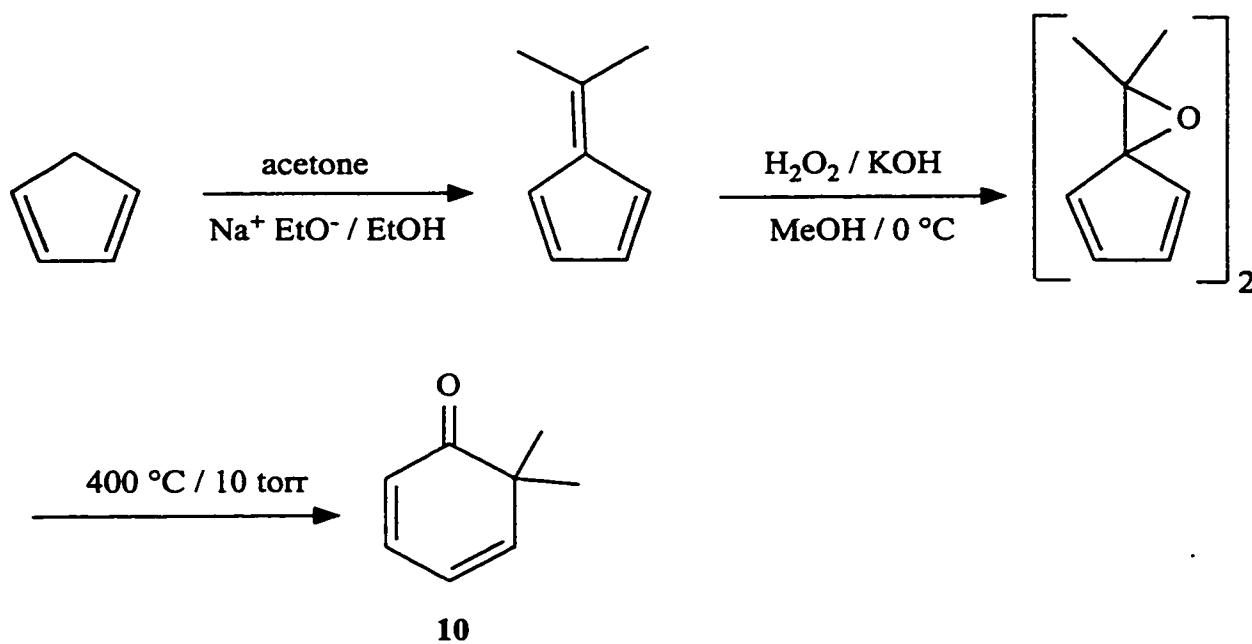


Figure 2.9: Preparation of 6,6-dimethylcyclohexa-2,5-dienone, 10.

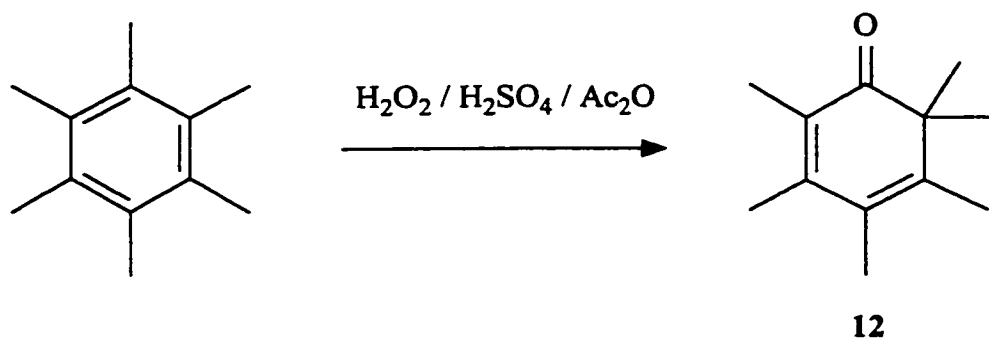


Figure 2.10: Preparation of hexamethylcyclohexa-2,4-dienone, 12.

### 2.3.1 Protonation

Protonation of phenols **1** and **3**, and ketones **4**, **6**, **8**, **10** and **12** in triflic acid resulted, in each case, in complete protonation to yield a single carbocation (Figure 2.11).

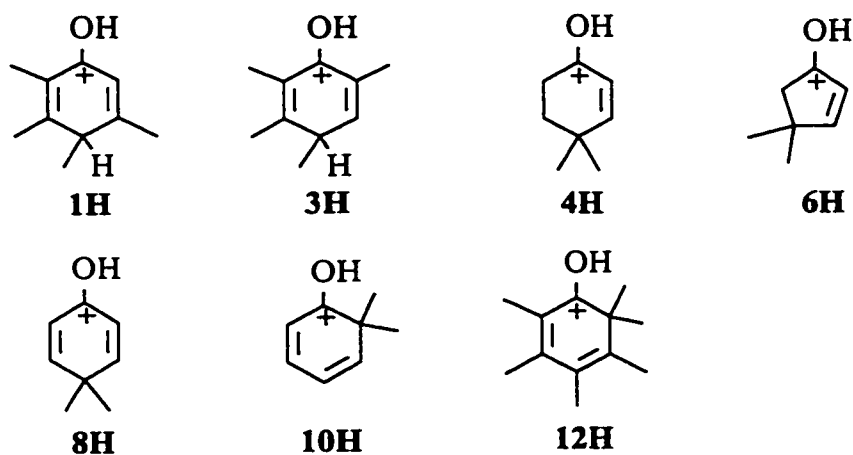


Figure 2.11: Cations that are cleanly formed in triflic acid.

The  $^1\text{H}$  NMR spectra (Table 2.1) of these hydroxy-substituted cyclohexadienyl and cycloalkenyl cations agreed well with previously published data for these or related ions

Table 2.1: <sup>1</sup>H NMR data for carbocations in triflic acid.<sup>a</sup>

cmpd	chemical shift (δ, ppm)				
	2	3	4	5	6
<b>1H</b>	2.10 s	2.41 s	1.53 d(7.5), 3.62 q(8)	2.41 s	6.87 s
<b>2H</b>	2.14 s	2.39 s	4.00 s	2.39 s	2.14 s
<b>3H</b>	2.17 s	2.46 s	1.55 s, <sup>b</sup>	8 bs	2.20 s
<b>4H</b>	6.71 d(10)	8.23 d(10)	1.28 s	2.08 t(7)	3.18 t(7)
<b>5H</b>	6.71 s	2.45 s	1.31 d(7.5), 3.02 m	2.07 m	3.02 m
<b>6H</b>	6.80 d(5.5)	8.92 d(5.5)	1.42 s	3.14 s	--
<b>7H</b>	6.75 s	2.58 s	1.32 d(7.5), 3.34 m	2.93 m, 3.34 m	--
<b>8H</b>	7.10 d(10)	8.35 d(10)	1.47 s	8.35 d(10)	7.10 d(10)
<b>10H</b>	7.1 m	8.58 t(7.5)	7.1 m	7.60 bd(9)	1.58 s
<b>11H</b>	2.16 s	2.47 s	4.07 bs	8.20 bd(8)	7.19 bd(8)
<b>12H</b>	2.16 s	2.59 s	2.16s	2.27 s	1.50 s
<b>13H</b>	2.16 s	2.40 s	1.40 s	2.40 s	2.16 s
<b>15H</b>	2.21 s	8.05 bs	4.03 bs	2.53 s	7.11 bs
<b>16H</b>	6.95 s	2.45 s	3.96 bs	2.45 s	6.95 s
<b>18H</b>	2.18 s	2.47 s	4.05 bs	8.03 bs	2.23 s

a) CF<sub>3</sub>SO<sub>3</sub>H at room temperature; relative to Me<sub>4</sub>N<sup>+</sup> BF<sub>4</sub><sup>-</sup> at 3.10 ppm; s = singlet, d = doublet, t = triplet, q = quartet, b = broad; coupling constants (Hz) are shown in brackets.  
 b) H4 not detected at room temperature.

in a variety of superacid media.[1,2,13,14] Ion **6H** has not been reported previously. The <sup>1</sup>H NMR spectrum for this ion is consistent with the assigned structure and is similar to the spectra of related ions found in Table 2.1 or the literature.[14] The smaller H2-H3



coupling constant observed for **6H** (5.5 Hz) compared with **4H** (10 Hz) is as expected for the smaller ring.[15]

The greater downfield shift of hydrogen or methyl groups located at C3 and C5 of the cyclohexadienyl cations and C3 of the cycloalkenyl cations as compared to those at C2 and C4 reveals that the positive charge is concentrated at these positions. This is consistent with the resonance picture of these ions (Figure 2.2).

In the case of phenols **9**, **14** and **17** which bear methyl substituents at the 4-position, broad spectra were observed (Table 2.2) indicative of exchange between more than one protonated species (Figure 2.12). Previous studies of 4-methyl substituted phenols in fluorosulfuric acid at low temperature (i.e. -50 °C) indicate that ortho, para and oxygen-protonated species are produced.[1b, 1d] For instance, Childs and Parrington[1b] found that in fluorosulfuric acid at -50 °C, **14**, was protonated at C6 (47%), oxygen (41%) and C4 (12%) (Figure 2.13). At higher temperatures, rapid interconversion between these ions would lead to broad peaks in the NMR spectrum as observed in triflic acid at room temperature. The formation of cyclohexadienyl cations during the protonation of compounds such as **9**, **14** and **17** explains why ions **9H**, **14H** and **17H** undergo isomerizations similar to those of the cleanly protonated phenols, cyclohexadienones and cycloalkenones shown in Figures 2.5 and 2.7.

Table 2.2:  $^1\text{H}$  NMR data for compounds for which protonation in triflic acid occurs at multiple sites.<sup>a</sup>

cmpd	chemical shift ( $\delta$ , ppm)
<b>9H</b>	2.10 bs, 2.55 s, 7.45 bs
<b>14H</b>	2.22 bs, 7.15 bs
<b>17H</b>	2.07 bs, 2.26 bs

a)  $\text{CF}_3\text{SO}_3\text{H}$  at room temperature; relative to  $\text{Me}_4\text{N}^+ \text{BF}_4^-$  at 3.10 ppm; s = singlet, b = broad.

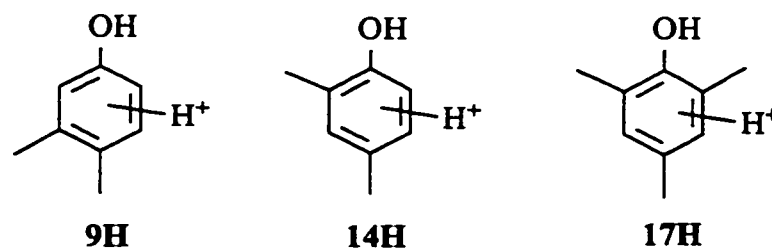


Figure 2.12: Ions consisting of more than one species in triflic acid.

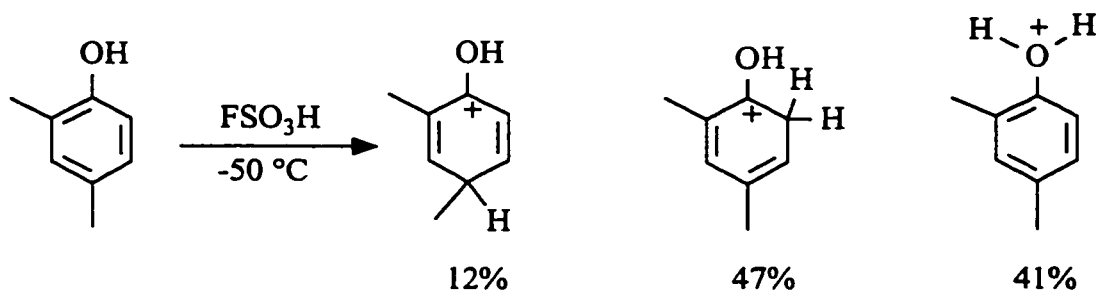


Figure 2.13: 2,4-Dimethylphenol gives three protonated species in fluorosulfuric acid.

### 2.3.2 Isomerizations

Cations **1H**, **3H**, **4H**, **6H**, **8H**, **9H**, **10H**, **12H**, **14H** and **17H** undergo isomerizations at temperatures ranging from room temperature to *ca.* 140°C (Figures 2.5-2.7). In each case isomerization results from a combination of 1,2-methyl and hydrogen migrations about the 5- or 6-membered rings. For example, ion **10H** can be converted to **11H** by two 1,2-migrations (Figure 2.14).

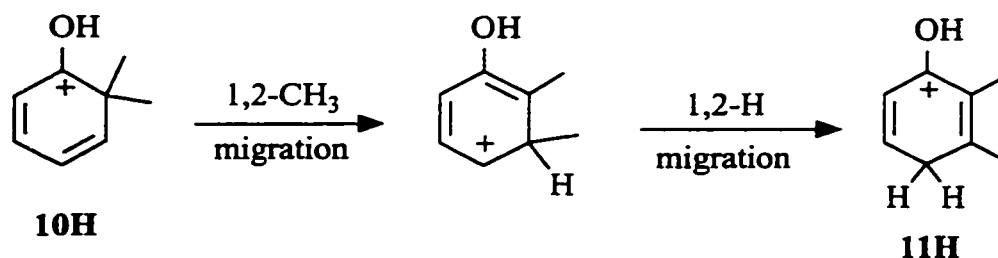


Figure 2.14: Mechanism for isomerization of **10H** to **11H** involves 1,2-methyl and hydrogen migrations. The hydroxy group is located at the centre of the  $\pi$ -system following isomerization.

The products of each isomerization were identified on the basis of their NMR spectra and/or comparison with the NMR spectra of authentic samples. Some of these isomerizations are known, or are closely related to known isomerizations such as the dienone to phenol rearrangements.[16] Thus, the isomerizations of **3H** to **2H** [17,18], **8H** to **9H** [19], **10H** to **11H** [20], **12H** to **13H** [21], **9H** to **16H** [17,22], and **17H** to **18H** [17] have been observed previously. In this work it was found that **14H** produced mainly **15H**, while it was previously reported to isomerize to **16H**. [17] Perhaps under the conditions used the literature, **15H** would have been further isomerized to **16H**.

The other isomerizations (**4H** to **5H**, **6H** to **7H**, and **1H** to **2H**) are closely related to the known reactions, and the observed products are as expected. Isomerization of **4** to **5** is thought to occur during electron impact ionization of **4**,[23a] and a similar reaction has been observed for steroidal derivatives in sulfuric acid.[23b] The known isomerization of 4-methylcyclopentenone to 3-methylcyclopentenone (*p*-toluenesulfonic acid/benzene)[23c] is a direct parallel of the **6H/7H** isomerization. The formation of **5H** from **4H** was confirmed by isolation and identification of 3,4-dimethylcyclohex-2-enone, **5**. The <sup>1</sup>H NMR, IR and mass spectral data for **5** were consistent with data reported in the literature.[11]

Protonated durenol, **2H**, is produced from both protonated prehnitol, **1H**, and protonated isodurenol, **3H**, upon heating at 100 °C. Both isomerizations move a methyl group onto an unsaturated carbon, however in the case of **1H** the methyl moves to the 6-position which does not formally bear charge in the cyclohexadienyl cation. The isomerizations of protonated 4,4-dimethyl-cyclohex-2-enone, **4H**, and protonated 4,4-dimethylcyclopent-2-enone, **6H**, to their 3,4-dimethyl isomers, **5H** and **7H**, respectively, are analogous to that of **3H** to **2H**, as a methyl group moves from an sp<sup>3</sup> centre to the terminal position of the π-system.

Methyl migrations were also observed for ions **8H**, **9H**, **14H** and **17H** (see Figure 2.6). Ion **8H** is composed of a single ion but isomerization results in protonated 3,4-dimethylphenol (**9H**) which consists of several different protonated species. With **9H**, **14H** and **17H**, the reactant consists of several protonated species in equilibrium. In addition, isomerization of **14H** and **17H** gives a mixture of products.

While the isomerizations of **10H** and **12H** also involve methyl migrations (see Figure 2.7), another important change occurs during these reactions. In the product, the hydroxy substituent is located on the central carbon of the  $\pi$ -system rather than a terminal carbon as in the reactant; a linearly-conjugated protonated cyclohexa-2,4-dienone is converted to a cross-conjugated protonated cyclohexa-2,5-dienone. This change does not involve cleavage of the C-O bond but is the result of methyl and hydrogen migrations (Figure 2.14).

Most of the isomerizations produce a single product and do so quantitatively, and thus, these reactions could be of synthetic utility. It is possible that isomerizations of the type studied in this work could be used to convert easily prepared phenols into those that are more difficult to prepare by conventional routes. For instance, durenol (**2**) could be prepared by methylation at the 4-position of 2,3,6-trimethylphenol to give isodurenol (**3**) and then isomerization in triflic acid to yield **2**.

The isomerizations of 4,4-disubstituted cycloalkenones in triflic acid have perhaps much greater potential for synthetic applications since enones are commonly used synthons. In all likelihood, this type of isomerization could be used for a variety of alkyl and aryl substituents, and it could be used with acyclic as well as cyclic enones. 4,4-Disubstituted cycloalkenones are readily prepared[24] and some are commercially available, however, the 3,4-disubstituted isomers can be more difficult to prepare.[11,25] Utilizing isomerizations such as **4H** to **5H** would provide a simple route to the 3,4-disubstituted isomers. For example, in a single unoptimized small-scale (240 mg) synthesis, **5** was isolated in 75% yield following purification.

### 2.3.3 Rates of Isomerization

The rates of isomerization (Table 2.3) were determined by monitoring changes in the  $^1\text{H}$  NMR spectrum with heating time. For instance, during the isomerization of **4H** the two vinyl doublets slowly disappear and are replaced by one singlet (Figure 2.15). Kinetic data for the isomerizations of **4H** and **6H** were measured accurately, but that for the other compounds should be considered as estimates, since the extent of isomerization was measured at a limited number of points during isomerization. In each case the rate data obeyed first-order kinetics. The rates of reaction compared well with values found in the literature for the isomerizations of ions **3H**,[18] **8H**,[19a] **9H**[22] and **12H**,[21a] whether in triflic acid or other superacid media. For instance, in this work isomerization of **3H** to **2H** in triflic acid was estimated to have a barrier of 27.7 kcal/mol at 100 °C compared with 27.1 kcal/mol determined at 60 °C in triflic acid.[18] The activation barrier for isomerization of ion **8H** was found to be 22 kcal/mol ( $\text{CF}_3\text{SO}_3\text{H}$ ,  $\approx 35$  °C) in this work compared with 21.65 kcal/mol (97%  $\text{H}_2\text{SO}_4$ , 25-40 °C).[19a]

In spite of the similarity between ions **4H** and **6H**, the isomerization of **6H** is 100 times slower and has an activation barrier 3.4 kcal/mol higher. This is likely due to the increased rigidity in the cyclopentenone ring. It is necessary to align the C4-methyl bond with the  $\pi$ -system for methyl migration to occur. This is easily accomplished in the cyclohexenone ring, but is more difficult in the less flexible cyclopentenone. The slow rate of isomerization made **6H** unsuitable for DSC. Cell rupture is a risk for DSC scans that end well above the boiling point of triflic acid (162 °C). Sulfuric acid (bp 330 °C) might allow DSC analysis of the **6H** to **7H** isomerization.

Table 2.3: First-order rate constants and activation barriers for isomerizations involving methyl migrations.

reaction	T (°C)	$10^5 k$ (s <sup>-1</sup> )	$\Delta G$ (kcal/mol)
<b>1H → 2H<sup>a</sup></b>	138	29.5	31.0
<b>3H → 2H</b>	100	46	27.7
<b>4H → 5H<sup>b</sup></b>	100	42.1	27.77 ± 0.03
<b>6H → 7H</b>	100	0.420	31.19 ± 0.03
<b>8H → 9H</b>	≈35	134	≈22
<b>10H → 11H</b>	≈35	445	≈21.4
<b>12H → 13H<sup>c</sup></b>	100	≈220	≈24.8
<b>14H → 15H</b>	100	≈10	≈29
<b>9H → 16H</b>	100	≈1	≈30
<b>17H → 18H</b>	100	≥100	≤27

a) At 135°C **2H** and **1H** exist as an equilibrium mixture (**2H:1H** = 93:7,  $\Delta G_0 = -2.11$  kcal/mol).

b)  $\Delta S^\ddagger = -10$  cal mol<sup>-1</sup> K<sup>-1</sup> based on measurements at 60, 100 and 128°C.

c) At 100°C **13H** and **12H** exist in an equilibrium mixture (**13H:12H** = 94.4:5.6,  $\Delta G_0 = -2.09$  kcal/mol).

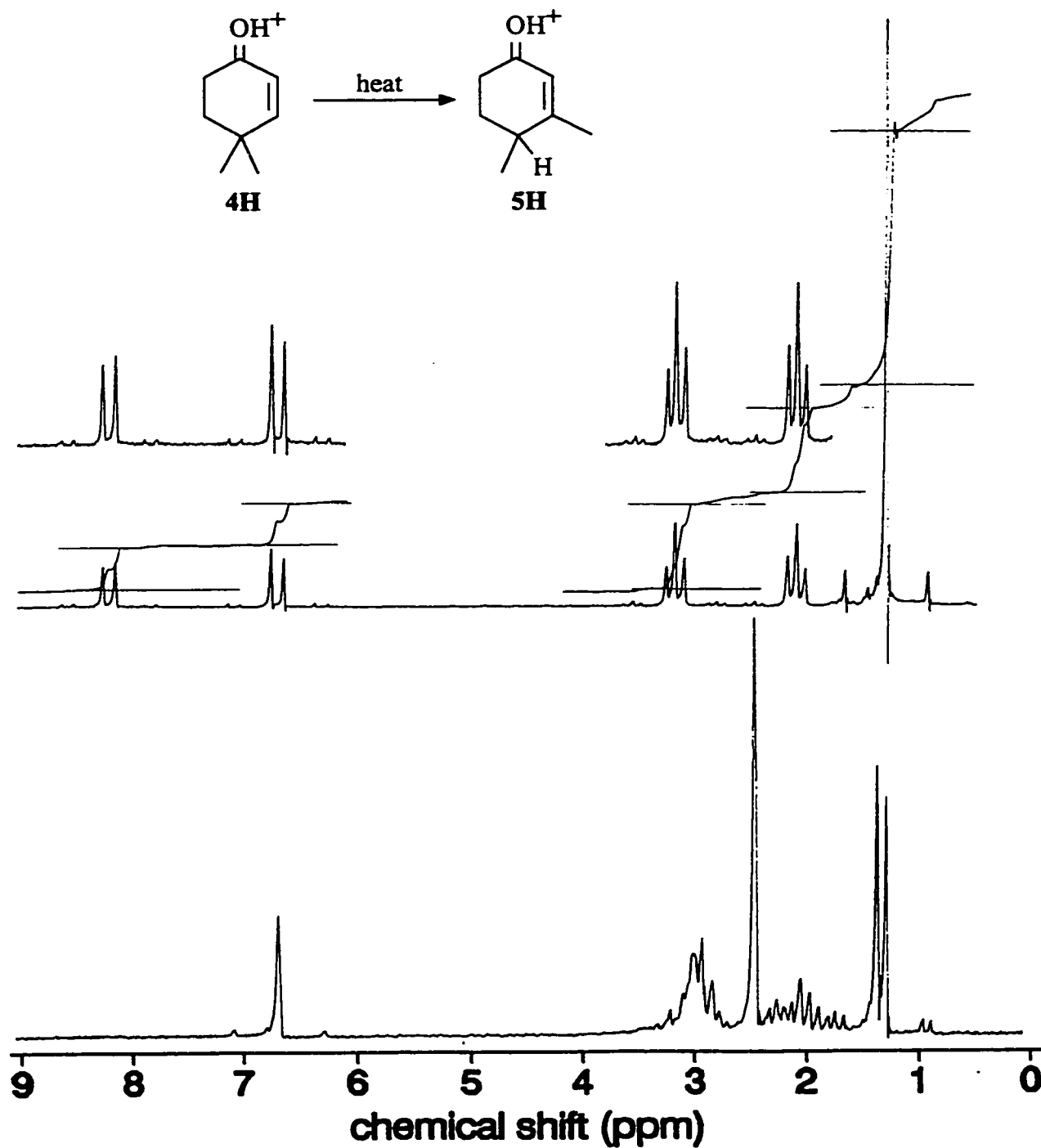


Figure 2.15: <sup>1</sup>H NMR spectrum of protonated 4,4-dimethylcyclohex-2-enone, **4H**, in triflic acid before (top) and after (bottom) isomerization to protonated 3,4-dimethylcyclohex-2-enone, **5H**, by heating at 110 °C for 100 min.



## 2.4 Measurement of Heats of Isomerization by DSC

### 2.4.1 Validation of DSC Technique

Differential scanning calorimetry (DSC) was used to measure the heats of isomerization ( $\Delta H_r$ ) for the reactions presented in the preceding sections. Since DSC has not been used previously to study the thermochemistry of carbocations it was necessary to confirm that this technique can provide accurate and meaningful results. This required that:

- 1) protonation occur to give a single, well characterized carbocation;
- 2) clean and quantitative reaction occur to give a single carbocation product;
- 3) DSC give accurate, reproducible thermochemical results which are consistent with other thermochemical measures.

As presented earlier,  $^1\text{H}$  NMR was used to investigate the protonation of the phenols and ketones which give rise to cations **1H**, **3H**, **4H**, **6H**, **8H-10H**, **12H**, **14H** and **17H** (Figures 2.11-2.12). With **9**, **14** or **17** more than one protonated species was produced. The presence of multiple species in the reactant or product of an isomerization makes it difficult to assign  $\Delta H_r$  to a particular structural change and, thus, cations **9H**, **14H** and **17H** were not suitable for investigation by DSC. Substrates **1**, **3**, **4**, **6**, **8**, **10**, and **12** (see Figure 2.11) were shown to be cleanly and completely protonated in triflic acid.

In order to get good precision in the DSC analysis the concentrations of carbocation need to be higher (0.5-1.5 M) than those typically used in NMR spectroscopic studies (0.1-0.5 M). The  $^1\text{H}$  NMR spectra of several compounds at these

higher concentration levels (1-1.5 M) in triflic acid were measured and, in each case, they very closely matched data found in the literature as illustrated in Table 2.4. Thus, completely protonated species are produced under the conditions used to measure  $\Delta H_R$ .

Table 2.4: Comparison of  $^1\text{H}$  NMR data at concentration used in DSC experiments with literature data.

ion	[ ](M), acid	chemical shift ( $\delta$ , ppm) <sup>a</sup>				
		2	3	4	5	6
<b>3H</b>	1.1, $\text{CF}_3\text{SO}_3\text{H}$	2.21	2.43	1.57 <sup>c</sup>	$\approx 8^f$	2.18
<b>3H<sup>b</sup></b>	$\approx 0.3$ , $\text{CF}_3\text{SO}_3\text{H}$	2.20	2.46	1.53 <sup>c</sup>	$\approx 8^f$	2.17
<b>2H</b>	1.2, $\text{CF}_3\text{SO}_3\text{H}$	2.14	2.38	3.99	2.38	2.14
<b>2H<sup>c</sup></b>	0.4, $\text{FSO}_3\text{H}$	2.20	2.46	4.05	2.46	2.20
<b>12H</b>	1.1, $\text{CF}_3\text{SO}_3\text{H}$	2.16	2.59	2.16	2.27	1.51
<b>12H<sup>d</sup></b>	$\approx 0.3$ , $\text{FSO}_3\text{H}$	2.17	2.62	2.17	2.29	1.52

a) Relative to  $(\text{CH}_3)_4\text{N}^+$  at 3.10 ppm.

b) From B.E. George, Ph.D. Thesis, McMaster University, Hamilton, Ontario, 1987, p. 53.

c) From R.F. Childs, B.D. Parrington, *Can. J. Chem.*, **1974**, *52*, 3303.

d) from R.F. Childs, B. Parrington, *Chem. Comm.*, **1970**, 1581.

e) Signal for H-4 and coupling to 4- $\text{CH}_3$  is not visible at room temperature due to rapid exchange with the solvent.

f) Signal for H-5 is a very broad singlet at room temperature, due to rapid exchange with the solvent.

The isomerizations of **1H**, **3H**, **4H**, **6H**, **8H-10H**, **12H**, **14H** and **17H** were discussed in a previous section. Only the isomerizations of **1H**, **3H**, **4H**, **6H**, **10H** and **12H** were found to proceed cleanly from a single reactant cation to a single product

cation (see Figures 2.5 and 2.7). The isomerizations yielded the product cation quantitatively with the exception of **1H** and **12H** which reach equilibria between reactant and product. In each case, the overall intensity of the  $^1\text{H}$  NMR spectrum was unchanged upon isomerization from reactant to product. The  $^1\text{H}$  NMR spectra measured before and after isomerization of **4H** are shown in Figure 2.15. (Note: the methyl signals are off-scale in Figure 2.15)

The isomerizations of **1H** and **12H** do not proceed completely to product but instead an equilibrium between the reactant and product is established. At 135 °C, **1H** and **2H** exist as 7:93 mixture, while **12H** and **13H** establish a 5.6:94.4 equilibrium at 100 °C. With this information the measured  $\Delta H_{\text{R}}$  values were corrected to give the true enthalpy difference between the product and reactant cations.

The accuracy of the values measured by DSC was ensured in several ways. The heats of fusion/melting were measured for pure samples of benzoic acid, naphthalene, acetanilide and indium and were found to deviate by  $\leq 3\%$  from the expected values.[12] Thus, the DSC instrument was capable of accurately measuring the heat absorbed/released during a thermochemical process.

Heats of isomerization of ions **1H**, **3H**, **4H**, **10H** and **12H** were determined on the basis of 4-7 individual measurements. The results obtained during individual runs on three separate reactants are given in Table 2.5. The  $\Delta H_{\text{R}}$  values are expressed as the mean  $\pm$  the standard deviation and the errors are on the order of 5%. The results show clearly that the DSC technique gives reproducible results for the isomerization of carbocations.

Table 2.5: Heats of isomerization ( $\Delta H_R$ ) measured for isomerizations of **4H**, **3H** and **12H** in triflic acid.

run	Heat of isomerization (kcal/mol)		
	<b>4H - 5H</b>	<b>3H - 2H</b>	<b>12H - 13H<sup>b</sup></b>
1	-4.21 <sup>c</sup>	-3.05	-1.99 <sup>c</sup>
2	-4.31	-3.70	-1.96
3	-4.30	-3.34	-1.81
4	-3.85	-3.43	-1.82
5	-4.20	-3.49	-1.75
6	-3.85	-3.22	--
7	-4.29	--	--
mean	$-4.1 \pm 0.2$	$-3.4 \pm 0.2$	$-1.9 \pm 0.1$

a) Samples are from stock solutions of reactant unless otherwise noted.

b) **13H/12H** = 94.4/5.6 at 100 °C. Used to correct measured values.

c) Individually prepared samples.

Samples for the DSC were prepared in two ways. Individual samples were prepared by mixing known amounts of substrate and triflic acid in a DSC cell at low temperature. In other cases, a stock solution of the reactant carbocation in triflic acid was prepared and then known volumes were transferred to the DSC cell with a micropipettor. Table 2.5 includes two examples in which the samples were individually prepared while all the other entries are for samples from stock carbocation solutions. The  $\Delta H_R$  values obtained by the two preparation techniques are in good agreement with each other.

It is possible that reproducible results might be obtained if isomerization was accompanied by a consistent degree of side reaction or charring in each run. The NMR

controls presented earlier show that this is not the case. NMR samples at the same concentration as the DSC samples were heated until isomerization was complete. The NMR spectra showed no peaks indicative of side reactions and there was no significant darkening of the solution due to charring.

Other thermochemical measures can be used to check the accuracy of the DSC measurements. Several comparisons are presented in the next section and in chapter 3. Overall, the DSC results are consistent with the other measures (principally heats of protonation). Also, the isomerizations of **1H** and **12H** result in an equilibrium mixture of reactant and product cations. The equilibrium ratio allows the free energy difference ( $\Delta G_R$ ) between the pairs of cations to be calculated ( $\Delta G_R = -2.1$  kcal/mol for **1H/2H** and  $-2.1$  kcal/mol for **12H/13H**). For a unimolecular reaction with a minor change in structure, the entropy ( $\Delta S_R$ ) should be small, and  $\Delta G_R \approx \Delta H_R$ . Therefore, the value of  $\Delta G_R$  provides an internal check of  $\Delta H_R$  measured by DSC. In both instances the  $\Delta H_R$  and  $\Delta G_R$  values are similar ( $\Delta G_R = -2.1$  and  $\Delta H_R = -2.18 \pm 0.11$  kcal/mol for **1H/2H**;  $\Delta G_R = -2.1$  and  $\Delta H_R = -1.86 \pm 0.10$  kcal/mol for **10H/12H**). This demonstrates that DSC is an accurate technique for the measurement of heats of isomerization.

#### *2.4.2 Heats of Isomerization*

The heats of isomerization ( $\Delta H_R$ ) of cations **1H**, **3H**, **4H**, **10H** and **12H** are given in Table 2.6. In this section, the chemical significance of these values is discussed. The magnitude of  $\Delta H_R$  is determined by several factors which include changes in bond and strain energies, changes in charge stabilization and changes in solvation. It is hoped that

conclusions may be reached about the effects of substituents on charge stabilization so it is essential that the other factors be kept in mind.

Table 2.6: Heats of reaction for isomerizations involving methyl migrations.

reaction	$-\Delta H_R$ (kcal/mol)	T(peak) <sup>a</sup> (°C)
<b>1H</b> → <b>2H</b> <sup>b</sup>	2.2 ± 0.1	125-195
<b>3H</b> → <b>2H</b>	3.4 ± 0.2	65-130
<b>4H</b> → <b>5H</b>	4.1 ± 0.2	85-150
<b>10H</b> → <b>11H</b>	10.0 ± 0.4	-10-50
<b>12H</b> → <b>13H</b> <sup>c</sup>	1.9 ± 0.1	40-100
<b>8</b> → <b>9</b> <sup>d</sup>	18.7 ± 0.1	50-105

a) temperature range from the beginning to the end of the peak at a scan rate of 1 °/min.

b) At 135°C **2H:1H** = 93:7 ( $\Delta G_0 = -2.11$  kcal/mol). This information was used to correct the measured  $\Delta H$  value.

c) At 100°C **13H:12H** = 94.4:5.6 ( $\Delta G_0 = -2.09$  kcal/mol). This information was used to correct the measured  $\Delta H$  value.

d) catalyzed reaction in 0.11M  $\text{CF}_3\text{SO}_3\text{H}$  in nitrobenzene.

During the isomerizations of **4H** to **5H** and **3H** to **2H**, a methyl group is moved from an  $\text{sp}^3$  carbon onto an unsaturated ( $\text{sp}^2$ ) carbon at the end of the  $\pi$ -system (Figure 2.16). The terminal position on an allyl or pentadienyl cation is a charge-bearing position. Conversely, the isomerization of **1H** to **2H** moves a methyl group onto the  $\pi$ -system at a position which does not formally bear charge in any of the resonance structures of the cyclohexadienyl cation. Thus, it is not surprising that  $\Delta H_R$  is more exothermic for the isomerizations of **3H** and **4H** ( $-3.4 \pm 0.2$  and  $-4.1 \pm 0.2$  kcal/mol, respectively) than for the isomerization of **1H** ( $-2.2 \pm 0.1$  kcal/mol).

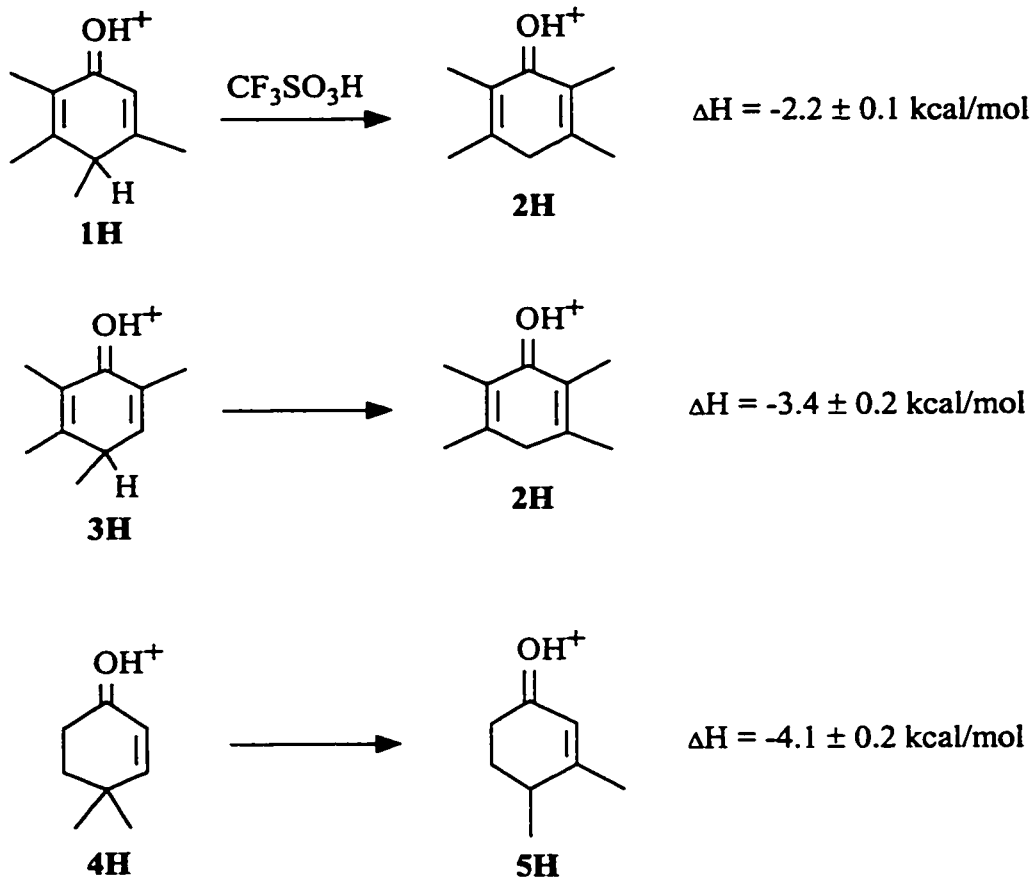


Figure 2.16: Heats of isomerization for reactions which move a methyl group onto the  $\pi$ -system.

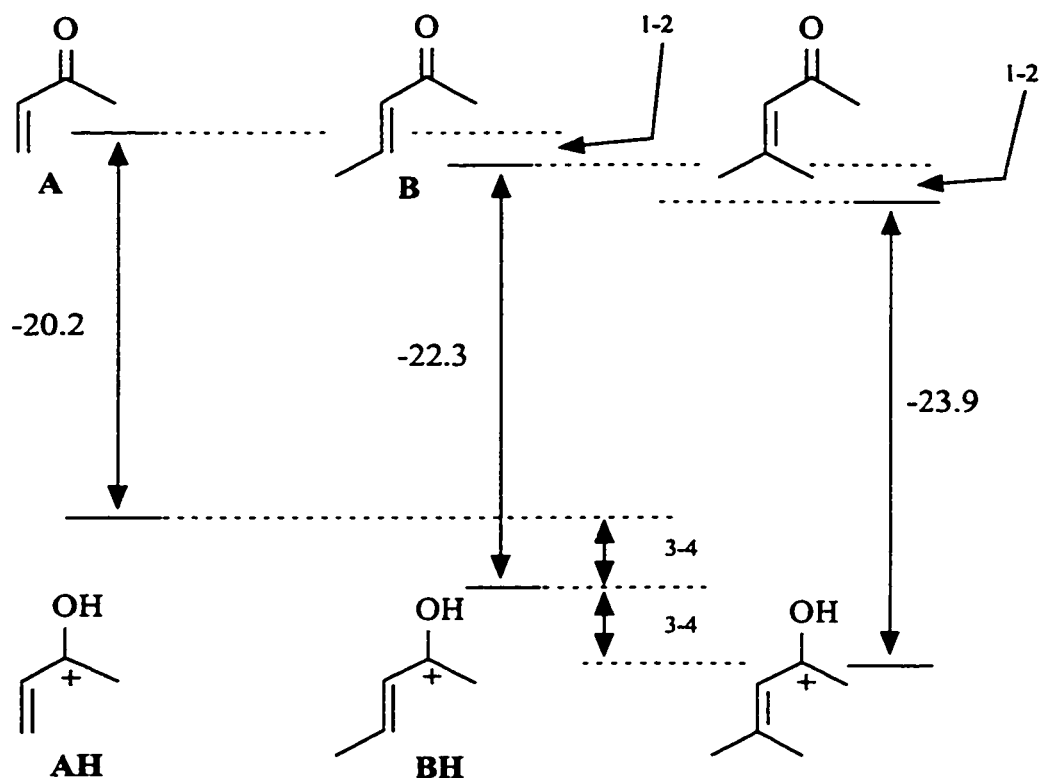
The isomerization of **1H** to **2H** is probably accompanied by a small increase in strain energy as the two gauche interactions (4-methyl with the 3- and 5-methyl groups) in **1H** are replaced by two ortho interactions (6-methyl with 5-methyl and 1-hydroxy) in **2H**. Group additivity tables[26] provide estimates of gauche (0.5 kcal/mol) and ortho interactions (0.6 kcal/mol) in neutral molecules, and so the strain increase would be small, on the order of 0.2 kcal/mol. Even with a small strain correction  $\Delta H_R$  for the **1H/2H** isomerization is only slightly more exothermic than might be expected for hypothetical reaction of a neutral species. Group additivity tables[26] reveal that moving

a methyl group from an  $sp^3$  carbon onto an unsaturated carbon reduces  $\Delta H_f$  by about 1 to 2 kcal/mol for alkenes and phenols. The relatively small effect of methyl migration in the **1H/2H** isomerization is consistent with a substituent which formally can only stabilize the cyclohexadienyl cation by inductive means.

The results shown in Table 2.6 show that  $\beta$ -methyl substitution stabilizes protonated enone **4H** by  $4.1 \pm 0.2$  kcal/mol, and protonated phenol **3H** by  $3.4 \pm 0.2$  kcal/mol. These values can be compared with those found in the literature based on the measurement of heats of protonation ( $\Delta H_p$ ) of enones in fluorosulfuric acid (Figure 2.17). As the number of  $\beta$ -methyl groups is increased the magnitude of  $\Delta H_p$  is also increased.[27] The differences ( $\Delta\Delta H_p$ ) between the heats of protonation give a measure of the added stability that each methyl group affords the cation. The two  $\Delta\Delta H_p$  values ( $-1.6$  and  $-2.1$  kcal/mol) are less than the two values obtained by DSC ( $-3.4$  and  $-4.1$  kcal/mol). However,  $\Delta H_R$  values from DSC measure the enthalpy difference between two isomeric ions, while  $\Delta\Delta H_p$  values depend on the heats of formation ( $\Delta H_f$ ) of four species, two neutral and two protonated ketones. As mentioned above, methyl substitution on the  $\beta$ -position of the  $\alpha,\beta$ -unsaturated ketone will stabilize the neutral species by 1-2 kcal/mol. Correcting for this effect, the  $\Delta\Delta H_p$  values indicate that the protonated enones with a  $\beta$ -CH<sub>3</sub> group are more stable than those without by ca. 3.5 kcal/mol, a value similar to that measured by DSC.

The isomerization of **4H** is more exothermic than that of **3H** by  $0.7 \pm 0.3$  kcal/mol. Ion **3H** spreads charge over a 5-carbon  $\pi$ -system substituted with one OH and three CH<sub>3</sub> groups. Ion **4H** delocalizes charge over a 3-carbon  $\pi$ -system with a single OH





$$\text{CH}_3 \text{ stabilization} = \Delta\Delta H_{\text{tr}} = \Delta H_{\text{tr}}(\text{B}) - \Delta H_{\text{tr}}(\text{A}) = -2.1 \text{ kcal/mol}$$

Figure 2.17: The differences in heats of protonation of the three ketones in  $\text{FSO}_3\text{H}$  give a measure of the stabilization provided by a methyl group. The relative energies of the neutral and protonated analogs are shown.

substituent on the  $\pi$ -system. Thus,  $\Delta H_{\text{R}}$  may be more exothermic for **4H** because there is more charge at C3 (than at C5 in **3H**) and the methyl provides greater stabilization. This is an example of the saturation effect in which a substituent has a greater effect in a less stable system than in a more stable system.[28]

In the isomerizations of **10H** and **12H** (Figure 2.7) the  $\pi$ -system is reorganized such that the hydroxy substituent moves from the end to the centre of the  $\pi$ -system. The driving force for rearranging the  $\pi$ -system such that the hydroxy group is on the

central carbon of the pentadienyl cation becomes clear when one examines the charge distribution in the cyclohexadienyl cation. The resonance or simple MO descriptions of the cyclohexadienyl cation predict the same charge distribution on terminal and central carbons.[4] However, higher order calculations and experimental results reveal that the lowest unoccupied orbital (LUMO) does not have equal sized lobes at the central and terminal positions.[29] The lobe at the central carbon of the cyclohexadienyl cation is larger than that at the terminal positions.

Olah[29a] has described the charge distribution in the cyclohexadienyl cation as 0.3 para, 0.25 ortho and 0.1 meta to proton attachment (Figure 2.18). Brouwer[29b] determined the relative stabilities of a series of di, tri and tetramethyl benzenium ions (cyclohexadienyl ions) and found that methyl substitution at the central carbon of the pentadienyl cation  $\pi$ -system was preferred by about 0.3 kcal/mol over substitution at the terminal position of the  $\pi$ -system, and by about 3.3 kcal/mol over substitution at C2 (the non-charge bearing position on the  $\pi$ -system). Thus, it is not surprising that the isomerizations of **10H** and **12H** place the best electron donor, the hydroxy group, on the central carbon. It is for this same reason that aryl compounds such as phenols are

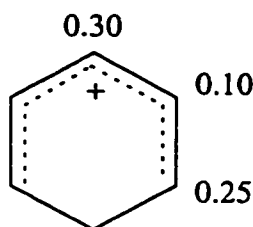


Figure 2.18: Estimated charge density in cyclohexadienyl cation.

preferentially protonated para to the best electron donor.[1,13]

During isomerization of **12H** to **13H** there is no change in the number or type of substituents on the  $\pi$ -system. The only change is that the hydroxy group changes position with one of the methyl groups and moves to the central carbon of the  $\pi$ -system while a methyl group moves to the end of the  $\pi$ -system. As a result of this switching of substituents the cation is stabilized ( $\Delta H_R = -1.9 \pm 0.1$  kcal/mol).

At first glance,  $\Delta H_R$  for the isomerizations of **10H/11H** and **12H/13H** seem remarkably different. However, the isomerization of **10H** involves not only a change in hydroxy position but also moves both methyl groups from  $sp^3$  to  $sp^2$  carbons. As revealed earlier, methyl migration from an  $sp^3$  position to a charge-bearing position was exothermic by ca. 4 kcal/mole, while migration to the 2-position was exothermic by ca. 2 kcal/mole. If these two contributions are subtracted from  $\Delta H_R$  for **10H** then it is possible to estimate  $\Delta H_R$  for repositioning the hydroxy group as  $\Delta H_R(\text{OH terminal} - \text{OH central}) \approx -4$  kcal/mol. The three contributions to  $\Delta H_R$  for **10H** are shown schematically in Figure 2.19.

Thus, the two  $\Delta H_R$  values for repositioning the hydroxy group are  $-1.9 \pm 0.1$  and approximately  $-4$  kcal/mole. While the latter value is an estimate, it is not surprising that this value is higher than the first. The isomerization of **10H** exchanges the position of the hydroxy group with a hydrogen atom, while the isomerization of **12H** switches the hydroxy group with a methyl group. One would expect that replacing a hydrogen atom with a hydroxy group on the most electron-deficient position of the cation would release more energy than replacing a methyl group at the same position. A second factor is also

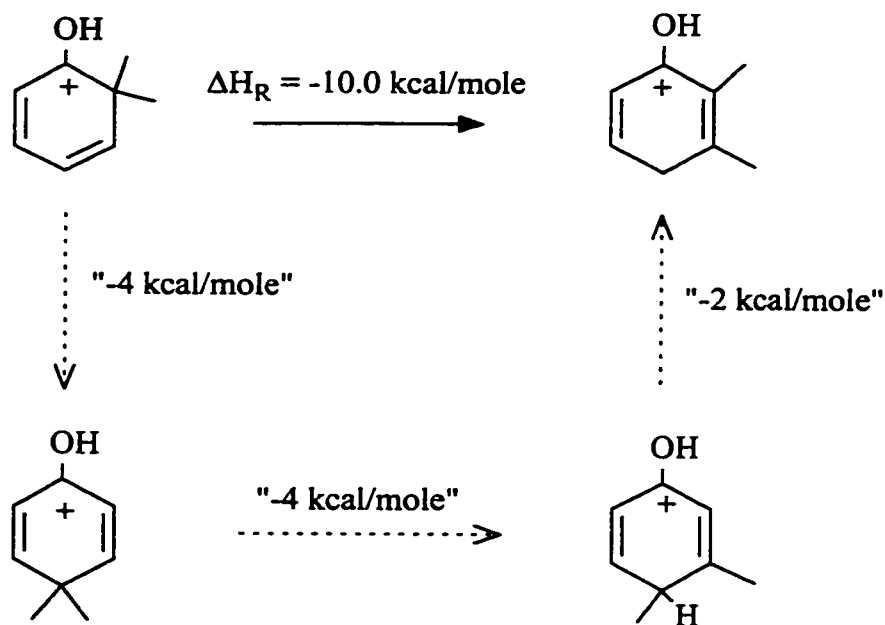


Figure 2.19: Schematic illustration of the contributions to  $\Delta H_R$  for **10H**.

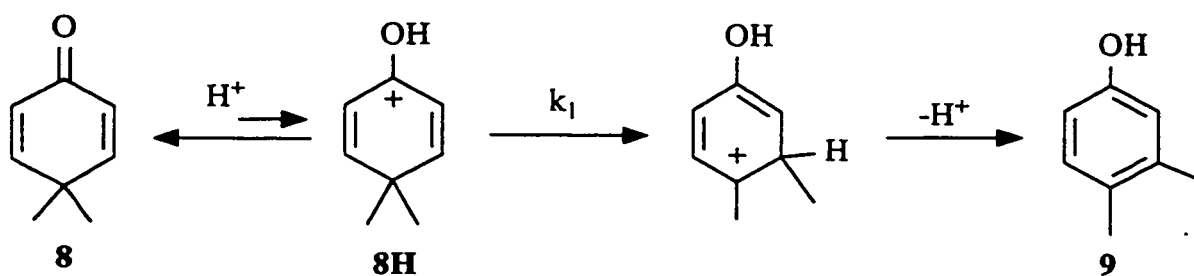
at play. Ion **12H** bears four methyl groups and one hydroxy group on the  $\pi$ -system, while **10H** has only two methyl groups in addition to the hydroxy function. The less exothermic reaction of **12H** may be another example of the saturation effect.[28]

#### 2.4.3 Catalyzed Isomerization: Energy Difference Between Neutral Isomers

In addition to the energy differences between isomeric carbocations, it was desirable to measure the energy difference between neutral isomers. For most, if not all, of the compounds studied, uncatalyzed isomerizations were not feasible because they required prohibitively high temperatures. Thus, it was decided to attempt acid-catalyzed isomerizations. Triflic acid dissolved in nitrobenzene was selected as the solvent because it was a high boiling, stable medium which did not interfere with DSC analysis of the

isomerization.

The catalyzed isomerization of 4,4-dimethylcyclohexa-2,5-dienone, **8**, to 3,4-dimethylphenol, **9**, was investigated (Figure 2.20). Vitullo and Grossman, in a previous study of this reaction, showed that the acid-catalyzed isomerization of **8** to **9** is consistent with the mechanistic scheme shown in Figure 2.20.[19a] For this reaction, the observed rate-constant is predicted to be equal to  $Fk_1$ , where  $F$  is the fraction of reactant that is protonated.  $F$  can be determined from the observed rate-constant, if  $k_1$  is independent of acid strength. In fact, Vitullo and Grossman[19a] found that  $k_1$  decreased slightly as the acid strength was lowered, and they proposed that the loss of one solvating water molecule during the rate-determining step accounted for the small decrease. In nitrobenzene, a poorer H-bonding solvent than water, the effect should be diminished. The rate of isomerization of **8** to **9** in 1.39 weight% (0.112 M) triflic acid in nitrobenzene at 65 °C was approximately 250 times slower than had been observed in concentrated



$$k_{\text{observed}} = Fk_1 \quad \text{where } F = \frac{[\mathbf{8H}]}{[\mathbf{8}] + [\mathbf{8H}]}$$

Figure 2.20: Mechanism of the acid catalyzed isomerization of **8** to **9**.

sulfuric acid.[19a] This allows the fraction of protonated dienone, **8H**, in solution to be estimated as 0.4 %, low enough that measurement of the heat released by isomerization will give an accurate measure of the relative energies of the neutral dienone and phenol.

The isomerization of **8** is an example of a dienone to phenol rearrangement and it reveals the energy released by aromatization. The catalyzed isomerization was found to have  $\Delta H_R = -18.7 \pm 0.1$  kcal/mole. The high exothermicity of this reaction points out the great stabilizing effect of aromaticity as it is the principal driving force for this reaction. This value can be compared with an estimate based on the relative energies of **9** and **8**. The measured heat of formation of **9** is -37.4 kcal/mole,[30] while the heat of formation estimated for **8** by the group additivity method[26] is about -20 kcal/mole; a difference of -17.4 kcal/mole. The  $\Delta H_f$  estimated for **8** is somewhat uncertain since several groups present in the molecule are not represented in the tabulated values and contributions for similar groups were used. A semi-empirical calculation found in the literature gives  $\Delta H_f = -18.36$  kcal/mol for the closely related 4,4-dichlorocyclohexa-2,5-dienone.[31]  $\Delta H_f$  for **8** should be almost identical since the  $\text{CCl}_2$  and  $\text{C}(\text{CH}_3)_2$  groups have identical contributions to the  $\Delta H_f$  in the group additivity method. If the  $\Delta H_f$  value for 4,4-dichlorocyclohexa-2,5-dienone is used to predict  $\Delta H_R$  for **8**, a value of -19.0 kcal/mole ( $-37.4 - (-18.36)$ ) is obtained (Figure 2.21), in excellent agreement with the value determined in this work ( $-18.7 \pm 0.1$  kcal/mol). Also shown in Figure 2.21 are the relative contributions to  $\Delta H_R$  of aromatization and moving the methyl groups from  $\text{sp}^3$  to  $\text{sp}^2$  carbons.

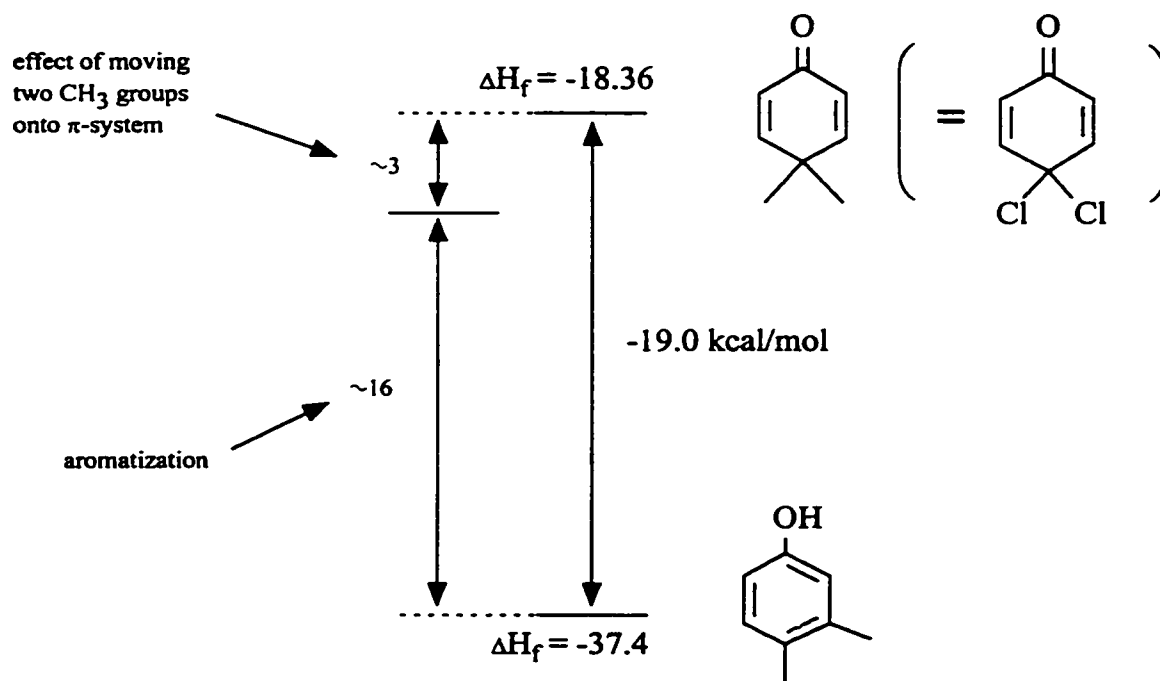


Figure 2.21: Estimate of  $\Delta H_R$  for isomerization of 8 to 9 based on  $\Delta H_f$  values measured for 9 and calculated for 8. The relative contributions of aromatization and moving the methyl groups onto the  $\pi$ -system are shown. Note: the calculated  $\Delta H_f$  value is for 4,4-dichlorocyclohexadienone which should have  $\Delta H_f$  identical to 8.

The isomerization of cyclohexadienones to phenols has been the topic of considerable interest.[16,19,33,34] This is due, in part, to the fact that cyclohexadienones or related species are key intermediates during electrophilic additions to aromatic compounds. Several estimates of the energy difference ( $\Delta G$  or  $\Delta H$ ) between phenol and cyclohexadienone are available and these can be compared to the  $\Delta H_R$  value measured in this work, in particular, the aromatization energy (-16 kcal/mol).

Shiner et al[32] used gas phase measurements to estimate the  $\Delta H_f$  values for phenol ( $-23.0 \pm 0.2$  kcal/mol), cyclohexa-2,5-dienone ( $-17 \pm 3$ ) and cyclohexa-2,4-dienone ( $-13 \pm 3$ ). This leads to the prediction that the cyclohexa-2,5-dienone to phenol

isomerization would have  $\Delta H_R = -6 \pm 3$  kcal/mol, while the cyclohexa-2,4-dienone to phenol isomerization would release  $-10 \pm 3$  kcal/mol. Both of these predicted  $\Delta H_R$  values are somewhat smaller than that derived from the  $\Delta H_R$  value (ca.  $-16$  kcal/mol for aromatization) measured in this work. The reason for this discrepancy is not clear.

Tee and Iyengar[33] concluded that for the cyclohexa-2,5-dienone/phenol system,  $\Delta G_0 = 15$  kcal/mole based on estimates of pKa for each compound. Capponi et al[34] estimated  $\Delta G_0$  for the closely related cyclohexa-2,4-dienone/phenol to be  $17.7 \pm 1.4$  kcal/mole. This value is based on the rate of isomerization of cyclohexa-2,4-dienone to phenol measured by flash photolysis and an estimate for the rate of the back reaction. These two estimates are free energy differences,  $\Delta G$ , while the enthalpy of isomerization,  $\Delta H_R$ , was measured in this work. It might be anticipated that the entropy of reaction ( $\Delta S$ ) will be small for this unimolecular reaction, so that  $\Delta G \approx \Delta H$  for this reaction. Both of the  $\Delta G$  estimates are substantially larger than the  $\Delta H_R$  values predicted from the data of Shiner et al,[32] but are in excellent agreement with the  $\Delta H_R$  value for aromatization (ca.  $-16$  kcal/mol) measured in this work.

## 2.5 Conclusion

A number of phenol and carbonyl precursors were protonated in triflic acid to produce a single carbocation in most but not all instances as revealed by  $^1\text{H}$  NMR spectroscopy. The chemical shifts were consistent with the known charge distribution in pentadienyl and allyl cations.

Thermal isomerizations involving methyl migration were observed for ten of the



carbocations which demonstrates that methyl migrations in hydroxy-substituted cyclohexadienyl and cycloalkenyl cations are relatively common. The isomerizations occur such that the methyl groups are moved onto the  $\pi$ -system preferably onto one of the charge bearing positions. In cations that bear the hydroxy substituent on the terminus of the cyclohexadienyl  $\pi$ -system, isomerization will reorganize the  $\pi$ -system so that the hydroxy group is on the central carbon.

The rates of isomerization measured in this work were consistent with values found in the literature, where available. The isomerization of protonated 4,4-dimethylcyclopent-2-enone is considerably slower than its cyclohexenone analogue. Alignment of the C-methyl bond with the  $\pi$ -system, which is needed for methyl migration to occur, is hindered by the rigidity of the cyclopentenone ring.

DSC proved to be a useful and accurate technique for measuring heats of isomerization, which in turn provide a direct quantitative measure of substituent effects in carbocations. Introduction of a methyl group onto the charge bearing terminal position of an allyl or pentadienyl cation stabilizes the system by 3.4–4.1 kcal/mol. A methyl group placed on the  $\pi$ -system but not at a formal charge bearing position (2-position in allyl, 2- or 4-positions in pentadienyl) lowers the cation energy by about 2 kcal/mol. Repositioning of the hydroxy substituent from the terminus to the centre of the pentadienyl  $\pi$ -system results in a 2–4 kcal/mol stabilization.

DSC was also used to measure the heat of isomerization of an acid-catalyzed cyclohexadienone to phenol rearrangement. The energy released by this isomerization ( $-18.7 \pm 0.1$  kcal/mol) was in good agreement with estimates of this energy difference made

by much less direct means.

DSC provides a powerful technique for determining thermochemical information essential to the understanding of chemical reactions of both neutral and charged species. Thus, it should find wider usage in the study of organic chemical reactions.

## 2.6 References

1. a) G.A. Olah, Y.K. Mo, *J. Org. Chem.*, **1973**, *38*, 353; b) R.F. Childs, B.D. Parrington, *Can. J. Chem.*, **1974**, *52*, 3303; c) G. Bertholon, R. Perrin, *Bull. Soc. Chim. Fr.*, **1974**, 113; d) S.M. Blackstock, M.P. Hartshorn, K.E. Richards, *Aust. J. Chem.*, **1980**, *33*, 2753; e) S.M. Blackstock, K.E. Richards, G.J. Wright, *Can. J. Chem.*, **1974**, *52*, 3313.
2. R.F. Childs, B.D. Parrington, *Chem. Comm.*, **1970**, 1581.
3. a) V.A. Koptug, *Top. Curr. Chem.*, **1984**, *122*, 1; b) D.M. Brouwer, E.L. Mackor, C. MacLean in *Carbonium Ions*, G.A. Olah, P.v.R. Schleyer (eds.), Wiley-Interscience, New York, 1970, vol. 2, chpt 20, p. 837.
4. T.H. Lowry, K.S. Richardson, *Mechanism and Theory in Organic Chemistry*, Harper & Row, New York, 1981, 2nd ed., p. 34; J. March, *Advanced Organic Chemistry: Reactions, Mechanisms, and Structure*, 4th ed., Wiley, Toronto, 1992, p. 502, 511.
5. G.A. Olah, *Acc. Chem. Res.*, **1970**, *4*, 240; G.A. Olah, Y. Halpern, Y.K. Mo, G. Liang, *J. Am. Chem. Soc.*, **1972**, *94*, 3554.
6. V.G. Shubin, *Top. Curr. Chem.*, **1984**, *116/117*, 267; J. March, *Advanced Organic*

- Chemistry: Reactions, Mechanisms, and Structure*, 4th ed., Wiley, Toronto, 1992, p. 1052-1062.
7. R.F. Childs, B.E. George, *Can. J. Chem.*, **1988**, *66*, 1343; B.E. George, Ph.D. Thesis, McMaster University, 1987, p. 181.
  8. H.E. Zimmerman, P. Hackett, D.F. Juers, J.M. McCall, B. Schroder, *J. Am. Chem. Soc.*, **1971**, *93*, 3653; V.P. Vitullo, *J. Org. Chem.*, **1970**, *35*, 3976.
  9. K. Alder, F.H. Flock, H. Lessenich, *Chem. Ber.*, **1957**, *90*, 1709; P. Yates, K.E. Stevens, *Tetrahedron*, **1981**, *37*, 4401.
  10. H. Hart, R.M. Lange, P.M. Collins, *Org. Synth.*, **1973**, *5*, 598; H. Hart, P.M. Collins, A.J. Waring, *J. Am. Chem. Soc.*, **1966**, *88*, 1005; H. Hart, *Acc. Chem. Res.*, **1971**, *4*, 337; J. Blum, Y. Pickholtz, H. Hart, *Synthesis*, **1972**, 195.
  11. W.G. Dauben, G.W. Shaffer, N.D. Vietmeyer, *J. Org. Chem.*, **1968**, *33*, 4060; A. Pons, J.-C. Milhavet, J.-P. Chapat, *Bull. Soc. Chim. Fr.*, **1979**, 381.
  12. R.J.L. Andon, J.E. Connett, *Thermochim. Acta*, **1980**, *42*, 241.
  13. B.E. George, Ph.D. Thesis, McMaster University, 1987, p. 53.
  14. R.F. Childs, K.E. Hine, F.A. Hung, *Can. J. Chem.*, **1979**, *57*, 1442.
  15. R.M. Silverstein, G.C. Bassler, T.C. Morrill, *Spectrometric Identification of Organic Compounds*, 5th ed., Wiley, Toronto, 1991, p.197
  16. a) B. Miller, *Acc. Chem. Res.*, **1975**, *8*, 245; b) J.N. Marx, J. Zuerker, Y.P. Hahn, *Tetrahed. Lett.*, **1991**, *32*, 1921; c) V.P. Vitullo, *J. Org. Chem.*, **1970**, *35*, 3976; d) V.P. Vitullo, N. Grossman, *J. Am. Chem. Soc.*, **1972**, *94*, 3844; e) A.J. Waring, *Adv. Alicyclic Chem.*, **1966**, *1*, 129.

17. L.A. Fury Jr, D.E. Pearson, *J. Org. Chem.*, **1965**, *30*, 2301.
18. R.F. Childs, B.E. George, *Can. J. Chem.*, **1988**, *66*, 1350.
19. a) V.P. Vitullo, N. Grossman, *J. Am. Chem. Soc.*, **1972**, *94*, 3844; b) K.L. Cook, A.J. Waring, *J. Chem. Soc., Perkin 2*, **1973**, 88; c) J.N. Marx, J.C. Argyle, L.R. Norman, *J. Am. Chem. Soc.*, **1974**, *96*, 2121; d) J.W. Pilkington, A.J. Waring, *J. Chem. Soc., Perkin 2*, **1976**, 1349.
20. B. Miller, *J. Am. Chem. Soc.*, **1970**, *92*, 6252; E.N. Marvell, E. Magoon, *J. Am. Chem. Soc.*, **1955**, *77*, 2542.
21. a) R.F. Childs, *Chem. Comm.*, **1969**, 946; b) H. Hart, *J. Am. Chem. Soc.*, **1967**, *89*, 1874; D.W. Swatton, H. Hart, *J. Am. Chem. Soc.*, **1967**, *89*, 5075.
22. V.I. Buraev, I.S. Isaev, V.A. Koptuyug, *J. Org. Chem. USSR*, **1979**, *15*, 697.
23. a) C. Fenselau, W.G. Dauben, G.W. Shaffer, N.D. Vietmeyer, *J. Am. Chem. Soc.*, **1969**, *91*, 112; b) P. Lupon, F. Canals, A. Iglesias, J.C. Ferrer, A. Palomer, J.J. Bonet, J.L. Brainso, J.F. Piniella, G. Germain, G.S.D. King, *J. Org. Chem.*, **1988**, *53*, 2193; c) G.W.K. Cavill, B.S. Goodrich, D.G. Laing, *Aust. J. Chem.*, **1970**, *23*, 83.
24. W.G. Dauben, G.W. Shaffer, N.D. Vietmeyer, *J. Org. Chem.*, **1968**, *33*, 4060; H.O. Krabbenhoft, *J. Org. Chem.*, **1979**, *44*, 4050; M.E. Flaugh, T.A. Crowell, D.S. Farlow, *J. Org. Chem.*, **1980**, *45*, 5399; H.E. Zimmerman, R. Keese, J. Nasielski, J.S. Swenton, *J. Am. Chem. Soc.*, **1966**, *88*, 4895; P.D. Magnus, M.S. Nobbs, *Synth. Commun.*, **1980**, *10*, 273; A.M. Badger, D.A. Schwartz, D.H. Picker, J.W. Dorman, F.C. Bradley, E.N. Cheeseman, M.J. DiMartino, N. Hanna, C.K. Mirabelli, *J. Med.*

- Chem.*, 1990, 33, 2963.
25. B.H. Freeman, J.M.F. Gagan, D. Lloyd, *Tetrahedron*, 1973, 29, 4307; J.W. Lyga, *J. Heterocycl. Chem.*, 1996, 33, 1631; J.M. Conia, M.L. Leriverend, *Bull. Soc. Chim. Fr.*, 1970, 2981.
  26. S.W. Benson, F.R. Cruickshank, D.M. Golden, G.R. Haugen, H.E. O'Neal, A.S. Rodgers, R. Shaw, R. Walsh, *Chem. Rev.*, 1969, 69, 279; H.K. Eigmann, D.M. Golden, S.W. Benson, *J. Phys. Chem.*, 1973, 77, 1687.
  27. R.F. Childs, D.L. Mulholland, A. Varadarajan, S. Yeroushalmi, *J. Org. Chem.*, 1983, 48, 1431; E.M. Arnett, R.P. Quirk, J.W. Larsen, *J. Am. Chem. Soc.*, 1970, 92, 3977.
  28. T.H. Lowry, K.S. Richardson, *Mechanism and Theory in Organic Chemistry*, Harper & Row, New York, 1981, 2nd ed., p. 271-3.
  29. a) G.A. Olah, *Acc. Chem. Res.*, 1970, 4, 240; b) D.M. Brouwer, *Rec. Trav. Chim.*, 1968, 87, 611; c) I. Fleming, *Frontier Orbitals and Organic Chemical Reactions*, Wiley, Toronto, 1976, p. 45.
  30. R.J.L. Andon, D.P. Biddiscombe, J.D. Cox, R. Handley, D. Harrop, E.F.G. Herington, J.F. Martin, *J. Chem. Soc.*, 1960, 5246.
  31. C. Decoret, G. Bertholon, C. Gaget, J. Vicens, J. Royer, M. Perrin, S. Lecocq, *Mol. Cryst. Liq. Cryst.*, 1983, 96, 49.
  32. C.S. Shiner, P.E. Vorndam, S.R. Kass, *J. Am. Chem. Soc.*, 1986, 108, 5699.
  33. O.S. Tee, N.R. Iyengar, *J. Am. Chem. Soc.*, 1985, 107, 455.
  34. M. Capponi, I. Gut, J. Wirz, *Angew. Chem., Int. Ed. Engl.*, 1986, 25, 344.

## **Chapter 3: Isomerization of Protonated Bicyclo[3.1.0]hex-3-en-2-ones to Protonated Phenols**

### **3.1 Introduction**

As presented in chapter 2, hydroxy-substituted cyclohexadienyl cations are formed when phenols or cyclohexadienones are dissolved in superacids. Many cyclohexadienyl cations can be transformed into bicyclo[3.1.0]hex-3-en-2-yl cations when irradiated with light of the appropriate wavelength.[1-4] In the case of hydroxycyclohexadienyl cations, these photoisomerizations produce the 2-hydroxybicyclo[3.1.0]hex-3-en-2-yl cations and then bicyclo[3.1.0]hex-3-en-2-ones when the acid solutions are quenched with base. Bicyclo[3.1.0]hex-3-en-2-ones can also be formed photochemically from unprotonated cyclohexadienones.[5]

While bicyclo[3.1.0]hexenyl cations are quite strained they are surprisingly stable and those substituted with a 2-hydroxy group are often stable at room temperature. The 2-hydroxybicyclo[3.1.0]hexenyl cations undergo isomerizations when heated with the principal thermal reaction being ring opening to regenerate the cyclohexadienyl system.[5,6] The photochemical and thermal reactions which interconvert cyclohexadienyl and bicyclo[3.1.0]hexenyl systems are illustrated in Figure 3.1.

Reviews of the chemistry of bicyclo[3.1.0]hexenyl cations can be found in papers

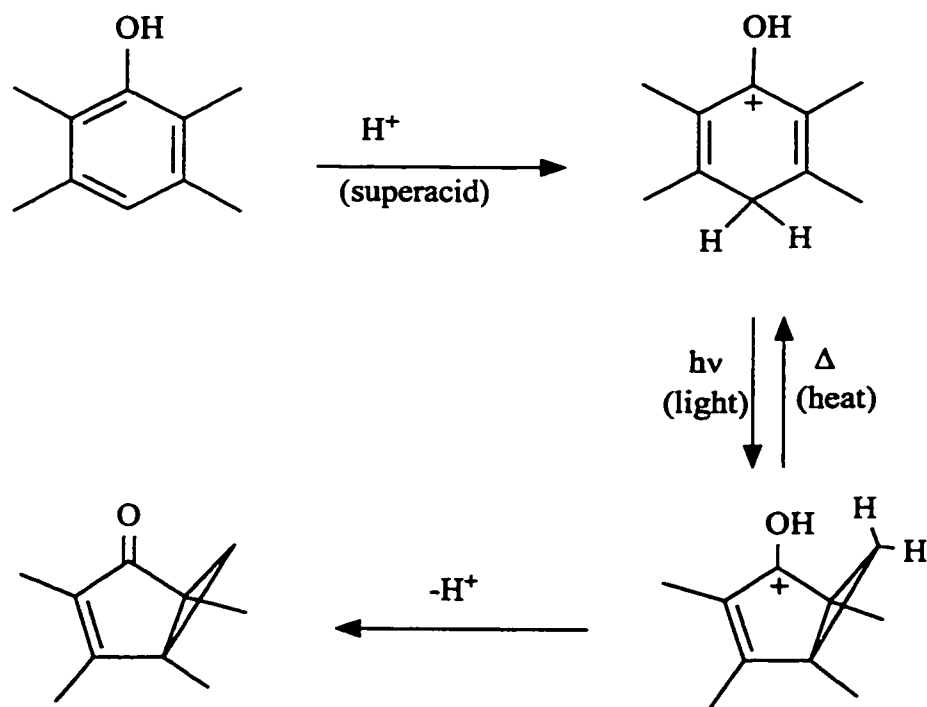


Figure 3.1: Protonation of a phenol yields a cyclohexadienyl cation. Irradiation transforms it to a protonated bicyclo[3.1.0]hexenone. Upon heating the protonated bicyclohexenone reverts to a cyclohexadienyl cation.

by Koptuyug[7] and by Childs, Cremer and Elia.[8] This chapter begins with a review of charge delocalization and photochemical formation of the bicyclo[3.1.0]hexenyl cation. The remainder of the introduction and chapter focuses on the thermal reactions of 2-hydroxy-substituted bicyclo[3.1.0]hex-3-en-2-yl cations, in particular, the effect of methyl substituents on the energy released during these isomerizations. The heat of isomerization depends on the energies of both the reactant and product ions. In chapter 2, the effect of methyl and hydroxy substituents on the stability of the cyclohexadienyl cation (the product ion) were presented. The heats of isomerization of the 2-hydroxybicyclo[3.1.0]hexenyl cations may be used with the information in chapter 2 to quantify the effect of methyl groups on the stability of the bicyclo[3.1.0]hexenyl cation.

### 3.1.1 Charge Delocalization in the Bicyclo[3.1.0]hex-3-en-2-yl Cation

The bicyclo[3.1.0]hex-3-en-2-yl cation is an interesting system. The cyclopropyl group spans the ends of the allyl portion of the ion. If the internal cyclopropane bond, the bond shared by the five and three-membered rings, were involved in charge delocalization, an antiaromatic, homocyclopentadienyl cation would result. Alternately, one or both of the external cyclopropyl bonds could be involved in charge delocalization, resulting in positive charge being transferred to C6.

NMR studies[1-4,9] of bicyclo[3.1.0]hex-3-en-2-yl cations were found to be consistent with charge delocalization via the external cyclopropane bonds. Firstly, there was no evidence for a ring current. The chemical shift difference ( $\Delta\delta$ ) between the endo and exo protons ( $\delta_{\text{endo}} - \delta_{\text{exo}}$ ) in the parent bicyclo[3.1.0]hex-3-en-2-yl cation is +0.3 ppm.[9a] In contrast, a homoaromatic system such as the homotropylium ion displays  $\Delta\delta = -5.8$  ppm consistent with a ring current due to cyclic delocalization (Figure 3.2).[10]

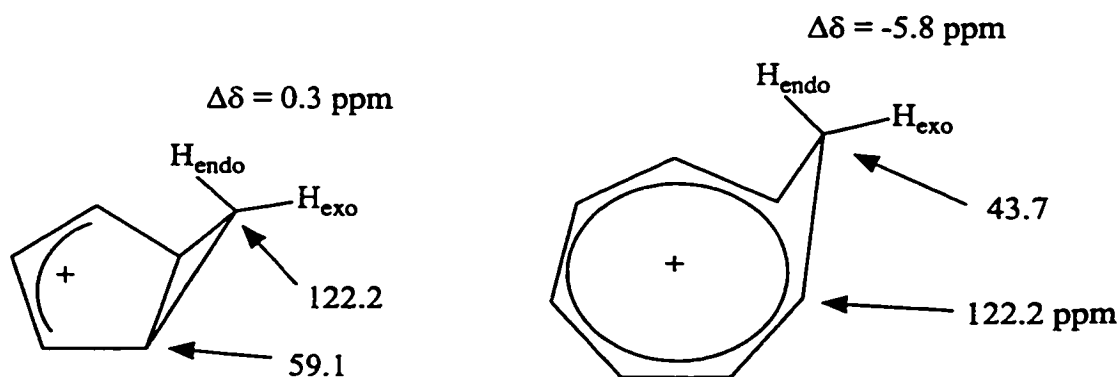


Figure 3.2:  $^1\text{H}$  NMR chemical shift difference ( $\Delta\delta$ ) between exo and endo protons and  $^{13}\text{C}$  chemical shifts of the bridging and bridgehead carbons in the bicyclo[3.1.0]hexenyl and homotropylium ions.



$^{13}\text{C}$  NMR studies[1,4f,9b] reinforced the conclusion that the nature of charge delocalization was different in the bicyclo[3.1.0]hex-3-en-2-yl and homotropylium ions (Figure 3.2). The signal for the bridging carbon in the bicyclohexenyl cation was found to resonate much further downfield than in the homotropylium ion (122 ppm vs. 44 ppm).[9b,10] In contrast, the bridgehead carbons of the homotropylium ion are deshielded relative to the bicyclohexenyl cation (122 vs. 59 ppm). This led to the conclusion that positive charge is delocalized via the external cyclopropyl bonds to the bridge position, C6, in the bicyclo[3.1.0]hex-3-en-2-yl ion, while the internal bond delocalizes charge in the homotropylium ion, resulting in charge being placed on the bridgehead carbons. The charge distribution in the bicyclohexenyl cation is well represented by the resonance structures in Figure 3.3.

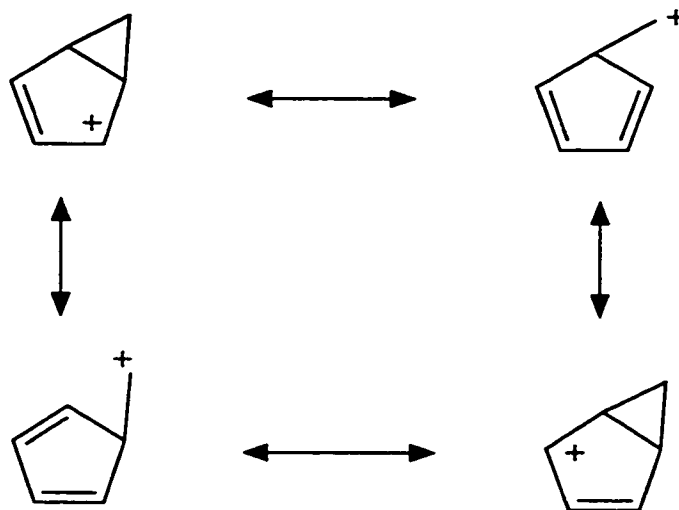


Figure 3.3: Resonance structures of bicyclo[3.1.0]hex-3-en-2-yl cation.

Childs and coworkers[11] isolated a hydroxy-substituted bicyclohexenyl cation as a crystalline solid and determined its structure by X-ray crystallography. The cation, shown in Figure 3.4, was prepared by the protonation of a bicyclo[3.1.0]hex-3-en-2-one. The structure was consistent with the resonance picture in Figure 3.3. The only lengthened cyclopropyl bond is the external bond (C1-C6), indicating that charge is delocalized to the bridging carbon (C6). The bond that joins C4 to its methyl group (1.479 Å) is considerably shorter than the C3-methyl bond (1.502 Å). Positive charge resides on C4, and this electron-deficient carbon would be expected to have shorter bonds to its substituents than a more electron-rich carbon (i.e. C3). In distinct contrast, the crystal structure of a homotropylium ion (protonated bicyclo[5.1.0]octa-3,5-dien-2-one) revealed structural changes consistent with cyclic delocalization -- a lengthened internal cyclopropane bond and shortened bonds connecting the  $\pi$ -system to the cyclopropyl ring.[12]

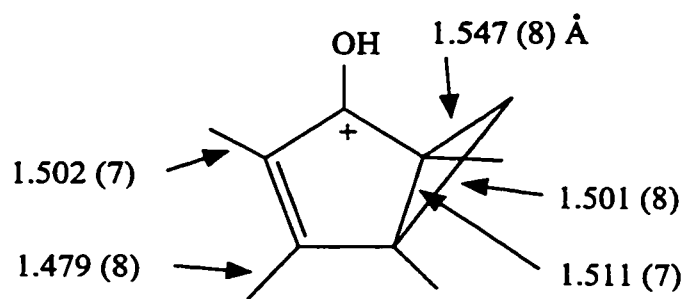


Figure 3.4: Key bond lengths in 2-hydroxy-1,3,4,5-tetramethylbicyclo[3.1.0]hex-3-en-2-yl cation.

Theoretical calculations[13] of the structure of the bicyclohexenyl cation found in the literature are consistent with charge delocalization as depicted in Figure 3.3.

<sup>13</sup>C NMR studies of protonated bicyclo[3.1.0]hexenones[1] further emphasize that the external cyclopropyl bonds are involved in delocalization. Comparison of the <sup>13</sup>C NMR spectra of three neutral and protonated bicyclo[3.1.0]hexenones showed that the most dramatic changes upon protonation of the ketone were the marked downfield shifts of C4 and C6. Thus, the bicyclo[3.1.0]hexenyl cation should be best stabilized by electron-donating substituents placed on C2, C4 and C6.

### 3.1.2 Photochemical Formation of Bicyclo[3.1.0]hex-3-en-2-one

The mechanism of the photoisomerization of neutral cyclohexadienones to bicyclo[3.1.0]hexenones (Figure 3.5) is well established.[14] The photochemical formation of bicyclo[3.1.0]hexenyl cations is proposed to occur by an analogous mechanism.[1-4]

Methyl-substituted cyclohexadienyl cations have absorption maxima at ca. 390nm ( $\log \epsilon \approx 4.0$ )[2] while the hydroxy-substituted ions absorb at ca. 320 nm ( $\log \epsilon \approx 3.8$ ).[1] After the absorption of light, the four electron, pentadienyl  $\pi$ -system can undergo ring closure, an electrocyclic reaction, to yield a cyclopentenyl cation. Orbital symmetry rules predict that this photochemical ring closure will occur in a disrotatory fashion, while the analogous thermal closure will occur in a conrotatory fashion.[15] Examples of both types of closure, principally thermal ones, are known for simple acyclic pentadienyl cations.[16] If the double bonds have *E,E* or *Z,Z* stereochemistry, the result of thermal

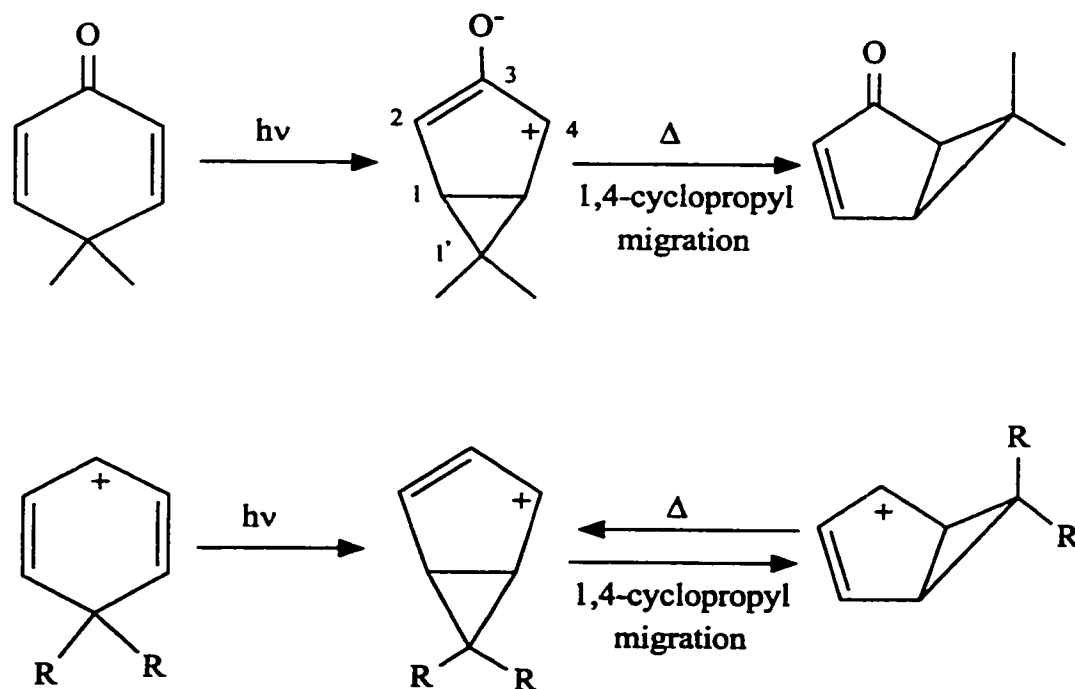


Figure 3.5: Proposed mechanism for the photochemical formation of the bicyclo[3.1.0]hexenyl framework from cyclohexadienones or cyclohexadienyl cations.

closure is a trans-fused product, while photochemical closure results in a cis-fused product (Figure 3.6). For a pentadienyl cation within a six membered ring, the thermally-allowed conrotatory closure would result in the highly strained, trans-fused bicyclo[3.1.0]hexenyl cation. Thermal ring closure of cyclohexadienyl systems is not observed, but photochemical closure is common.[1-4]

In many cases the initially formed bicyclo[3.1.0]hexenyl framework rearranges to yield a more stable bicyclic system. In the case of hydroxycyclohexa-2,5-dienyl cations (protonated phenols or cyclohexa-2,5-dienones), the initial closure would result in a bicyclo[3.1.0]hexenyl system containing a 2-hydroxy substituted allyl cation (see Figure 3.7). A 1,4 cyclopropyl migration about the five membered ring would convert this to the

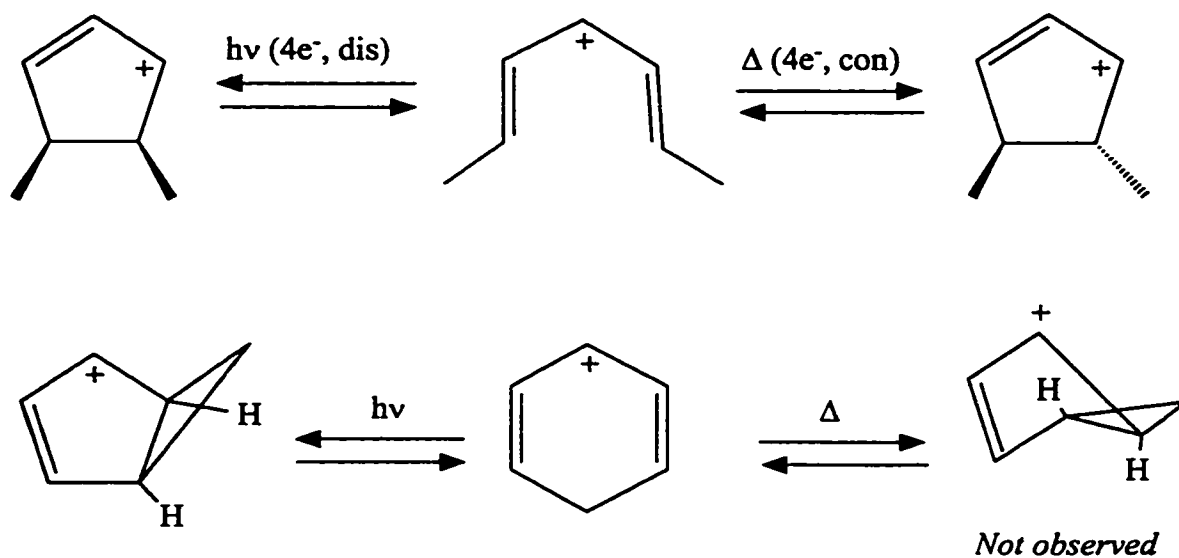


Figure 3.6: The stereochemical outcome of thermal and photochemical ring closures of pentadienyl cations.

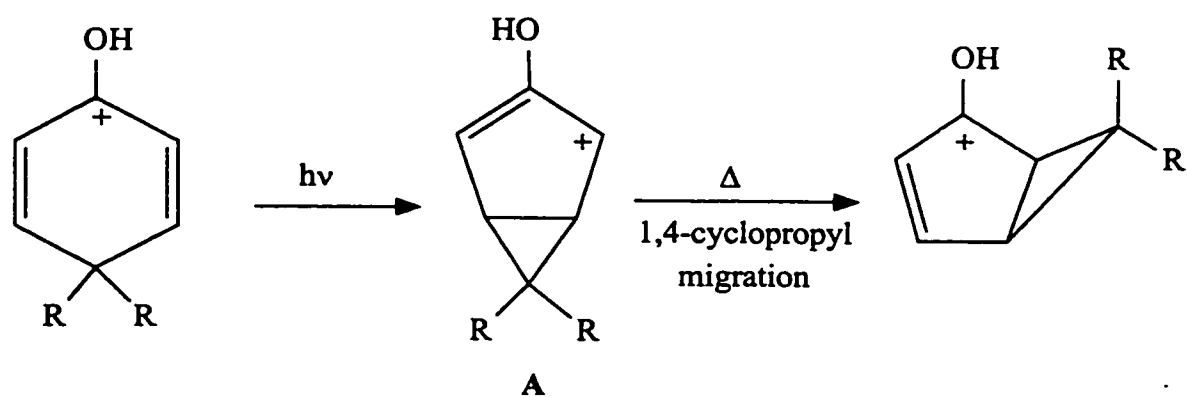


Figure 3.7: Ring closure produces the 3-hydroxybicyclo[3.1.0]hex-3-en-2-yl cation (A) which can isomerize to a more stable 2-hydroxybicyclo[3.1.0]hex-3-en-2-yl cation.

much more stable 1-hydroxy allyl cation function.

Childs and George[1] studied the photoisomerization of a number of protonated phenols to protonated bicyclo[3.1.0]hex-3-en-2-ones. The efficiency of the photochemical reaction which converts the protonated phenol into a protonated bicyclo[3.1.0]hexenone was found to be strongly dependent on the location of substituents (Figure 3.8). The variations in quantum efficiency were rationalized based on the effects of methyl substitution on the initially formed 3-hydroxybicyclo[3.1.0]hex-3-en-2-yl cation (A in Figure 3.7). Methyl groups at the 3 and 5-positions of the phenol end up on the bridgeheads of intermediate A. Substitution at the bridgeheads of bicyclo[3.1.0]hexenyl cations or bicyclo[2.1.0]pentenes is known to promote ring opening. Ring opening of A regenerates the starting material. Methyl groups at the 2 and 6-positions of the phenol will end up on the  $\pi$ -system of intermediate A. Methyl groups on the  $\pi$ -system of bicyclo[3.1.0]hexenyl cations or bicyclo[2.1.0]pentenes have been found to stabilize those molecules and retard ring opening. With ring opening slowed, cyclopropyl migration leading to a protonated bicyclo[3.1.0]hex-3-en-2-one is able to occur.

### *3.1.3 Thermal Reactions of Protonated Bicyclo[3.1.0]hex-3-en-2-ones*

The thermal reactions of protonated bicyclo[3.1.0]hexenones have been found to fall into two categories: 1) migrations of the cyclopropyl ring around the periphery of the cyclopentenyl ring (circumambulatory rearrangements),[17] and 2) opening of the bicyclic system to a six-membered ring.

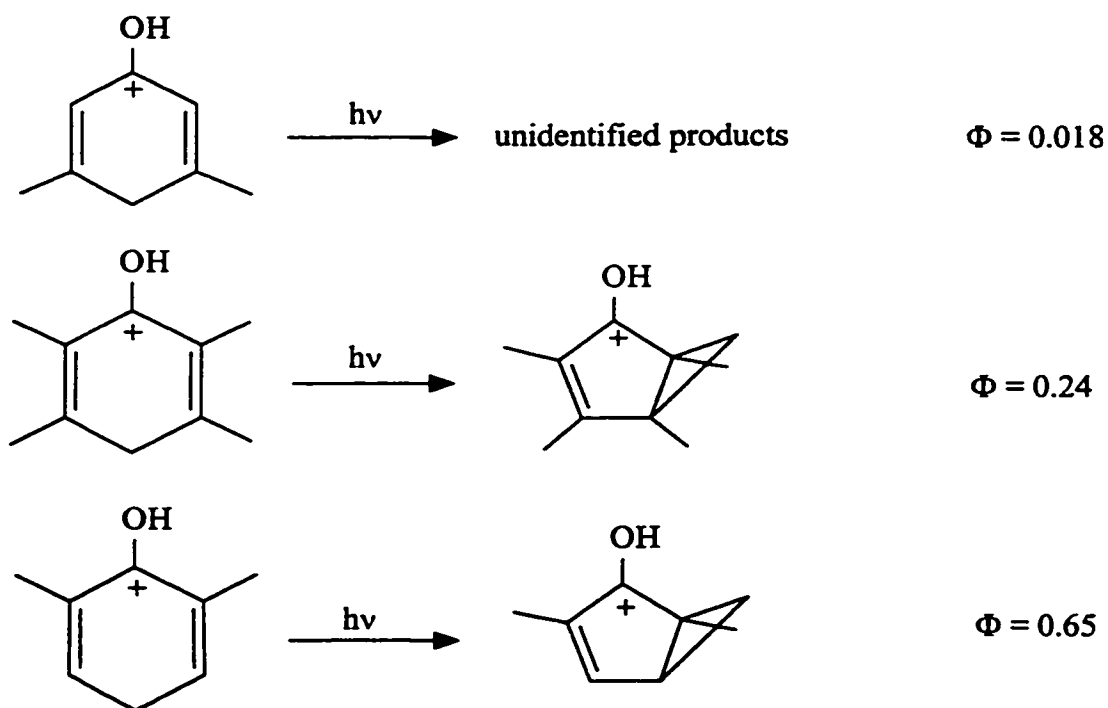


Figure 3.8: Quantum yields for the photoisomerization of several methyl-substituted protonated phenols.

Ions such as the 1,2,3,4,5,6-hexa and 1,2,3,4,5,6,6-heptamethyl bicyclo[3.1.0]hexenyl cations (Figure 3.9) display temperature dependent line-broadening  $^1\text{H}$  NMR spectra.[2] The signals due to the five cyclopentenyl methyl groups coalesce into a singlet when the samples are warmed. The occurrence of a rapid circumambulatory rearrangement was used to explain these observations (Figure 3.9).

Circumambulatory rearrangements are not as easily detected for protonated bicyclo[3.1.0]hex-3-en-2-ones but they have been shown to be operative.[3,5,6] As outlined above, cyclopropyl migrations are believed to occur during the photochemically initiated formation of neutral or protonated bicyclo[3.1.0]hex-3-en-2-ones.[1,3,5,14] Thermal ring opening of protonated bicyclo[3.1.0]hexenones often results in a

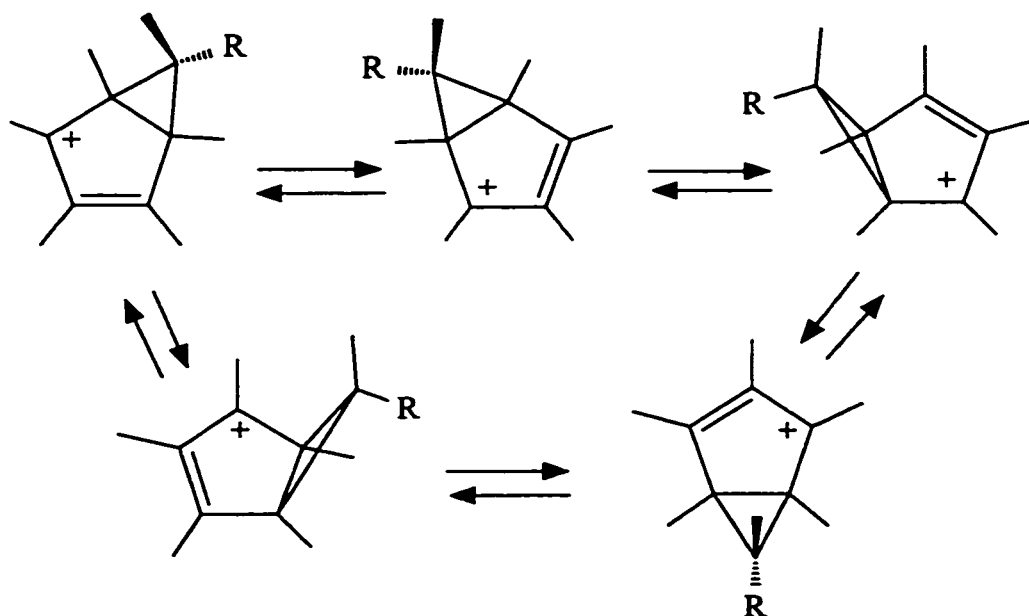


Figure 3.9: Cyclopropyl migration in hexamethyl ( $R = H$ ) or heptamethyl ( $R = CH_3$ ) bicyclo[3.1.0]hexenyl cations causes methyl group bound to the five-membered ring to be averaged. Note that the  $R$  group remains in an *exo* orientation.

repositioning of methyl groups on the ring system which provides evidence that cyclopropyl migrations preceded ring opening.[3,5,6] Further evidence comes from the study of deuterium labelled bicyclo[3.1.0]hex-3-en-2-ones.[5b,6] Protonated bicyclo[3.1.0]hex-3-en-2-ones (one example is shown in Figure 3.10) were found to exhibit scrambling of a deuterium labelled methyl group between C4 and C5 in the recovered starting material, which indicated that the bicyclo[3.1.0]hexenyl system had undergone a circumambulatory rearrangement.

In the examples found in the literature,[2,3,4a,4e,5b] the relative orientation of the substituents at C6 was found to be unaffected by the circumambulatory rearrangement. Thus, cyclopropyl migration occurs by a route which maintains the *exo* and *endo*



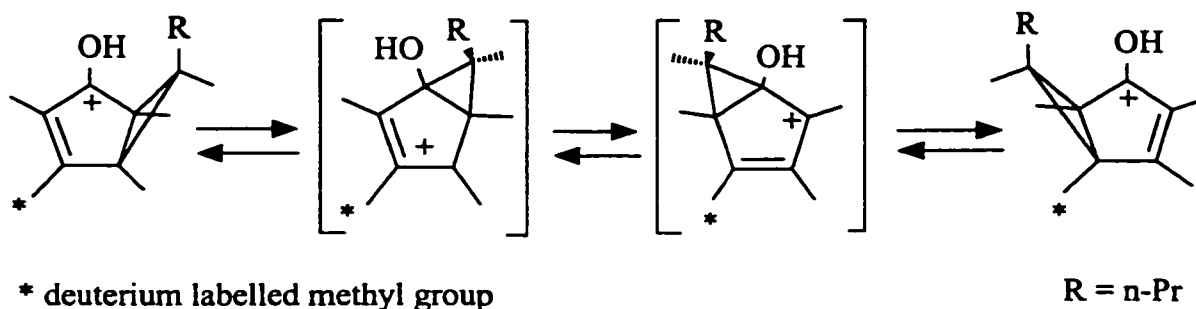


Figure 3.10: Scrambling of labelled methyl group shows that cyclopropyl migration (circumambulation) has occurred.

orientation of the substituents at C6. This has been rationalized as being due to orbital symmetry constraints. Cyclopropyl migration is an example of a [1,4]-sigmatropic rearrangement, a concerted reaction during which one bond to C6 is broken while, at the same time, a new bond to C6 is formed. Orbital symmetry rules predict that this four-electron [1,4]-migration will occur via a transition state in which the stereochemistry of the migrating centre is inverted.[18] If the migrating centre (C6) inverts its stereochemistry, the exo and endo groups maintain their orientation relative to the five-membered ring. The experimental results found in the literature are in accord with the predictions of orbital symmetry.

Cyclopropyl migration is favoured by the introduction of charge stabilizing groups at C6, the migrating carbon.[2,4e] For example, the two ions shown in Figure 3.9 differ in the number of methyl groups on C6. The barrier to cyclopropyl migration in the heptamethyl bicyclo[3.1.0]hexenyl cation was found to be 10.1 kcal/mol, while for the hexamethyl bicyclo[3.1.0]hexenyl cation, the barrier increased to 17.5 kcal/mol. This is presumably due to an increase in the degree of positive charge at C6 in the transition state

which is better stabilized in the ion with two methyl groups on C6.

Bicyclo[3.1.0]hexenyl compounds possess considerable ring strain and as a result they are of higher energy than the isomeric cyclohexadienyl compounds. Essentially all bicyclo[3.1.0]hexenyl systems undergo a thermal ring opening to a cyclohexadienyl framework.[1-8] In spite of the driving force, the activation barrier for this reaction is remarkably high. Ring opening is an electrocyclic reaction. For the 4-electron ring opening of the bicyclo[3.1.0]hex-3-en-2-yl framework, reaction in a conrotatory fashion is predicted to be of lower energy than a disrotatory opening (Figure 3.6).[15] However, conrotatory opening would produce a cyclohexadienyl cation with a trans double bond, a very high energy molecule (Figure 3.6). The observed cyclohexadienyl cation corresponds to opening in a disrotatory fashion, a mode of reaction which is predicted to be forbidden (of higher energy) than the conrotatory opening on the basis of orbital symmetry considerations. The reaction has a high energy barrier because the ring opening is forced by steric constraints to occur in a disrotatory fashion, the forbidden reaction pathway.

Childs and George[6] studied ring openings of a series of methyl substituted bicyclo[3.1.0]hexenones in  $\text{CF}_3\text{SO}_3\text{H}$  and they found that the activation barrier for ring opening ranges from 20 to 30 kcal/mole. Electron donors on the  $\pi$ -system, which stabilize the bicyclo[3.1.0]hexenyl cation, were found to raise the activation barrier for ring opening. Methyl substituents on the bridgehead positions (C1, C5) lowered the barrier for the ring opening by stabilizing the transition state for ring opening. The effect of methyl substitution at C6 was variable. In some cases, there was little effect on the

barrier to ring opening, while in others, methyl substitution on C6 lowered the barrier. For example, the 1,3,4,6-*exo*-tetramethyl-bicyclohexenyl ion (Figure 3.11) was found to have a barrier to ring opening 3 kcal/mol less than the 1,3,4-trimethyl cation. The methyl group on C6 facilitates cyclopropyl migration which produces an intermediate with a much lower ring-opening barrier than the initial bicyclo[3.1.0]hexenyl ion.

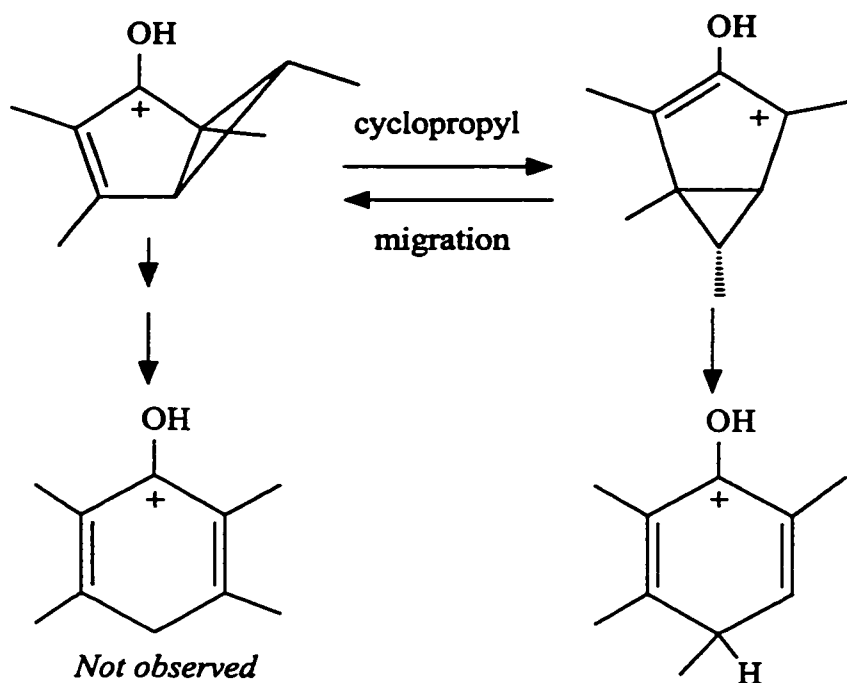


Figure 3.11: Cyclopropyl migration precedes ring opening during the isomerization of protonated 1,3,4,6-*exo*-tetramethylbicyclo[3.1.0]hexenone.

As a result of their studies, Childs and George[6] proposed that the ring openings of protonated bicyclo[3.1.0]hexenones took place by three closely related mechanisms (Figures 3.12-3.14).

This work demonstrated that the energy required for cyclopropyl migration and ring opening in the protonated bicyclo[3.1.0]hexenones were closely matched. With

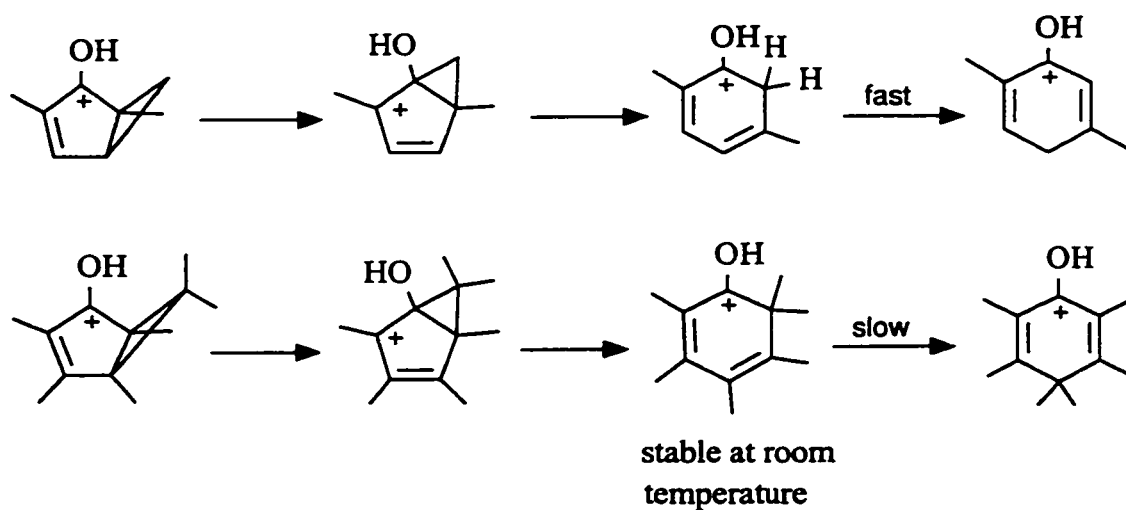


Figure 3.12: Examples of isomerizations in which cyclopropyl migration towards oxygen precedes ring opening.

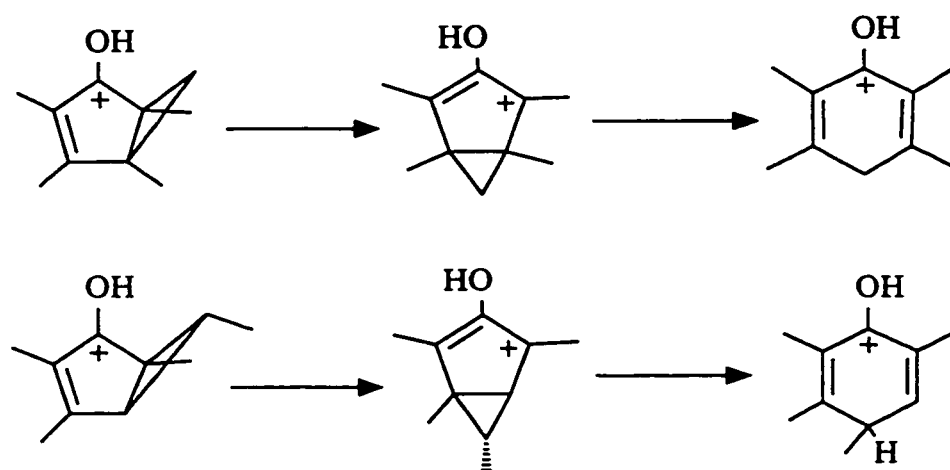


Figure 3.13: Examples of isomerization in which cyclopropyl migration away from oxygen precedes ring opening.

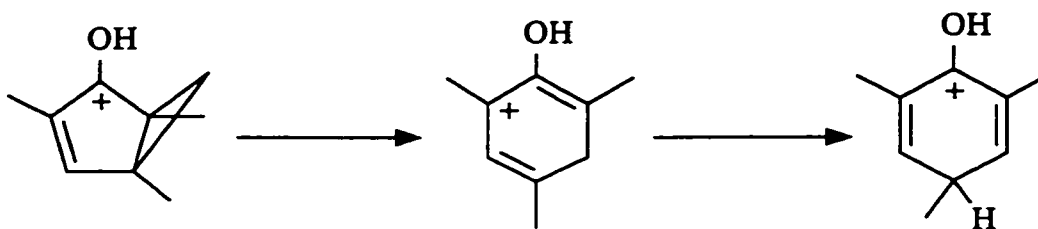


Figure 3.14: Example of isomerization in which ring opening occurs without cyclopropyl migration.

some substitution patterns, cyclopropyl migration can occur to yield bicyclic systems for which ring opening is rapid. With other substitution patterns, ring opening may occur at a lower temperature than is required for cyclopropyl migration and thus no scrambling of substituents is seen. It was clear that when scrambling was observed, it had occurred before ring opening since control experiments had shown that substituent migrations about the cyclohexadienyl framework require higher temperatures than is needed for ring opening. For example, during the isomerization of protonated 1,3,4,5-tetramethylbicyclo[3.1.0]hexenone to protonated durenol (Figure 3.15), it is conceivable that the initial product of isomerization might be protonated isodurenol. However, protonated isodurenol isomerizes to protonated durenol about 20 times slower than the ring opening reaction[6] and isodurenol would be detected if it were the initial product of ring opening.

The ready photochemical/thermal interconversion of cyclohexadienyl and bicyclo[3.1.0]hexenyl cations led Childs and coworkers[19] to propose that these transformations might form the basis of a solar energy storage system (Figure 3.16).[20] However, it appears unlikely that a practical system will be developed because of poor

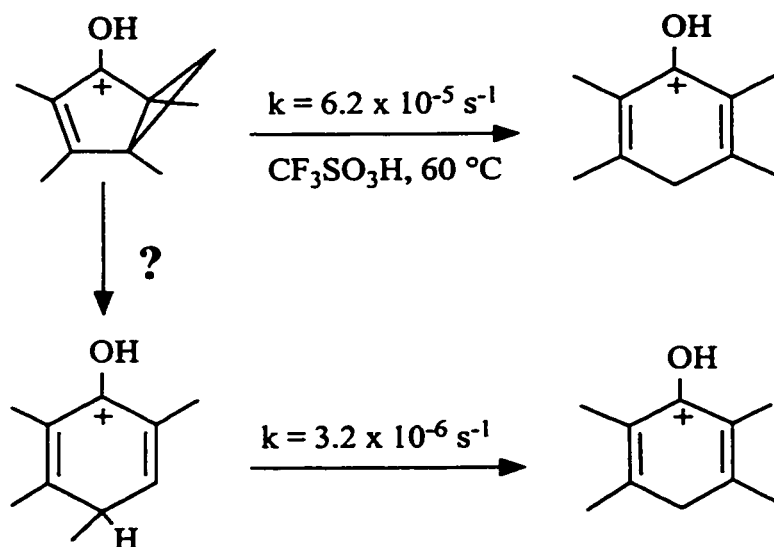


Figure 3.15: Rates of formation of protonated durenol from protonated 1,3,4,5-tetramethylbicyclo[3.1.0]hexenone and from protonated isodurenol.

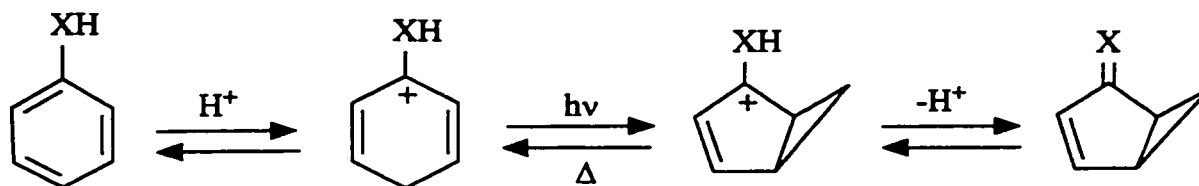


Figure 3.16: Reaction scheme for the storage of photochemical energy in a bicyclo[3.1.0]hexenyl compound.

overlap with the solar spectrum and an inability to transfer this chemistry to an acid catalyzed regime.

### 3.1.4 Thermochemistry

Thermochemical information about the ring opening of bicyclo[3.1.0]hexenyl cations would be valuable as it would reveal the amount of photochemical energy stored

in the bicyclic system and the effect of structural changes upon the stability of the cations. However, only a limited amount of information is available.

Childs and Mulholland[21] determined the energy difference between a bicyclo[3.1.0]hexenyl cation and its cyclohexadienyl isomer for two pairs of isomers. This was accomplished with a calorimetric technique in which the heats of protonation ( $\Delta H_p$ ) of neutral precursors in fluorosulfuric acid are measured. The heat released by the protonation of the bicyclo[3.1.0]hexenyl isomer of hexamethylbenzene was measured at -20 and 65 °C (Figure 3.17). At the lower temperature, a bicyclo[3.1.0]hexenyl cation is produced, while isomerization to protonated hexamethylbenzene accompanies protonation at the higher temperature. The difference between the two  $\Delta H_p$  values provides the heat of isomerization ( $\Delta H_R$ ), the enthalpy difference between the two isomeric cations.  $\Delta H_R$  was found to be  $-8.9 \pm 0.8$  kcal/mol as illustrated in Figure 3.17. Similarly, the energy difference between hexamethylcyclohexa-2,4-dienone and its bicyclic isomer was determined to be  $-12 \pm 2$  kcal/mol (Figure 3.18).

The heat of protonation technique also allows the energy difference between the isomeric neutral precursors to be determined. The relationship between the neutral precursors and cations is conveniently illustrated in the form of an energy diagram. Childs and Mulholland[21] generated energy diagrams for the two examples described in the preceding paragraph and similar diagrams are shown in Figures 3.19 and 3.20.<sup>1</sup>

---

1

Note:  $\Delta H_{tr}$  is obtained by correcting the heat of solution in fluorosulfuric acid by the heat of solution in an inert solvent such as carbon tetrachloride. This procedure corrects for the energy associated with the separation of molecules (eg. lattice and H-bonding energy). Thus, the

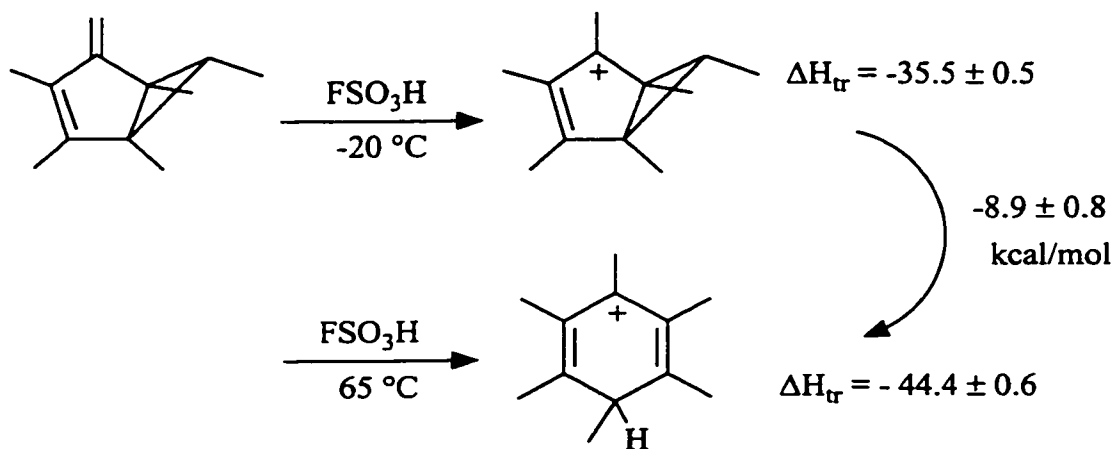


Figure 3.17:  $\Delta H_R$  determined from heats of protonation measured at two different temperatures.

Estimates of the enthalpy difference between the bicyclo[3.1.0]hexenyl and cyclohexadienyl cations is also available from theoretical calculations. Calculations at the STO-3G level of approximation revealed that the cyclohexadienyl cation was more stable by 21 kcal/mol.[13a] Earlier calculations predicted an even larger energy difference of 22 (STO-3G) and 34 (4-31G) kcal/mol.[23]

More thermochemical information about the bicyclo[3.1.0]hexenyl/cyclohexadienyl system is needed. Measurement of the heat of

---

reference state for  $\Delta H_{tr}$  is a dilute solution of the cation precursor in an inert solvent (eg.  $\text{CCl}_4$ ). This has been found to be comparable to the use of the gas phase as the reference state.[22] On the other hand, the heat of formation ( $\Delta H_f$ ) refers to the compound in its standard state. For example, hexamethylbenzene is a solid at 25 °C. In reference [21] there is some inconsistency in the use of reference states for the  $\Delta H$  values considered in the discussion and used to generate Figure 1. For this reason, Figure 3.19 should be viewed as a corrected version of Figure 1 in reference [21].



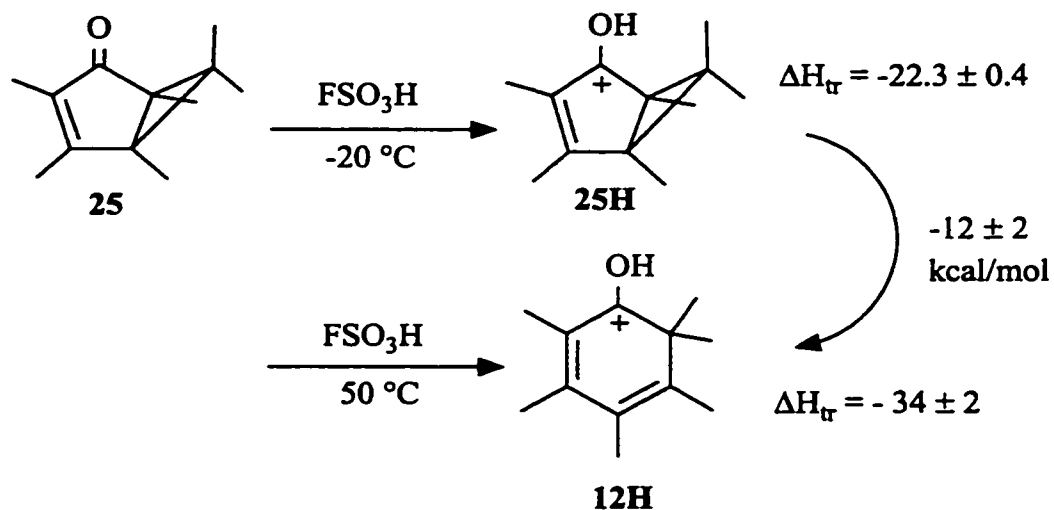


Figure 3.18:  $\Delta H_R$  determined from heats of protonation measured at two different temperatures.

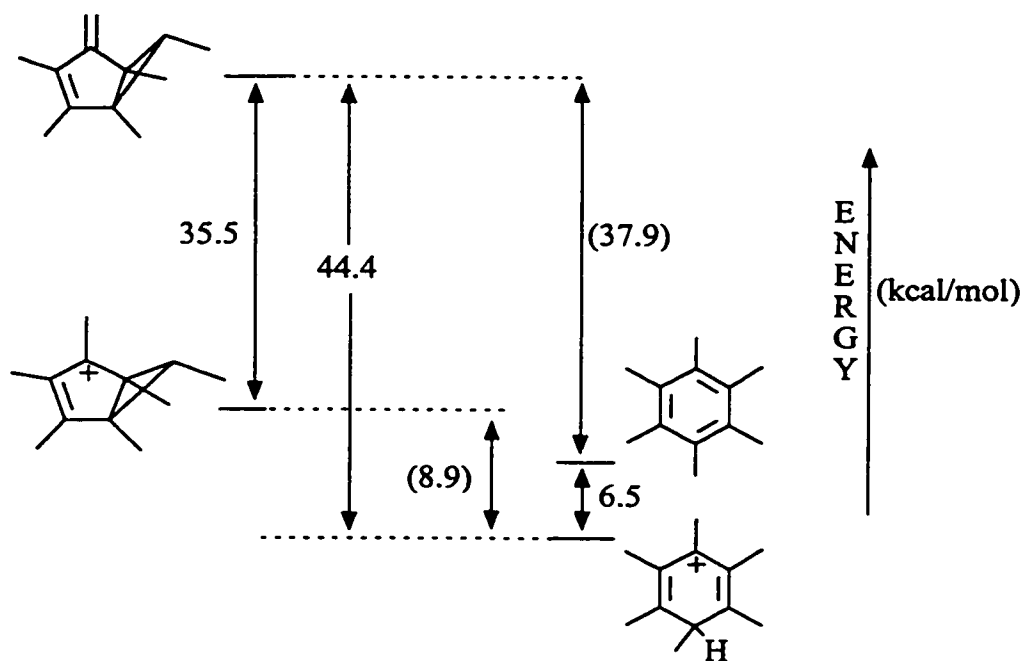


Figure 3.19: Relative energies (in kcal/mol) of neutral and protonated hexamethylbenzene and bicyclic isomers determined in  $\text{FSO}_3\text{H}$ . Values in brackets are differences between measured heats of protonation ( $\Delta H_{tr}$ ). Data from ref. 21.

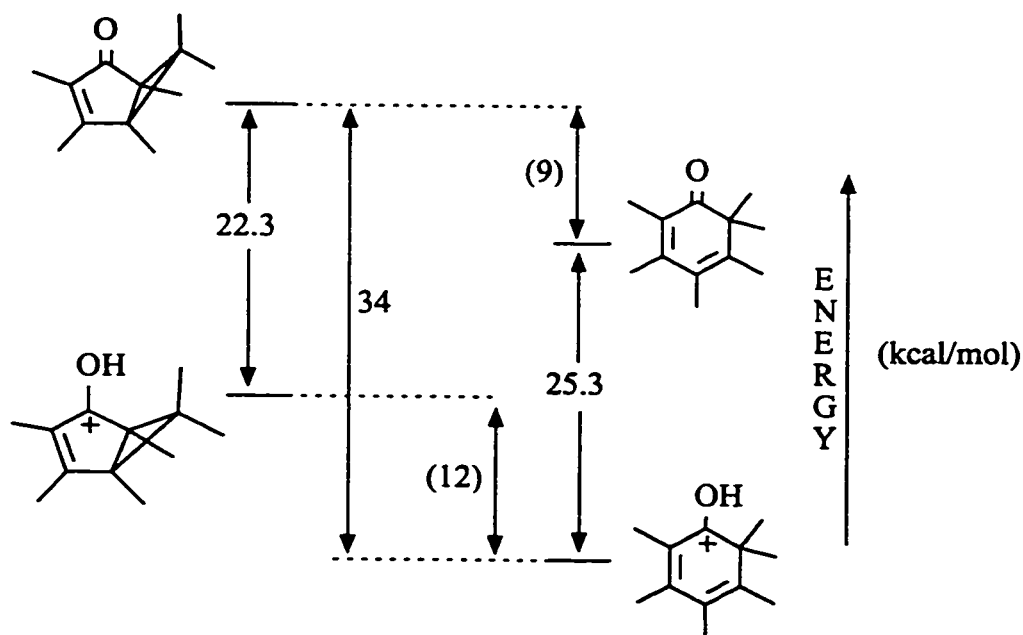


Figure 3.20: Relative energies (in kcal/mol) of neutral and protonated hexamethyl ketones in  $\text{FSO}_3\text{H}$ . Values in brackets are differences in measured heats of protonation ( $\Delta H_{\text{TP}}$ ). Data from ref. 21.

isomerization with DSC provides an ideal route to this information. Determination of the heat of isomerization would provide additional measures of the energy difference between the bicyclo[3.1.0]hexenyl and cyclohexadienyl frameworks and also provide quantitative information about the effect of substituents upon the stability of these cations.

### 3.1.5 Goals

The goal of this research was to find the heat of isomerization ( $\Delta H_{\text{isom}}$ ) for the conversion of the 2-hydroxybicyclo[3.1.0]hex-3-en-2-yl cation (protonated bicyclo[3.1.0]hex-3-en-2-one) to the hydroxy-cyclohexadienyl cation (protonated

phenol), and to determine how this energy is affected by methyl substituents. This information would provide the storage capacity of a photochemical energy storage system and could suggest substitution patterns to maximize energy storage capability of the bicyclo[3.1.0]hexenone framework. In addition, the heats of isomerization can be used to quantify the stabilizing effects of methyl substituents in the bicyclo[3.1.0]hexenyl cation. When this information is combined with that in chapter 2 it should be possible to prepare energy diagrams which show the relationship between isomeric cations.

### 3.2 Experimental

<sup>1</sup>H NMR spectra were measured with Bruker AM200 (200 MHz) or Varian EM390 (90 MHz) spectrometers and are reported as  $\delta$  in ppm relative to tetramethylsilane and coupling constants in Hz. Compounds **2**, **11**, **15** and **19** were commercially available (Aldrich). The preparation of compound **12** was described in chapter 2 while compound **20** had been prepared in this laboratory previously.[1] Compounds **21-24** [1] and **25**[5c] were prepared by procedures found in the literature.

*3,4-Dimethylbicyclo[3.1.0]hex-3-en-2-one, 21* - This compound was prepared from **11** by the method described by Childs and George.[1] NMR (CCl<sub>4</sub>): 1.00 (q(4), 1H, endo-H-6), 1.32 (ddd(8.5, 7.5, 3.5), 1H, exo-H-6), 1.49 (s, 3H, 3-CH<sub>3</sub>), 1.94 (m, 1H, 5-H), 2.03 (s, 3H, 4-CH<sub>3</sub>), 2.17 (m, 1H, H-1).

*1,3-Dimethylbicyclo[3.1.0]hex-3-en-2-one, 22* - Prepared by the same procedure used to produce **21** but starting from **19**. NMR (CCl<sub>4</sub>): 1.09 (t(2.5), 1H, endo-H-6), 1.14 (m, 1H, exo-H-6), 1.29 (s, 3H, 1-CH<sub>3</sub>), 1.55 (d(2), 3H, 3-CH<sub>3</sub>), 2.01 (p(3), 1H, 5-H), 7.08 (m, 1H, 4-H).

*1,3,4,5-Tetramethylbicyclo[3.1.0]hex-3-en-2-one, 23* - Prepared by the same procedure used to produce **21** but starting from **2**. NMR (CCl<sub>4</sub>): 0.82 (d(3), 1H, endo-H-6), 1.21 (d(3), 1H, exo-H-6), 1.25 (s, 3H, 5-CH<sub>3</sub>), 1.32 (s, 3H, 1-CH<sub>3</sub>), 1.51 (s, 3H, 3-CH<sub>3</sub>), 1.96 (s, 3H, 4-CH<sub>3</sub>).

*1,3,4,5,endo-6-Pentamethylbicyclo[3.1.0]hex-3-en-2-one, 24* - Prepared by the same procedure used to produce **21** but starting from **20**. NMR (CCl<sub>4</sub>): 0.91 (d(5.5), 3H, endo-6-CH<sub>3</sub>), 1.18 (s, 3H, 5-CH<sub>3</sub>), 1.31 (s, 3H, 1-CH<sub>3</sub>), 1.58 (s, 3H, 3-CH<sub>3</sub>), 1.89 (s, 3H, 4-CH<sub>3</sub>). Note: Signal for exo-H-6 was obscured by stronger signals.

*1,3,4,5,6,6-Hexamethylbicyclo[3.1.0]hex-3-en-2-one, 25* - Prepared by the literature procedure[5c] by irradiation of a deoxygenated ether solution of 2,3,4,5,6,6-hexamethylcyclohexa-2,4-dienone, **12**, in a Rayonet RPR-100 photoreactor (300 nm). mp 48-50 °C (lit 50-52 °C [5c]). NMR (CCl<sub>4</sub>): 0.92 (s, 3H, endo-6-CH<sub>3</sub>), 1.11 (s, 6H, 5-CH<sub>3</sub> and exo-6-CH<sub>3</sub>), 1.21 (s, 3H, 1-CH<sub>3</sub>), 1.57 (s, 3H, 3-CH<sub>3</sub>), 1.89 (s, 3H, 4-CH<sub>3</sub>).

*Protonation, Kinetics and Heats of Isomerization* were studied as described in chapter 2.

*Catalyzed Isomerization of 23* - As described in chapter 2 except that 0.18 M triflic acid in nitrobenzene was used as the solvent.

### 3.3 Results and Discussion

Bicyclo[3.1.0]hex-3-en-2-ones **21-24**[1] and **25**[5c] were prepared by methods found in the literature. To prepare **21-24** triflic acid solutions of the precursor phenols were irradiated (300 nm) at room temperature, neutralized and then extracted with ether. It was not necessary to purify the products by preparative GC as described in reference [1] because the irradiations provided exclusively or predominantly one bicyclic ketone. Instead, base extraction to remove phenol(s) followed by bulb-to-bulb distillation gave pure ketones which had spectroscopic properties consistent with the assigned structure and with those found in the literature. <sup>1</sup>H NMR data for the ketones is given in Table 3.1.

The <sup>1</sup>H NMR spectra (Table 3.1) of the bicyclic ketones in triflic acid were identical to those observed previously[1] and revealed that cleanly and completely oxygen-protonated species **21H-25H** were produced. The <sup>1</sup>H NMR results are fully in accord with the picture of charge delocalization presented in the Introduction (Figure 3.3). Thus, substituents to C2, C4 or C6 should provide the greatest stabilization of the carbocation.

#### 3.3.1 Isomerization of Protonated Bicyclo[3.1.0]hex-3-en-2-ones

The thermal isomerizations of protonated bicyclo[3.1.0]hex-3-en-2-ones shown in

Figure 3.21 were investigated. In each case, a cyclohexadienyl cation (protonated phenol or protonated cyclohexadienone) was the exclusive product of isomerization and there were no signs of decomposition caused by heating. The reactant and product ions were identified on the basis of their  $^1\text{H}$  NMR spectra (Tables 3.1, 3.2 and 2.1), and in each case the products were identical to those observed previously.[2,3b,5,6] The  $^1\text{H}$  NMR spectra measured before and after isomerization of **22H** are shown in Figure 3.22.

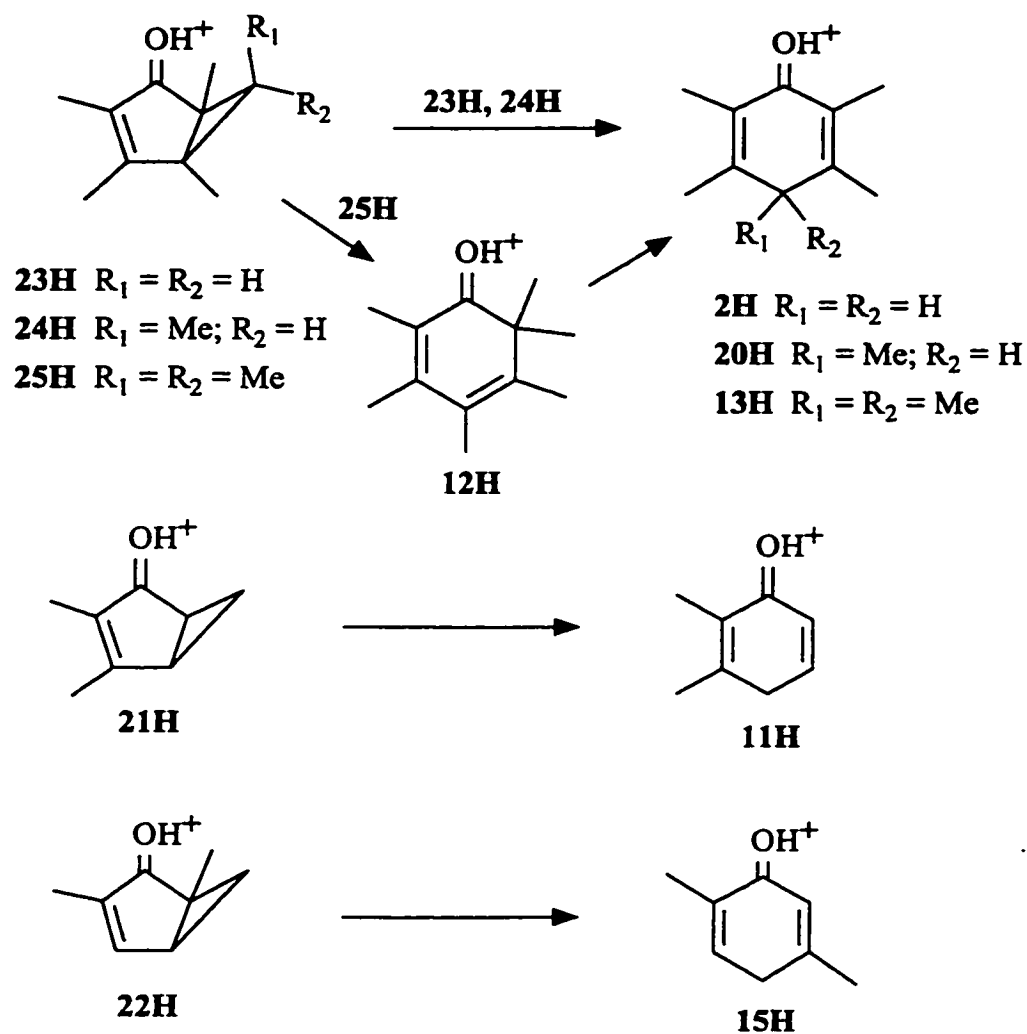


Figure 3.21: Isomerizations of protonated bicyclo[3.1.0]hex-3-en-2-ones to protonated phenols or cyclohexadienones.

Table 3.1: <sup>1</sup>H NMR data for neutral and protonated bicyclo[3.1.0]hex-3-en-2-ones.<sup>a,b</sup>

cmpd	chemical shift (δ, ppm)					
	3	1	5	6-exo	6-endo	
<b>21</b>	2.17 m	1.49 s	2.03 s	1.94 m	1.32 ddd(8.5, 7.5, 3.5)	1.00 q(4)
<b>22</b>	1.29 s	1.55 d(2)	7.08 m	2.01 p(3)	1.14	1.09 t(2.5)
<b>23</b>	1.32 s	1.51 s	1.96 s	1.25 s	1.21 d(3)	0.82 d(3)
<b>24</b>	1.31 s	1.58 s	1.89 s	1.18 s	<sup>c</sup>	0.91 d(5.5)
<b>25</b>	1.21 s	1.57 s	1.89 s	1.11 s	1.11 s	0.92 s
<b>21H</b>	3.27 m	1.75 s	2.45 s	3.52 p(3.5)	2.36 m	2.59 q(4)
<b>22H</b>	1.74 s	1.92 s	8.41 bs	3.57 m	2.37 dd(6.5, 3.5)	2.99 t(4)
<b>24H</b>	1.63 s	1.90 s	2.33 s	1.58 s	2.9	1.21 d(6.5)

a) s = singlet, d = doublet, t = triplet, q = quartet, p = pentet, b = broad. Values in brackets are coupling constants in Hz.

b) Neutral ketones in CCl<sub>4</sub>; relative to TMS. Protonated ketones in CF<sub>3</sub>SO<sub>3</sub>H; relative to (CH<sub>3</sub>)<sub>4</sub>N<sup>+</sup> BF<sub>4</sub><sup>-</sup> at 3.10 ppm.

c) Signal for H-6<sub>exo</sub> was not detected.

Table 3.2: <sup>1</sup>H NMR data for protonated phenols.<sup>a</sup>

cmpd	chemical shift (δ, ppm)				
	2	3	4	5	6
<b>19H</b>	2.30 s	8.23 bs	4.1 bs <sup>b</sup>	8.23 bs	2.30 s
<b>20H</b>	2.14 s	2.39 s	1.49 d(8) 3.62 q(8)	2.39 s	2.14 s

a) in CF<sub>3</sub>SO<sub>3</sub>H; relative to (CH<sub>3</sub>)<sub>4</sub>N<sup>+</sup> BF<sub>4</sub><sup>-</sup> at 3.10 ppm. s = singlet, d = doublet, q = quartet, b = broad. Values in brackets are coupling constants in Hz.

b) broad signal is barely detectable at room temperature.

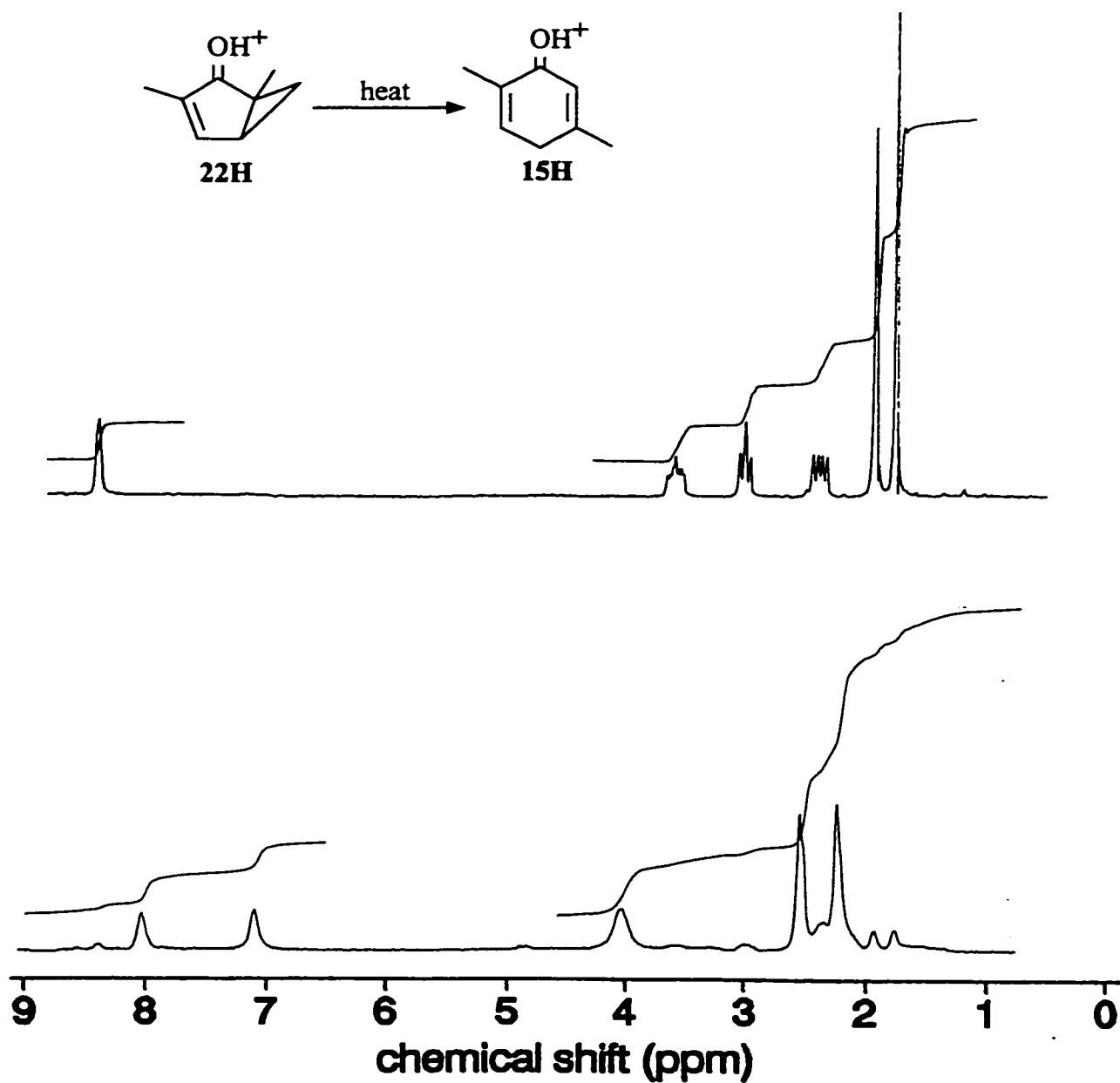


Figure 3.22:  $^1\text{H}$  NMR spectrum of protonated 1,3-dimethylbicyclo[3.1.0]hex-2-enone, **22H**, in triflic acid before (top) and after (bottom) isomerization to protonated 2,5-dimethylphenol, **15H**, by heating at  $100\text{ }^\circ\text{C}$  for ca. 80 min. Note: after 80 min. isomerization is incomplete and the solution contains ca. 7% of **22H**.



The rates of isomerization and activation barriers were determined for three isomerizations (Table 3.3) and were similar to those found in the literature.[6]

Table 3.3: Rate constants, activation barriers, and enthalpies of reaction for isomerization of protonated bicyclo[3.1.0]hex-3-en-2-ones to protonated phenols in triflic acid.

rxn	T (°C)	$10^4k$ (s <sup>-1</sup> )	$\Delta G^\ddagger$ (kcal/mol)	$-\Delta H_R$ (kcal/mol)	T(peak) <sup>a</sup> (°C)
21H - 11H	130	1.14	31.1 <sup>b</sup>	12.0 ± 0.2	110 - 180
22H - 15H	100	5.3	27.6 <sup>c</sup>	18.1 ± 0.6	75 - 140
23H - 2H			26.3 <sup>d</sup>	13.7 ± 0.7	50 - 125
24H - 20H			25.8 <sup>d</sup>	11.6 ± 0.6	55 - 115
25H - 12H			20.5 <sup>e</sup>	8.4 ± 0.5	0 - 50
12H - 13H	100	≈220	≈24.8 <sup>f</sup>	1.86 ± 0.10	40 - 100
25H - 13H				10.3 ± 0.5 <sup>g</sup>	
23 - 2 <sup>h</sup>				≈21	

a) temperature range from beginning to end of peak for scan rate of 1 °C/min.

b) cf.  $\Delta G^\ddagger = 30.7$  kcal/mol at 100 °C (R.F. Childs, B.E. George, *Can. J. Chem.*, 1988, 66, 1350).

c) cf.  $\Delta G^\ddagger = 27.2$  kcal/mol at 100 °C (R.F. Childs, B.E. George, *Can. J. Chem.*, 1988, 66, 1350).

d) from R.F. Childs, B.E. George, *Can. J. Chem.*, 1988, 66, 1350.

e) from R.F. Childs, S. Winstein, *J. Am. Chem. Soc.*, 1974, 96, 6409; in FSO<sub>3</sub>H.

f) cf.  $\Delta G^\ddagger = 24.1$  kcal/mol at 61 °C in FSO<sub>3</sub>H (R.F. Childs, *Chem. Comm.*, 1969, 946).

g) sum of preceding two entries.

h) Acid catalyzed isomerization in 0.18 M CF<sub>3</sub>SO<sub>3</sub>H/nitrobenzene.

### 3.3.2 Heats of Isomerization

As outlined in chapter 2 the accurate measurement of heats of isomerization by DSC requires a clean and quantitative reaction from a single reactant to a single product. The  $^1\text{H}$  NMR results outlined in the preceding section show that each of the reactions under investigation met this requirement.

The  $^1\text{H}$  NMR spectra of a 1.2 M solution of bicyclic ketone **21** in triflic acid was found to be nearly identical to that found in the literature.[1] Thus, the bicyclo[3.1.0]hexenones are cleanly and completely protonated at the higher cation concentrations needed for DSC analysis. In chapter 2, the protonation of phenols at the concentrations needed for DSC analysis was discussed.

The heats of isomerization ( $\Delta H_{\text{R}}$ ) for the reactions shown in Figure 3.21 were measured by DSC and the results are presented in Table 3.3. A typical thermogram for the **22H** to **15H** isomerization is shown in Figure 3.23.

The question of reliability of the DSC values will be addressed in the following sections as these values are compared to other experimental measures. It is possible to make a preliminary comparison of the magnitude of  $\Delta H_{\text{R}}$  measured by DSC with those determined by Childs and Mulholland for the isomerization of two bicyclo[3.1.0]hex-3-en-2-yl ions.[21] As illustrated in Figures 3.17 and 3.18, they determined  $\Delta H_{\text{R}}$  values from heats of protonation in fluorosulfuric acid. While the DSC and solution calorimetry experiments involve quite different procedures, the  $\Delta H_{\text{R}}$  values from solution calorimetry ( $-8.9 \pm 0.8$  and  $-12 \pm 2$  kcal/mol) are of comparable magnitude to those measured by DSC which range from  $-8.4$  to  $-18.1$  kcal/mol.

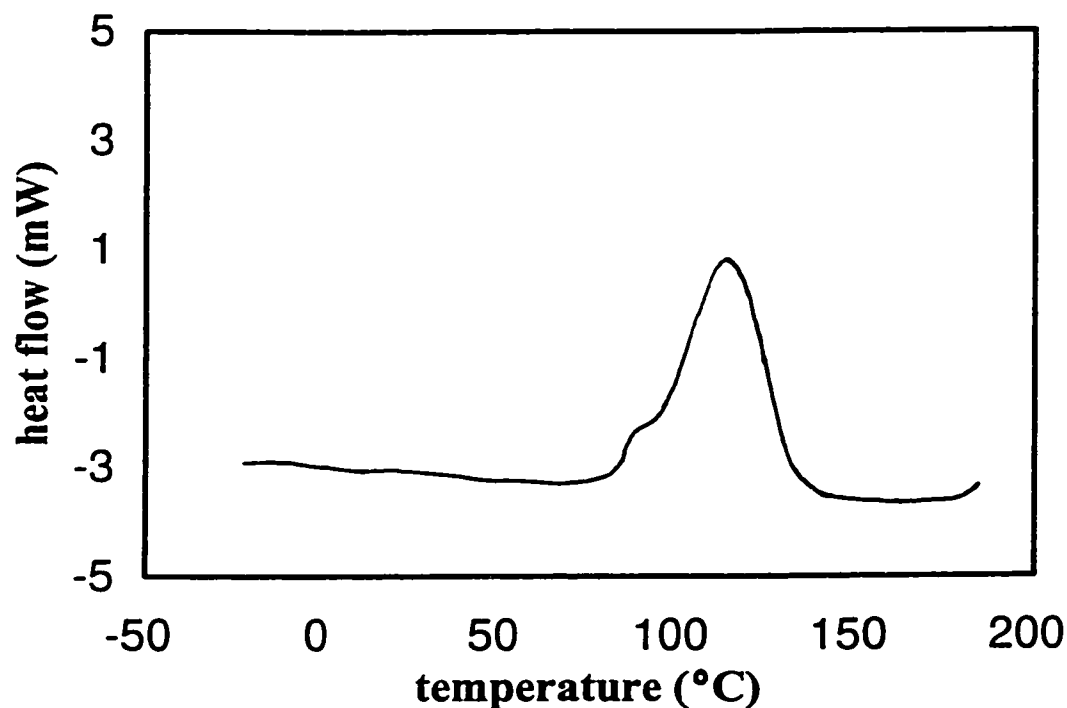


Figure 3.23: DSC thermogram for the isomerization of protonated 1,3-dimethylbicyclo[3.1.0]hexenone, **22H**, to protonated 2,5-dimethylphenol, **15H**, in triflic acid. Scan rate = 1 °C/min; sample size = 10.6 mg of **22**.

Discussion of the  $\Delta H_R$  values is presented in three sections: 1) the effect of methyl substitution at C6, the bridging carbon, of the bicyclo[3.1.0]hex-3-en-2-ones, 2) the effect of methyl substitution on the five-membered ring of the bicyclo[3.1.0]hex-3-en-2-one, and 3) discussion of the factors that determine the magnitude of  $\Delta H_R$ .

### 3.3.3 Effect upon $\Delta H_R$ of Methyl Substitution at C6

Ions **23H-25H** differ in the number of methyl groups at C6 while the remainder of the substituents are identical (Figure 3.24). Each of **23H-25H** isomerizes to a cyclohexadienyl cation in which the  $sp^3$  centre, C4, bears the same substituents as those on C6 of the reactant. The isomerization of **25H** to **13H** occurs in two distinct steps (**25H**

to **12H**; **12H** to **13H**) and  $\Delta H_R$  for the **25H/13H** isomerization is the sum of the  $\Delta H_R$  values for the two steps. The changes in  $\Delta H_R$  for the cations **23H-25H** provide information about the charge distribution at C6 of the bicyclo[3.1.0]hexenyl cation and C4 of the cyclohexa-2,5-dienyl cation.

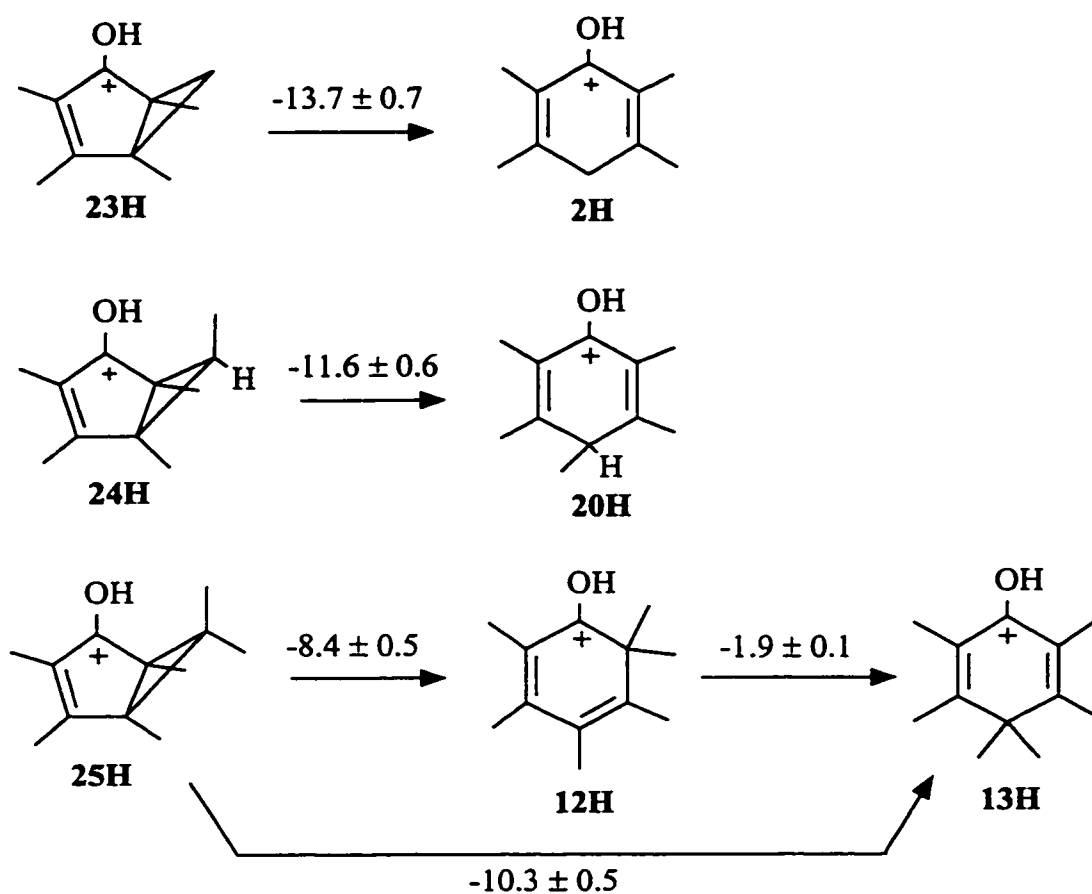


Figure 3.24: Isomerizations of protonated bicyclo[3.1.0]hex-3-en-2-ones which differ in the degree of methyl substitution at C6.  $\Delta H_R$  in kcal/mol are shown above the arrows.

The trend in  $\Delta H_R$  values shown in Figure 3.24 is clear; as methyl groups are added to C6 of the bicyclo[3.1.0]hex-3-en-2-one, the isomerization becomes less exothermic. ( $\Delta H = -13.7 \pm 0.7$ ;  $-11.6 \pm 0.6$ ;  $-10.3 \pm 0.5$  kcal/mol) Thus, methyl substitution at C6

of the bicyclohexenyl cation causes the energy of the reactant to be lowered to a greater extent than that of the product cyclohexadienyl cation.

Methyl substitution will affect  $\Delta H_R$  if isomerization causes changes in the charge delocalization, steric interactions or solvation involving the substituent.  $\Delta H_R$  will become less exothermic if methyl substitution causes greater steric strain or greater hindrance of solvation in the cyclohexadienyl cation, or if more charge is delocalized to C6 of the bicyclohexenyl cation than to C4 of the cyclohexadienyl cation.

There is no evidence that the methyl groups are placed in a more sterically-constricted environment in the cyclohexadienyl cation than in the bicyclohexenyl cation, however, the effect of the methyl groups on solvation may be important. While electrostatic solvation of both ions (at C2 and C4 of the bicyclohexenyl ion, and C3 and C5 of the cyclohexadienyl ion) may be hindered by the addition of methyl groups,[24] the loss of hydrogen-bonding to H4 in the cyclohexadienyl ion may be key.  $^1\text{H}$  NMR studies[25] of phenols in strong acids clearly show the strong interaction between H4 and solvent since this hydrogen is rapidly exchanged with the solvent. Methyl substitution at the site of protonation in aromatic compounds is believed to reduce the basicity by a factor of about 10-20.[26] However, Childs and Mulholland[21] observed that hexamethyl and pentamethylbenzene have nearly identical heats of protonation;  $\Delta H_p = -6.5 \pm 0.1$  and  $-6.3 \pm 0.2$  kcal/mol, respectively. Protonation of pentamethylbenzene would be more exothermic than that of hexamethylbenzene if solvation via the ring protons were of great importance.

In the cyclohexa-2,5-dienyl cation charge is delocalized principally to C1, C3 and

C5 and to substituents on these positions. The substituent(s) at C4 plays, at best, a minor role via a weak inductive effect. The nearly identical heats of protonation of hexa- and pentamethylbenzenes indicate that substitution of a methyl group at C4 causes no increase (or decrease) in stabilization of the cyclohexadienyl cation.

Charge delocalization in the bicyclo[3.1.0]hexenyl cations was discussed earlier. A variety of studies[1-9,11,13] have concluded that charge is delocalized to C6 of the bicyclo[3.1.0]hexenyl cation, so methyl substitution at this site should stabilize the cation. Thus, the changes in  $\Delta H_R$  with C6 methyl substitution is entirely consistent with the picture of the charge delocalization and it seems clear that C6 methyl groups provide stabilization of charge in the bicyclo[3.1.0]hex-3-en-2-yl ion.

As presented earlier, Childs and Mulholland[21] determined  $\Delta H_R$  for the **25H/12H** isomerization from the difference in heats of protonation in  $\text{FSO}_3\text{H}$  (see Figure 3.18). The  $\Delta H_R$  value measured by DSC ( $-8.4 \pm 0.5$  kcal/mol) is more than 3 kcal/mol lower than that measured by Childs and Mulholland ( $-12 \pm 2$  kcal/mol).[21] However, the experiments involve quite different procedures and conditions. Triflic acid ( $H_0 \approx -13$ ) used in the DSC measurements and fluorosulfuric acid ( $H_0 \approx -14$ ) used in solution calorimetry differ in acid strength by a factor of about ten.[27] The heat of isomerization determined by solution calorimetry includes a correction for the heat capacity of the substrate, which is at room temperature. Another drawback to the solution calorimetry technique is that the neutral bicyclic ketone, **25**, is a low melting solid which makes handling difficult. It was introduced to the calorimeter as a solution in carbon tetrachloride, and the  $\Delta H_R$  value must be corrected for contributions due to the carbon

tetrachloride. In light of the corrections (heat capacities of **25** and  $\text{CCl}_4$ ) required in solution calorimetry, the different acid media and the magnitude of the errors, the two values are in reasonable agreement. The  $\Delta H_R$  value determined by DSC would be expected, for this isomerization at least, to give a more accurate measure of the energy differences between reactant and product cations.

#### *3.3.4 Effect upon $\Delta H_R$ of Methyl Substitution on the Five-Membered Ring of the Bicyclo[3.1.0]hexenyl Cation*

Ions **21H-23H** are unsubstituted at C6 but differ in the substitution pattern on the five-membered ring of the bicyclo[3.1.0]hexenyl ion (Figure 3.25). In each case, isomerization of the bicyclohexenyl ion produces a cyclohexadienyl ion in which the methyl groups are attached to unsaturated carbons.

The  $\Delta H_R$  values (Figure 3.25) show that the location of the methyl groups on the five-membered ring in the bicyclo[3.1.0]hexenyl reactant has a pronounced effect on the heat of isomerization. For instance, the heat of isomerization of **22H** is 6 kcal/mole more exothermic than the rearrangement of the closely related ion **21H**.

Methyl substitution will affect  $\Delta H_R$  by changing the energy of the reactant and/or the product. In the case of the **21H** and **22H** isomerizations, the energy of the two products, **11H** and **15H**, would be expected to be similar. In both products, there is one methyl group at C2 while the other is at a charge-bearing centre (C3 or C5). Cation **11H** has an ortho interaction between the methyl groups which is not present in **15H** and this will raise the energy of **11H**

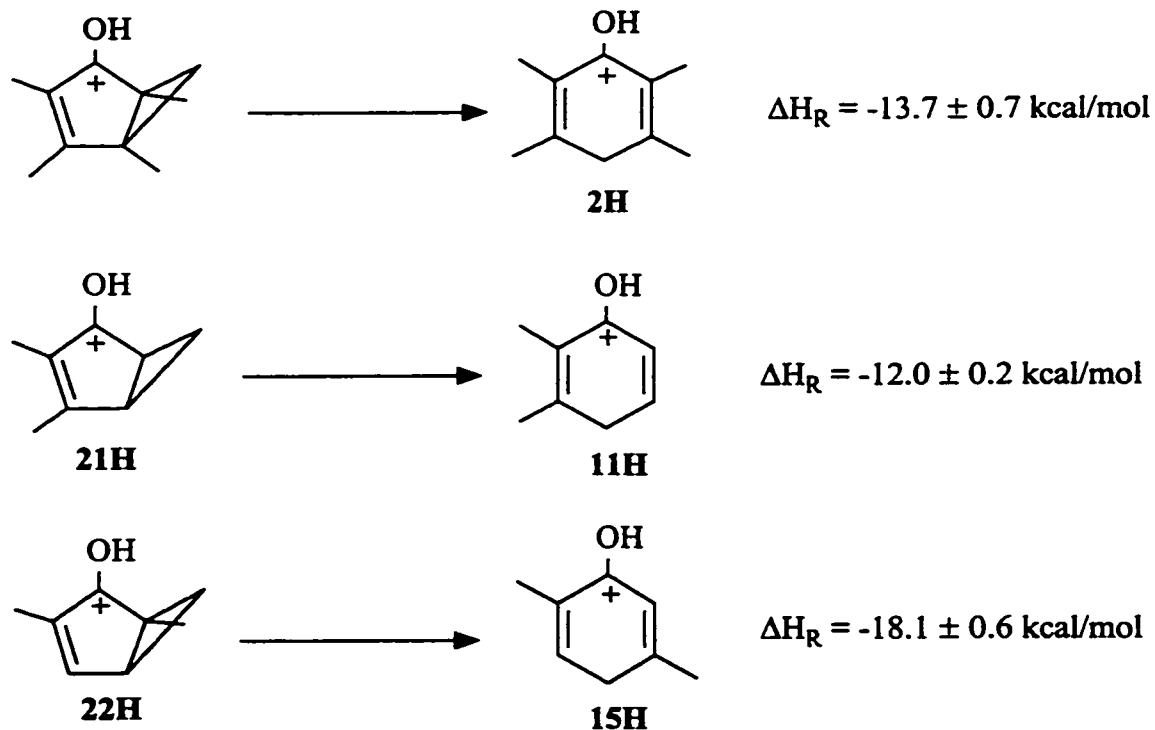


Figure 3.25: Isomerizations for bicyclo[3.1.0]hexenyl ions with different substitution patterns on cyclopentyl ring.

by about 1 kcal/mol relative to **15H**.<sup>[28-30]</sup> This means that **22H**, the 1,3-dimethylbicyclo[3.1.0]hexenyl ion, must be about 5 kcal/mol higher in energy than the 3,4-dimethyl isomer, **21H**. The relative energies of the ions are illustrated in Figure 3.26.

The estimated 5 kcal/mole energy difference between **21H** and **22H** can be compared to the analogous isomerizations involving methyl migration from an  $sp^3$  to an  $sp^2$  centre (discussed in chapter 2). The isomerizations of **4H** and **3H**, which involved methyl migration from an  $sp^3$  centre to the electron-deficient terminal position of the  $\pi$ -system, had  $\Delta H_R$  values of  $-4.1 \pm 0.2$  and  $-3.4 \pm 0.2$  kcal/mole, respectively. The best comparison can be made between **21H/22H** and **5H/4H** since each pair of ions is



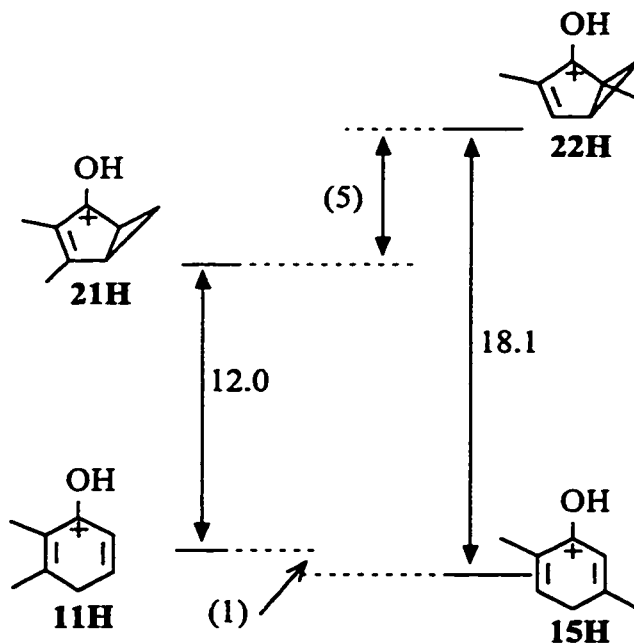


Figure 3.26: Relative energies (kcal/mol) of dimethyl isomers in triflic acid. Values in brackets are estimates.

interconverted by moving a methyl group from an  $sp^3$  centre to the 3-position of a 1-hydroxy-allyl cation (Figure 3.27). The estimated energy difference between **21H** and **22H** of ca. 5 kcal/mole is in fairly good agreement with this value.

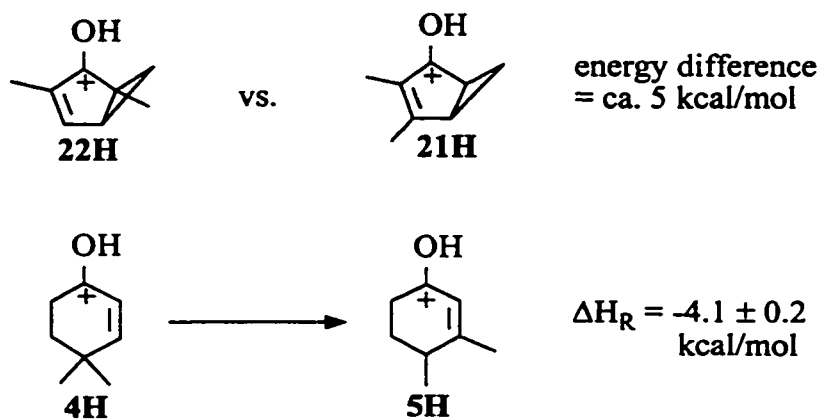


Figure 3.27: Comparison of energy difference between the two dimethyl bicyclohexenyl isomers with  $\Delta H_R$  for the isomerization of protonated 4,4-dimethylcyclohex-2-enone.

The comparison of  $\Delta H_r$  values for the isomerization of **23H** with that of either **22H** or **21H** is more problematic. The addition of methyl groups at C1 and C5 of bicyclo[3.1.0]hex-3-en-2-yl ion **21H** (see Figure 3.26) should formally have little effect on the relative stability of the ion. On the other hand, methyl groups at C5 and C6 of cyclohexa-2,5-dienyl ion **11H** should lead to a marked stabilization of this cation. In chapter 2, it was found that methyl groups on C5 and C6 stabilized the cyclohexadienyl ion by 3.4 and 2.2 kcal/mol, respectively. This would be offset by two new ortho interactions (ca. 0.6 kcal/mol each) and, thus, the extra methyl groups might lower the energy of the cyclohexadienyl cation by about 4 to 4.5 kcal/mole. Based on this rationale, the isomerization of **23H** should be more exothermic than that of **21H**, by ca. 4 to 4.5 kcal/mole. The isomerization of **23H** is more exothermic than that of **21H** but only by 1.7 kcal/mole. The reason for this discrepancy is not clear. Further study of the bicyclo[3.1.0]hex-3-en-2-yl and cyclohexadienyl ions (theoretical calculations of their energies, ion solvation studies) may clarify this problem.

### 3.3.5 The Bicyclo[3.1.0]hexenyl/Cyclohexadienyl Energy Difference

The energy difference between the bicyclo[3.1.0]hexenyl and cyclohexadienyl cations is a combination of several contributions: 1) bond energies; 2) strain energies; and 3) charge stabilization.

The bond energy will be changed upon isomerization if there is a change in the number and type of bonds. For instance, isomerization of the bicyclo[3.1.0]hexenyl framework (formally one double and six single bonds) to the cyclohexadienyl framework

(two double and four single bonds) results in the loss of two C-C single bonds and the creation of one new C-C double bond.

There is a significant decrease in the strain energy with isomerization from the bicyclo[3.1.0]hexenyl to cyclohexadienyl cations. Isomerization converts a system with a cyclopropane ring fused to a cyclopentenyl ring (bicyclo[3.1.0]hexane ring strain = 32.7 kcal/mol) to one with a single cyclohexadienyl ring (cyclohexadiene ring strain = 0.5–4.8 kcal/mol).[29]

Differing charge stabilizing abilities between the bicyclo[3.1.0]hexenyl or cyclohexadienyl frameworks will also be important. If one of the systems is more effective at stabilizing positive charge in the cation this will contribute to the overall energy difference.

The magnitude of the bond and strain contributions can be estimated. For instance, the 9.9 kcal/mol energy difference between bicyclo[3.1.0]hexane ( $\Delta H_f = 9.1$  kcal/mol) and cyclohexene ( $\Delta H_f = -0.8$  kcal/mol) calculated with the group additivity method[29] provides an approximation of the combined bond/strain energy contribution. Childs and Mulholland were also able to estimate the magnitude of the bond/strain contribution from differences in heats of protonation in  $\text{FSO}_3\text{H}$ . [21] In cases where isomeric bicyclo[3.1.0]hexenyl and benzenoid precursors gave the same cation upon protonation, the difference between the heats of protonation gave the relative energies of neutral precursors (see Figures 3.19 and 3.20 for two examples). The energy differences were then corrected for contributions due to resonance or conjugation so that an estimate of the bond/strain contribution could be extracted (Figure 3.28). Two of the estimates

(4.9 and 7.7 kcal/mol) are similar to that from the group additivity method but the 0 kcal/mol estimate based on the pentamethylbenzene system seems anomalously low. If the lowest estimate is disregarded, the bond/strain energy contribution is predicted to fall in the rather broad range of 5-10 kcal/mol.<sup>2</sup>

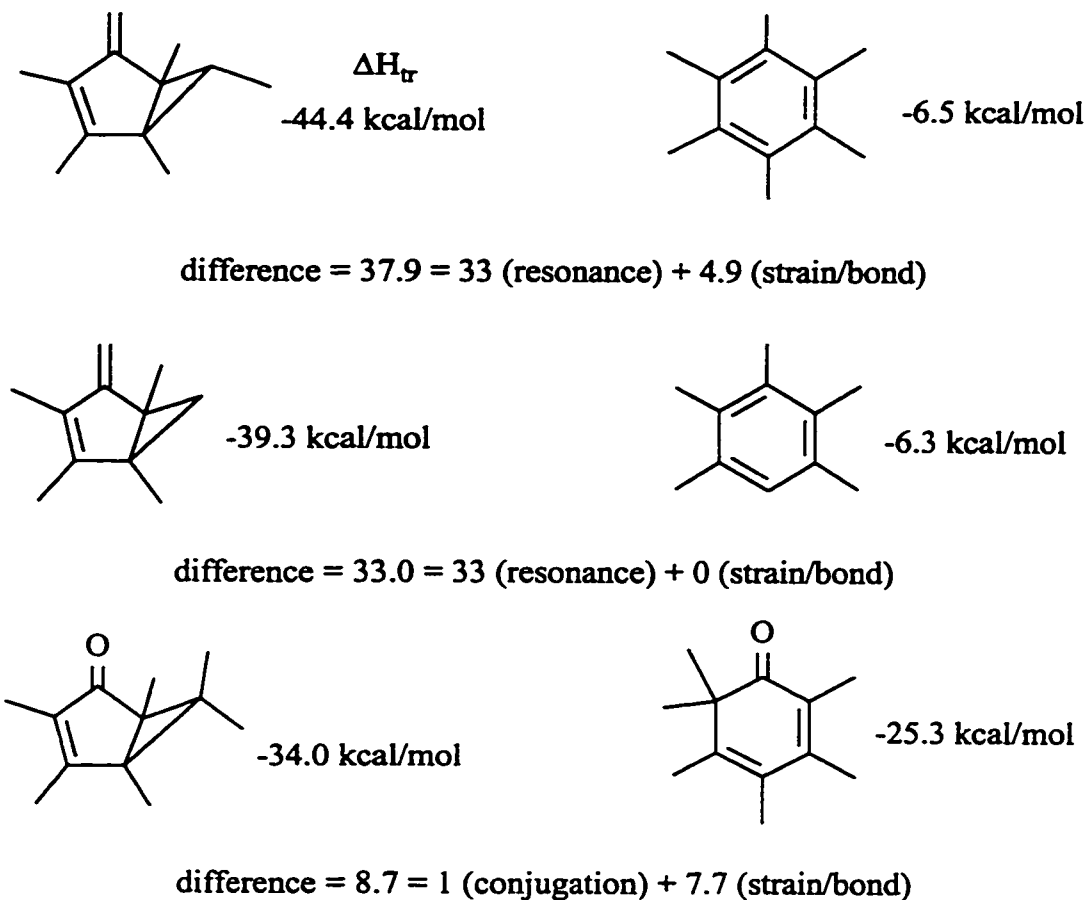


Figure 3.28: Each pair of molecules give the same cation upon protonation. The difference in the heats of protonation ( $\Delta H_{tr}$ ) reveals the relative energies of the molecules. The strain/bond energy contribution to the energy difference can be extracted by correcting for the contributions of resonance or conjugation.

<sup>2</sup> The bond/strain energy estimates in Figure 3.28 are somewhat different than those found in reference [21]. As mentioned earlier, an error was made in the calculation of the relative energies of some compounds in reference [21]. The raw data from reference [21] was used to generate the corrected values found in Figure 3.28.

The  $\Delta H_R$  values measured in this thesis for the isomerizations of protonated bicyclo[3.1.0]hex-3-en-2-ones are in almost all cases greater than the bond/strain energy estimates. For instance, in the **21H** to **11H** isomerization the methyl and hydroxy substituents are similarly placed in reactant and product, and thus  $\Delta H_R$  gives a measure of the energy difference between the bicyclo[3.1.0]hex-3-en-2-yl and cyclohexa-2,5-dienyl cations. The  $\Delta H_R$  value of  $-12.0 \pm 0.2$  kcal/mol is more exothermic than the strain/bond energy estimates. Improved charge stabilization must account for the additional exothermicity. This leads to the conclusion that charge stabilization by the cyclopropyl ring in the bicyclo[3.1.0]hexenyl cations is less efficient (by 2-7 kcal/mol) than that provided by the second double bond in the cyclohexadienyl cations.

Childs and Mulholland[21] had concluded that charge stabilization in the bicyclo[3.1.0]hexenyl cations was as effective as that in the cyclohexadienyl cations, and that the bond/strain energy changes were the sole driving force for isomerization. However, when the corrected bond/strain energy estimates in Figure 3.28 are used, their conclusions must be modified slightly; for both pairs of isomeric cations studied in their work (see Figures 3.17 and 3.18), the cyclohexadienyl cation provides about 4 kcal/mol more charge stabilization than the bicyclo[3.1.0]hexenyl isomers. This is in good agreement with the conclusion based on  $\Delta H_R$  values measured by DSC.

The theoretical calculations (STO-3G) of Cremer et al[13a] further support this conclusion. The energy of the parent bicyclo[3.1.0]hex-3-en-2-yl and cyclohexadienyl cations were calculated to differ in energy by 21 kcal/mole, well in excess of the bond/strain energy contribution. A similar energy difference is obtained if the reaction is

naively viewed as being driven by the change in the bond/strain energy (5-10 kcal/mol) plus the additional charge stabilization provided by a pentadienyl cation vs. an allyl cation. The resonance energy of the pentadienyl cation has been estimated to be 13 kcal/mol higher than an allyl cation[21,31], and thus  $\Delta H_R$  is predicted to be about -20 kcal/mol for the parent ion by this simple approach. Both the calculated value and the simple estimate are well in excess of the bond/strain estimates which indicates that improved charge stabilization in the cyclohexadienyl cation is an important driving force for the isomerization of bicyclo[3.1.0]hexenyl cations.

The discrepancy between the experimental and calculated values for  $\Delta H_R$  is due in part to the fact that the experimental values are for substituted ions in the condensed phase, while the calculations deal with isolated unsubstituted ions in the gas phase. It might be anticipated that the  $\Delta H_R$  value calculated for the parent ion would be attenuated in the presence of charge stabilizing substituents and solvation.

### *3.3.6 Catalyzed Isomerization: Energy Difference Between a Bicyclo[3.1.0]hexenone and a Phenol*

In order to get a more complete picture of the relative energies of species in the bicyclo[3.1.0]hexenyl/cyclohexadienyl family it would be valuable to have an experimental measure of the energy difference between neutral bicyclo[3.1.0]hexenones and phenols. Towards this end, the acid-catalyzed isomerization of **23** to **2** (Figure 3.29) in 2.26 weight% (0.18 M) triflic acid/nitrobenzene was investigated. The isomerization is 25 times slower than the rate for the fully protonated species,[6] so the fraction of

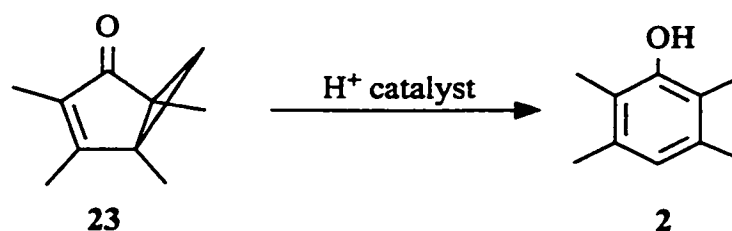


Figure 3.29: Acid catalyzed isomerization.

protonated bicyclo[3.1.0]hex-3-en-2-one **23H** can be estimated as 4%. The  $\Delta H_R$  value for this isomerization was found to be ca. -21 kcal/mole. It is based on only two measurements and the peaks in the DSC trace were oddly shaped, consisting of a sharp peak superimposed on a broad peak. Thus, this  $\Delta H_R$  value should be treated as tentative.

The rearrangement of the **23** to **2** is driven by both aromatization and strain/bond energy changes, and the  $\Delta H_R$  value can be compared to other estimates of these energies. It is useful to break the isomerization into two hypothetical steps, as illustrated in Figure 3.30. The first step, conversion of the bicyclo[3.1.0]hexenone to a cyclohexadienone, would be driven by bond/strain energy changes and these are estimated to be 5-10 kcal/mol. The second step, aromatization of a cyclohexa-2,5-dienone, is similar to the catalyzed isomerization of 4,4-dimethylcyclohexa-2,5-dienone, **8**, to 3,4-dimethylphenol, **9**, studied in chapter 2. The isomerization of **8** to **9** released  $-18.7 \pm 0.1$  kcal/mol so this leads to the prediction that ring opening of **23** to **2** should release about 24-29 kcal/mol. The uncertainty in the measured value as well as the discrepancy between the estimate of  $\Delta H_R$  (ca. -24 to -29 kcal/mol) and the measured value (-21 kcal/mol) shows that further work is required.





carbocations and their neutral precursors, and 2) ones which displays the relative energies of isomeric carbocations and the transition states which connect them. A variety of data is used to make the diagrams:  $\Delta H_R$  values in triflic acid,  $\Delta H_{tr}$  values in fluorosulfuric acid, and  $\Delta G^\ddagger$  values in triflic, fluorosulfuric, or sulfuric acid. Obviously the combination of  $\Delta H$  and  $\Delta G^\ddagger$  values is not strictly correct, and the use of data from acids of differing acid strengths introduces some uncertainty. However, it is useful to see a graphical representation of the relative energies of the cations and related compounds.

It should be pointed out that Childs[32] found that the rate of isomerization of **12H** to **13H** was the same in 85% and 95 % sulfuric and fluorosulfuric acid, which differ in acid strength by several orders of magnitude. This indicates that, at least for this reaction, there is not a strong interaction between the carbocations and the strong acid solvent. (Note: the presence of  $\text{SO}_3$  and other strong electrophiles did cause a dramatic rate acceleration[32]). Thus, the use of kinetic data measured in differing strong acid systems may be reasonable.

#### *The $\text{C}_6\text{H}_5\text{O}(\text{CH}_3)_2^+$ Isomers*

An energy diagram for several  $\text{C}_6\text{H}_5\text{O}(\text{CH}_3)_2^+$  isomers (protonated dimethylphenols and bicyclo[3.1.0]hex-3-en-2-ones) is shown in Figure 3.31. This diagram was constructed with measured  $\Delta H_R$  values, and by using some simple approximations based on the effects of methyl substitution on cation stability. For instance, the measured  $\Delta H_R$  values do not reveal the relative energies of protonated 2,3- and 2,5-dimethylphenols. Protonated 2,3-dimethylphenol would be ca. 1 kcal/mol higher

in energy due to the steric interaction of the ortho methyl groups.[28-30] With this correction the two halves of the energy diagram may be tied together. Similarly, protonated 2,6-dimethylphenol can be added to the energy diagram since it will be ca. 2 kcal/mol higher than protonated 2,3-dimethylphenol.

A second energy diagram (Figure 3.32) can be constructed from the activation barriers ( $\Delta G^\ddagger$ ) measured in this work and by Childs and George[6] in combination with the  $\Delta H_R$  values measured in this thesis.

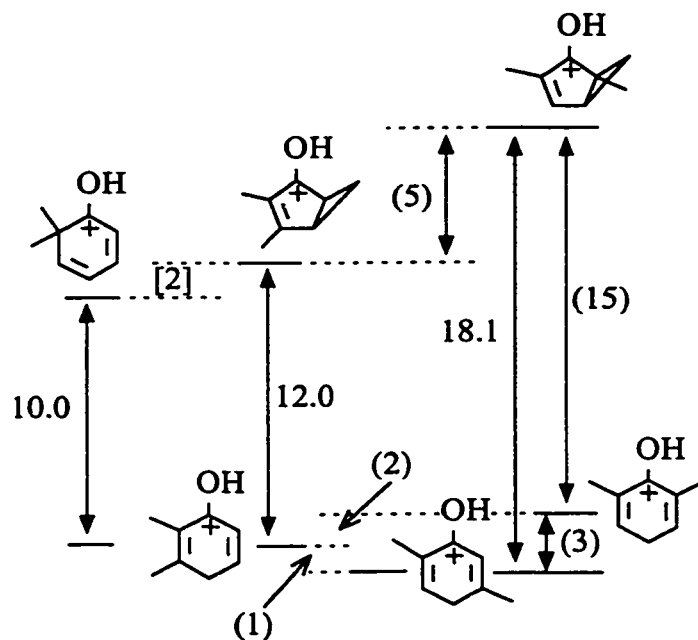


Figure 3.31: Relative energies (kcal/mol) of dimethyl isomers in triflic acid. Value in [ ] is the difference between measured  $\Delta H_R$  values. Values in ( ) brackets are estimates.

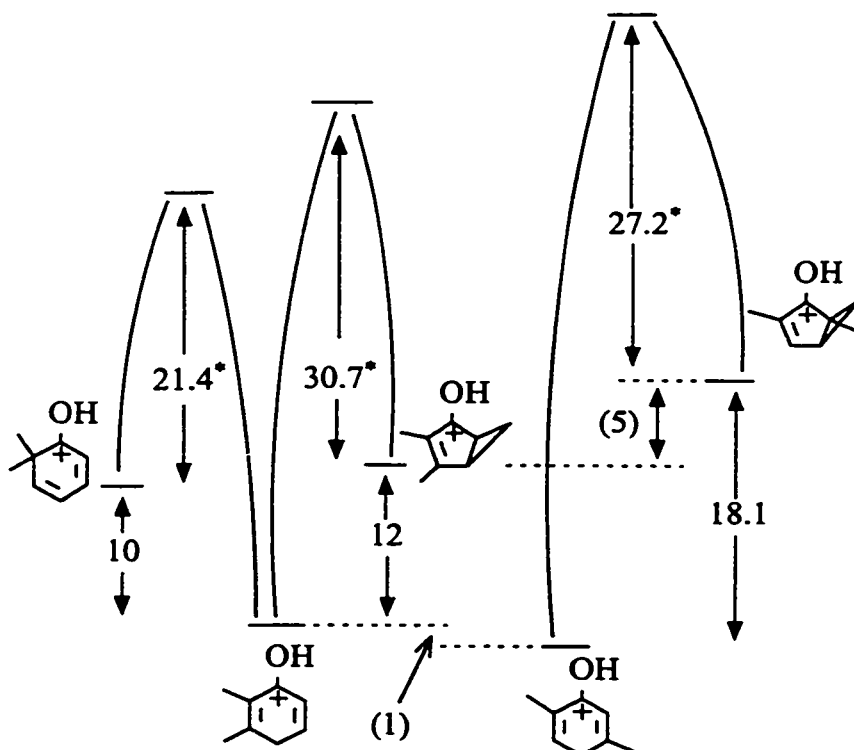


Figure 3.32: Relative energies (kcal/mol) of dimethyl isomers and transition states linking them.  $\Delta G^\ddagger$  (denoted by \*) and  $\Delta H_R$  are in kcal/mol in triflic acid. Values in brackets are estimates.

### *The $C_6H_3O(CH_3)_4^+$ Isomers*

The  $\Delta H_R$  values determined in this thesis were used to draw the energy diagram shown in Figure 3.33 for the  $C_6H_3O(CH_3)_4^+$  isomers. A second diagram (Figure 3.34) was drawn by combining the  $\Delta H_R$  values with  $\Delta G^\ddagger$  values,[6] and the  $\Delta H_r$  for 1,3,4,5-tetramethylbicyclo[3.1.0]hex-3-en-2-one in  $FSO_3H$ . [24]

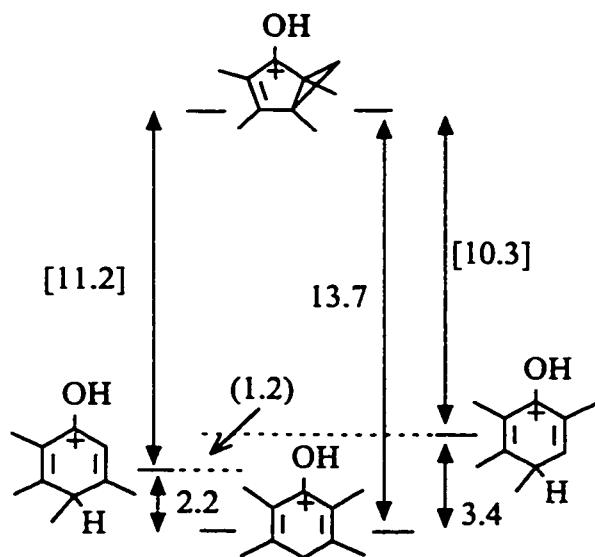


Figure 3.33: Relative energies (kcal/mol) of tetramethyl isomers in triflic acid. Values in brackets are differences between  $\Delta H_R$  values.

### *The $C_6HO(CH_3)_6^+$ Isomers*

An energy diagram (Figure 3.35) for the  $C_6HO(CH_3)_6^+$  isomers was constructed from the measured  $\Delta H_R$  values in combination with  $\Delta G^\ddagger$ [2,32] and  $\Delta H_\tau$  values[21] found in the literature and measured in  $FSO_3H$ .

### 3.4 Conclusion

DSC has proven to be a useful technique for measuring the heats of isomerization of protonated methyl-substituted bicyclo[3.1.0]hex-3-en-2-ones. Five methyl-substituted bicyclo[3.1.0]hex-3-en-2-ones were prepared by photochemical isomerization of their isomeric phenols in triflic acid solution. The bicyclo[3.1.0]hexenones were shown to be cleanly and completely protonated on the carbonyl oxygen, and to undergo quantitative

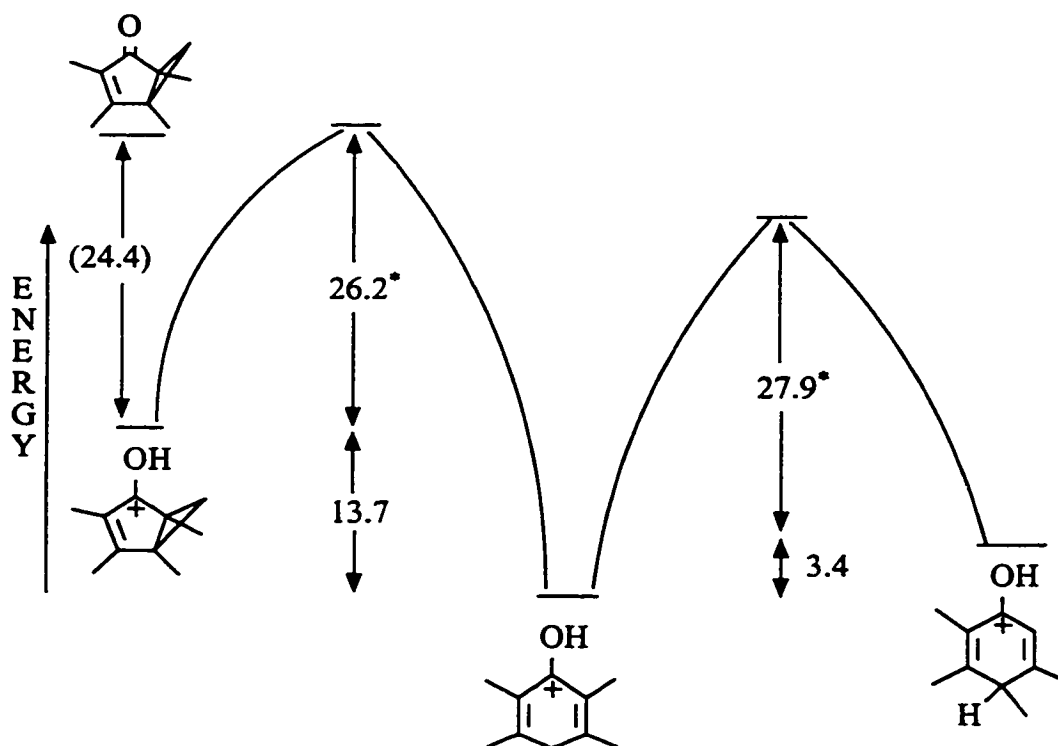


Figure 3.34: Relative energies (kcal/mol) of tetramethyl isomers and transition states linking them.  $\Delta G^\ddagger$  (denoted with \*) and  $\Delta H_R$  were measured in  $\text{CF}_3\text{SO}_3\text{H}$ . The value in brackets is  $\Delta H_T$  in  $\text{FSO}_3\text{H}$ .

isomerizations to cyclohexadienyl cations as revealed by  $^1\text{H}$  NMR.

Comparison of the heats of isomerization allowed conclusions to be drawn about the effect of methyl substituents on the stability of the 2-hydroxybicyclo[3.1.0]hexenyl cation. A methyl group placed on C6, the bridging carbon, of the bicyclo[3.1.0]hexenyl ion stabilizes this ion by 2 kcal/mol. A methyl group at C4, a formal charge bearing position, results in a 5 kcal/mol stabilization. These results were found to be consistent with the picture of charge delocalization derived from  $^1\text{H}$  NMR and other techniques.

The isomerization of the 2-hydroxybicyclo[3.1.0]hexenyl cation is driven by both

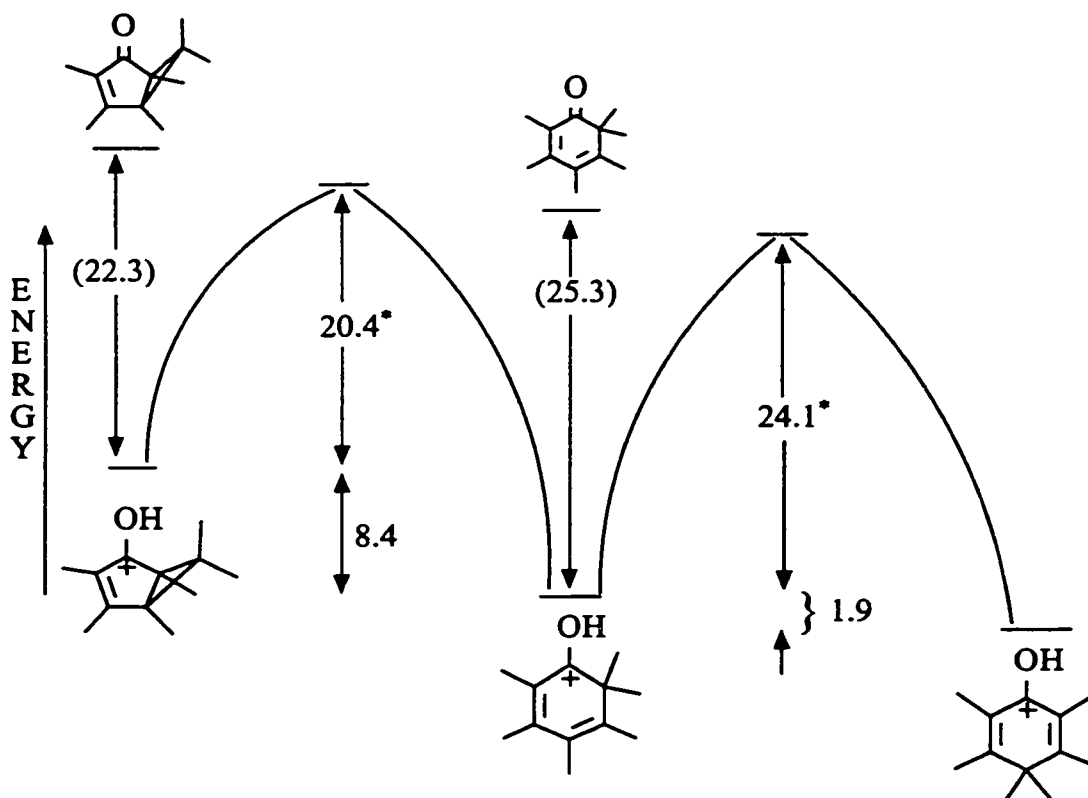


Figure 3.35: Relative energies (kcal/mol) of hexamethyl isomers and transition states linking them.  $\Delta H_R$  were measured in  $CF_3SO_3H$ .  $\Delta G^\ddagger$  (marked with \*) and  $\Delta H_{tr}$  (in brackets) were measured in  $FSO_3H$ .

a decrease in the bond and strain energies (5-10 kcal/mol for both) and to an increase in the stabilization of positive charge (2-7 kcal/mol) by the cyclohexadienyl cation vs. the bicyclohexenyl cation.

Previous work[21] had concluded that the strain/bond energy contribution accounted for the entire energy difference between the bicyclo[3.1.0]hexenyl and cyclohexadienyl frameworks. It is now clear that this conclusion was incorrect, due in part to arithmetical errors in the calculation of the strain/bond energies. Recalculation of the strain/bond energy contribution revealed that it fell in the broad range of 5-10

kcal/mole. The results described in this chapter show that energy released (ca. -12 kcal/mol) by ring opening of the bicyclohexenyl cation is greater than this value, and thus charge stabilization is more efficient in the cyclohexadienyl cation than in the bicyclo[3.1.0]hexenyl cation by at least 2 kcal/mol.

The thermodynamic information provided by DSC is consistent with that furnished by a variety of other techniques. Heats of isomerization provide a valuable quantitative measure of substituent effects in carbocations without some of the complications inherent in other measures of estimating stability (e.g. heats of protonation, rates of solvolysis, etc.).

### 3.5 References

1. R.F. Childs, B.E. George, *Can. J. Chem.*, **1987**, *66*, 1343.
2. R.F. Childs, M. Sakai, B.D. Parrington, S. Winstein, *J. Am. Chem. Soc.*, **1974**, *96*, 6403; R.F. Childs, S. Winstein, *J. Am. Chem. Soc.*, **1974**, *96*, 6409; R.F. Childs, M. Sakai, S. Winstein, *J. Am. Chem. Soc.*, **1968**, *90*, 7144; R.F. Childs, S. Winstein, *J. Am. Chem. Soc.*, **1968**, *90*, 7146.
3. a) R.F. Childs, B. Parrington, *Chem. Comm.*, **1970**, 1540; b) B. Parrington, R.F. Childs, *Chem. Comm.*, **1970**, 1581; c) R.F. Childs, B.D. Parrington, M. Zeya, *J. Org. Chem.*, **1979**, *44*, 4912.
4. a) V.A. Koptug, L.I. Kuzubova, I.S. Isaev, V.I. Mamatyuk, *Chem. Commun.*, **1969**, 389; b) V.A. Koptug, V.I. Mamatyuk, L.I. Kuzubova, I.S. Isaev, *Bull. Acad.*

- Sci. USSR, Div. Chem. Sci.*, 1969, 1524; c) I.S. Isaev, V.I. Mamatyuk, T.G. Egorova, L.I. Kuzubova, V.A. Koptug, *Bull. Acad. Sci. USSR, Div. Chem. Sci.*, 1969, 1954; d) V.A. Koptug, L.I. Kuzubova, I.S. Isaev, V.I. Mamatyuk, *J. Org. Chem. USSR*, 1970, 6, 1854; e) I.S. Isaev, V.I. Mamatyuk, L.I. Kuzubova, T.A. Gordymova, V.A. Koptug, *J. Org. Chem. USSR*, 1970, 6, 2493; f) V.I. Mamatyuk, A.I. Rezvukhin, I.S. Isaev, V.I. Buraev, V.A. Koptug, *J. Org. Chem. USSR*, 1974, 10, 662.
5. a) D.W. Swatton, H. Hart, *J. Am. Chem. Soc.*, 1967, 89, 5075; b) H. Hart, T.R. Rodgers, J. Griffiths, *J. Am. Chem. Soc.*, 1969, 91, 754; c) H. Hart, P.M. Collins, A.J. Waring, *J. Am. Chem. Soc.*, 1966, 88, 1005; d) H. Hart, D.W. Swatton, *J. Am. Chem. Soc.*, 1967, 89, 1874.
6. R.F. Childs, B.E. George, *Can. J. Chem.*, 1988, 66, 1350.
7. V.A. Koptug, *Top. Curr. Chem.*, 1984, 122, 1.
8. R.F. Childs, D. Cremer, G. Elia in *The Chemistry of the Cyclopropyl Group*, Z. Rappaport (ed.), Wiley, 1995, vol. 2, chpt. 8, p. 411.
9. a) P. Vogel, M. Saunders, N.M. Hasty, Jr., J.A. Berson, *J. Am. Chem. Soc.*, 1971, 93, 1551; b) G.A. Olah, G. Liang, S.P. Jindal, *J. Org. Chem.*, 1975, 40, 3259.
10. P. Warner, D.L. Harris, C.H. Bradley, S. Winstein, *Tetrahed. Lett.*, 1970, 4013; G.A. Olah, G. Liang, L.A. Paquette, M.J. Broadhurst, P. Warner, *J. Am. Chem. Soc.*, 1973, 95, 3386; J.F.M. Oth, D.M. Smith, U. Prange, G. Schröder, *Angew. Chem., Int. Ed. Engl.*, 1973, 12, 327.
11. S.K. Chadda, R.F. Childs, R. Faggiani, C.J.L. Lock, *J. Am. Chem. Soc.*, 1983, 105,



- 5069.
12. R.F. Childs, A. Varadarajan, C.J.L. Lock, R. Faggiani, C.A. Fyfe, R.E. Wasylshen, *J. Am. Chem. Soc.*, **1982**, *104*, 2452.
  13. D. Cremer, E. Kraka, T.S. Slee, R.F.W. Bader, C.D.H. Lau, T.T. Nguyen-Dang, P.J. MacDougall, *J. Am. Chem. Soc.*, **1983**, *105*, 5069; W.J. Hehre, *J. Am. Chem. Soc.*, **1972**, *94*, 8908; W.J. Hehre, *J. Am. Chem. Soc.*, **1974**, *96*, 5207; W.L. Jorgensen, *J. Am. Chem. Soc.*, **1976**, *98*, 6784; D. Cremer, R.F. Childs, E. Kraka in *The Chemistry of the Cyclopropyl Group*, Z. Rappaport (ed.), Wiley, 1995, vol. 2, chpt. 7, p. 339.
  14. H.E. Zimmerman, D.I. Schuster, *J. Am. Chem. Soc.*, **1962**, *84*, 4527; H.E. Zimmerman, J.S. Swenton, *J. Am. Chem. Soc.*, **1967**, *89*, 906; H.E. Zimmerman, *Pure Appl. Chem.*, **1964**, *9*, 493; D.I. Schuster, *Acc. Chem. Res.*, **1978**, *11*, 65; P.J. Kropp, *Org. Photochem.*, **1967**, *1*, 1.
  15. R.B. Woodward, R. Hoffmann, *The Conservation of Orbital Symmetry*, Academic Press, New York, 1970, p. 38; F.A. Carey, R.J. Sundberg, *Advanced Organic Chemistry*, Plenum Press, New York, 1990, part A, p. 596; T.H. Lowry, K.S. Richardson, *Mechanism and Theory in Organic Chemistry*, Harper & Row, New York, 1981, 2nd ed., p. 792, 862.
  16. T.S. Sorensen, A. Rauk, *Pericyclic Reactions*, A.P. Marchand, R.E. Lehr (eds.), Academic Press, New York, 1977, vol. 2, p. 1; C.W. Shoppee, B.J.A. Cooke, *J. Chem. Soc., Perkin Trans. 1*, **1972**, 2271; C.W. Shoppee, B.J.A. Cooke, *J. Chem. Soc., Perkin Trans. 1*, **1973**, 1026; N.W.K. Chiu, T.S. Sorensen, *Can. J. Chem.*,

- 1973, 51, 2776.
17. R.F. Childs, *Tetrahedron*, **1982**, 38, 567.
  18. R.B. Woodward, R. Hoffmann, *The Conservation of Orbital Symmetry*, Academic Press, New York, 1970, p. 114; F.A. Carey, R.J. Sundberg, *Advanced Organic Chemistry*, Plenum Press, New York, 1990, part A, p. 609; T.H. Lowry, K.S. Richardson, *Mechanism and Theory in Organic Chemistry*, Harper & Row, New York, 1981, 2nd ed., p. 764, 869.
  19. R.F. Childs, D.L. Mulholland, M. Zeya, A.K. Goyal, *Solar Energy*, **1983**, 30, 155
  20. H.-D. Scharf, J. Fleischhauer, H. Leismann, I. Ressler, W. Schleker, R. Weitz, *Angew. Chem. Int. Ed. Engl.*, **1979**, 18, 652.
  21. R.F. Childs, D.L. Mulholland, *J. Am. Chem. Soc.*, **1983**, 105, 96
  22. E.M. Arnett, R.P. Quirk, J.J. Burke, *J. Am. Chem. Soc.*, **1970**, 92, 1260.
  23. energies for the cyclohexadienyl cation are given in W.J. Hehre, J.A. Pople, *J. Am. Chem. Soc.*, **1972**, 94, 6901; energies for the bicyclo[3.1.0]hexenyl cation are given in W.J. Hehre, *J. Am. Chem. Soc.*, **1974**, 96, 5207.
  24. R.F. Childs, D.L. Mulholland, A. Varadarajan, S. Yeroushalmi, *J. Org. Chem.*, **1983**, 48, 1431.
  25. G.A. Olah, Y.K. Mo, *J. Org. Chem.*, **1973**, 38, 353; R.F. Childs, B.D. Parrington, *Can. J. Chem.*, **1974**, 52, 3303; S.M. Blackstock, K.E. Richards, G.J. Wright, *Can. J. Chem.*, **1974**, 52, 3313; G. Bertholon, R. Perrin, *Bull. Soc. Chim. Fr.*, **1974**, 113; S.M. Blackstock, M.P. Hartshorn, K.E. Richards, *Aust. J. Chem.*, **1980**, 33, 2753; B.E. George, Ph.D. Thesis, McMaster University, 1987, p53.

26. D.M. Brouwer, E.L. Mackor, C. MacLean, in *Carbonium Ions*, G.A. Olah, P.v.R. Schleyer (eds.), Wiley-Interscience, New York, 1970, vol. 2, p. 837.
27. G.A. Olah, G.K.S. Prakash, J. Sommer, *Superacids*, Wiley, New York, 1985, p.34; R. Jost, J. Sommer, *Rev. Chem. Intermediates*, **1988**, *9*, 171.
28. a)  $\Delta H_f$  (2,3-dimethylphenol) = -37.6 kcal/mol and  $\Delta H_f$  (2,5-dimethylphenol) = -38.7 kcal/mol from R.J.L. Andon, D.P. Biddiscombe, J.D. Cox, R. Handley, D. Harrop, E.F.G. Herington, J.F. Martin, *J. Chem. Soc.*, **1960**, 5246; b) D.M. Brouwer, *Rec. Trav. Chim.*, **1968**, *87*, 611.
29. S.W. Benson, F.R. Cruickshank, D.M. Golden, G.R. Haugen, H.E. O'Neal, A.S. Rodgers, R. Shaw, R. Walsh, *Chem. Rev.*, **1969**, *69*, 279; H.K. Eigmann, D.M. Golden, S.W. Benson, *J. Phys. Chem.*, **1973**, *77*, 1687.
30. D.M. Brouwer, *Rec. Trav. Chim.*, **1968**, *87*, 611.
31. N.C. Baird, *Tetrahedron*, **1972**, *28*, 2355.
32. R.F. Childs, *Chem. Comm.*, **1969**, 946.

## **Chapter 4: Isomerization of Protonated Cyclopropyl Ketones to Oxolanylium Ions**

In this and the following chapter the isomerization of protonated cyclopropyl ketones is explored. This chapter covers the characterization of the protonated cyclopropyl ketones, the identification and characterization of the isomerization products, and the thermochemistry of the isomerization. In the following chapter, kinetic and mechanistic aspects of the isomerizations are investigated.

### **4.1 Introduction**

Molecules containing the cyclopropyl group have a rich chemistry and as such the cyclopropyl group provides a fascinating research subject.[1] Cyclopropane, the most strained monocyclic alkane (strain energy = 27.6 kcal/mole[2]), has formal bond angles of 60°, a significant deviation from the optimum of 109° for an sp<sup>3</sup> hybridized atom. Both experimental[3,4] and theoretical[4] evidence reveal that the ring bonds of cyclopropane are bent so that the region of highest electron density lies not along the internuclear vector but is instead bowed out, away from the ring centre.

One consequence of the "bent" bonds is that the electron density is more accessible to electrophiles or adjacent conjugating groups. The same may be said of the  $\pi$ -electrons in an alkene and in many ways the properties of the cyclopropyl ring are similar to those of a double bond. For example, the cyclopropyl ring is a powerful

stabilizing group for carbocations,[5] and may act as an electronic relay in carbocations capable of forming a homoaromatic systems.[6] As well, cyclopropyl compounds exhibit many reactions (electrocyclic reactions, conjugate addition, electrophilic attack, reductive hydrogenation) typically associated with double bonds.[7]

#### *4.1.1 Cyclopropylcarbinyl Cations*

Cyclopropylcarbinyl carbocations in which the cyclopropyl ring is directly bound to the cation centre, have been well studied.[5,8,9] The cyclopropyl ring is an excellent stabilizing group for carbocations. For example, the relative rates of solvolysis found in the literature[9] for compounds substituted with isopropyl and cyclopropyl groups (Figure 4.1) show this clearly. Although each of the compounds has the same number of carbons, the rate of solvolysis becomes dramatically faster as each isopropyl group is replaced by a cyclopropyl ring. The isopropyl group has similar steric size, and thus ionization is not driven by relief of steric strain. In none of the reactions is the cyclopropyl ring broken, so the high rate of reaction is not caused by the release of ring strain upon ionization. The accelerated rates of solvolysis for cyclopropyl substituted compounds are due to the ability of this group to stabilize the carbenium ion formed upon ionization.

The lowest energy structure of the parent cyclopropylcarbinyl cation has been the subject of considerable study.[5,10,11] Theoretical calculations[5,10] and NMR studies[5,11] indicate similar energies for a bisected cyclopropylcarbinyl cation or a set of equilibrating bicyclobutonium ions. For most other cyclopropylcarbinyl cations the

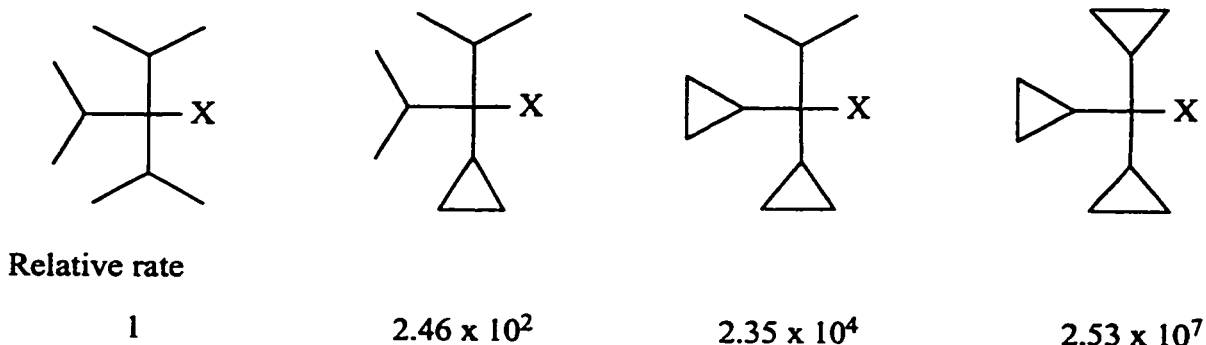


Figure 4.1: Rates of solvolyses of isopropyl/cyclopropyl substituted compounds. X = p-nitrobenzoate except for last compound where X=benzoate.

energetically preferred structure appears to be the bisected cyclopropylcarbinyl cation. For example, the  $^1\text{H}$  NMR spectrum of the 1,1-dimethyl substituted ion revealed a static species consistent with the bisected cyclopropylcarbinyl cation.[12,13] The methyl groups display two distinct signals separated by 0.5 ppm ( $^1\text{H}$  NMR) or 8.8 ppm ( $^{13}\text{C}$  NMR). A bisected geometry in which one methyl group sits in the face of the cyclopropyl ring (Figure 4.2) accounts for this observation. Shielding by the ring causes the signal for this methyl group to move upfield of the signal for the other methyl group.

As with double bonds, the extent of the interaction between the cyclopropyl ring and the conjugating group is dependent on molecular conformation. For a double bond, maximum conjugation is achieved when the  $\pi$ -orbital of the double bond is aligned (parallel) with the p or  $\pi$ -orbitals of the neighbouring group, however with a cyclopropyl ring the conformation of maximum overlap occurs when the p or  $\pi$ -orbital on the neighbouring carbon is aligned parallel to the distal bond (Figure 4.3).

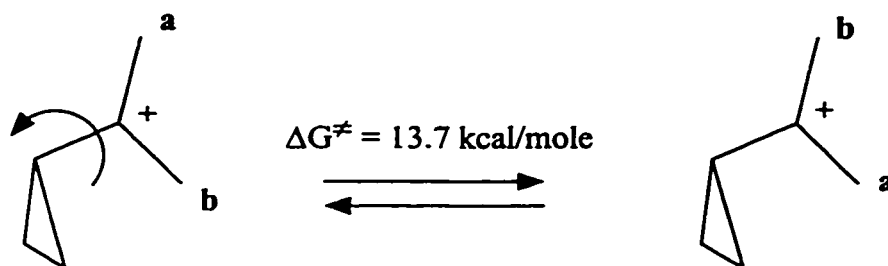


Figure 4.2: Rotation about C<sup>+</sup>-cyclopropyl bond exchanges methyl groups a and b.

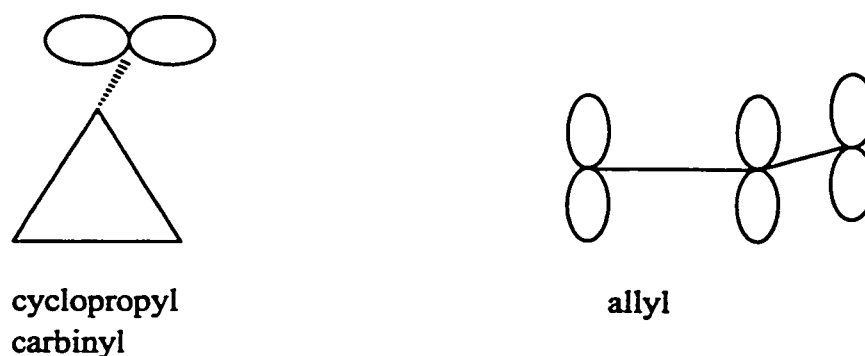


Figure 4.3: The geometry required for maximum orbital overlap in the cyclopropylcarbinyl and allyl systems.

The energetic preference for a bisected geometry is revealed by the barrier for rotation about the bond joining the cyclopropyl ring to the cation centre in the 1,1-dimethylcyclopropylcarbinyl cation (Figure 4.2).[14] The large energy barrier to rotation ( $13.7 \pm 0.4$  kcal/mol) illustrates the strength of the interaction between the cyclopropyl ring and cation centre.

One consequence of the conjugation of the cyclopropyl ring with an electron deficient centre is that electron density is transferred from the cyclopropyl ring to the cation centre. This leads to a weakening of the two vicinal cyclopropane bonds and the transfer of considerable positive charge to the two  $\beta$ -positions. Comparison of the  $^{13}\text{C}$

NMR spectra of cyclopropylcarbinyl cations and neutral precursors[5,11,12,13] confirms this charge transfer since the chemical shifts of the  $\beta$ -positions are affected to a greater extent than the  $\alpha$ -position. This behaviour is consistent with the resonance picture displayed in Figure 4.4.

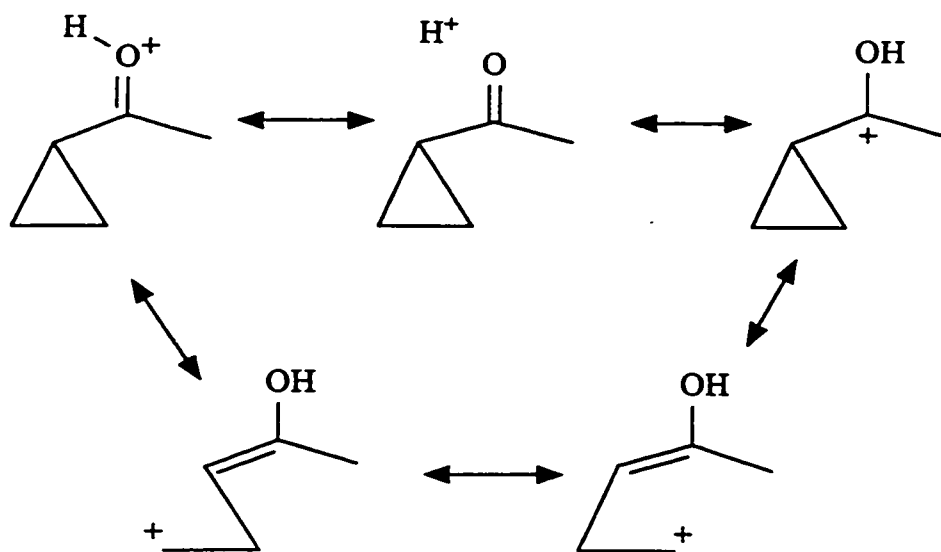


Figure 4.4: Resonance structures of a protonated cyclopropyl ketone.

Protonated cyclopropyl ketones can be viewed as hydroxy-substituted cyclopropylcarbinyl cations (Figure 4.4). While a significant fraction of the charge may reside on the oxygen atom, experimental studies have shown that protonated cyclopropyl ketones exhibit many of the properties of the cyclopropylcarbinyl cation. NMR studies of protonated cyclopropyl ketones have shown that a considerable amount of positive charge is delocalized into the cyclopropyl ring.

The crystal structures of several protonated cyclopropyl ketones, determined by



Childs and coworkers,[15] also show the cyclopropylcarbinyl nature of these ions. The structures of the five protonated cyclopropyl ketones were found to deviate no more than  $7^\circ$  from a perfectly bisected geometry. The cations displayed a lengthening of the vicinal bonds, and shortening of the distal and cyclopropyl-C+ bonds. The degree to which the bond lengths were altered was found to fall between that observed for neutral ketones and that calculated for the parent cyclopropylcarbinyl cation. The resonance structures of a protonated cyclopropyl ketone (Figure 4.4) help to explain the observed structural changes.

#### *4.1.2 Ring Expansion Reactions of Cyclopropyl Compounds*

The reactions of cyclopropyl compounds are dominated by reactions which open the ring and thus, reduce the strain energy. While ring openings are the most commonly observed reactions of cyclopropyl compounds, ring expansions form another important class of cyclopropyl reactions.[16] Ring expansion typically involves the cyclopropyl ring and a double bond with which it is conjugated and leads to a five-membered ring. The earliest examples of this type of reaction include the ring expansions of N-benzoylaziridine[17a] and 1,1-cyclopropanedicarboxylic acid[17b] and the acid catalyzed ring expansion of a cyclopropyl ketimine.[18] Perhaps the best known example of the ring expansion is the vinylcyclopropane to cyclopentene rearrangement which was first observed in 1959,[19] and continues to be the subject of mechanistic[20] and synthetic interest.[21] Examples of the cyclopropyl ketimine and vinylcyclopropane reactions are shown in Figure 4.5.

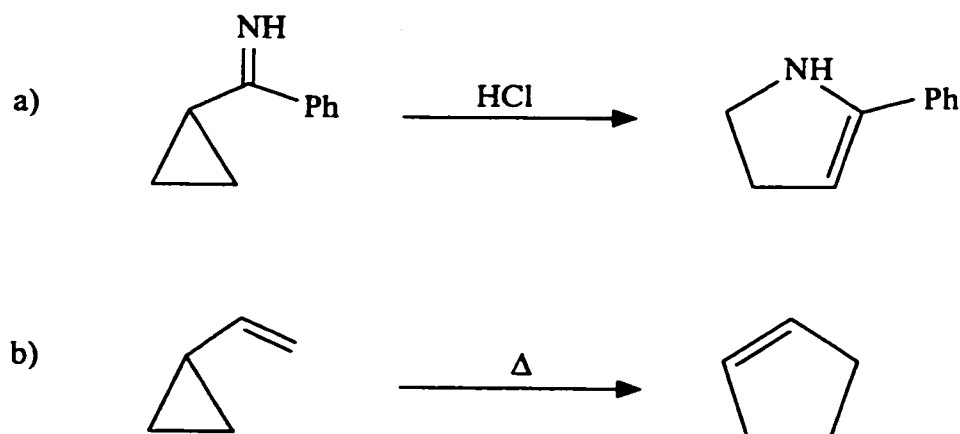


Figure 4.5: Ring expansion of a) cyclopropyl phenyl ketimine to 2-phenylpyrroline and b) vinylcyclopropane to cyclopentene.

There are many examples of the two reactions in Figure 4.5 as well as many other systems in which one or more of the carbon atoms of vinylcyclopropane have been replaced by heteroatoms. Ring expansion has been observed for compounds in which the cyclopropyl ring is conjugated to vinyl,[19-21] imine,[18,22] carboxylic acid,[17b,23] carbonyl,[24,25] azo,[26] and other functional groups.[27] There are also examples in which one or more of the carbon atoms of the cyclopropyl ring have been replaced with a heteroatom.[28] Several examples of ring expansions are displayed in Figure 4.6.[24,28d,28e,26a,28a]

As mentioned earlier, protonation of compounds such as cyclopropyl ketones, imines or carboxylic acids causes the transfer of positive charge to the cyclopropyl ring. However, unlike alkenes (eg. vinylcyclopropane) these functional groups can be protonated without loss of the  $\pi$ -system, and thus ring expansion to five membered rings is still available to these compounds. Formation of the protonated cyclopropyl compound

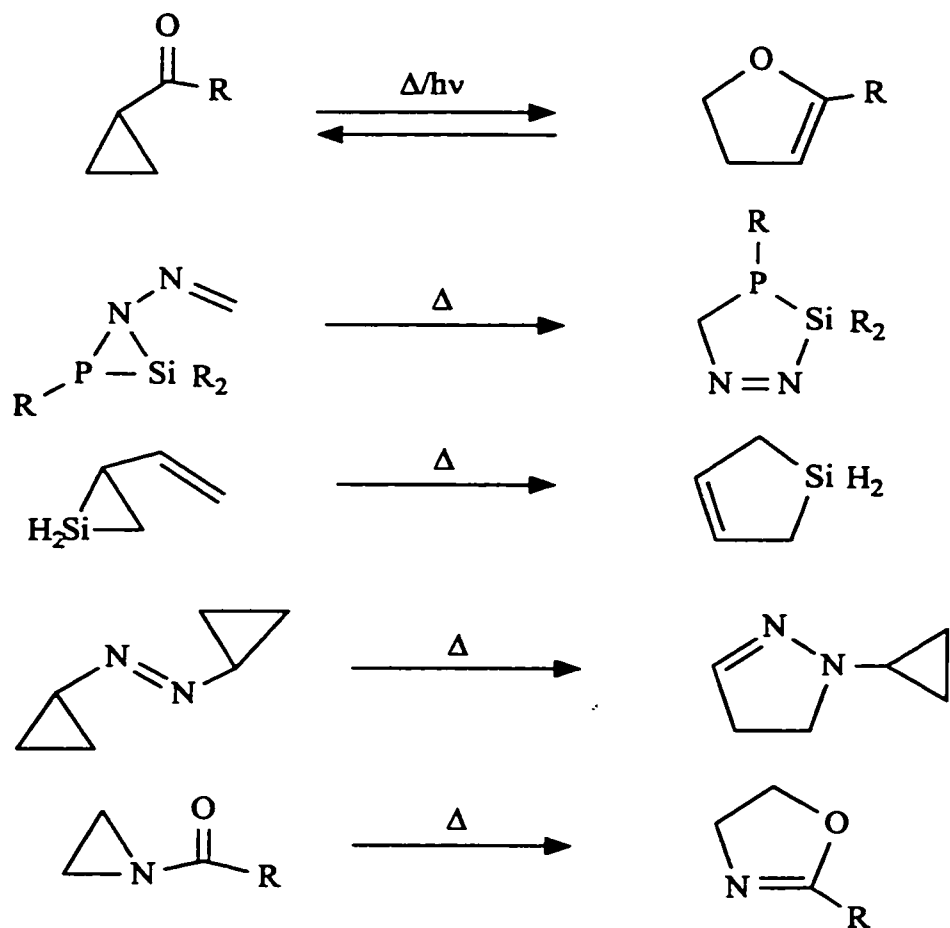


Figure 4.6: Reactions which involve ring expansion of cyclopropyl group and adjacent double bond to a five-membered ring.

can cause a weakening of the vicinal bonds of the cyclopropyl ring which facilitates reactions such as ring opening or ring expansion. There are a number of examples of cyclopropyl compounds which undergo ring expansion only when protonated.[22,23c,25a] The best known example is the ring expansion of protonated cyclopropyl imines.[22]

In many cases, ring expansion is a minor pathway for both protonated and neutral cyclopropyl compounds and the bulk of the product consists of acyclic material (alkenes,

enones, etc.) or decomposition products. For instance, thermolysis of vinylcyclopropanes[19-21] and protonated cyclopropanecarboxylic acids[23c] can lead to appreciable amounts of ring opened products.

In contrast to this behaviour, Pittman and McManus found that the exclusive reaction of several protonated cyclopropyl ketones in strong acids was ring expansion.[25a] The cyclopropyl ketones were shown to be quantitatively protonated on oxygen, and quantitatively converted to oxolanylium ions (Figure 4.7) at temperatures ranging from 15-100 °C depending on substitution pattern. In the absence of acid, the cyclopropyl ketones were shown to be stable for extended periods at 80-115 °C.

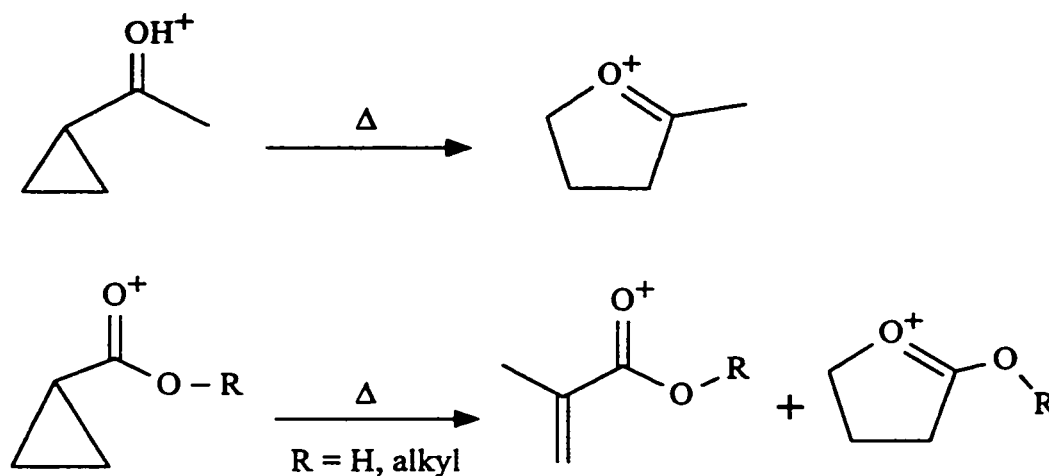


Figure 4.7: Reactions in strong acids of cyclopropyl ketones and cyclopropanecarboxylic acids.

Few studies of the ring expansion of protonated cyclopropyl ketones can be found in the literature.[25] The relative lack of information concerning the ring expansion of protonated cyclopropyl ketones coupled with a strong ongoing interest in the reactions of cyclopropyl compounds,[1] including ring expansions, made this reaction an ideal

candidate for a more systematic investigation. Also, the quantitative nature of the isomerization made it suitable for the determination of heats of isomerization by differential scanning calorimetry which would reveal the thermochemical forces at play in this reaction.

The mechanism(s) by which protonated cyclopropyl ketones undergo ring expansion is examined in detail in chapter 5.

#### *4.1.3 Goals*

This chapter concentrates on the identification and characterization of the reactants and products involved in the isomerization of protonated cyclopropyl ketones to oxolanylium ions. This was done to gain an understanding of the charge distribution in these cations which can be used in conjunction with the thermodynamic results (heats of isomerization) and the kinetic results presented in chapter 5 to interpret the effect of substituents on the energies of the ions. Information about the regio and stereochemical pathways of these ring expansions is coupled with the kinetic results to propose a mechanistic scheme for the isomerizations.

## 4.2 Experimental

$^1\text{H}$  and  $^{13}\text{C}$  NMR spectra were measured with Bruker AM200 (200 MHz), WM250 (250 MHz), AM500 (500 MHz) or Varian EM390 (90 MHz) spectrometers. All chemical shifts are reported in ppm relative to tetramethylsilane, and coupling constants (J) are reported in Hz. Compounds **26-32**, **61** and **62** were commercially available (Aldrich). Ketones **33**[29] and **35**[30] were prepared from the corresponding cyclopropanecarboxylic acids by reaction with methyl lithium.[31] Ketone **37**[32] was prepared in a similar fashion from cyclopropyl lithium and 2-methylcyclopropanecarboxylic acid. Compound **34**, kindly supplied by Marianne Kostyk, was prepared in an analogous manner by the addition of phenyl lithium to 1-methylcyclopropanecarboxylic acid. Compounds **36**[33] and **41**[34] were prepared by the cyclopropanation of the corresponding  $\alpha,\beta$ -unsaturated ketone with dimethyl sulfoxonium ylide.[35] Ketone **42**, generously provided by Dr. Mailvaganam Mahendran, was prepared in a similar fashion from cyclohexenone. The method of Andrist et al[36] was used to prepare compound **38**. Ketones **39** and **40**, which were new compounds, were prepared by a similar sequence of reactions. Descriptions of the preparations follow.

*Methyl 1-Phenylcyclopropyl Ketone, 33* - Prepared by methods found in the literature.[29,31] Flash chromatography on silica (eluant: petroleum ether/ether (95:5)) yielded 3.5 g (yield 71%) of methyl 1-phenylcyclopropyl ketone, **33**. NMR ( $\text{CCl}_4$ ): 1.07 (q(3.5), 2H, cis- $\text{CH}_2$ ), 1.50 (q(3.5), 2H, trans- $\text{CH}_2$ ), 1.92 (s, 3H,  $\text{CH}_3$ ), 7.35 (m, 5H,

C<sub>6</sub>H<sub>5</sub>). <sup>13</sup>C NMR data for **33** can be found in Table 4.2. IR: 1691 cm<sup>-1</sup> (CO stretch).

*Methyl 2-Methylcyclopropyl Ketone, 35* - Prepared by methods found in the literature.[30,31] Distillation at reduced pressure (ca. 20 torr) yielded 2 g (yield 41%) of methyl 2-methylcyclopropyl ketone, **35**. NMR (CCl<sub>4</sub>): 0.59 (m, area 1H), 1.13 (m, area 2H), 1.13 (s, area 3H, 2-CH<sub>3</sub>), 1.57 (m, area 1H), 2.13 (s, area 3H, CH<sub>3</sub>-CO); (500 MHz, CDCl<sub>3</sub>): 0.66 (m, area 1H, H-3), 1.05 (d(6.0), area 3H, 2-CH<sub>3</sub>), 1.16 (p(4.3), area 1H, H-3), 1.34 (m, area 1H, H-2), 1.61 (p(3.9), area 1H, H-1), 2.14 (s, area 3H). <sup>13</sup>C NMR data for **35** can be found in Table 4.2.

*2-Methylcyclopropyl Phenyl Ketone, 36* - Prepared using Corey's cyclopropanation method.[35] Trimethylsulfoxonium iodide (5.5 g, 25 mmol) and sodium hydride (1 g (60% dispersion in oil), 25 mmol) and a magnetic stirring bar were placed under a nitrogen atmosphere in a three-necked flask. Dimethylsulfoxide (30 mL distilled from CaH<sub>2</sub>) was added with the flask maintained at 5-10 °C. The reaction mixture was stirred for 10 minutes, the ice bath was removed and stirring was continued for 90 min. A solution of 1-phenylbut-2-en-1-one (3.5 g, 24 mmol) in DMSO (7 mL) was added from a dropping funnel. The reaction mixture was stirred for 15 min at room temperature, and then heated to 50-60 °C for 1 hour before being poured into 150 ml of water. The aqueous solution was extracted with ether (3 x 50 mL). The combined organic extracts were dried over MgSO<sub>4</sub>, and then the solvent was removed on a rotary evaporator. A <sup>1</sup>H NMR spectrum of the crude product revealed that none of the phenylbutenone reactant

remained. Vacuum distillation (ca. 5 torr) yielded a clear, colourless liquid but  $^1\text{H}$  NMR revealed some impurities. Flash chromatography of the distilled product on silica with petroleum ether/ether (95:5) yielded pure 2-methylcyclopropyl phenyl ketone, **36**. NMR ( $\text{CCl}_4$ ): 0.80 (m, 1H), 1.21 (d(4.5), 3H,  $\text{CH}_3$ ), 1.43 (m, 2H), 2.29 (dt(7.5, 4), 1H, H-1), 7.41 (m, 3H, Ar-H), 7.93 (m, 2H, Ar-H).

*Cyclopropyl 2-Methylcyclopropyl Ketone, 37* - A solution of 19.16 g (158 mmol) of bromocyclopropane in anhydrous ether (25 mL) was added to 3 g of lithium sand in 100 mL anhydrous ether under an argon atmosphere. The reaction mixture was stirred for 30 min at room temperature and then cooled to  $-78\text{ }^\circ\text{C}$  before a solution of 6.05 g (60 mmol) of 2-methylcyclopropanecarboxylic acid in anhydrous ether (30 mL) was slowly added from a dropping funnel. After addition was complete, the flask was warmed to room temperature at which time cyclopropane boiled off. The reaction mixture which had solidified was left overnight at room temperature. The reaction was quenched with saturated aqueous  $\text{NH}_4\text{Cl}$  which was added so that the aqueous layer remained alkaline. The ether layer was removed, and then the aqueous layer was washed with ether (2 x 50 mL). The combined organic layers were washed with water (1 x 100 mL) and dried over  $\text{MgSO}_4$  before solvent removal on a rotary evaporator. A  $^1\text{H}$  NMR spectrum of the crude product showed the absence of 2-methylcyclopropanecarboxylic acid. Vacuum distillation produced a clear, colourless liquid boiling over at  $68\text{-}72\text{ }^\circ\text{C}$  (ca. 20 torr). An infrared absorption at  $1680\text{ cm}^{-1}$  showed that a ketone had been formed but NMR revealed that the distillate was contained some impurities. Preparative GC (Aerograph



A90-P<sub>3</sub>, 0.25" x 5' copper column with 10% OV-17 on Chromosorb W, He carrier, 10 mL/min, 145 °C column temperature) yielded two major fractions ( $t_R = 5.5$  and 7 min) both with NMR spectra consistent with the desired product (cis and trans isomers?). The larger fraction (ca. 300 mg) with  $t_R = 7$  min was used in all subsequent experiments. NMR (CCl<sub>4</sub>): a continuum of highly coupled signals between 0.5-2.0 ppm including multiplets at 1.65 and 1.9 for the two  $\alpha$ -protons. IR: 1672 cm<sup>-1</sup> (CO stretch); 1690 cm<sup>-1</sup> (minor fraction). MS (EI, m/z): 124 (M<sup>+</sup>), 109 (M<sup>+</sup> - CH<sub>3</sub>), 95, 83 (M<sup>+</sup> - cyclopropyl), 69 (M<sup>+</sup> - 2-Me-cyclopropyl), 55 (2-Me-cyclopropyl<sup>+</sup>).

*cis,trans-2,3-Dimethylcyclopropyl Methyl Ketone, 38* - A literature procedure[36] was used to make compound **38**. The intermediate and final compounds are described below.

*Ethyl cis,trans-2,3-Dimethylcyclopropanecarboxylate* - Vacuum distillation (bp 62-4 °C (ca. 30 torr)) gave ethyl *cis,trans-2,3-dimethylcyclopropanecarboxylate* (2.1 g, 20%) as a clear, colourless liquid. NMR (CCl<sub>4</sub>): 1.2 (m, 12H), 4.16 (q(7.5), 2H, O-CH<sub>2</sub>).

*cis,trans-2,3-Dimethylcyclopropanecarboxylic acid* - *cis,trans-2,3-dimethylcyclopropanecarboxylic acid* was obtained as clear, colourless oil (1.5 g, 89%).

NMR (CCl<sub>4</sub>): 1.2 (m, 9H), 11.27 (s, 1H, COOH).

*cis,trans-2,3-Dimethylcyclopropyl Methyl Ketone, 38* - Column chromatography (alumina, pentane eluant) yielded *cis,trans-2,3-dimethylcyclopropyl methyl ketone, 38*, as a clear, colourless liquid. NMR (CCl<sub>4</sub>): 0.98 (d(2), 3H, *cis*-CH<sub>3</sub>), 1.08 (d(2), 3H, *trans*-CH<sub>3</sub>), 1.1 (m, 2H, H-2 and H-3), 1.54 (m, 1H, H-1), 2.07 (s, 3H, CH<sub>3</sub>-CO).

*cis,cis-2,3-Dimethylcyclopropyl Methyl Ketone, 39 and trans,trans-2,3-*

*Dimethylcyclopropyl Methyl Ketone, 40* - Compounds 39 and 40 were prepared from *Z-2-butene* by the same procedure[36] as for 38. The synthesis is described below.

*Ethyl cis,cis- and trans,trans-2,3-dimethylcyclopropanecarboxylate* - *Z-2-Butene* (ca 50 mL), ether and Cu(II) acetate were added to a flask before ethyl diazoacetate (20 g, 175 mmol) in ether was added. Reaction did not commence until the flask was warmed to room temperature. The reaction and work-up were conducted as described above for ethyl *cis,trans-2,3-dimethylcyclopropanecarboxylate*. The crude product contained diethyl fumarate and maleate. Vacuum distillation afforded 5.6 g (23%) of ethyl *cis,cis- and trans,trans-2,3-dimethylcyclopropanecarboxylate* (bp 107-110 (ca. 100 torr)) as a clear, colourless liquid. NMR (CCl<sub>4</sub>): (broad m, 12H), 4.04 (q(7), 2H, CH<sub>2</sub>-O). MS (EI, m/z): 142 (M<sup>+</sup>), 127 (M<sup>+</sup> - CH<sub>3</sub>), 114 (M<sup>+</sup> - CH<sub>2</sub>=CH<sub>2</sub>), 99 (M<sup>+</sup> - CH<sub>3</sub> - CH<sub>2</sub>=CH<sub>2</sub>), 97 (M<sup>+</sup> - OCH<sub>2</sub>CH<sub>3</sub>), 69 (M<sup>+</sup> - COOCH<sub>2</sub>CH<sub>3</sub>).

*cis,cis- and trans,trans-2,3-Dimethylcyclopropanecarboxylic Acid* - The ester (5.6 g, 39 mmol) prepared above was hydrolyzed with formic acid/H<sub>2</sub>SO<sub>4</sub> as described in the preparation of compound 38. Water and ether were added to the reaction mixture. The ether layer was washed with 5% HCl (4 x 25 mL) to remove formic acid. The product was extracted from ether with 6% KOH (4 x 25 mL). (Note: the ether layer at this point contains unreacted ester (5-20%) which can be isolated.) The combined KOH fractions were acidified with concentrated HCl and then extracted with ether. The ether layer was dried over Na<sub>2</sub>SO<sub>4</sub> before the ether was removed on a rotary evaporator to give 3.0 g (80% based on reacted ester) of *cis,cis- and trans,trans-2,3-*

dimethylcyclopropanecarboxylic acid as a clear, colourless oil which crystallized on standing. NMR (CDCl<sub>3</sub>): 1.12 (m, 7H, (CH<sub>3</sub>)<sub>2</sub> and H-1), 1.53 (m, 2H, H-2 and H-3), 10.03 (bs, 1H, COOH).

*cis,cis- and trans,trans-2,3-Dimethylcyclopropyl Methyl Ketone, 39 and 40* - As described in the preparation of compound 38,[36] *cis,cis-* and *trans,trans-2,3-*

*dimethylcyclopropanecarboxylic acid* were reacted with excess methyl lithium. <sup>1</sup>H NMR of the crude product revealed two CH<sub>3</sub>-CO signals for the *cis,cis* and *trans,trans* isomers as well as the presence of the tertiary alcohol. The two ketone isomers were separated by preparative TLC (silica, eluant: petroleum ether/ether 97:3). The eluant was allowed to run up the plate several times until two resolved bands were visible with a UV lamp. The band with higher R<sub>f</sub> proved to be *cis,cis-2,3-dimethylcyclopropyl methyl ketone, 39*.

NMR (CDCl<sub>3</sub>): 1.11 (dd(4.2, 1.9), 6H, 2- and 3-CH<sub>3</sub>), 1.48 (m, 2H, H-2 and H-3), 1.92 (t(8.5), 1H, H-1), 2.19 (s, 3H, CH<sub>3</sub>-CO). The band with lower R<sub>f</sub> had a <sup>1</sup>H NMR spectrum consistent with *trans,trans-2,3-dimethylcyclopropyl methyl ketone, 40*. NMR (CDCl<sub>3</sub>): 1.07 (dd(4.1, 1.9), 6H, 2- and 3-CH<sub>3</sub>), 1.52 (m, 2H, H-2 and H-3), 1.31 (t(4.3), 1H, H-1), 2.16 (s, 3H, CH<sub>3</sub>-CO). <sup>13</sup>C NMR spectra for both 39 and 40 can be found in Table 4.2. A 2,4-dinitrophenylhydrazone derivative of 40 was prepared and following recrystallization from methanol the derivative had mp = 159-61 °C. Further recrystallization from benzene yielded crystals suitable for structure analysis by X-ray diffraction techniques. Crystallographic data can be found in the Appendix.

*Bicyclo[3.1.0]hexan-2-one, 41* - Prepared by methods found in the literature.[34,35]

Vacuum distillation (ca. 100 torr) of the crude product provided 1.50 g (26% yield) of bicyclo[3.1.0]hexanone, **41**, as a clear, colourless oil.  $^1\text{H}$  NMR ( $\text{CDCl}_3$ ): 0.87 (td(4.6, 3.2), 1H, endo-H-6), 1.14 (m, 1H, exo-H-6), 1.70 (m, 1H, H-5), 1.92-2.11 (m, 5H).  $^{13}\text{C}$  NMR data for **41** can be found in Table 4.3.

*Protonation* - As described in chapter 2.

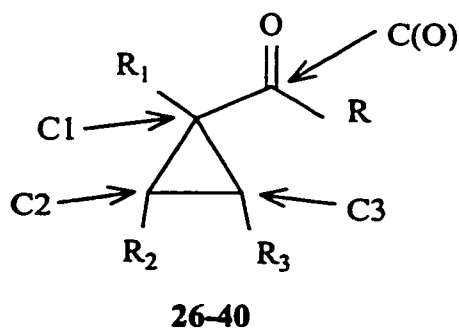
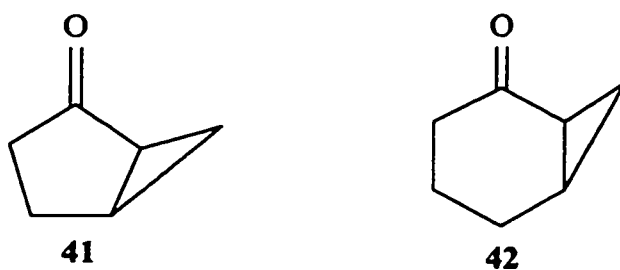
*Isomerization* - Isomerization of protonated cyclopropyl ketones was conducted in a steam bath, oil bath or constant-temperature bath as described in the experimental section of chapter 2.  $^1\text{H}$  NMR, and in some cases  $^{13}\text{C}$  NMR, spectroscopy was used to identify the products of isomerization.

*Heats of Isomerization* - As described in chapter 2.

*Photochemical Isomerization of Protonated Cyclopropyl Ketones* - Triflic acid solutions of **27H** and **28H** were placed in quartz NMR tubes and irradiated with 254 nm (**27H**) or 300 nm (**28H**) light in a Rayonet RPR-100 photochemical reactor (Southern New England Ultraviolet Co.). The course of the photochemical reactions were monitored by  $^1\text{H}$  NMR spectroscopy.

### 4.3 Results and Discussion

A series of cyclopropyl ketones, **26-42**, were studied (Figure 4.8). Compounds **26-32** were commercially available (Aldrich Chemical Co.). Standard routes to cyclopropyl ketones, such as the addition of alkyl lithiums to cyclopropanecarboxylic



	R	R <sub>1</sub>	R <sub>2</sub>	R <sub>3</sub>		R	R <sub>1</sub>	R <sub>2</sub>	R <sub>3</sub>
<b>26</b>	H	H	H	H	<b>34</b>	Ph	Me	H	H
<b>27</b>	Me	H	H	H	<b>35</b>	Me	H	Me	H
<b>28</b>	Ph	H	H	H	<b>36</b>	Ph	H	Me	H
<b>29</b>	p-An	H	H	H	<b>37</b>	cp	H	Me	H
<b>30</b>	p-Cl-Ph	H	H	H	<b>38</b>	Me	H	cis-Me	trans-Me
<b>31</b>	cp	H	H	H	<b>39</b>	Me	H	cis-Me	cis-Me
<b>32</b>	Me	Me	H	H	<b>40</b>	Me	H	trans-Me	trans-Me
<b>33</b>	Me	Ph	H	H					

Figure 4.8: Cyclopropyl Ketones studied in this work.

acids[31] or the addition of dimethylsulfoxonium ylide to  $\alpha,\beta$ -unsaturated ketones,[35] were used to prepare the remaining compounds (Figure 4.9). Thus, known ketones 33[29] and 35[30] were prepared from the corresponding cyclopropanecarboxylic acids by reaction with methyl lithium. Compound 34, kindly supplied by Marianne Kostyk, was prepared in an analogous manner by the addition of phenyl lithium to 1-methylcyclopropanecarboxylic acid. Known compounds 36[33] and 41[34] were

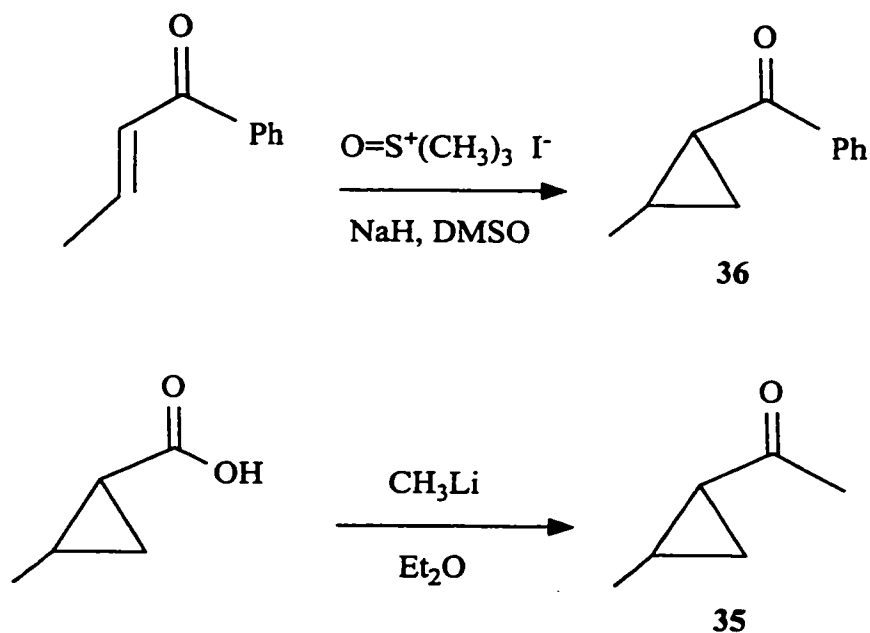


Figure 4.9: Synthetic routes to cyclopropyl ketones.

prepared by cyclopropanation of the appropriate  $\alpha,\beta$ -unsaturated ketone with dimethyl sulfoxonium ylide. Compound **42** was prepared by the same route by Dr. Mailvaganam Mahendran and a sample was generously provided for this work.

A synthetic route to compound **37** described by Hanack and Eggensberger[32] involved base-catalyzed condensation of butyrolactone and 4-methyl butyrolactone and led to a mixture of three closely related cyclopropyl ketones (Figure 4.10) which could prove difficult to separate. In this work, compound **37** was prepared by a new route which involved the addition of cyclopropyl lithium to 2-methyl-cyclopropanecarboxylic acid (Figure 4.10).

The method of Andrist et al[36] was used to prepare compound **38** beginning from E-2-butene. Ketones **39** and **40** were prepared by a similar sequence of reactions

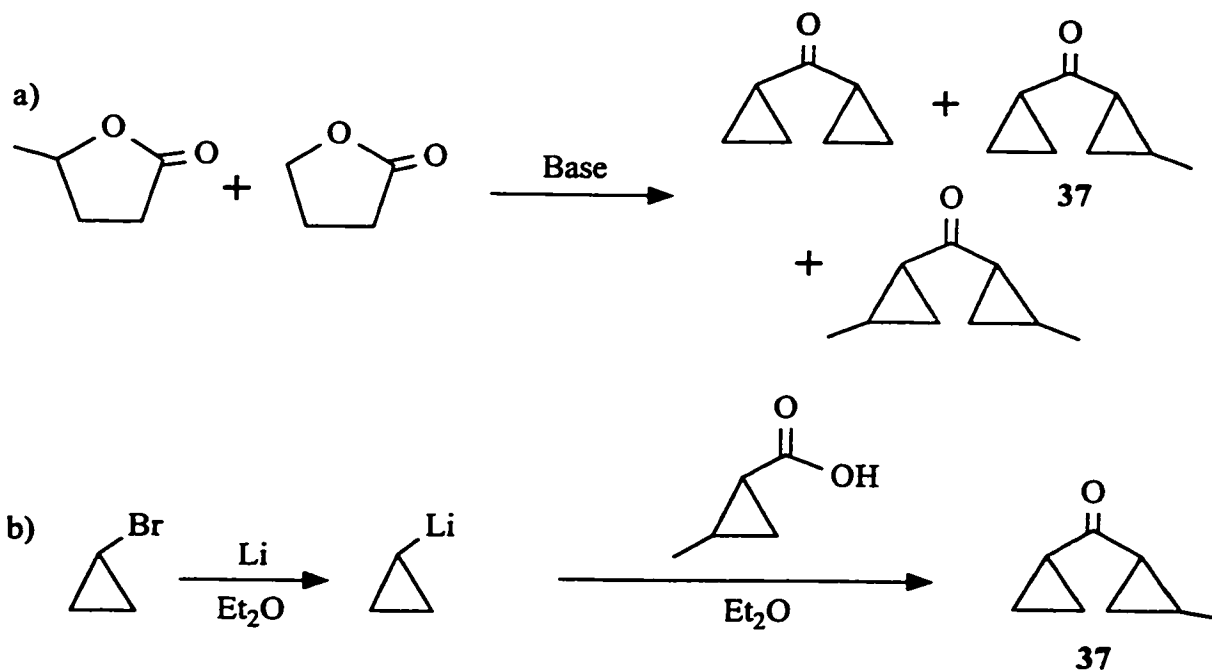


Figure 4.10: Synthesis of 37 by a) base catalyzed condensation of  $\gamma$ -valerolactone and  $\gamma$ -butyrolactone, and b) alkylation of 2-methylcyclopropanecarboxylic acid with cyclopropyl lithium.

starting from *Z*-2-butene. The synthetic routes to 38–40 are outlined in Figures 4.11–4.12.

#### 4.3.1 Protonated Cyclopropyl Ketones

Dissolution of ketones 26–42 in triflic acid at reduced temperature ( $\leq -20\text{ }^\circ\text{C}$ ) followed by warming to room temperature, yielded oxygen-protonated cyclopropyl ketones 26H–42H (see Figure 4.8).  $^1\text{H}$  and  $^{13}\text{C}$  NMR spectra are shown in Tables 4.1–4.3.

At 90 MHz, the  $^1\text{H}$  NMR spectra of 41, 42, 41H, and 42H were poorly resolved. At 500 MHz, the  $^1\text{H}$  NMR spectra were somewhat simplified although substantial overlap still existed. The  $^1\text{H}$  NMR spectrum of ion 42H was assigned on the basis of a 2D spectrum and, thus, these assignments are more secure.

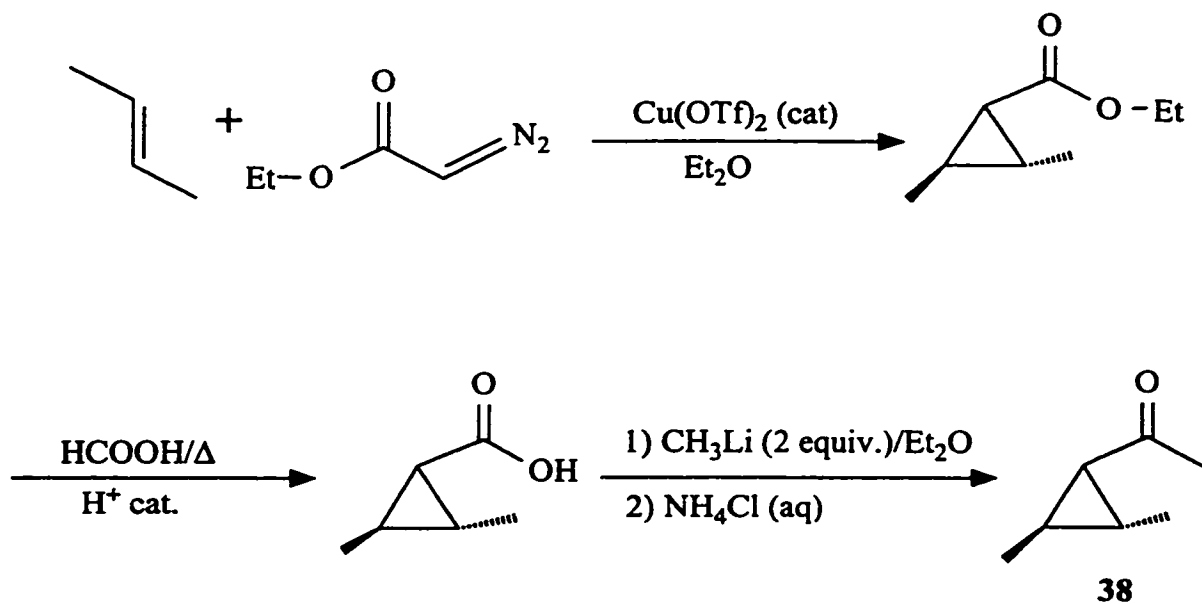


Figure 4.11: Synthesis of compound 38 by the route of Andrist et al.[36]

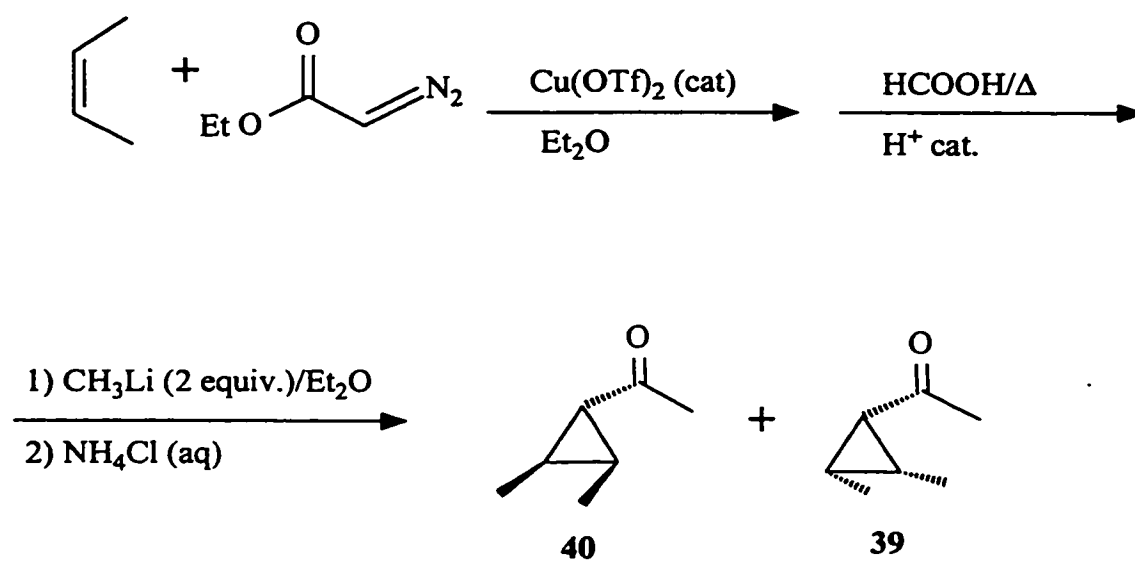


Figure 4.12: Synthesis of compounds 39 and 40 by route analogous to that for 38 (see Fig. 4.11) but with cis-2-butene as a starting material.



Table 4.1: <sup>1</sup>H NMR of protonated cyclopropyl ketones.<sup>a</sup>

cmpd	chemical shift (ppm) at position noted			
	R	H1/R <sub>1</sub>	H2/R <sub>2</sub>	H3/R <sub>3</sub>
<b>26H</b>	8.76 d(9)	2.73 m	2.52 m	2.52 m
<b>27H</b>	2.79 s	2.70 m	2.27 m 2.33 m	2.27 m 2.33 m
<b>28H</b>	7.73 t(8) 8.06 t(7.5) 8.23 d(7.5)	3.25 m	2.34 bs 2.42 bs	2.34 bs 2.42 bs
<b>29H</b>	8.32 d(9) 7.22 d(9) 4.06 s	3.10 bp(6)	2.07 bd	2.07 bd
<b>30H</b>	7.73 d(9) 8.24 d(9)	3.24 p(6)	2.50 d(6)	2.50 d(6)
<b>31H</b>	1.94 bs 2.00 s 2.19 m	2.19 m	1.94 bs 2.00 s	1.94 bs 2.00 s
<b>32H</b>	2.62 s	1.50 s	2.08 m 2.34 m	2.08 m 2.34 m
<b>33H</b>	2.66 m	7.47 m	2.72 m 2.91 m	2.72 m 2.91 m
<b>34H</b>	7.82 m	1.70 s	2.18 m 2.54 m	2.18 m 2.54 m
<b>35H</b>	2.76 m	2.49 dt(7.2,3.8)	2.84 m 1.43 d(5.9)	2.28 ddd(8,8,4) 2.56 dt(9.1,4.4)
<b>35H<sup>b,c</sup></b>	2.98 s	2.54 m	2.95 m 1.43 d(6)	2.26 m 2.54 m
<b>36H<sup>c</sup></b>	7.71 t(8) 8.02 t(7) 8.21 d(7.5)	3.00 m	3.00 m 1.49 d(5.5)	2.28 m 2.74 m
<b>37H<sup>c</sup></b>	1.97 m 2.28 m	2.28 m	2.28 m 1.34 d(6)	1.97 m
<b>38H</b>	2.89 s	2.57 dd(7,4.5)	2.96 m 1.39 d(5.5)	2.96 m 1.51 d(5.9)

Table 4.1 continued

cmpd	R	H1/R <sub>1</sub>	H2/R <sub>2</sub>	H3/R <sub>3</sub>
<b>39H</b>	2.82 s	2.82 t(7.5)	3.32 m 1.39 d(6)	3.32 m 1.39 d(6)
<b>40H</b>	2.74 s	2.23 t(3.5)	3.11 bs 1.42 d(4.5)	3.11 bs 1.42 d(4.5)

a) At 90 or 500 MHz in triflic acid;  $(\text{CH}_3)_4\text{N}^+ \text{BF}_4^-$  at 3.10 ppm. s = singlet, d = doublet, t = triplet, q = quartet, p = pentet, b = broad.

b) as  $\text{SbCl}_6^-$  salt in  $\text{CD}_2\text{Cl}_2$ ; reference  $\text{CH}_2\text{Cl}_2$  at 5.30 ppm; low solubility of salt makes the assignment of some signals difficult.

c) Some assignments may be reversed.

#### 4.3.2 Comparison of NMR Data for Neutral and Protonated Cyclopropyl Ketones

Comparison of the  $^1\text{H}$  and  $^{13}\text{C}$  NMR spectra (Tables 4.1-4.3) of the protonated ketones, **26H-42H**, with those of the neutral ketones, **26-42**, and those found in the literature[13,37] indicates that positive charge is primarily located at C(O), C2 and C3. This is consistent with strong conjugation of the cyclopropyl ring with the protonated carbonyl function. For ketones **27**, **32** and **33**, which are unsubstituted on the  $\beta$ -positions, the  $^{13}\text{C}$  signals for C(O) and C2 (or C3) are shifted approximately 30 and 19 ppm downfield, respectively. Protonation of ketones **39** or **40**, monosubstituted at each  $\beta$ -position, causes the  $^{13}\text{C}$  NMR chemical shifts of C(O) and C2 (or C3) to move 25 and 30 ppm downfield, respectively. Compound **35**, with both an unsubstituted and a substituted  $\beta$ -carbon, shows behaviour characteristic of both groups of ketones; the C(O) signal moves 27 ppm downfield and the C2 and C3 signals move 26.5 and 18 ppm downfield, respectively. Bicyclic ketones **41** and **42** show similar changes in the NMR spectra.

Table 4.2:  $^{13}\text{C}$  NMR data: neutral and protonated cyclopropylketones<sup>a-c</sup>

cmpd	chemical shift (ppm) at position noted				
	C(O)	R	C1/R <sub>1</sub>	C2/R <sub>2</sub>	C3/R <sub>3</sub>
27	209.4	30.6	21.7	11.2	11.2
32	209.9 s	26.0 q(127.5)	27.5 s 20.4 q(126.7)	18.3 t(163.8)	18.3 t(163.8)
33	209.0	29.8	38.2 128.0 129.2 131.3 141.8	19.1	19.1
35	208.7	30.9	30.7	20.5 18.6	19.8
39	207.5	28.0	33.5	22.4 6.6	22.4 6.6
40	208.6	30.4	38.5	25.1 11.9	25.1 11.9
27H	240.1	26.6	29.1	29.5	29.5
32H	238.4 s	24.5 q	36.2 s 16.9 q	36.8 t	36.8 t
33H	239.9 s	26.9 q(134)	45.1 s 130.3 d(162) 130.8 d(159) 132.8 s	38.6 t(168)	38.6 t(168)
35H	235.9	26.9	38.7	47.0 18.0	37.9
39H	233.5 s	30.9 q(132.5)	40.6 d(175.2)	53.4 d(167.5) 7.4 q(129.4)	53.4 d(167.5) 7.4 q(129.4)
40H	232.9 s	27.5 q(133.3)	48.0 d(177.6)	53.9 d(171.9) 12.6 q(129.3)	53.9 d(171.9) 12.6 q(129.3)

a) At 125.721 and 62.86 MHz in  $\text{CDCl}_3$  and  $\text{CF}_3\text{SO}_3\text{H}$ . Protonated ketones referenced to  $\text{CF}_3\text{SO}_3\text{H}$  at 119.0 ppm which corresponds to  $\text{CDCl}_3$  at 77.2 ppm.

b) Multiplicity: s = singlet; d = doublet; t = triplet; q = quartet.  $^1\text{H}$ - $^{13}\text{C}$  coupling constants (Hz) shown in brackets.

c) Some assignments may be reversed.

Table 4.3:  $^1\text{H}$  and  $^{13}\text{C}$  NMR Data for neutral and protonated bicyclo[3.1.0]alkan-2-ones, **41**, **41H**, **42** and **42H**.<sup>a,b,c</sup>

cmpd	chemical shift (ppm) at position noted						
	1	2	3	4	5	6	7
<b>41</b>	2.00m	--	2.00 m	2.00 m	1.72 p(4)	0.86 td (4.6, 3.2) 1.15 m	
	28.0	215.8	31.9	23.2	22.1	14.0	
<b>41H</b>	2.95m	--	2.77 bd (9.2) 2.95 m	2.32 dd (13.5, 6.2) 2.58 m	3.37 p(5)	2.18 m 2.58 m	
	36.5	242.8	33.0	23.8	41.4	32.1	
<b>42</b>	1.87m	--	1.99 ddd (18.2, 11.4, 6.8) 2.23 dt (18.3, 4.6)	1.61 m	1.61 m	1.87 m	1.03 ddd (9.8, 8.2, 5.3) 1.15 q(5.2)
	26.3	209.8	37.2	18.3	21.8	17.9	10.7
<b>42H</b>	2.76m	--	2.76 m 2.99 dd (21.8, 6.0)	1.94 m	1.94 m 2.20 bd (14.4)	3.18 bq(6)	2.50 bq(7) 2.76 m
	34.1	237.5	33.9	16.4	19.8	40.1	28.8

a) Neutral ketones measured at 500 MHz in  $\text{CDCl}_3$ ; ref.  $\text{CDCl}_3$  at 7.24 ppm( $^1\text{H}$ ) and 77.6 ppm( $^{13}\text{C}$ ).

b) Protonated ketones measured at 500 MHz in  $\text{CF}_3\text{SO}_3\text{H}$ ; ref.  $(\text{CH}_3)_4\text{N}^+\text{BF}_4^-$  at 3.10 ppm( $^1\text{H}$ ) and  $\text{CF}_3\text{SO}_3\text{H}$  at 119.0 ppm( $^{13}\text{C}$ ).

c) some assignments may be reversed.

Other interesting features are evident in the  $^{13}\text{C}$  NMR data for the series of neutral and protonated ketones (Tables 4.2 and 4.3). The chemical shifts of the methyl substituents on C2 and C3 of **35**, **39** and **40** are unaffected by protonation, even though the carbon to which they are attached undergoes a 30 ppm downfield shift. For each ketone, protonation causes a downfield shift for the C1 signal of 7-9.5 ppm, markedly less than the changes that occur for the C(O), C2 and C3 signals. Most surprising is that, with the exception of **39**, each of the ketones with  $\text{R} = \text{CH}_3$  displays an upfield shift (3-4 ppm) of the signal for this methyl group following protonation. A similar upfield shift of C3 (the  $\text{CH}_2$   $\alpha$  to the carbonyl) is observed in **41H** and **42H**. One would expect a downfield shift for the carbon beside the cation centre. In one of the two possible bisected geometries, the  $\alpha$ -carbon is placed in the face of the cyclopropyl ring, and restricted rotation about the bond joining the cyclopropyl ring and C(O) might hold it in this position. This might be expected to shield the  $\alpha$ -carbon. However, this explanation seems unlikely since a similar upfield shift of the  $\alpha$ -carbons following protonation has been observed for other ketones not containing cyclopropyl rings.[13,38]

The chemical shift of C(O) changes as the electron-donating ability of the cyclopropyl ring is varied. The chemical shift for C(O) moves upfield and  $\Delta\delta (= \delta_{\text{cation}} - \delta_{\text{neutral}})$  becomes smaller as the electron-donating ability of the cyclopropyl ring increases (Figure 4.13). Presumably, the more electron-rich cyclopropyl rings can supply more electron density to the cation centre (carbonyl carbon). The  $^{13}\text{C}$  NMR results are compared with literature data for the rates of solvolysis of cyclopropylcarbinyll derivatives[9] with the same substitution pattern as the ketones shown in Figure 4.13. As

the ring becomes a better donor, the chemical shift of C(O) moves upfield,  $\Delta\delta$  becomes smaller and the rate of solvolysis for the cyclopropylcarbonyl 3,5-dinitrobenzoate derivatives becomes faster. In fact, a plot in which the  $^{13}\text{C}$  NMR data is compared with the solvolysis rates provides a straight line with high correlation coefficient ( $r = 0.99$ , see Figure 4.14).

Caution must be exercised in the use of  $^{13}\text{C}$  NMR shifts to predict the electron density on a particular carbon.[13,39] While  $^{13}\text{C}$  NMR chemical shifts are related to electron density other factors are also important. It has been shown that the cyclopropyl group causes a significant neighbouring group deshielding of the cation centre, an effect unrelated to the charge delocalizing ability of this group.[40] It is generally agreed that conclusions about charge density is best made by comparing compounds of closely related structure. Thus, the comparison of  $^{13}\text{C}$  NMR spectra of neutral and protonated cyclopropyl ketones is on sound footing.

#### *4.3.3 Rearrangement of Protonated Cyclopropyl Ketones*

When heated at temperatures between 30-130 °C, the protonated cyclopropyl ketones, **26H-40H**, isomerized to oxolanylium ions, **43-60**. In those systems where the  $\beta$ -positions are not symmetrically substituted, the more substituted  $\beta$ -carbon of the cyclopropyl ketone is bound to the oxygen atom in the product. The net result of isomerization is to break the C1-C2 bond of the cyclopropyl ring, form a bond between C2 and oxygen and move a hydrogen atom from oxygen to C1 (Figure 4.15).

The course of the isomerization, and the identity of the products of isomerization

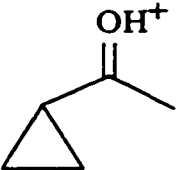
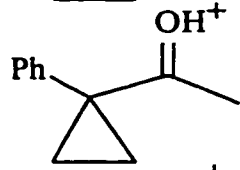
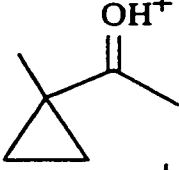
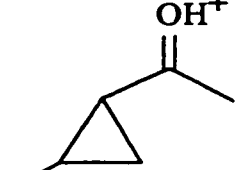
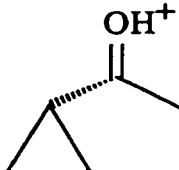
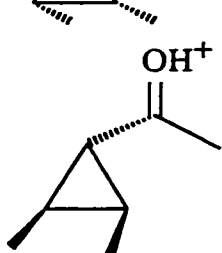
	$\delta(\text{C}(\text{O}))$ (ppm)	$\Delta\delta(\text{C}(\text{O}))$ (ppm)	Relative rate of solvolysis
	240.1	30.7	1
	239.9	30.9	1.3 ( $\text{PhSO}_3^-$ )
	238.4	28.5	5
	235.9	27.2	11
	233.5	26	82
	232.9	24.3	124

Figure 4.13: Comparison of  $^{13}\text{C}$  NMR data for protonated ketones with solvolysis rates found in the literature for cyclopropylcarbinyl 3,5-dinitrobenzoates with the same substitution pattern on the ring.  $\delta(\text{C}(\text{O}))$  is the chemical shift of the carbonyl carbon in the protonated ketone.  $\Delta\delta(\text{C}(\text{O}))$  is the difference in chemical shift of the carbonyl carbon in the protonated vs. neutral ketone.

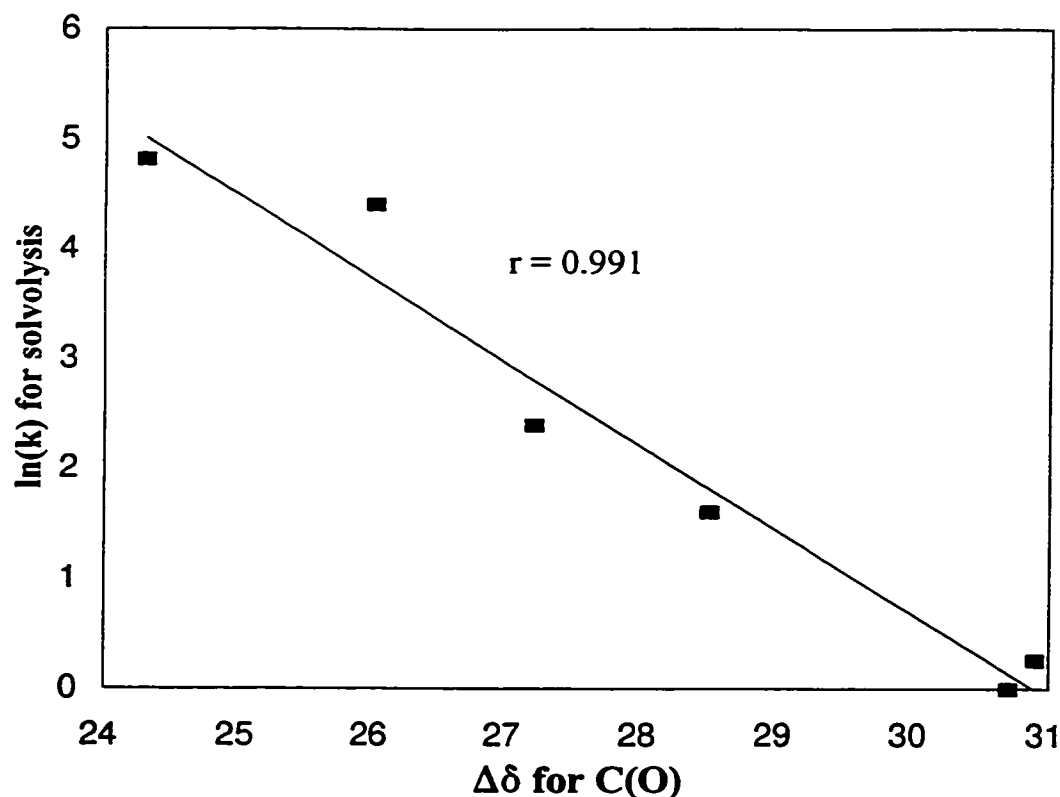


Figure 4.14: Correlation of  $\Delta\delta$ , the change in the  $^{13}\text{C}$  chemical shift of C(O), of cyclopropyl ketones when protonated in triflic acid with rates of solvolysis found in the literature for similarly substituted cyclopropylcarbonyl 3,5-dinitrobenzoates.

was established by  $^1\text{H}$  NMR spectroscopy. Figures 4.16 and 4.17 show the change that occurs in the  $^1\text{H}$  NMR spectra of protonated cyclopropyl methyl ketone, **27H**, and protonated cyclopropyl phenyl ketone, **28H**, when heated at 100 °C in triflic acid. The signals due to the protonated cyclopropyl ketone disappear, and the characteristic peaks of the oxolanylium ion appear at about 2.5, 4 and 6 ppm. The  $^1\text{H}$  NMR spectrum of each oxolanylium ion was measured and the data are summarized in Table 4.4. The  $^{13}\text{C}$  NMR spectra of several oxolanylium ions are presented in Table 4.5.



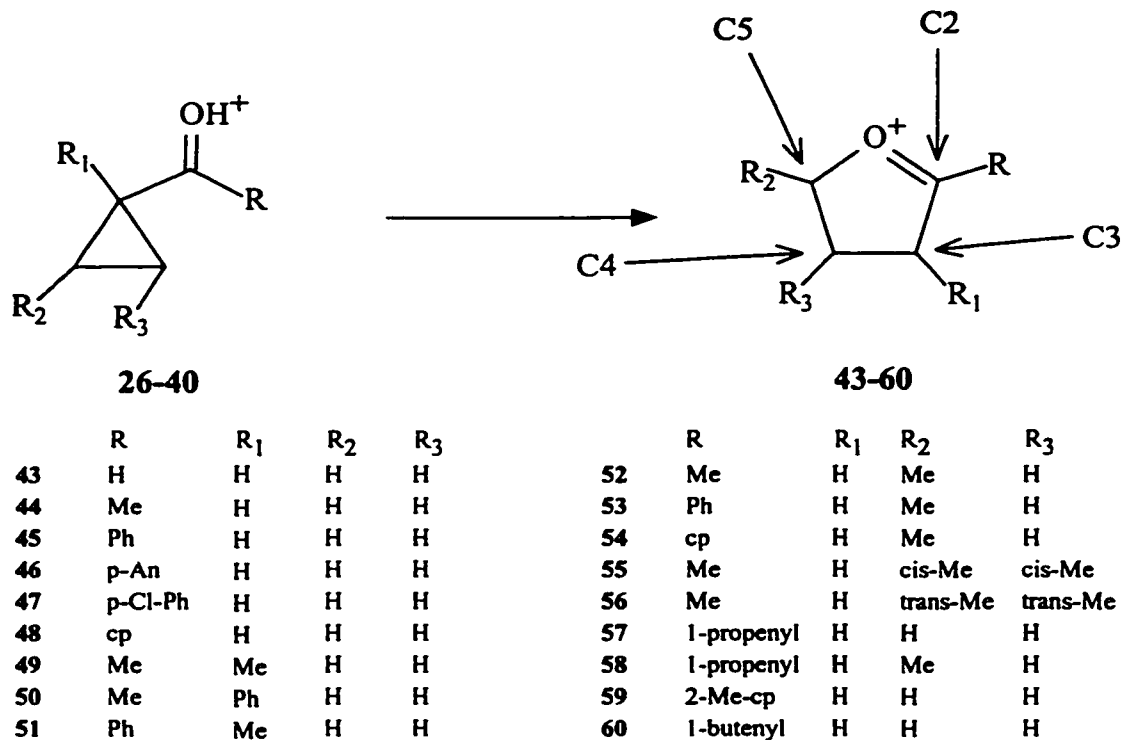


Figure 4.15: Oxolanylium ions produced by isomerization of protonated cyclopropyl ketones 26-40.

When the cyclopropyl ketone is part of a bicyclo[n.1.0] system bonding of a  $\beta$ -cyclopropyl carbon to the oxygen is prevented. Thus when bicyclo[3.1.0]hexan-2-one, **41**, and bicyclo[4.1.0]heptan-2-one, **42**, were heated in triflic acid, they isomerized to protonated enones (Figure 4.18). **41H** yielded protonated cyclohex-2-enone, **61H**, while **42H** produced a 2:1 mixture of protonated 3-methylcyclohex-2-enone, **62H**, and protonated cyclohept-2-enone, **63H**. The products were identified on the basis of their  $^1\text{H}$  NMR spectra (Table 4.6). In addition, the  $^1\text{H}$  NMR spectrum of a commercial sample of 3-methylcyclohex-2-enone, **62**, in triflic acid was identical to that of the major product of **42H** isomerization.

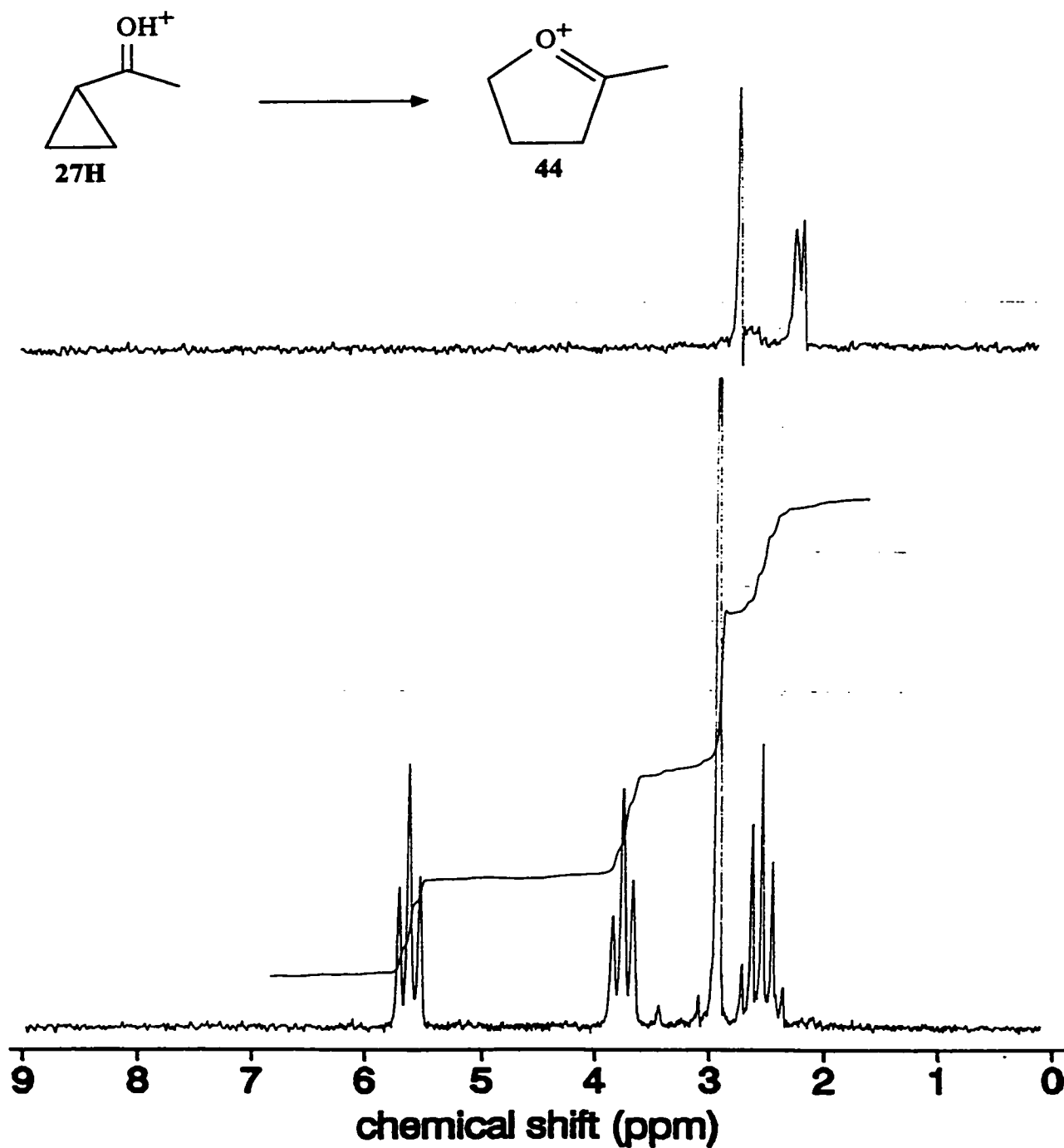


Figure 4.16:  $^1\text{H}$  NMR spectra of protonated cyclopropyl methyl ketone, 27H, before (top) and after (bottom) isomerization to 2-methyloxolanylium ion, 44, by heating in triflic acid at 100 °C for 150 min.

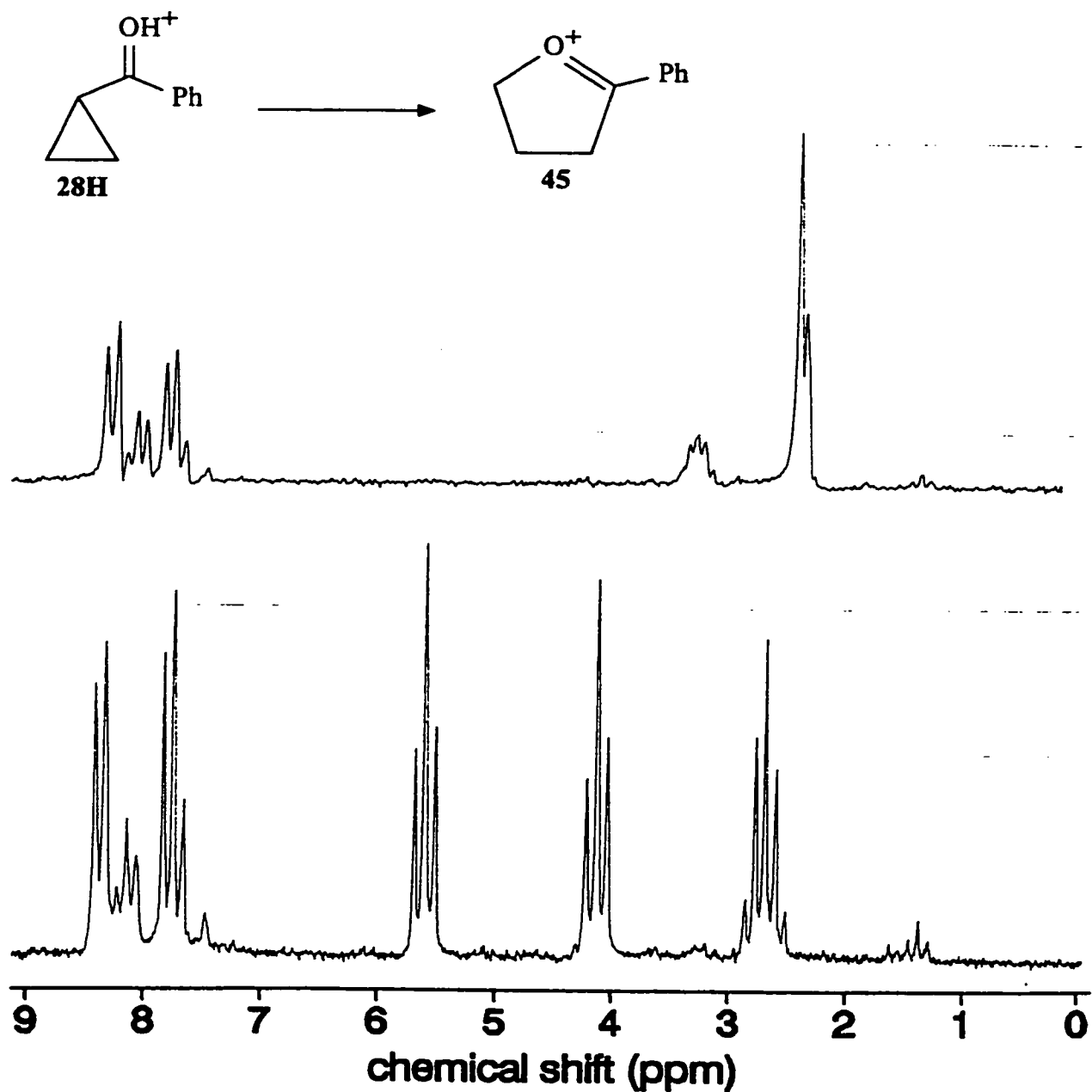


Figure 4.17:  $^1\text{H}$  NMR spectra of protonated cyclopropyl phenyl ketone, 28H, before (top) and after (bottom) isomerization to 2-phenyloxolanylium ion, 45, by heating in triflic acid at  $100^\circ\text{C}$  for 150 min.

Table 4.4: <sup>1</sup>H NMR of oxolanylium ions<sup>a,b</sup>

cmpd	chemical shift (ppm) at position noted			
	R	H3/R <sub>1</sub>	H4/R <sub>3</sub>	H5/R <sub>2</sub>
43	10.25 s	4.04 t(8)	2.69 p(8)	5.95 t(8)
44	2.94s	3.76 t(7.5)	2.54 p(7.5)	5.63 t(7.5)
44 <sup>c</sup>	3.12 s	3.98 t(7)	2.67 p(8)	5.79 t(8)
45	7.73 t(8) 8.11 t(8) 8.34 d(8)	4.08 t(8)	2.65 p(8)	5.57 t(8)
45 <sup>c</sup>	7.85 t(8) 8.22 t(8) 8.50 d(8)	4.33 t(8)	2.78 p(8)	5.78 t(8)
46	7.18 d(9) 8.33 d(9) 4.27 s	3.88 t(7.5)	2.56 p(7.5)	5.36 t(7.5)
47	7.75 d(9.5) 8.33 d(9.5)	4.05 t(8)	2.66 p(8)	5.59 t(8)
49	2.90 s	3.79 m 1.56 d(7.3)	2.17 m 2.77 m	5.41 q(9.4) 5.64 td (10.1, 3.8)
50	2.78 s	4.94 t(9.5) 7.28 dd (7.6, 1.8) 7.48m	2.72m 3.13m	5.63 q(9.5) 5.92 td (10.2, 4.2)
51	7.80 t(7.5) 8.15 t(7.5) 8.41 d(7.5)	4.47 p(8) 1.62 d(7.5)	2.60 m 2.78 m	5.54 m
52	2.90 s	3.70 dt (23.1, 9.2) 3.82 ddd (23.1, 9.6, 3.6)	2.15 dq (13.4, 8.9) 2.72 m	6.06 h(7.2) 1.78 d(6.4)
52 <sup>c</sup>	2.93 s	3.83 bt(8)	2.13 m 2.65 m	6.07 bh(7) 1.75 d(6)
52 <sup>f</sup>	3.16 s	4.06 bt(8)	2.24 m 2.80 m	6.24 bq(7.5) 1.87 d(6)

Table 4.4 continued over

Table 4.4 continued

cmpd	chemical shift (ppm) at position noted			
	R	H3/R <sub>1</sub>	H4/R <sub>3</sub>	H5/R <sub>2</sub>
<b>53</b>	7.75 t(8) 8.12 t(7) 8.38 d(8)	4.12 m	2.28 m 2.84 m	6.00 h(6.5) 1.82 d(6)
<b>54<sup>d</sup></b>	?	3.53 m	?	5.78 bp(6.5) 1.65 d(6.5)
<b>55</b>	2.91 s	3.46 dd (22.7, 4.6) 3.88 dd (22.7, 8.4)	3.04 m 1.08 d(7.3)	6.06 p(6.9) 1.67 d(6.9)
<b>56</b>	2.92 s	3.34 dd (22.6, 9.2) 3.95 dd (22.7, 8.4)	2.62 m 1.25 d(6.8)	5.57 bp(7.5) 1.79 d(6.5)
<b>57</b>	2.35 d(6.5) 6.87 d(16) 8.34 dq(16, 6.5)	3.71 t(7.5)	2.51 p(7.5)	5.38 t(7.5)
<b>58</b>	2.33 d(6.5) 6.83 d(16) 8.29 dq(16, 6.5)	3.67 m	?	5.82 bp(6.5) 1.69 d(6.5)
<b>59<sup>d</sup></b>	?	3.41 t(7.5)	?	5.21 t(7.5)
<b>60<sup>d</sup></b>	?	3.67 m	?	5.38 t(7.5)
	1.19 t(6.5)			

a) Measured at 90 or 500 MHz in CF<sub>3</sub>SO<sub>3</sub>H at 25 °C unless otherwise noted.

b) reference (CH<sub>3</sub>)<sub>4</sub>N<sup>+</sup> BF<sub>4</sub><sup>-</sup> at 3.10 ppm; b = broad, s = singlet, d = doublet, t = triplet, q = quartet, p = pentet, h = hextet.

c) as SbCl<sub>6</sub><sup>-</sup> salt in CD<sub>3</sub>NO<sub>2</sub> at 25 °C; 200 MHz; ref CD<sub>2</sub>HNO<sub>2</sub> at 4.33 ppm. A trace of CH<sub>2</sub>Cl<sub>2</sub> in one sample gave a signal at 5.44 ppm using this reference.

d) <sup>37</sup>H yields several products (**54**, **58-60**) with overlapping signals which makes interpretation of the signals difficult and the identification of the products tentative.

e) as CF<sub>3</sub>SO<sub>3</sub><sup>-</sup> salt in CD<sub>2</sub>Cl<sub>2</sub>; reference. CDHCl<sub>2</sub> at 5.32 ppm.

f) as SbCl<sub>6</sub><sup>-</sup> salt in CD<sub>2</sub>Cl<sub>2</sub>; reference CH<sub>2</sub>Cl<sub>2</sub> at 5.30 ppm; low solubility of this salt makes identification of signals for H2 difficult.

Table 4.5:  $^{13}\text{C}$  NMR data for oxolanylium ions.<sup>a,b,c</sup>

compd	chemical shift (ppm) at position noted				
	C2	R	C3/R <sub>1</sub>	C4/R <sub>3</sub>	C5/R <sub>5</sub>
44	243.9 s	23.2 q(138)	45.8 t(138)	20.1 t(136)	93.9 t(161)
44 <sup>d</sup>	244.8	24.8	47.1	21.6	95.1
45	222.0	126.9 131.9 136.8 145.0	40.5	22.0	91.7
49	246.6 s	22.2 q(133)	52.9 d(133) 14.5 q(132)	28.5 t(139)	92.0 t(164)
50	243.5 s	22.7 q(137)	63.8 d(134) 128.5 d(152) 130.7 d(152) 132.1 s	29.4 t(143)	92.9 t(164)
52	241.5	23.6	46.3	27.7	109.1 19.2
55	241.8 s	24.1 q(133.3)	53.3 t(136)	33.1 d(137.4) 12.6 q(127.1)	110.6 d(158.6) 13.8 q(129.8)
56	242.1	24.1	53.1	37.9 14.6	112.9 17.8

a) spectra were collected at 125.721, 62.86 and 50.323 MHz (500, 250 and 200 MHz for  $^1\text{H}$ ).

b) ref.  $\text{CF}_3\text{SO}_3\text{H}$  at 119.0 ppm. One sample contained a trace of  $\text{CDCl}_3$  which gave a peak at 77.2 ppm using this reference.

c) For coupled spectra, the multiplicity (s = singlet; d = doublet; t = triplet; q = quartet) and  $^1\text{H}$ - $^{13}\text{C}$  coupling constants (Hz) are shown.

d) as an  $\text{SbCl}_6^-$  salt in  $\text{CD}_3\text{NO}_2$ ; 50.323 MHz; reference  $\text{CD}_3\text{NO}_2$  at 62.8 ppm.

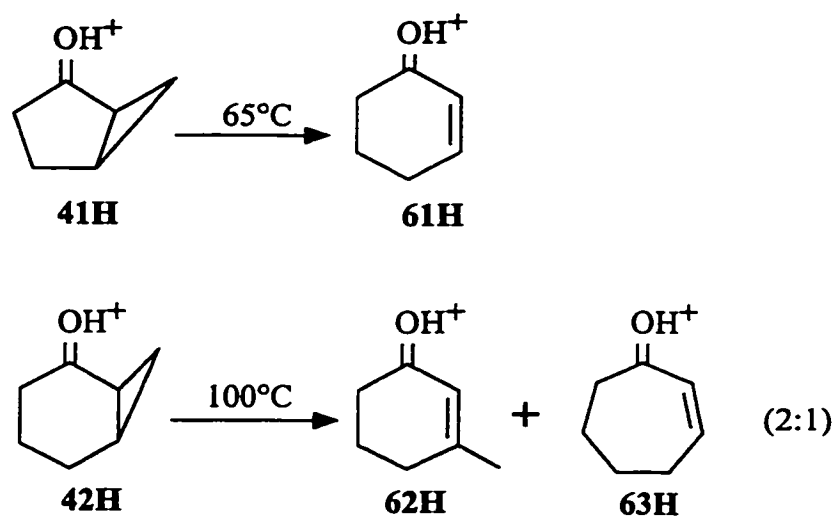


Figure 4.18: Isomerization of protonated bicyclo[3.1.0]hexanone, **41H**, and bicyclo[4.1.0]heptanone, **42H**, yields protonated enones.

Table 4.6:  $^1\text{H}$  NMR data for protonated enones produced by the isomerization of **41H** and **42H**.<sup>a</sup>

position	chemical shift (ppm) for compound noted		
	<b>61H</b>	<b>62H</b>	<b>63H<sup>b</sup></b>
2	6.88 dt(10.5, 1)	6.76 s	6.81 d(11)
3	8.60 dt(10.5, 4)	2.41 s	8.24 dt(11, 6)
4	2.88 bq(5)	2.78 t(6.5)	
5	2.25 p(6.5)	2.14 p(6.5)	
6	3.13 t(6.5)	2.94 t(6.5)	
7	--	--	

a) Measured at 25°C in triflic acid.

b) other signals for **63H** are obscured by the stronger signals of **62H**.

Different regioselectivities of bond cleavage have been observed for these two ketones previously,[41] but the reason is not immediately clear. Alignment of the cyclopropyl bonds with the vacant p-orbital at C<sup>+</sup> is known to be an important factor, but not the only factor, responsible for the regioselectivity of reductive, photochemical, acid-catalyzed and solvolytic ring openings of bicyclo[n.1.0] systems.[42]

Bicyclo[4.1.0]heptan-2-one is fairly flexible and, in fact, a crystal structure of a salt of **42H** shows that this ion adopts a nearly bisected conformation in the solid state, such that the C1-C7 and C1-C6 bonds are equally well aligned with the p-orbital at C<sup>+</sup>. [15b] This is consistent with the observation that both bonds are cleaved during isomerization. In contrast, ion **41H** is quite rigid and the external C1-C6 bond is best aligned with the p-orbital at C<sup>+</sup>. The exclusive cleavage of the internal C1-C5 bond is puzzling and indicates that other factors are at work.

In all but a few instances, discussed later, isomerization of protonated cyclopropyl ketones **26H-40H** yielded oxolanylium ions quantitatively and the oxolanylium ions were found to be stable upon extended heating. Oxonium ions, which include oxolanylium ions, are well known,[43] and the formation of oxolanylium ions is not surprising, as this ion appears to be the most stable of many possible isomeric ions. Under strong acid conditions, oxolanylium ions are formed from a variety of starting materials (Figure 4.19): a) cyclopropyl ketones[25]; 2)  $\alpha,\beta$ -,  $\beta,\gamma$ - or  $\gamma,\delta$ -unsaturated ketones[25c,44,45]; c) 4,5-dihydrofurans[46]; d)  $\gamma$ -substituted ketones[46,47]; e) acylium ions plus alkenes.[48]



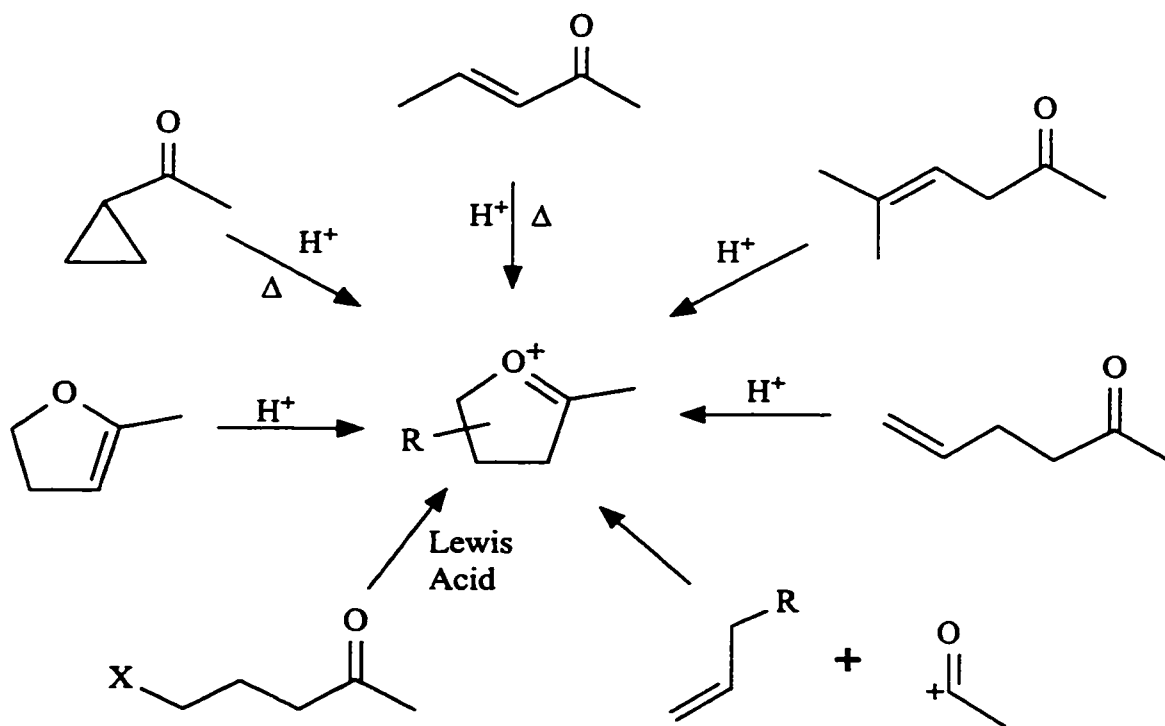


Figure 4.19: Oxolanylium ions result from a number of precursors: enones, cyclopropyl ketones, dihydrofuran,  $\gamma$ -substituted ketones, and acylium ions/alkenes.

#### 4.3.4 Characterization of Oxolanylium Ions: $^1\text{H}$ and $^{13}\text{C}$ NMR

The  $^1\text{H}$  NMR data in Table 4.4 agrees very well with that found in the literature.[25a,25c,43-47] It should be noted that some of the literature data was measured in sulfuric acid with TMS as an external reference. In these cases, all of the signals are found about 0.5 ppm further downfield than when measurement is made in triflic acid with the tetramethyl ammonium ion as reference. This difference is most likely the result of using different zero references rather than a change in structure or magnetic environment. Correction of the chemical shifts by approximately 0.5 ppm gives

results which closely match those measured in this thesis. The entries in Table 4.4 for ions **44**, **45** and **52** reveal only minor variations in the NMR spectrum when the oxolanylium ions are prepared as triflate or hexachloroantimonate salts in organic solvents such as  $\text{CD}_2\text{Cl}_2$  and  $\text{CD}_3\text{NO}_2$ .

There are several distinctive features in the  $^1\text{H}$  NMR data of the oxolanylium ions. The C5 hydrogens resonate quite far downfield with chemical shifts between 5.4 and 6.1 ppm in triflic acid. In an uncharged cyclic ether such as p-dioxane or tetrahydrofuran, these peaks would appear at ca. 3.7-4.0 ppm.[49] The greater downfield shift of the hydrogens in the oxolanylium ions is not surprising since the oxygen atom bears partial positive charge.

For several oxolanylium ions (**52**, **55**, **56**), it is possible to observe the magnitude of the geminal coupling constant between the two hydrogens on C3. For all three of these ions, the geminal coupling constant,  $^2J_{\text{HH}}$ , is about 23 Hz, among the largest geminal coupling constants measured. A large geminal coupling constant,  $^2J_{\text{HH}} = 21.8$  Hz, is also seen for the hydrogen atoms on C3 of the protonated bicyclic ketone **42H** (see Table 4.3). Geminal coupling constants generally range from -9 to -21 Hz.[50] Substitution of inductive electron acceptors, such as halogen atoms, causes the absolute value of  $^2J$  to decrease while  $\pi$ -type electron acceptors (hyperconjugative acceptors) cause an increase in the absolute values of  $^2J$ . [50,51] For example,  $^2J$  for the methylene hydrogens in malonitrile is 20.0 Hz.[51] Thus,  $^2J$  of 23 Hz seen for the oxolanylium ions and 21.8 Hz observed for **42H** are reasonable for hydrogens adjacent to a strongly electron withdrawing  $\text{sp}^2$  atom, the cation centre.

The  $^{13}\text{C}$  NMR spectra measured in this work (Table 4.5) agree well with spectra found in the literature.[25h,47] The chemical shifts of the oxolanylium ions are nearly invariant as the solvent and counter-anion are varied. For instance, the  $^{13}\text{C}$  NMR spectra of **44** measured in triflic acid ( $\text{CF}_3\text{SO}_3^-$  counterion) and in nitromethane ( $\text{SbCl}_6^-$  counterion) exhibit chemical shifts which differ by no more than 1.6 ppm (Table 4.4).

The most distinctive feature of the  $^{13}\text{C}$  NMR spectra of oxolanylium ions is the C5 signal, found at 91 - 95 ppm when C5 is unsubstituted, and at 106 - 112 ppm when C5 is monosubstituted. This can be compared to data for tetrahydrofurans,[52] pyrans,[53] and dioxanylium ions and dioxolanylium ions[54] (Figure 4.20). The chemical shift of C5 is moved markedly downfield in the oxolanylium ions relative to the neutral models and the related dioxygen containing carbocations. This is consistent with significant positive charge on C5.

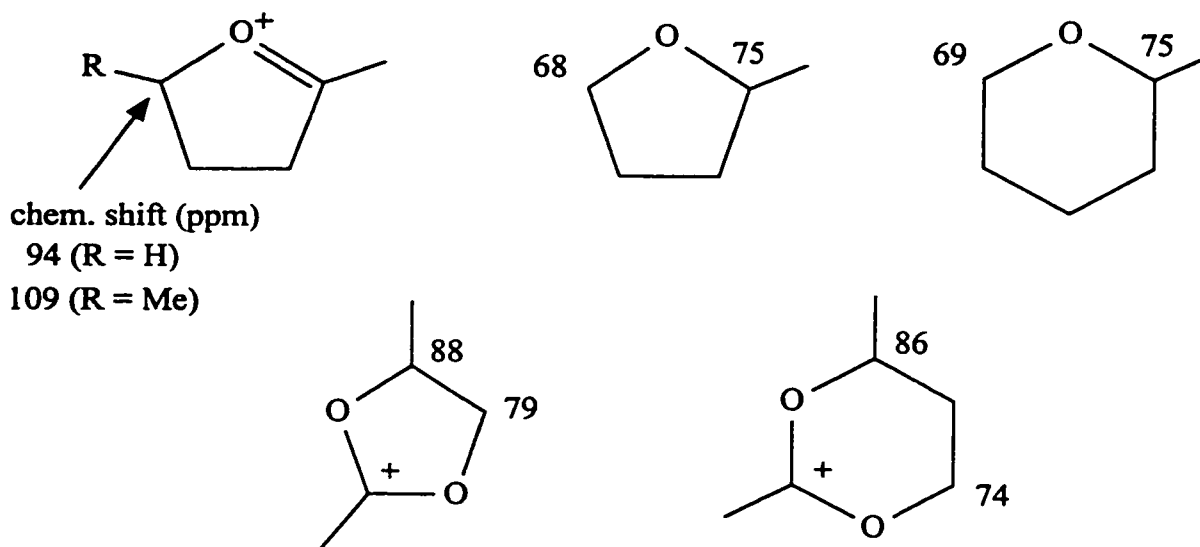


Figure 4.20: Comparison of  $^{13}\text{C}$  chemical shifts (ppm) of oxolanylium ions with neutral and ionic model compounds.

The coupling constant,  $^1J_{\text{CH}}$ , between C5 and H5 increases to ca. 160 Hz in the oxolanylium ions from ca. 145 Hz in tetrahydrofuran. In contrast, the C-H coupling constants for C4/H4 and C3/H3 do not differ significantly for the charged and neutral compounds. This points to increased charge on C5, resulting in a change towards  $sp^2$  hybridization. The downfield shift of C5 and H5 and the increase in  $^2J_{\text{CH}}(\text{C5/H5})$  are consistent with the third resonance structure for the oxolanylium ion (Figure 4.21), in which the positive charge is on C5.

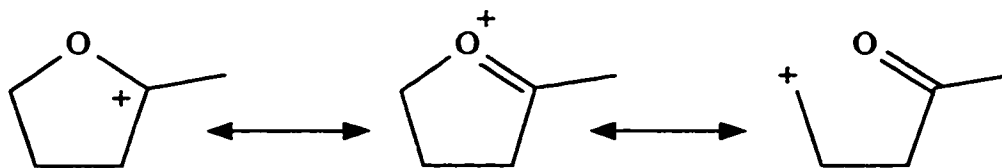


Figure 4.21: Resonance structures for the oxolanylium ion.

Further evidence for the existence of positive charge at C5 comes from the reactions of oxolanylium ions. Nucleophilic attack can occur at C5 of oxolanylium ions leading to rupture of the C5-O bond.[43] In this work, the direct isomerization between two oxolanylium ions was observed for the first time. The *cis* 2,4,5-trimethyl oxolanylium ion, **55**, isomerizes to its *trans* stereoisomer **56** (Figure 4.22) upon heating at 100 °C. An equilibrium mixture of **55/56** (19.5/80.5) is established after extended heating ( $\Delta G = 1.05$  kcal/mol). While isomerization may occur by a series of nucleophilic attacks at C5, it seems more likely that isomerization occurs by directly breaking the C5-O bond to form an alkyl cation. C4-C5 bond rotation and reformation of the C5-O bond would complete the isomerization as illustrated in Figure 4.22. The observed C5-O bond

breaking is consistent with the resonance picture shown in Figure 4.21.

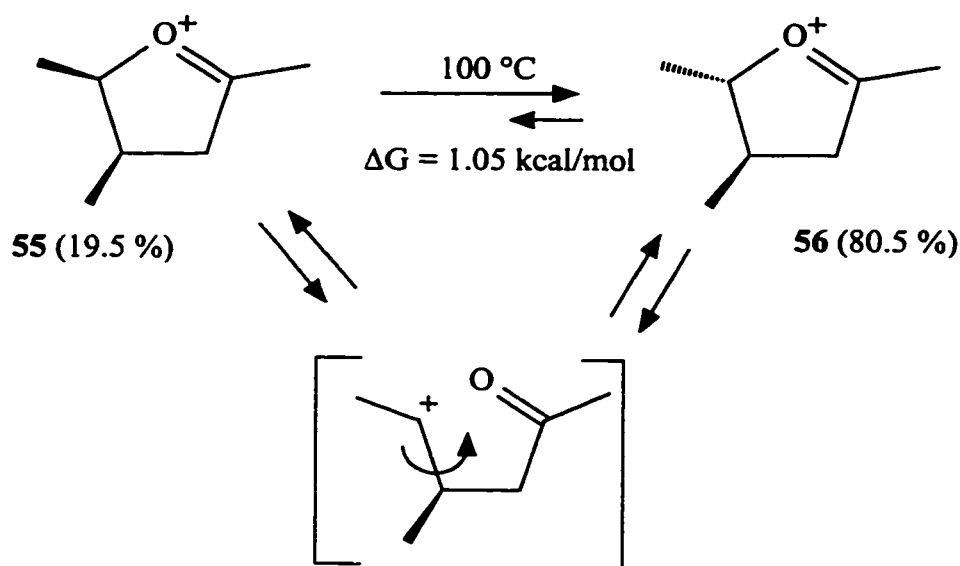


Figure 4.22: Cis and trans 2,4,5-trimethyloxolanylium ion isomers exist as an equilibrium mixture at 100 °C in triflic acid.

#### 4.3.5 Stereochemistry of Dimethyl Substituted Cyclopropyl Ketones and Oxolanylium Ions

Cyclopropyl ketones **38–40** and oxolanylium ions **55** and **56** are dimethyl substituted. It was necessary to determine the relative stereochemistry of the the methyl groups, primarily for the mechanistic studies presented in Chapter 5. This was accomplished with a variety of information. With both the neutral (Table 4.7) and protonated cyclopropyl ketones (Table 4.1), the  $^1\text{H}$  NMR signal for H1 is particularly diagnostic; the H1 signal moves upfield as more methyl groups are placed cis to this hydrogen. The signal for H1 is found at 1.92, 1.54 and 1.31 ppm for **39**, **38** and **40**, and

Table 4.7: <sup>1</sup>H NMR data for the 2,3-dimethylcyclopropyl methyl ketones, **38-40**.<sup>a</sup>

cmpd	chemical shift (ppm) at position noted			
	R	H1	H2/R <sub>2</sub>	H3/R <sub>3</sub>
<b>38</b>	2.07 s	1.54 m	1.10 m 0.98 d(2)	1.10 m 1.08 d(2)
<b>39</b>	2.19 s	1.92 t(8.5)	1.48 m 1.11 dd(4.2, 1.9)	1.48 m 1.11 dd(4.2, 1.9)
<b>40</b>	2.16 s	1.31 t(4.3)	1.52 m 1.07 dd(4.1, 1.9)	1.52 m 1.07 dd(4.1, 1.9)

a) **38** measured at 90 MHz and **39** and **40** measured at 500 MHz at room temperature.

2.82, 2.57 and 2.23 ppm for **39H**, **38H** and **40H**, respectively. Also, the coupling constants between H1 and H2/H3 provide information about the structure. The cis coupling constants (<sup>3</sup>J<sub>cis</sub>) in cyclopropyl systems are larger than the trans coupling constants (<sup>3</sup>J<sub>trans</sub>).<sup>[55]</sup> The triplets for H1 in **39** (<sup>3</sup>J = 8.5 Hz, two cis couplings) and **40** (<sup>3</sup>J = 4.3 Hz, two trans couplings) illustrate this relationship clearly. The protonated ketones reveal a similar pattern: **39H** (triplet, <sup>3</sup>J = 7.5 Hz), **40H** (triplet, <sup>3</sup>J = 3.5 Hz), while **38H** (doublet of doublets, <sup>3</sup>J = 7, 4.5 Hz) displays both a trans and a cis coupling constant (Figure 4.23).

The <sup>13</sup>C chemical shifts of the methyl signals in **39** and **40** (Table 4.2) gives information about the orientation of the methyl groups relative to the acetyl function. It is known that in substituted cyclopropyl compounds cis-substituents cause considerable shielding of each other.<sup>[37a,56]</sup> The <sup>13</sup>C NMR chemical shifts of the methyl groups in **40** and **39** (11.9 vs. 6.6 ppm, respectively) are consistent with the methyl groups of **40** being

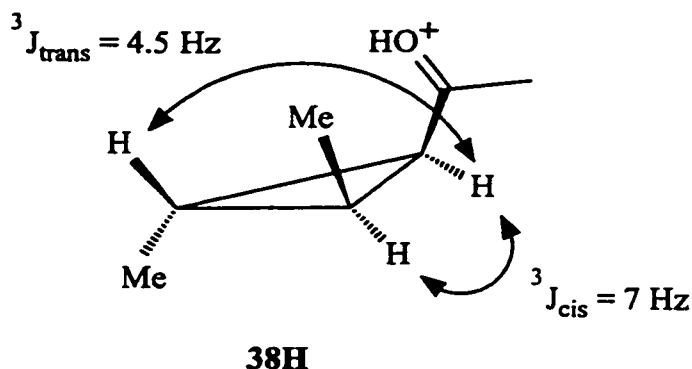


Figure 4.23: Signal for H1 of **38H** shows cis and trans coupling constants.

trans to the acetyl function and those of **39** being cis to the acetyl function. Similarly, the methyl resonances of **40H** and **39H** (Table 4.2) are found at 12.6 and 7.4 ppm, respectively, supporting the assigned stereochemistries.

In addition, during the preparation of **39** and **40** a mixture of the cis,cis- and trans,trans-2,3-dimethylcyclopropanecarboxylic acids were obtained. The solid was recrystallized and a single crystal was investigated by X-ray diffraction techniques. The space group and cell parameters for this crystal were identical to those found in the literature[57] for the trans,trans isomer.

Finally, the stereochemistry of **40** was confirmed by the determination of the crystal structure of its 2,4-dinitrophenylhydrazone derivative (Figure 4.24). The structure of this molecule was determined in a single crystal X-ray diffraction experiment. Crystallographic data can be found in the Appendix. The crystallographically determined structure is shown in Figure 4.25. This confirmed that the two methyl groups in **40** were cis to each other and trans to the acetyl function.

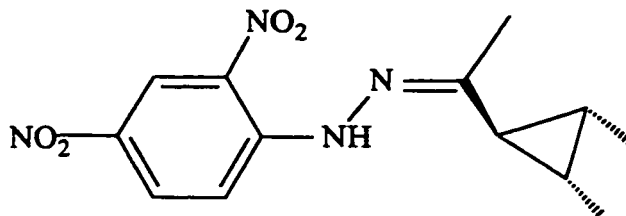


Figure 4.24: The 2,4-dinitrophenylhydrazone derivative of **40**.

The relative stereochemistry of the methyl groups in the oxolanylium ions **55** and **56** was assigned on the basis of  $^1\text{H}$  and  $^{13}\text{C}$  NMR data (Tables 4.4 and 4.5). The oxolanylium ion is a fairly rigid system so the methyl groups in the cis isomer will be partially eclipsed and, thus, would be expected to resonate upfield of those in the trans isomer. This has been observed for other rigid dimethyl-substituted systems.[58] In the case of the oxolanylium ions, the methyl resonances of the cis-dimethyl isomer, **55**, appear upfield of those of the trans isomer in both the  $^1\text{H}$  (1.08 and 1.67 vs. 1.25 and 1.79 ppm) and the  $^{13}\text{C}$  (12.6 and 13.8 vs. 14.6 and 17.8 ppm) NMR spectra. In the trans isomer, **56**, both H4 and H5 are cis to a methyl group on the neighbouring carbon. The chemical shifts of H4 and H5 in **56** (2.62 and 5.57 ppm) are upfield of those for **55** (3.04 and 6.06 ppm), consistent with the assigned stereochemistry.

Confirmation of the assignments is provided by the relative stabilities of the two isomers. As described earlier, ion **55** isomerizes to its trans stereoisomer **56** (Figure 4.22) forming an equilibrium mixture after extended heating at 100 °C in triflic acid. The free energy difference ( $\Delta G$ ) between the trans and cis isomers is 1.05 kcal/mol; **56** is 1.05 kcal/mol more stable than **55**.



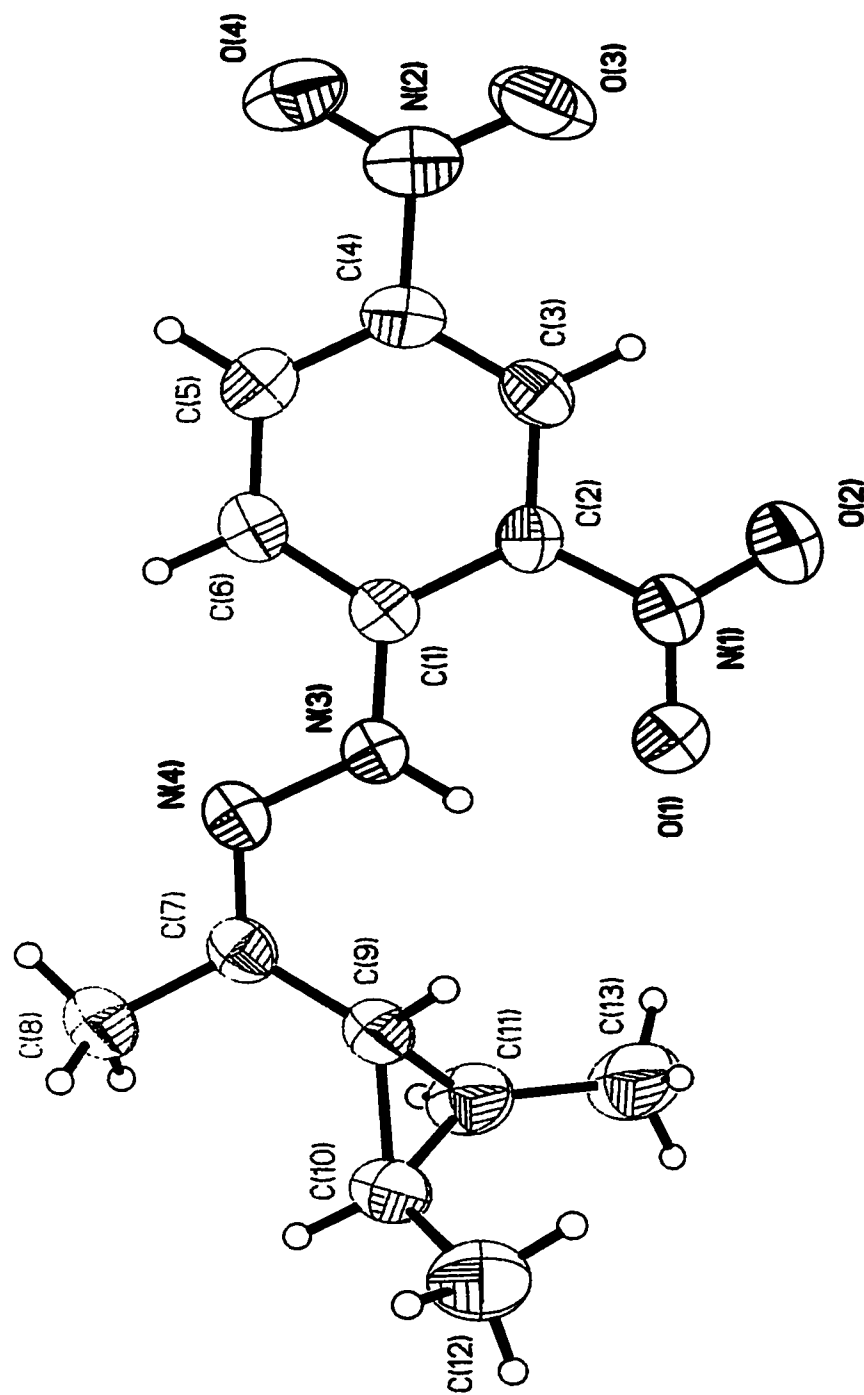


Figure 4.25: ORTEP diagram of the crystal structure of the 2,4-dinitrophenylhydrazone derivative of **40**. Note that both methyl groups are trans to the carbonyl (hydrazone) group.

#### 4.3.6 Products Other Than Oxolanylium Ions

With the exception of the bicyclic ketones **41** and **42**, oxolanylium ions are produced during every isomerization of a protonated cyclopropyl ketone in triflic acid. However, in a few instances, they were not the exclusive product of isomerization.

Protonation of cyclopropane carboxaldehyde, **26**, was often accompanied by some charring, but the only species detected in the  $^1\text{H}$  NMR spectrum is protonated cyclopropane carboxaldehyde, **26H**. Upon heating at 35 °C, a single product is formed, having a  $^1\text{H}$  NMR spectrum (see Table 4.4) consistent with that of other oxolanylium ions. If this same solution is heated at a higher temperature (i.e.  $\geq 65^\circ\text{C}$ ), one or more new products appear. Some of the peaks (triplets at 5.82 and 4.65 ppm and a singlet at 9.58 ppm) in the  $^1\text{H}$  NMR spectrum are similar to those of the initial isomerization product indicating a similar structure, perhaps a ring opened product such as the  $\gamma$ -substituted aldehyde (protonated 4-triflatobutanal). Two possible reaction pathways are shown in Figure 4.26.

In one experiment, isomerization of **35H** to **52** (Figure 4.27) produced a trace (2%) of protonated hex-3-en-2-one (signals at 1.23 t, 6.82 d(15.5 Hz), 8.56 dt(15.5, 5.9)). Extended heating of this sample at 100 °C did not lead to an increase in the amount of protonated hexenone. This indicates that protonated hex-3-en-2-one was not derived from **52**. It is possible that this sample experienced extended exposure to light causing the photochemical formation of protonated hex-3-en-2-one (see Section 4.3.7).

The two dicyclopropyl ketones, **31** and **37**, gave several products upon heating in triflic acid. Protonated dicyclopropyl ketone, **31H**, gives two or more products upon

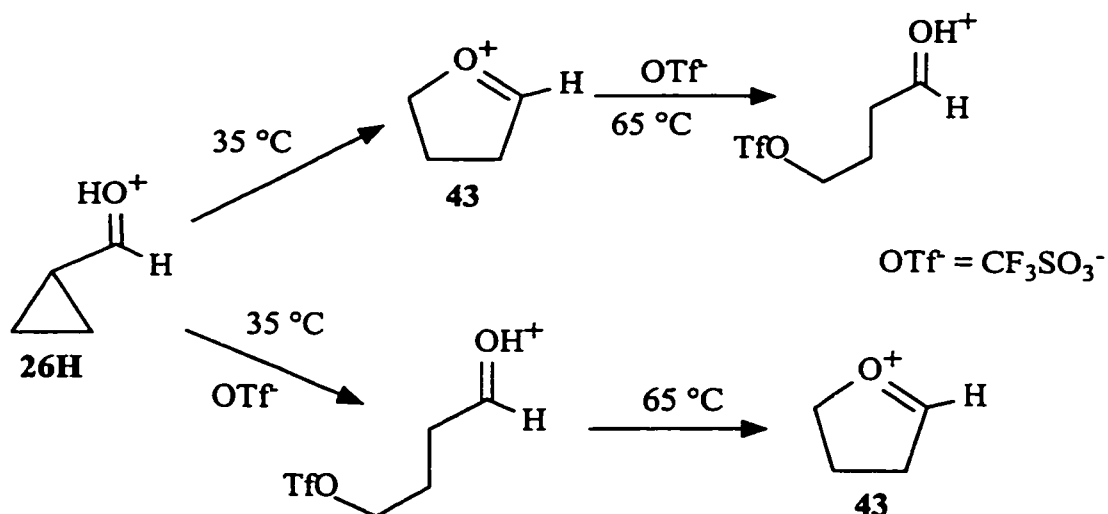


Figure 4.26: Two possible reaction paths for protonated cyclopropanecarboxaldehyde, 26H.

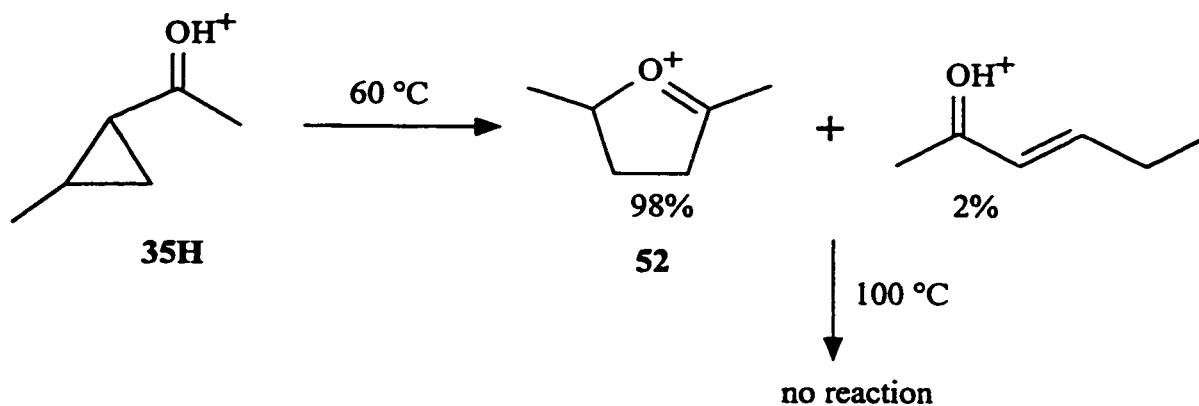


Figure 4.27: During a single isomerization of 35H, protonated hexenone was formed in addition to the oxolanylium ion product 52. Extended heating at 100 °C did not change the composition of the product mixture.

heating at 100 °C (Figure 4.28). The major product has a <sup>1</sup>H NMR spectrum consistent with cyclopropyl oxolanylium ion 48 (triplets at 5.3 and 3.5 ppm). Upon extended heating, the 2-(1-propenyl)oxolanylium ion, 57, is formed as evidenced by the appearance of vinyl signals at 6.87 and 8.34 ppm. It appears that each of the initial products from

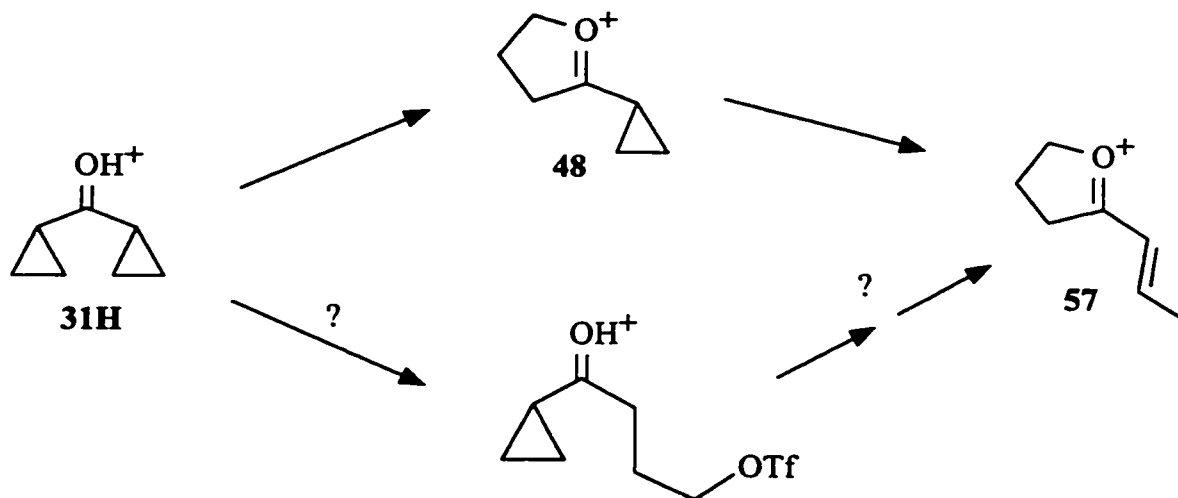


Figure 4.28: Protonated dicyclopropyl ketone, **31H**, isomerizes to 2-cyclopropyl-oxolanylium ion, **48**, which isomerizes to 2-(1-propenyl)-oxolanylium ion, **57**. A second route may be partially responsible for the formation of **57**.

protonated dicyclopropyl ketone is able to form the propenyloxolanylium ion. Thus, one of the initial products may be a  $\gamma$ -substituted ketone (Figure 4.28) which could furnish **57** upon extended heating.

Aryl-substituted cyclopropyl ketones might yield tetralones or indanones upon treatment with strong acids. Murphy and coworkers<sup>[25d-25i]</sup> have prepared tetralones from aryl-substituted cyclopropyl ketones by treatment with Lewis acids (Figure 4.29). In this work, tetralone production is possible for compounds **28-30**, **34**, and **36**, but in each case the sole product of isomerization in triflic acid was an oxolanylium ion.

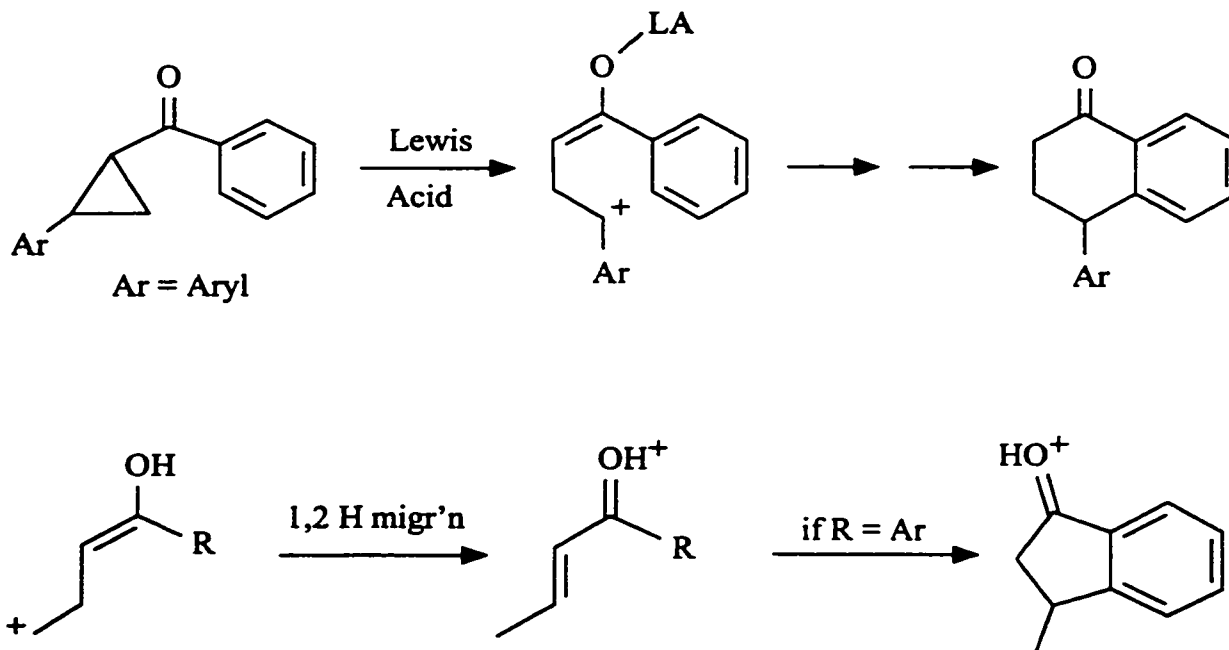


Figure 4.29: Tetralones or indanones (via enones) could be formed from aryl cyclopropyl ketones in strong acids.

#### 4.3.7 Attempted Photoisomerization of Protonated Cyclopropyl Ketones

The photochemistry of protonated cyclopropyl ketones was investigated to check for the occurrence of ring expansion in the photochemical reaction. It was anticipated that protonated cyclopropyl ketones might undergo a facile ring expansion upon irradiation similar to the thermal reaction.

Preliminary experiments were conducted with cyclopropyl methyl ketone, **27**, and cyclopropyl phenyl ketone, **28**. Irradiation of a solution of **27H** in triflic acid with 254 nm light led to ring opening; protonated pent-3-en-2-one was formed. Following 18 hours of irradiation, about 15% of **27H** had been isomerized to protonated pentenone (Figure 4.30). Similarly, irradiation of **28H** for 14 hours with 300 nm light provided

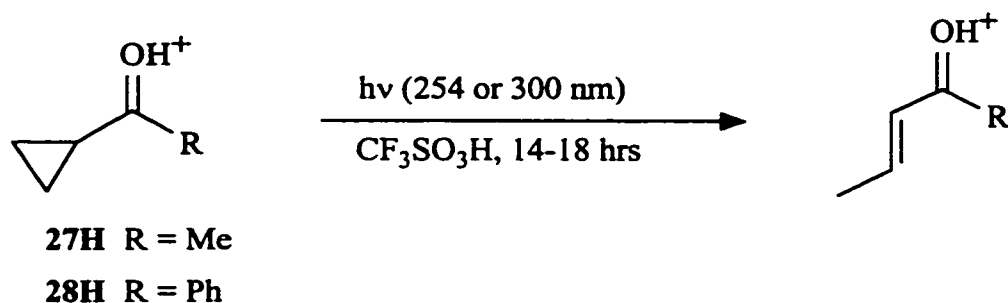


Figure 4.30: Irradiation of **27H** at 254 nm or **28H** at 300 nm leads to formation of the corresponding protonated enone.

about 70% of the ring opened product, protonated 1-phenylbut-2-en-1-one (Figure 4.30). A doublet ( $J = 16$  Hz) at 7.32 ppm is consistent with H2 of protonated 1-phenylbut-2-en-1-one. New signals also appeared at 2.4 and 7.6-8.4 ppm but these were obscured by the remaining signals of **28H**. Since products of ring expansion were not detected, the photochemical studies were not extended to the 2,3-dimethylcyclopropyl methyl ketones (**38-40**), which had been used to check for the stereoselectivity of thermal isomerization.

The two examples studied did not undergo photochemical ring expansion in triflic acid. Presumably, with the the energy available in the excited state, the cyclopropyl ring opens to form a primary cation followed by a rapid 1,2 H-migration to produce the protonated enone. While ring expansion was not observed in these cases, it is possible that photochemical ring expansion may be observed for protonated cyclopropyl ketones with a different substitution pattern.

#### 4.3.8 Heats of Isomerization of Protonated Cyclopropyl Ketones

The quantitative nature of protonated cyclopropyl ketone isomerizations made them ideal candidates for measurement of the heat of isomerization ( $\Delta H_R$ ). DSC was used to measure the heats of isomerization ( $\Delta H_R$ ) for several cyclopropyl ketones in triflic acid. All of the reactions proceeded cleanly and quantitatively to the product cation (oxolanylium ion or protonated enone). DSC thermograms for the isomerizations of protonated cyclopropyl methyl ketone, **27H**, and protonated cyclopropyl phenyl ketone, **28H**, are shown in Figures 4.31 and 4.32. The results are displayed in Table 4.8. All of the reactions are strongly exothermic and give good reproducibility with standard deviations typically  $\leq 5\%$ .

Table 4.8: Heats of reaction ( $\Delta H_R$ ) for the isomerization of protonated cyclopropyl ketones as determined by DSC.

reaction	$-\Delta H_R$ (kcal/mol)	$T_{\text{peak}}$ ( $^{\circ}\text{C}$ ) <sup>a</sup>
<b>27H - 44</b>	$9.8 \pm 0.3$	80-140
<b>28H - 45</b>	$13.0 \pm 0.6$	70-145
<b>32H - 49</b>	$10.8 \pm 0.4$	70-150
<b>33H - 50</b>	$8.5 \pm 0.3$	55-130
<b>35H - 52</b>	$11.7 \pm 0.2$	30-110
<b>36H - 53</b>	$12.1 \pm 0.3$	45-105
<b>38H - 55/56</b>	$11.8 \pm 0.4$	45-115
<b>39H - 55/56</b>	$10.8 \pm 0.7$	20-80
<b>41H - 61H</b>	$8.4 \pm 0.5$	50-115

a) temperature at beginning and end of exotherm in DSC trace.

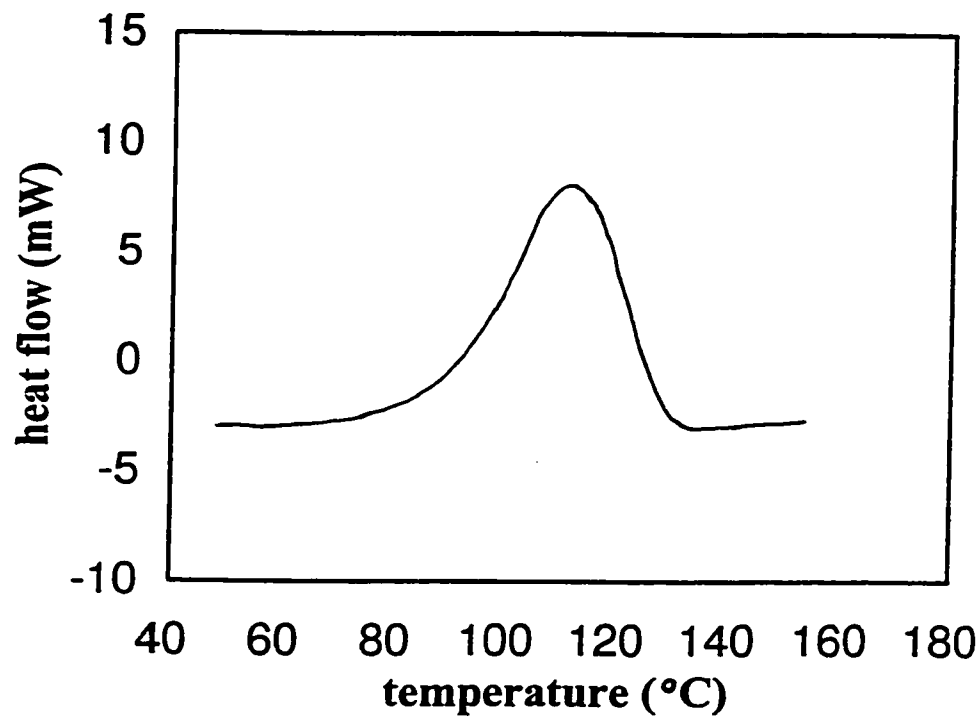


Figure 4.31: DSC thermogram for the isomerization of protonated cyclopropyl methyl ketone, **27H**, to 2-methyloxolanylium ion, **44**. Scan rate = 1 °C/min; sample size = 18.4 mg of **27**.

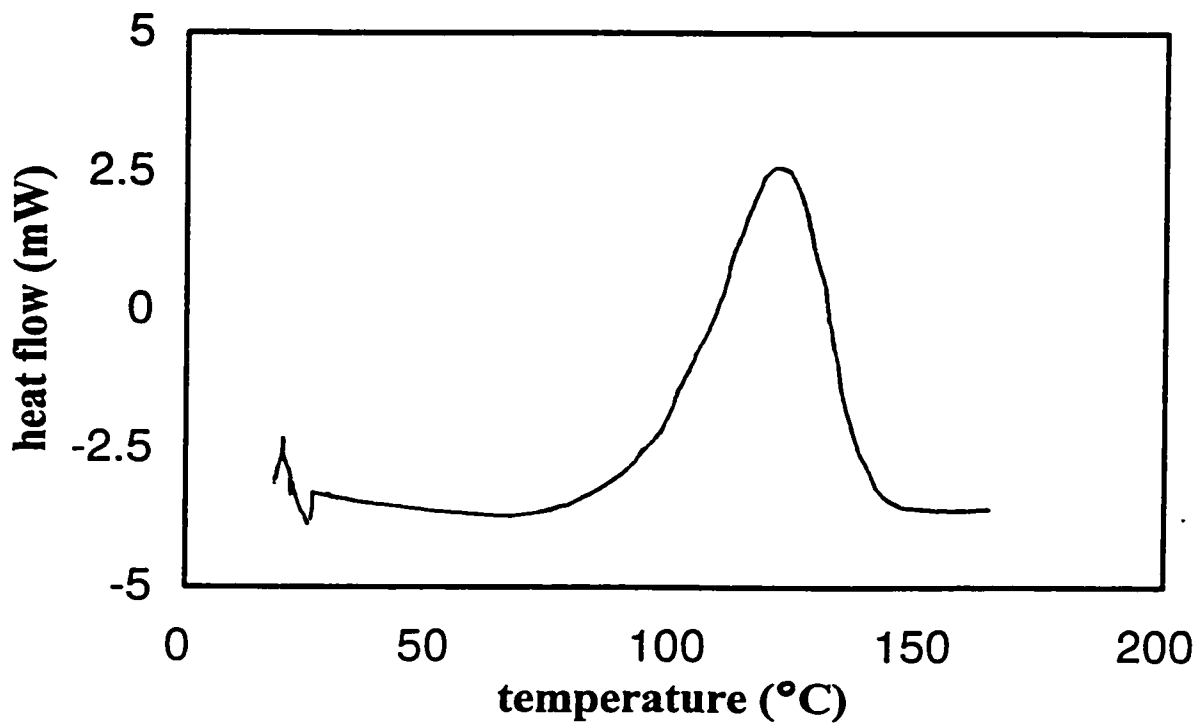


Figure 4.32: DSC thermogram for the isomerization of protonated cyclopropyl phenyl ketone, **28H**, to 2-phenyloxolanylium ion, **45**. Scan rate = 1 °C/min; sample size = 13.4 mg of **28**.



The  $\Delta H_R$  values for ring expansion (Note: **41H** - **61H** is a ring opening) fall in a fairly narrow range with all but one found in the range of  $-11 \pm 2$  kcal/mol. Thus, the substituent effects must be similar in the reactant and product cations. It is difficult to discern any trends in the  $\Delta H_R$  values in Table 4.8. For example, the isomerization of **27H** is  $3.2 \pm 0.7$  kcal/mol less exothermic than that of **28H**. The analogous pair, **35H** and **36H**, should show a similar effect, but instead, have the same  $\Delta H_R$  within error. Similarly, methyl substitution at the  $\beta$ -carbon of the cyclopropyl ring makes  $\Delta H_R$  more exothermic for **27H** vs. **35H** ( $\Delta\Delta H_R = -1.9 \pm 0.4$  kcal/mol) but the same is not true for **28H** vs. **36H** ( $\Delta\Delta H_R = 0.9 \pm 0.7$  kcal/mol). It is not clear whether one of the  $\Delta H_R$  values is in error, or another factor is at work.

Compounds **27H**, **32H**, **33H** differ only in the substituent at the  $\alpha$ -carbon (C1) of the cyclopropyl ring. When a methyl group is added to **27H**,  $\Delta H_R$  is more exothermic ( $\Delta\Delta H_R = -1.0 \pm 0.5$  kcal/mol), but when a phenyl group is added  $\Delta H_R$  decreases ( $\Delta\Delta H_R = 1.3 \pm 0.4$  kcal/mol). The changes in  $\Delta H_R$  may be due to the inductive effects of the substituents, possibly coupled with their effects on solvation. In terms of inductive effect, a phenyl group is electron-withdrawing and a methyl group electron-donating relative to hydrogen and, thus, consistent with the observed trend in  $\Delta H_R$  values.

Structural studies[15,59] of carbocations, including protonated cyclopropyl ketones and dioxolanylium ions have provided valuable information about solvent-ion interactions. H-bonding between solvent (or counter-ion) and the proton is an important interaction for protonated ketones. In systems without a protonated oxygen, the principal interaction will be between the cation centre and counter-ion (or solvent). This

interaction is also present in protonated ketones. An  $\alpha$ -substituent will not hinder H-bonding in the protonated cyclopropyl ketone but it may hinder solvent approach to one side of the oxolanylium ion (Figure 4.33). Further experiments would be required to elucidate the role of solvation in these rearrangements.

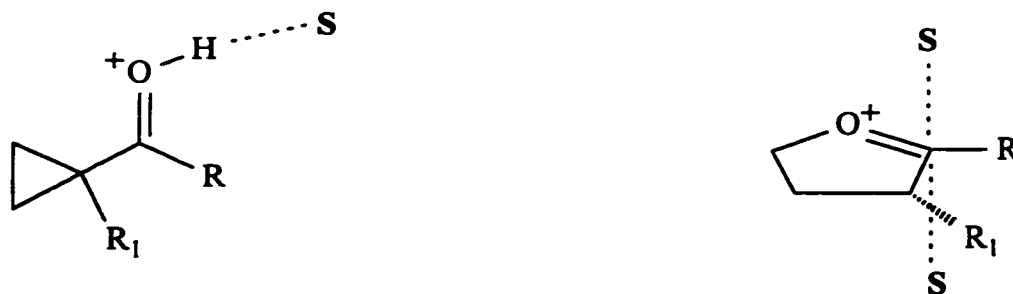


Figure 4.33: The principal ion-solvent interaction for protonated cyclopropyl ketone will be H-bonding to the proton on the carbonyl oxygen. With the oxolanylium ion, solvent will interact most strongly with the cation centre.

Compounds **35H** and **41H** have a similar substitution pattern about the cyclopropyl ketone portion of the molecule but one undergoes ring expansion while the other isomerizes to a protonated enone. Comparison of the  $\Delta H_r$  values for the isomerization of these two ions gives a guide to the relative energies of protonated cyclopropyl ketones, enones and oxolanylium ions. Apparently, the energy of the protonated cyclopropyl ketone lies about 8 kcal/mol above that of a protonated enone, and about 11 kcal/mol above that of an oxolanylium ion.

The magnitude of  $\Delta H_r$  is determined by the changes in: a) ring strain, b) bond energy (bonds broken/made), c) charge stabilization, and d) substituent effects. Estimates of the strain/bond energy contributions can be obtained by comparing the  $\Delta H_r$  values for

suitable model compounds. The  $\Delta H_f$  values for cyclopropylmethanol (-30.2 kcal/mol), tetrahydrofuran (-43.4) and 2-buten-1-ol (-37.3) can be estimated by the group additivity method.[60] The differences between these values gives a rough measure of the strain/bond energy contributions to the  $\Delta H_R$  values; about -13 kcal/mol for ring expansion and -7 for ring opening. These rough estimates are similar to the measured  $\Delta H_R$  values.

One final piece of thermodynamic information is available. The free energy difference,  $\Delta G$ , between the 4,5-dimethyloxolanylium ions **55** and **56** can be calculated from the equilibrium ratio (19:81) formed at 100 °C. Thus, the cis isomer is 1.1 kcal/mol less stable than the trans isomer.

#### 4.4 Summary and Conclusions

Eight cyclopropyl ketones were synthesized including all three diastereomers of 2,3-dimethylcyclopropyl methyl ketone. A total of seventeen cyclopropyl ketones were investigated.

The  $^1\text{H}$  and  $^{13}\text{C}$  NMR spectra of the protonated ketones, **26H-42H**, reveal that the ketones are cleanly protonated and that positive charge is concentrated at C(O), C2 and C3, consistent with strong conjugation of the cyclopropyl ring with the protonated carbonyl function. In the oxolanylium ion, C(O) and C5 bear significant positive charge.

The isomerization of cyclopropyl ketones in strong acids is generally a clean and quantitative reaction producing oxolanylium ions as the exclusive products. Protonated enones are produced only when the formation of oxolanylium ions is prevented by other

constraints (i.e. strain). Thus, the energies of the three ions must increase in the order: oxolanylium ion < protonated enone < protonated cyclopropyl ketone.

The stereochemistry of the methyl groups in all three diastereomers of 2,3-dimethylcyclopropyl methyl ketone was established on the basis of a variety of spectroscopic information. The stereochemistry of the two 4,5-dimethyloxolanylium ions was determined by NMR spectroscopy and the relative stabilities of the two ions. The trans isomer is more stable than the cis isomer ( $\Delta G = -1.05$  kcal/mol).

Instead of photochemical ring expansion, the protonated cyclopropyl ketones underwent ring opening to protonated enones upon irradiation.

DSC proved to be a valuable technique for determination of the heats of isomerization of protonated cyclopropyl ketones. The heats of isomerization for ring expansion were found to fall in a narrow range ( $-11 \pm 2$  kcal/mol). The heats of isomerization for ring expansion and ring opening were similar to estimates of the strain and bond energy changes that occur upon isomerization. The narrow range of heats of isomerization reveals that substituents have similar stabilizing effects in both protonated cyclopropyl ketones and oxolanylium ions.

#### 4.5 References

1. *The Chemistry of the Cyclopropyl Group*, Z. Rappoport (ed.), Wiley, Toronto, 1987 (vol. 1) and 1995 (vol. 2); G. Boche, H.M. Walborsky, *Cyclopropane Derived Reactive Intermediates*, Wiley, Toronto, 1990; A. de Meijere, *Ang. Chem. Int. Ed. Engl.*, **1979**, *18*, 809.

2. T.H. Lowry, K.S. Richardson, *Mechanism and Theory in Organic Chemistry*, Harper & Row, New York, 1981, 2nd edn., p. 150.
3. B. Rozsondai in *The Chemistry of the Cyclopropyl Group*, Z. Rappoport (ed.), Wiley, Toronto, 1995, vol. 2, chpt. 3, p. 139
4. D. Cremer, E. Kraka, K.J. Szabo in *The Chemistry of the Cyclopropyl Group*, Z. Rappoport (ed.), Wiley, Toronto, 1995 vol. 2, chpt. 2, p. 43; K.B. Wiberg in *The Chemistry of the Cyclopropyl Group*, Z. Rappoport (ed.), Wiley, Toronto, 1987, vol. 1, chpt. 1, p. 1.
5. G.A. Olah, P.V. Reddy, G.K.S. Prakash in *The Chemistry of the Cyclopropyl Group*, Z. Rappoport (ed.), Wiley, New York, 1995, vol. 2, chpt. 14, p. 813.
6. R.F. Childs, D. Cremer, G. Elia in *The Chemistry of the Cyclopropyl Group*, Z. Rappoport (ed.), Wiley, Toronto, 1995, vol. 2, chpt. 8, p. 411; D. Cremer, R.F. Childs, E. Kraka in *The Chemistry of the Cyclopropyl Group*, Z. Rappoport (ed.), Wiley, Toronto, 1995, vol. 2, chpt. 7, p. 339.
7. H.U. Reissig in *The Chemistry of the Cyclopropyl Group*, Z. Rappoport (ed.), Wiley, Toronto, 1987, vol. 1, chpt. 8, p. 375; R. Verhe, N. DeKimpe in *The Chemistry of the Cyclopropyl Group*, Z. Rappoport (ed.), Wiley, Toronto, 1987, vol. 1, chpt. 9, p. 445; T.T. Tidwell in *The Chemistry of the Cyclopropyl Group*, Z. Rappoport (ed.), Wiley, Toronto, 1987, vol. 1, chpt. 10, p. 565.
8. K.B. Wiberg, B.A. Hess, Jr., A.J. Ashe III in *Carbonium Ions*, G.A. Olah, P.v.R. Schleyer (eds.), Wiley, Toronto, 1972, vol. 3, chpt. 25, p. 1295.
9. H.G. Richey Jr. in *Carbonium Ions*, G.A. Olah, P.v.R. Schleyer (eds.), Wiley,

- Toronto, 1972, vol. 3, chpt. 25, p. 1201.
10. G.A. Olah, P.V. Reddy, G.K.S. Prakash, *Chem. Rev.*, **1992**, *92*, 69.
  11. G.A. Olah, D.P. Kelly, C.L. Jeuell, R.D. Porter, *J. Am. Chem. Soc.*, **1970**, *92*, 2544;  
G.A. Olah, C.L. Jeuell, D.P. Kelly, R.D. Porter, *J. Am. Chem. Soc.*, **1972**, *94*, 146;  
P.C. Myhre, G.G. Webb, C.S. Yannoni, *J. Am. Chem. Soc.*, **1990**, *112*, 8992.
  12. C.U. Pittman, Jr., G.A. Olah, *J. Am. Chem. Soc.*, **1965**, *87*, 2998 and 5123; G.A. Olah, P.W. Westerman, *J. Am. Chem. Soc.*, **1973**, *95*, 7530.
  13. G.A. Olah, P.W. Westerman, J. Nishimura, *J. Am. Chem. Soc.*, **1974**, *96*, 3548.
  14. D.S. Kabakoff, E. Namanworth, *J. Am. Chem. Soc.*, **1970**, *92*, 3234.
  15. R.F. Childs, R. Faggiani, C.J.L. Lock, M. Mahendran, S.D. Zweep, *J. Am. Chem. Soc.*, **1986**, *108*, 1692; R.F. Childs, M.D. Kostyk, C.J.L. Lock, M. Mahendran, *J. Am. Chem. Soc.*, **1990**, *112*, 8912; R.F. Childs, M. Mahendran, S.D. Zweep, G.S. Shaw, S.K. Chadda, N.A.D. Burke, B.E. George, R. Faggiani, C.J.L. Lock, *Pure Appl. Chem.*, **1986**, *58*, 111.
  16. R.V. Stevens, *Acc. Chem. Res.*, **1977**, *10*, 193; Z. Goldschmidt, B. Crammer, *Chem. Soc. Rev.*, **1988**, *17*, 229; J. Salaun in *The Chemistry of the Cyclopropyl Group*, Z. Rappoport (ed.), Wiley, Toronto, 1987, vol. 1, chpt. 13, p. 809; T. Hudlicky, T.M. Kutchan, S.M. Naqvi, *Org. React. (N.Y.)*, **1985**, *33*, 247; H.W. Heine in *Mechanisms of Molecular Migrations*, B.S. Thyagarajan (ed.), Wiley, New York, 1971, vol. 3, p. 145.
  17. a) S. Gabriel, R. Stelzner, *Chem. Ber.*, **1895**, *28*, 2929; b) R. Fittig, F. Röder, *Ann.*

- Chem.*, **1885**, 227, 1; c) W.H. Perkin, *J. Chem. Soc.*, **1885**, 47, 801; d) R. Marburg, *Ann. Chem.*, **1897**, 294, 89.
18. J.B. Cloke, *J. Am. Chem. Soc.*, **1929**, 51, 1174.
19. N.P. Neureiter, *J. Org. Chem.*, **1959**, 24, 2044.
20. Z. Goldschmidt, B. Crammer, *Chem. Soc. Rev.*, **1988**, 17, 229; E.R. Davidson, J.J. Gajewski, *J. Am. Chem. Soc.*, **1997**, 119, 10543; K.N. Houk, M. Nendel, O. Wiest, J.W. Storer, *J. Am. Chem. Soc.*, **1997**, 119, 10545; J.P. Dinnocenzo, D.A. Conlon, *J. Am. Chem. Soc.*, **1988**, 110, 2324. J. E. Baldwin, N. D. Ghatlia, *J. Am. Chem. Soc.* **1991**, 113, 6273; J.J. Gajewski, M. Warner, *J. Am. Chem. Soc.*, **1984**, 106, 802; W.E. Doering, K. Sachdev, *J. Am. Chem. Soc.*, **1974**, 96, 1168; W.E. Doering, K. Sachdev, *J. Am. Chem. Soc.*, **1975**, 97, 5512; J.E. Baldwin, K.A. Villarica, D.I. Freedberg, F.A.L. Anet, *J. Am. Chem. Soc.*, **1994**, 116, 10845; J.E. Baldwin, S.J. Bonacorsi, *J. Am. Chem. Soc.*, **1996**, 118, 8258; G. D. Andrews, J.E. Baldwin, *J. Am. Chem. Soc.* **1976**, 98, 6705; J.J. Gajewski, G.C. Paul, *J. Org. Chem.* **1991**, 56, 1986; J.J. Gajewski, L.P. Olsen, *J. Am. Chem. Soc.* **1991**, 113, 7432; J.J. Gajewski, M.P. Squicciarini, *J. Am. Chem. Soc.*, **1989**, 111, 6717; J.J. Gajewski, L.P. Olson, M.R. Willcott, *J. Am. Chem. Soc.*, **1996**, 118, 299.
21. T. Hudlicky, T.M. Kutchan, S.M. Naqvi, *Org. React. (N.Y.)*, **1985**, 33, 247; T. Hudlicky, N.E. Heard, A. Fleming, *J. Org. Chem.*, **1990**, 55, 2570; R.L. Danheiser, C. Martinez-Davila, J.M. Morin, Jr., *J. Org. Chem.*, **1980**, 45, 1340; R.L. Danheiser, C. Martinez-Davila, R.J. Auchus, J.T. Kadonaga, *J. Am. Chem. Soc.*,

- 1981, 103, 2443; R.L. Danheiser, J.J. Bronson, K. Okano, *J. Am. Chem. Soc.*, 1985, 107, 4579; D.F. Harvey, M.F. Brown, *Tetrahed. Lett.*, 1991, 32, 2871; H.W.L. Davies, B. Hu, *J. Org. Chem.*, 1992, 57, 3186.
22. R.V. Stevens, *Acc. Chem. Res.*, 1977, 10, 193; R.K. Boeckman, Jr., P.F. Jackson, J.P. Sabatucci, *J. Am. Chem. Soc.*, 1985, 107, 2191; R.K. Boeckman, Jr., J.P. Sabatucci, S.W. Goldstein, D.M. Springer, P.F. Jackson, *J. Org. Chem.*, 1986, 51, 3742; R.K. Boeckman, Jr., S.W. Goldstein, M.A. Walters, *J. Am. Chem. Soc.*, 1988, 110, 8250; R.K. Boeckman, Jr., M.A. Walters, in *Advances in Heterocyclic Natural Product Synthesis*, W.H. Pearson (ed.), JAI Press, Greenwich, Conn., 1990, Vol. 1, p. 1; H.H. Wasserman, R.P. Dion, *Tetrahed. Lett.*, 1983, 24, 3409; H.H. Wasserman, R.P. Dion, *Tetrahed. Lett.*, 1982, 23, 1413; P.C. Heidt, S.C. Bergmeier, W.H. Pearson, *Tetrahed. Lett.*, 1990, 31, 5441; R.B. Bennett, J.K. Cha, *Tetrahed. Lett.*, 1990, 31, 5437; P.-L. Wu, W.S. Wang, *J. Org. Chem.*, 1994, 59, 622.
23. a) J. Bus, H. Steinberg, T. J. de Boer, *Rec. Trav. Chim.*, 1972, 91, 657; b) J. Bus, H. Steinberg, T.J. deBoer, *Tetrahed. Lett.*, 1966, 1979; c) N.C. Deno, W.E. Billups, D. LaVietes, P.C. Scholl, S. Schneider, *J. Am. Chem. Soc.*, 1970, 92, 3700; d) R.F. Childs, T. DiClemente, E.F. Lund-Lucas, T.J. Richardson, C.V. Rogerson, *Can. J. Chem.*, 1983, 61, 856.
24. C.L. Wilson, *J. Am. Chem. Soc.*, 1947, 69, 3002; D.M.A. Armitage, C.L. Wilson, *J. Am. Chem. Soc.*, 1959, 81, 2437; D.E. McGreer, J.W. McKinley, *Can. J. Chem.*,



- 1973, 51, 1487; H. Hiraoka, *Tetrahedron*, 1973, 29, 2955; M.E. Alonso, A. Morales, *J. Org. Chem.*, 1980, 45, 4530.
25. a) C.U. Pittman, S.P. McManus, *J. Am. Chem. Soc.*, 1969, 91, 5915; b) T. Nakai, E. Wada, M. Okawara, *Tetrahed. Lett.*, 1975, 1531; c) R.F. Childs, T. DiClemente, E.F. Lund-Lucas, T.J. Richardson, C.V. Rogerson, *Can. J. Chem.*, 1983, 61, 856; d) W.S. Murphy, S. Wattanasin, *Tetrahed. Lett.*, 1980, 21, 1887; e) W.S. Murphy, S. Wattanasin, *Tetrahed. Lett.*, 1980, 21, 3517; f) W.S. Murphy, S. Wattanasin, *J. Chem. Soc., Perkin Trans. II*, 1981, 2920; g) W.S. Murphy, S. Wattanasin, *J. Chem. Soc., Perkin Trans. II*, 1982, 1029; h) W.S. Murphy, S. Wattanasin, *J. Chem. Soc., Perkin Trans. II*, 1983, 817; i) K. Hantawong, W.S. Murphy, D.K. Boyd, G. Ferguson, M. Parvez, *J. Chem. Soc., Perkin Trans. II*, 1985, 1577; j) E. Lee-Ruff, P. Khazanie, *Can. J. Chem.*, 1975, 53, 1708; k) E. Lee-Ruff, P.G. Khazanie, *Can. J. Chem.*, 1978, 56, 803; l) P.G. Khazanie, E. Lee-Ruff, *Can. J. Chem.*, 1978, 56, 808.
26. a) P.S. Engel, D.B. Gerth, *J. Am. Chem. Soc.*, 1981, 103, 7689; b) J. Bonnekesel, C. Ruchardt, *Chem. Ber.*, 1973, 106, 2890
27. T. Nakajima, H. Miyaji, M. Segi, S. Suga, *Chem. Lett.*, 1986, 181; T. Nakajima, M. Tanabe, K. Ohno, M. Segi, S. Suga, *Chem. Lett.*, 1986, 177.
28. a) H.W. Heine in *Mechanisms of Molecular Migrations*, B.S. Thyagarajan (ed.), Wiley, New York, 1971, vol. 3, p. 145; b) J. Legters, L. Thijs, B. Zwanenburg, *Rec. Trav. Chim.*, 1992, 111, 16; c) S.-H. Jung, H. Kohn, *J. Am. Chem. Soc.*, 1985, 107,

- 2931; d) M. Driess, H. Pritzkow, *Angew. Chem. Int. Ed. Engl.*, **1992**, *31*, 751; e) M.P. Clarke, I.M.T. Davidson, M.P. Dillon, *J. Chem. Soc., Chem. Commun.*, **1988**, 1139;
29. H. Langhals, C. Ruchardt, *Chem. Ber.*, **1981**, *114*, 3831.
30. J.J. Gajewski, M.P. Squicciarini, *J. Am. Chem. Soc.*, **1989**, *111*, 6717.
31. C.H. DePuy, F.W. Breitbeil, K.R. DeBruin, *J. Am. Chem. Soc.*, **1966**, *88*, 3347
32. M. Hanack, H. Eggensperger, *Chem. Ber.*, **1963**, *96*, 1259.
33. Y. Masuyama, Y. Ueno, M. Okawara, *Chem. Lett.*, **1977**, 1439.
34. N. DiBello, L. Pellacani, P.A. Tardella, *Synthesis*, **1978**, 227; W.G. Dauben, G.H. Berezin, *J. Am. Chem. Soc.*, **1967**, *89*, 3449.
35. E.J. Corey, M. Chaykovsky, *J. Am. Chem. Soc.*, **1965**, *87*, 1353.
36. A.H. Andrist, R.M. Angello, D.C. Wolfe, *J. Org. Chem.*, **1978**, *43*, 3422.
37. a) N.C. Rol, A.D. Clague, *Org. Magn. Reson.*, **1981**, *16*, 187; b) C.G. Andrieu, D. DeBruyne, D. Paquer, *Org. Magn. Reson.*, **1978**, *11*, 528; c) G.A. Olah, R.J. Spear, P.C. Hiberty, W.J. Hehre, *J. Am. Chem. Soc.*, **1976**, *98*, 7470.
38. K. Müllen, E. Kotzamani, H. Shmickler, B. Frei, *Tetrahed. Lett.*, **1984**, *25*, 5623.
39. B. Eliasson, D. Johnels, I. Sethson, U. Edlund, K. Müllen, *J. Chem. Soc. Perkin Trans. 2*, **1991**, 897; D. Farcasiu, S. Sharma, *J. Org. Chem.*, **1991**, *56*, 126.
40. G.A. Olah, R.J. Spear, *J. Am. Chem. Soc.*, **1975**, *97*, 1539.
41. E. Giacomini, M.A. Loreto, L. Pellacani, P.A. Tardella, *J. Org. Chem.*, **1980**, *45*, 519.

42. W.G. Dauben, L. Schutte, R.E. Wolf, E.J. Deviny, *J. Org. Chem.*, **1969**, *34*, 2512; A. Padwa, T.J. Wisnieff, E.J. Walsh, *J. Org. Chem.*, **1989**, *54*, 299; E.C. Friedrich, M.A. Saleh, *J. Am. Chem. Soc.*, **1973**, *95*, 2617; E.C. Friedrich, G. Biresaw, M.A. Saleh, *J. Org. Chem.*, **1983**, *48*, 1435.
43. H. Perst in *Carbonium Ions*, G.A. Olah, P.v.R. Schleyer (eds.), Wiley, New York, 1976, vol. 5, chpt. 34, p. 1361; C.U. Pittman, Jr., S.P. McManus, J.W. Larsen, *Chem. Rev.*, **1972**, *72*, 357; H. Perst, *Oxonium Ions in Organic Chemistry*, Verlag Chemie-Academic Press, New York, 1971.
44. D.M. Brouwer, J.A. vanDoorn, A.A. Kiffen, *Rec. Trav. Chim.*, **1975**, *94*, 198.
45. a) D.M. Brouwer, *Rec. Trav. Chim.*, **1969**, *88*, 530; b) G.A. Olah, Y. Halpern, Y.K. Mo, G. Liang, *J. Am. Chem. Soc.*, **1972**, *94*, 3554; c) C.U. Pittman, Jr., S.P. McManus, *Chem. Commun.*, **1968**, 1479.
46. H.R. Ward, P.D. Sherman, Jr., *J. Am. Chem. Soc.*, **1968**, *90*, 3812.
47. J.P. Begue, D. Bonnet-Delpon, *Org. Magn. Reson.*, **1980**, *14*, 349.
48. O.V. Lubinskaya, A.S. Shashkov, V.A. Chertkov, W.A. Smit, *Synthesis*, **1976**, 742.
49. C.J. Pouchert, J.R. Campbell, *The Aldrich Library of NMR Spectra*, Aldrich Chemical Co., Milwaukee, 1974.
50. D.J. Pasto, C.R. Johnson, *Laboratory Text for Organic Chemistry*, Prentice-Hall, Englewood Cliffs, NJ, 1979, p. 202.
51. R.M. Silverstein, G.C. Bassler, T.C. Morrill, *Spectrometric Identification of Organic Compounds*, Wiley, Toronto, 1991, p. 197.
52. A. Accary, J. Huet, Y. Infaret, *Org. Magn. Reson.*, **1978**, *11*, 287.

53. H. Duddeck, P. Wolff, *Org. Magn. Reson.*, **1976**, *8*, 593; N. Pothier, *Can. J. Chem.*, **1981**, *59*, 1132.
54. H. Paulsen, R. Dammeyer, *Chem. Ber.*, **1976**, *109*, 1837; H. Paulsen, E. Schüttpelz, *Org. Magn. Reson.*, **1979**, *12*, 616.
55. D.J. Pasto, C.R. Johnson, *Laboratory Text for Organic Chemistry*, Prentice-Hall, Englewood Cliffs, NJ, 1979, p. 203; R.M. Silverstein, G.C. Bassler, T.C. Morrill, *Spectrometric Identification of Organic Compounds*, Wiley, Toronto, 1991, p. 221.
56. M. Barfield, E.D. Canada, Jr., C.R. McDaniel, Jr., J.L. Marshall, S.R. Walter, *J. Am. Chem. Soc.*, **1983**, *105*, 3411.
57. P.A. Luhan, A.T. McPhail, *J. Chem. Soc. Perkin Trans. 2*, **1972**, 2372.
58. E. Breitmaier, W. Voelter, *Carbon-13 NMR Spectroscopy*, VCH, Weinheim, 1987, p. 187; J.K. Whitesell, M.A. Minton, *Stereochemical Analysis of Alicyclic Compounds by C-13 NMR Spectroscopy*, Chapman and Hall, London, 1987, p. 41.
59. T. Laube in *Stable Carbocation Chemistry*, G.K.S. Prakash, P.v.R. Schleyer (eds.), Wiley, New York, 1997, p. 453.
60. S.W. Benson, F.R. Cruickshank, D.M. Golden, G.R. Haugen, H.E. O'Neal, A.S. Rodgers, R. Shaw, R. Walsh, *Chem. Rev.*, **1969**, *69*, 279; H.K. Eigmann, D.M. Golden, S.W. Benson, *J. Phys. Chem.*, **1973**, *77*, 1687.

## **Chapter 5: Mechanism of the Protonated Cyclopropyl Ketone to Oxolanylium Ion Isomerization**

This chapter is the second of two parts dealing with the isomerization of protonated cyclopropyl ketones to oxolanylium ions. The subject of chapter 4 was identification and characterization of the reactants and products, while in this chapter the focus is on the mechanism(s) of the isomerization.

### **5.1 Introduction**

As mentioned in chapter 4, there exists a considerable variety of cyclopropyl systems for which ring expansion has been observed. The mechanism of ring expansion of vinylcyclopropane to cyclopentene has been investigated in considerable detail[1-4] since this reaction, and that of analogous systems, provides a simple test of the orbital symmetry predictions for a 1,3-sigmatropic migration.[5] In addition, the ring expansion of cyclopropyl compounds is finding increasing use in synthetic chemistry[4,6] and information about the mechanism, in particular the stereochemical outcome of ring expansion, is of great value.

The introduction will focus on the mechanism of ring expansion of protonated cyclopropyl ketones and related carbocationic systems with reference to comparable pathways occurring for neutral cyclopropyl compounds. Several mechanisms exist by

which protonated cyclopropyl ketones might undergo ring expansion, and there is evidence that each mechanism is operative for certain substrates (cyclopropyl ketones or closely related compounds) under certain conditions. Four potential mechanisms are considered:

- 1) Reaction via a protonated cyclopropyl ring
- 2) Reaction via an alkyl cation
- 3) Double nucleophilic displacement
- 4) Concerted ring expansion

Determination of the stereochemical outcome of reactions often provides essential information needed to differentiate between mechanistic pathways. A brief review of some stereochemical studies of the ring expansion of cyclopropyl compounds makes up the second part of the introduction.

### *5.1.1 Reaction via a Protonated Cyclopropyl Ring*

In the initial study of the ring expansion of cyclopropyl ketones in strong acids,[7] several potential mechanisms were put forward. The mechanism favoured by the authors was one in which protonation of the cyclopropyl ring (Figure 5.1) was a key step. Protonated cyclopropanes have been implicated in the reactions of some cyclopropanes and they are believed to occur as intermediates in the isomerizations of some carbocations,[8] however, current evidence[9,10] indicates that this mechanism is not active for cyclopropyl ketones in strong acids.

Ring protonation is believed to be responsible for isomerizations of some

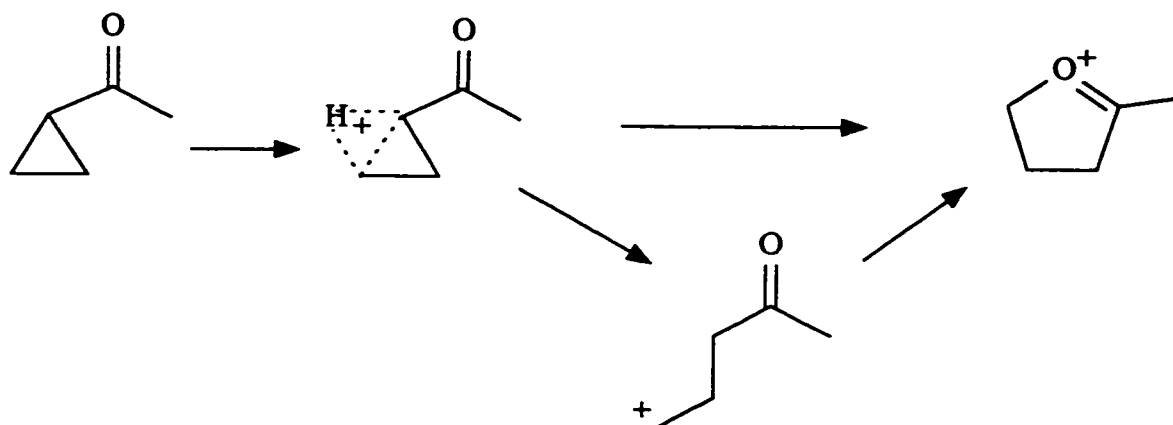


Figure 5.1: Ring protonation mechanism: protonated cyclopropyl ring opens to alkyl cation or undergoes direct expansion to oxolanylium ion.

cyclopropanecarboxylic acids in strong acids. Deno et al[9] studied the reactions of six different cyclopropanecarboxylic acids in sulfuric or fluorosulfuric acid. Products of ring expansion were noted in only two cases. Ring opening or decomposition were more commonly observed. Two mechanisms were proposed to account for the reactions of the cyclopropanecarboxylic acid. Both mechanisms involved diprotonation (cyclopropane ring and carboxylic acid group), where ring protonation produced either a non-classical ion or an alkyl cation as illustrated in Figure 5.2.

Two distinct effects are noted for cyclopropanecarboxylic acids for which ring protonation is suspected: 1) nearly exclusive C2-C3 bond cleavage, and 2) deuteration of all the ring carbons when the isomerization is carried out in deuterated acid (Figure 5.3).[9] In distinct contrast, the cyclopropyl ketones studied by Pittman and McManus[7] and others[10,11] exhibit only C1-C2 bond cleavage in strong acids, and deuteration occurs only at C3 in the oxolanylium ion ring (Figure 5.4). In fact, only a single deuterium was incorporated at C3 during ring expansion in  $D_2SO_4$ [7] or  $FSO_3D$ [10], with

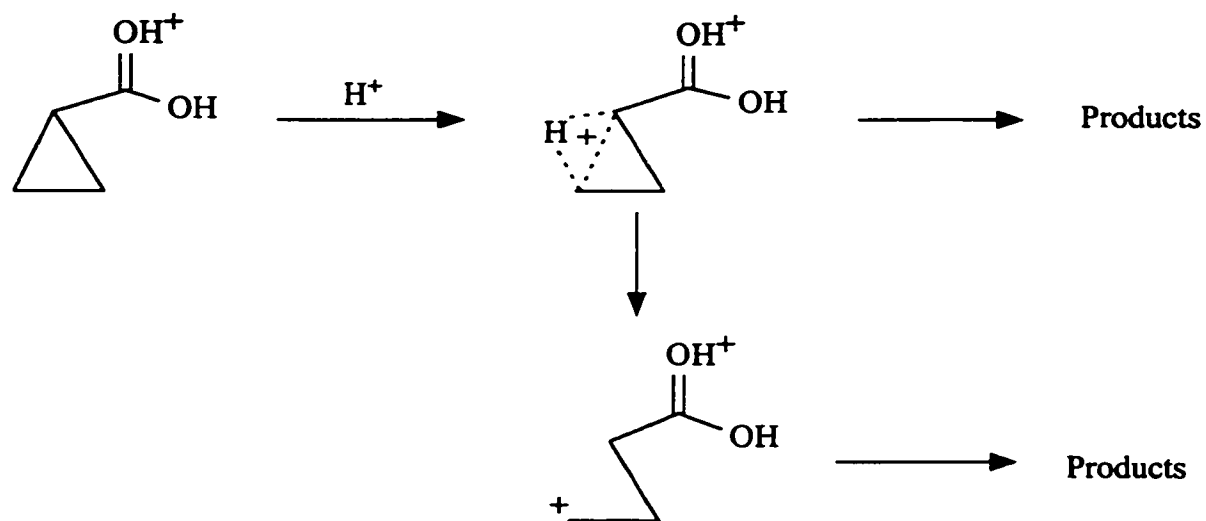


Figure 5.2: Reactions of cyclopropanecarboxylic acids *via* protonated cyclopropyl ring. The ring protonated species may produce an alkyl cation.

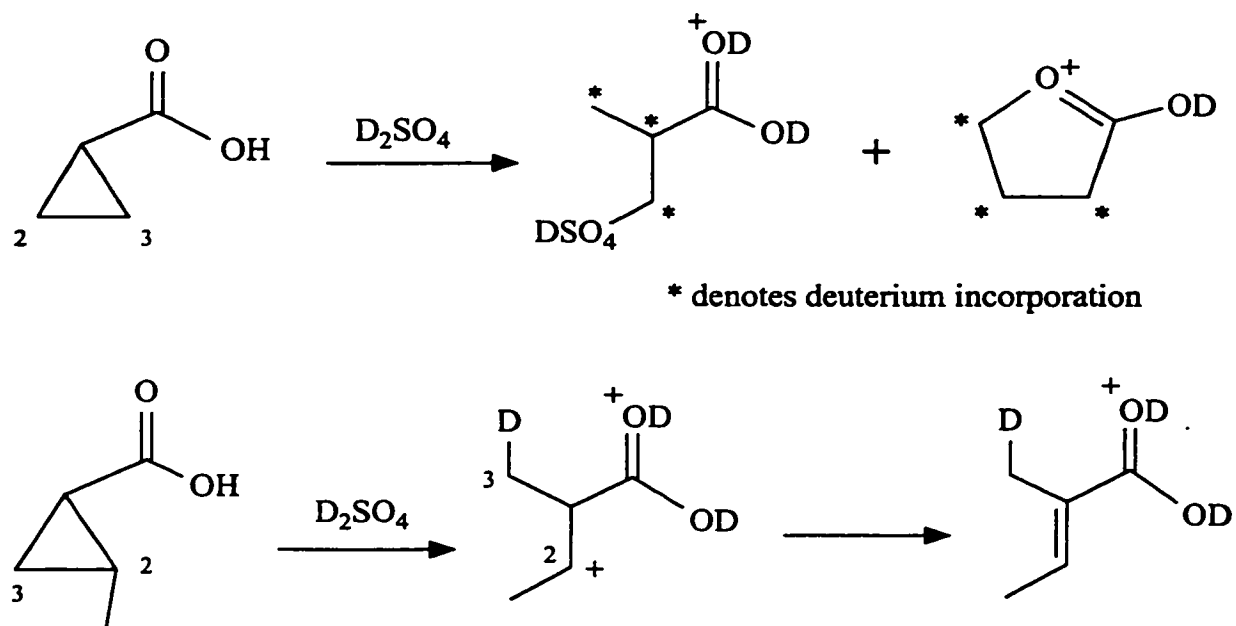


Figure 5.3: Evidence for cyclopropyl ring protonation: deuteration of all ring carbons and C2-C3 cleavage.



further deuteration of the oxolanylium ion occurring upon extended heating. This evidence demonstrates that ring protonation is not involved in the ring expansion of cyclopropyl ketones in strong acids. In reference to the mechanism proposed by Pittman and McManus,[7] Deno et al[9] commented that "protonated cyclopropane intermediates seem unlikely despite this suggestion in the literature".

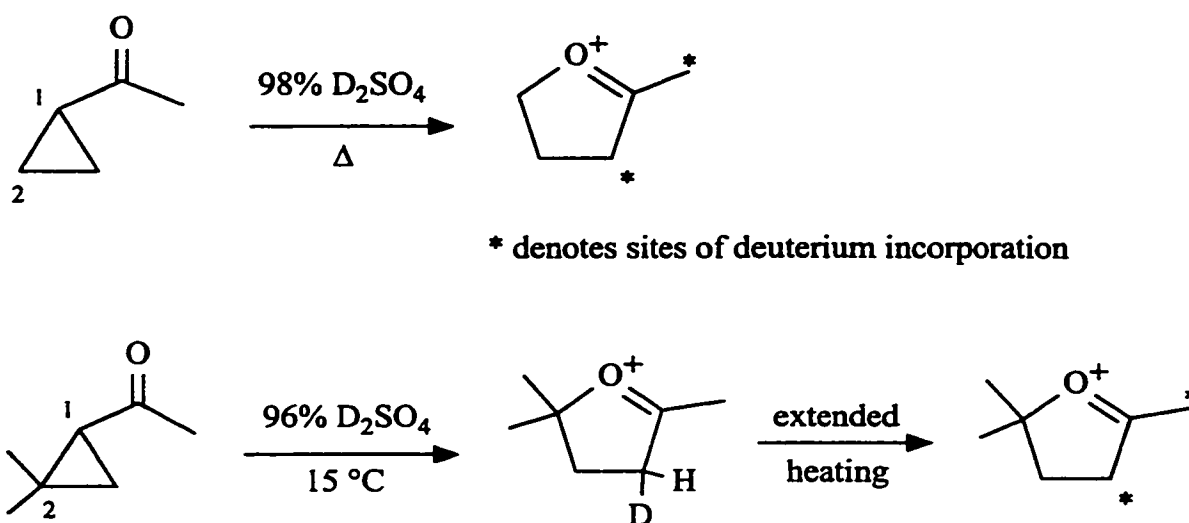


Figure 5.4: Protonated cyclopropyl ketones give only C1-C2 cleavage and deuteration only at  $\alpha$ -positions.

### 5.1.2 Reaction via an Alkyl Cation Intermediate

Ring expansion may occur via a ring opening-cyclization pathway (Figure 5.5) in which the cyclopropyl ring is opened to yield an alkyl cation in the initial step of isomerization. Subsequent cyclization of the alkyl cation intermediate would generate the five-membered ring.

Alkyl cations have been implicated in the ring openings and ring expansions of cyclopropanecarboxylic acids, esters and cyclopropyl ketones in strong acids.[9-13] Two

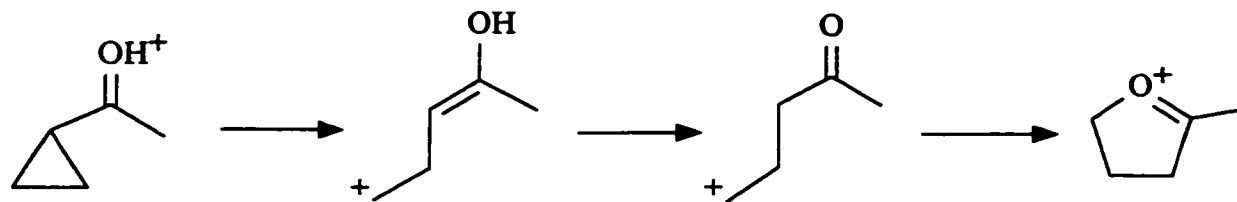


Figure 5.5: Alkyl cation mechanism: ring opening to an alkyl cation precedes ring closure to oxolanylium ion.

examples are shown in Figure 5.6.

Harvey and Brown[12] studied the Lewis acid induced reactions of cyclopropyl compounds that were conjugated with both an ester group and an alkene. A ring expansion to a cyclopentenyl system occurred and a highly stabilized alkoxy-allyl cation was believed to be the intermediate.

Murphy and coworkers[11] gave convincing evidence that alkyl cations were formed during Lewis acid treatment of diaryl substituted cyclopropyl ketones. While oxolanylium ions were observed as intermediates in some cases, the ultimate products of isomerization were often tetralones (Figure 5.7). Stable benzyl cations in equilibrium with oxolanylium ions were proposed to be the intermediates responsible for these transformations. Compounds in which the aryl rings were not activated reacted sluggishly if at all.

Alkyl cation intermediates formed from protonated cyclopropyl ketones, might also undergo 1,2-hydrogen shifts to yield protonated enones (Figure 5.8). In  $\text{H}_2\text{SO}_4$ , only oxolanylium ions were observed as products from the protonated cyclopropyl ketones investigated by Pittman and McManus,[7] however, enones have been observed under

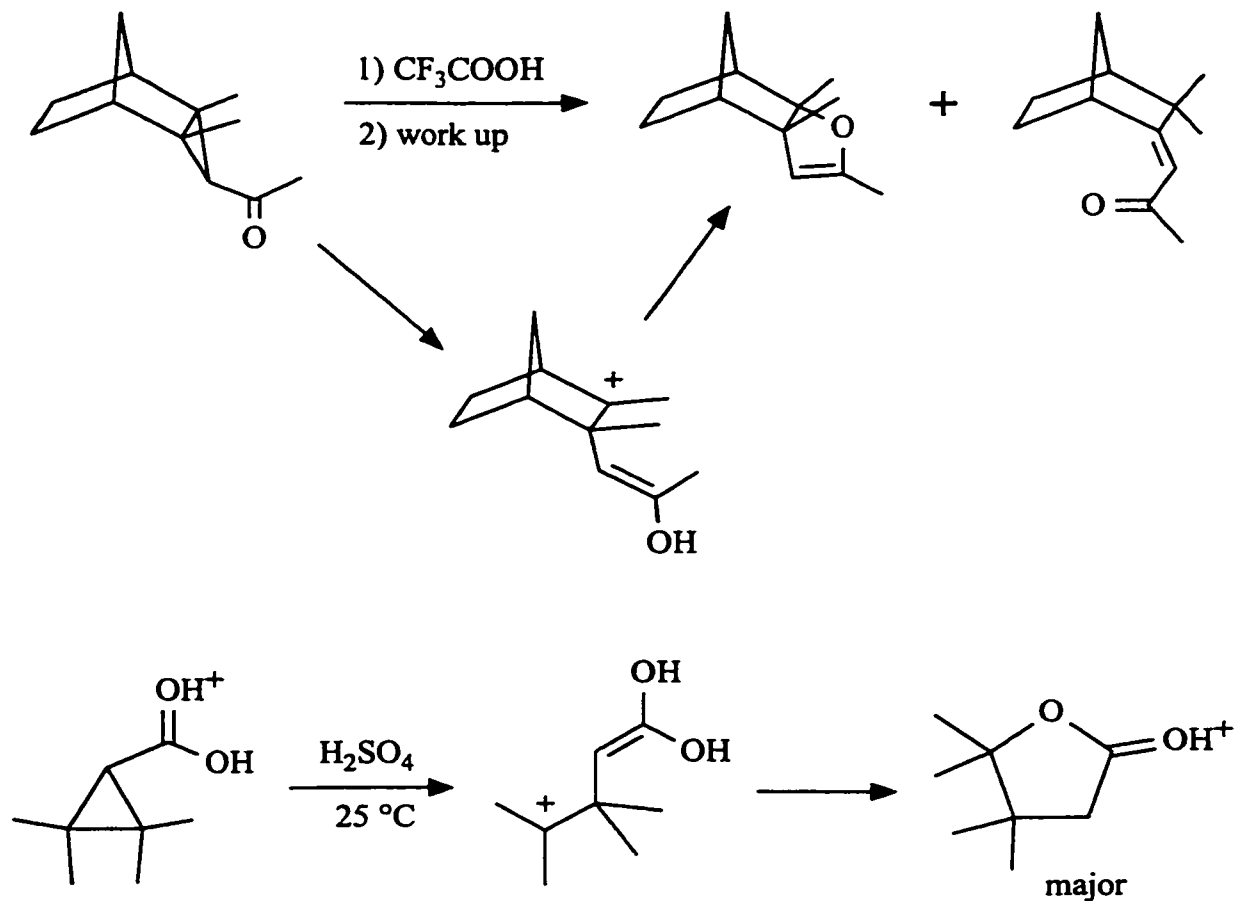


Figure 5.6: Isomerizations believed to occur via alkyl cation intermediates in strong acids.

other conditions.[10,13] Childs and coworkers[10] found that 2,2-dimethylcyclopropyl methyl ketone isomerized to a protonated enone and an oxolanylium ion in  $\text{FSO}_3\text{H}/\text{SO}_2\text{ClF}$  at  $-50^\circ\text{C}$ , with the enone undergoing further reaction to the oxolanylium ion when the acid solution was warmed to  $34^\circ\text{C}$  (Figure 5.9). The use of  $\text{H}_2\text{SO}_4$  requires temperatures above  $0^\circ\text{C}$  so it is possible that enones were produced as short lived intermediates. However, some substrates ( $\text{R}_1 = \text{R}_2 = \text{H}$  or  $\text{R}_1 = \text{alkyl}$ ,  $\text{R}_2 = \text{H}$  in Figure 5.9) would have yielded enones that were stable in  $\text{H}_2\text{SO}_4$  at the temperatures used for the

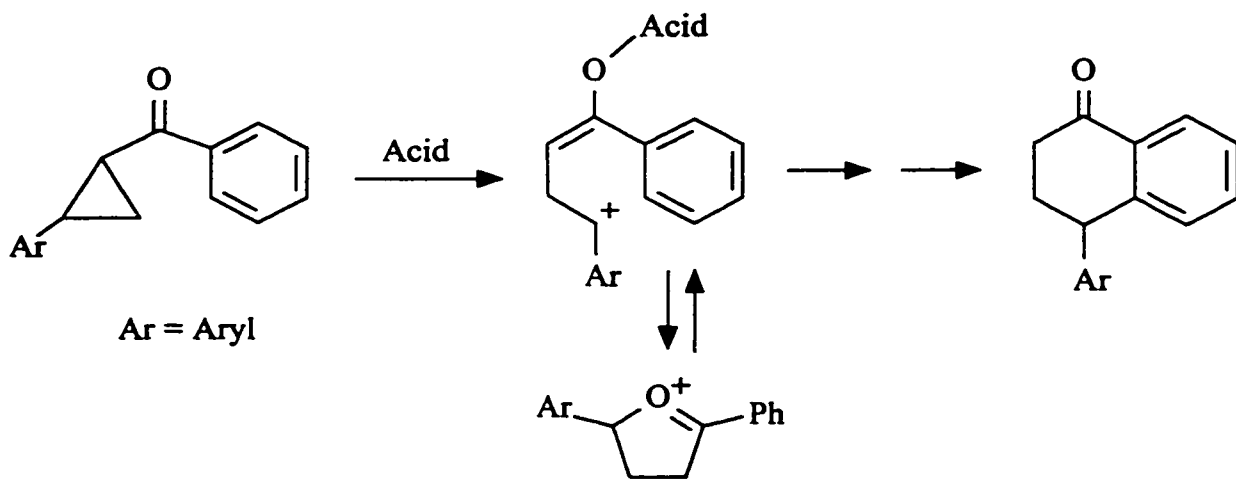


Figure 5.7: Aryl-substituted cyclopropyl ketones produce tetralones presumably via an alkyl cation intermediate.

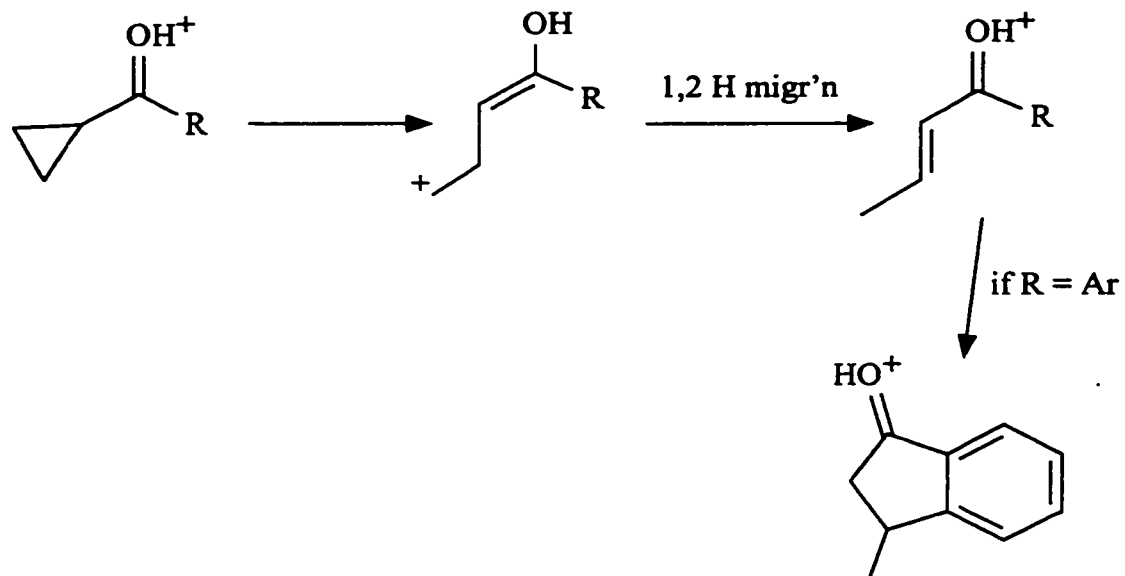


Figure 5.8: Enones should result from an alkyl cation intermediate. In the case of aryl substituted systems, indanones could be formed.

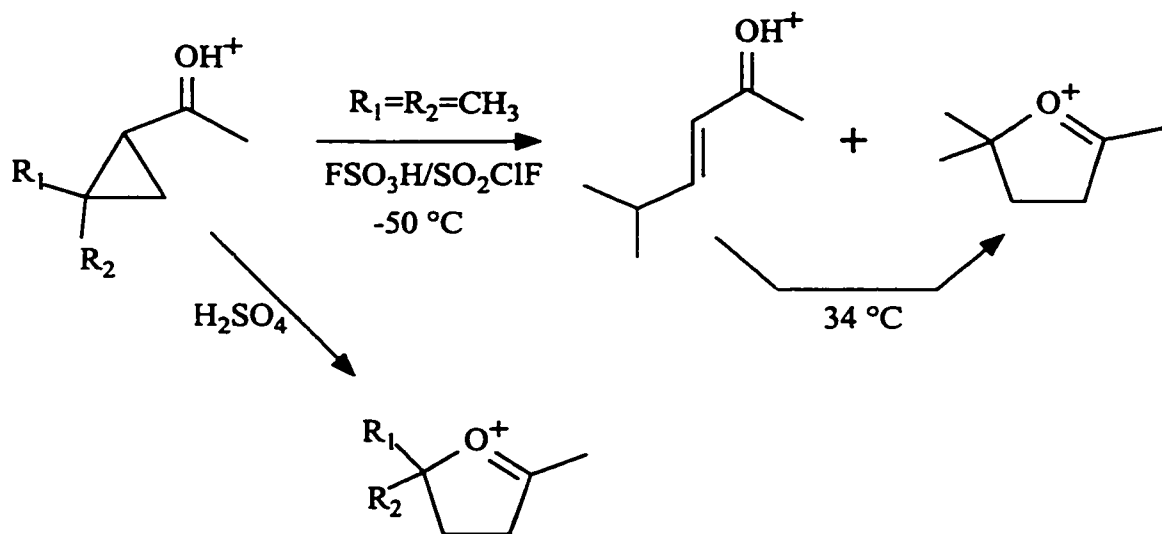


Figure 5.9: Most simple alkyl-substituted cyclopropyl ketones yield oxolanylium ions in sulfuric acid but the 2,2-dimethyl analog gives a protonated enone in addition to the oxolanylium ion in  $FSO_3H/SO_2ClF$  at  $-50\text{ }^\circ\text{C}$ .

isomerization of the cyclopropyl ketones to oxolanylium ions. Cyclization of these protonated enones to oxolanylium ions only occurs under more forcing conditions; protonated pent-3-en-2-one is unchanged upon heating in  $FSO_3H$  or  $H_2SO_4$  at  $100\text{ }^\circ\text{C}$ .<sup>[14]</sup>

As the examples above indicate, evidence for the intermediacy of alkyl cations is limited, not surprisingly, to those systems capable of producing a highly stabilized cation (i.e. tertiary, allylic, benzylic).

It is interesting to note that the reactions of a number of uncharged cyclopropyl compounds are thought to occur by conceptually similar mechanisms in which ring opening produces a biradical or zwitterion which then cyclizes to a five-membered ring. This type of mechanism has been proposed for the ring expansion of compounds such as vinylcyclopropanes,<sup>[2]</sup> cyclopropyl ketones,<sup>[15,16]</sup> 2-alkoxy-3-cyano-2,3-dihydrofurans,<sup>[17]</sup> trans-azocyclopropane<sup>[18]</sup> and acceptor-donor-substituted

cyclopropanes.[19] One example is shown in Figure 5.10.

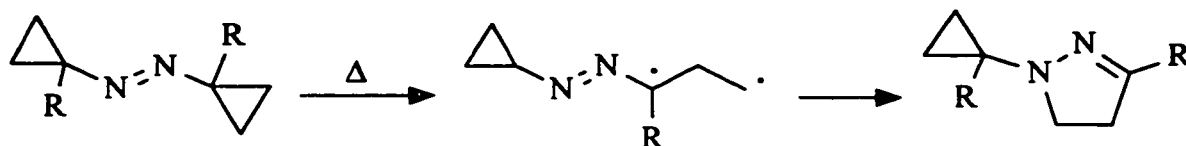


Figure 5.10: Thermal isomerization of azocyclopropanes is thought to occur via biradical intermediates.

### 5.1.3 Double Nucleophilic Displacement

Ring expansion of protonated cyclopropyl ketones might also occur via a ring opening-cyclization sequence in which both reactions are nucleophilic displacements (Figure 5.11). Attack by an external nucleophile would cause ring opening, and then the carbonyl oxygen would displace the initial nucleophile.

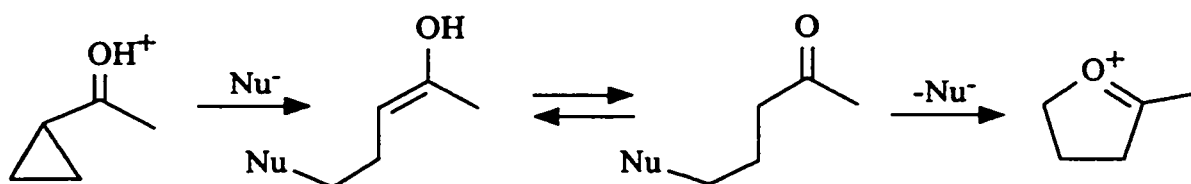


Figure 5.11: Double nucleophilic displacement mechanism: a nucleophile opens the cyclopropyl ring and is subsequently displaced by the carbonyl oxygen during ring closure.

There is ample evidence for the occurrence of both nucleophilic displacements. The first step is a well known reaction of strong nucleophiles with cyclopropyl ketones [20] and has also been observed in the reactions of compounds such as cyclopropyl imines[6a,6b,21] and cyclopropanecarboxylic acids in strong acids.[9,22] The second nucleophilic displacement in Figure 5.11 which forms an oxolanylium ion from a ketone by intramolecular displacement of a leaving group on the  $\gamma$ -position is also known. The solvolyses of  $\gamma$ -substituted ketones are much faster than that of simple alkyl analogues (Figure 5.12).[23] The accelerated rate of solvolysis was postulated to involve intramolecular nucleophilic displacement of the leaving group by the carbonyl oxygen wherein an oxolanylium ion was formed. Oxolanylium ions have been isolated as both stable solutions and crystalline salts following the reaction of  $\gamma$ -chloro ketones with Lewis acids.[24] Thus, there is ample evidence that both displacements needed for a double nucleophilic displacement are feasible.

The ring expansion reaction of 1,1-cyclopropanedicarboxylic acid in media ranging from water to concentrated sulfuric acid has been studied.[9,22,25] It was proposed that in aqueous solutions the rate determining step for this reaction was the nucleophilic attack of water on the cyclopropyl ring. In concentrated sulfuric acid, nucleophilic attack by  $\text{HSO}_4^-$  competes with intramolecular attack by one of the  $\text{COOH}$  groups (Figure 5.13). Deno et al[9] suggested that mechanisms such as these might also account for the ring expansions of cyclopropyl ketones in strong acids observed by Pittman and McManus.[7]

The ring expansion of cyclopropyl ketimines to pyrrolines has attracted attention

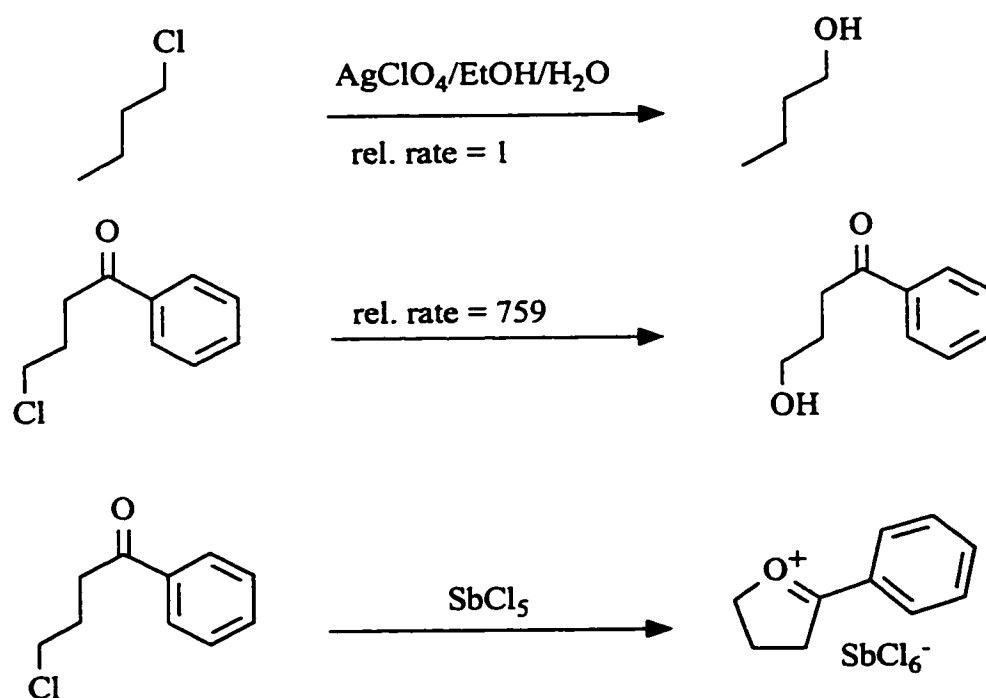


Figure 5.12: Enhanced solvolysis of 4-chlorobutyrophenone is believed to be due to the formation of a stable oxolanylium ion intermediate. The intermediate can be isolated in the absence of nucleophiles.

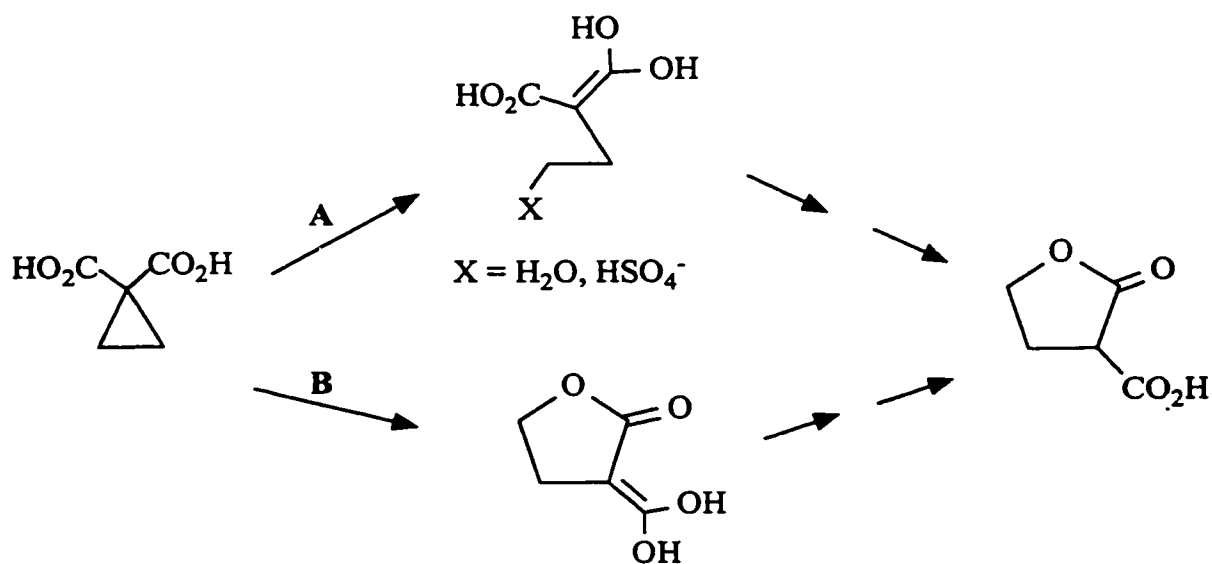


Figure 5.13: Ring expansion of 1,1-cyclopropanedicarboxylic acid in 0-98% sulfuric acid occurs by two pathways. Pathway A occurs at all acid strengths while pathway B occurs only in concentrated sulfuric acid.



for use in natural product synthesis.[6a,6b,21] The reaction requires an acid to proceed and a nucleophilic counterion, such as a halide.[6a,6b,21,26] Nucleophilic attack on the cyclopropyl iminium ion is presumably the first step in the ring expansion (Figure 5.14). In fact, during some experiments the ring-opened product of nucleophilic attack on the cyclopropyl iminium ion is isolated.

Ring expansion mediated by the attack of an external nucleophile has also been observed with a number of other related compounds in which the cyclopropyl carbons are replaced by one or more heteroatoms.[27-32]

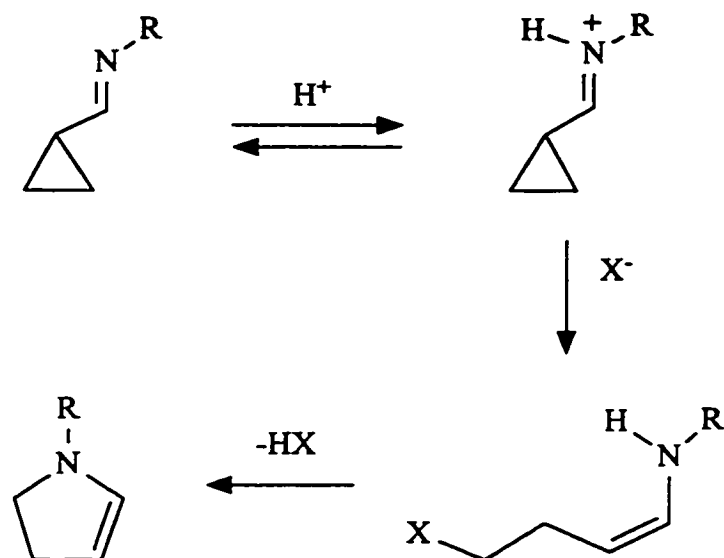


Figure 5.14: Cyclopropylimine rearrangement requires protonation and the presence of a nucleophile.

### 5.1.4 Concerted Ring Expansion

Since the ring expansion of protonated cyclopropyl ketones is formally a [1,3]-migration (Figure 5.15) it provides a potential test of the orbital symmetry rules for a 1,3-migration.[5,33] A four electron, [1,3]-alkyl migration is predicted to occur by a suprafacial/inversion (*si*) or antarafacial/retention (*ar*) pathway (Figure 5.16). An *si* pathway involves migration of the alkyl carbon along one face of the  $\pi$ -system with inversion of the stereochemistry at the migrating carbon. In an *ar* pathway the stereochemistry of the migrating carbon is retained as it moves from one side of the  $\pi$ -system to the other.

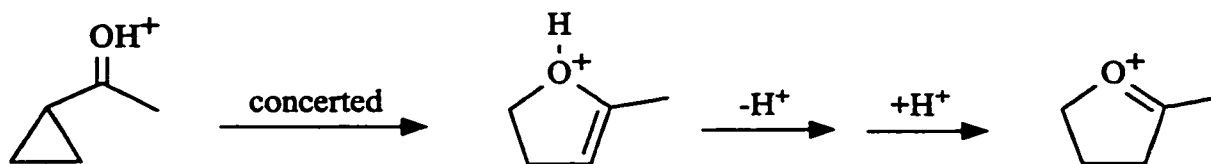


Figure 5.15: Concerted ring expansion mechanism: concerted ring expansion to an oxygen protonated dihydrofuran followed by deprotonation and reprotonation to produce the oxolanylium ion.

Most ring expansions of cyclopropyl compounds appear to occur via non-concerted pathways although concerted reactions have been considered in several instances.[3,7,9,16,34]

The mechanism of the vinylcyclopropane to cyclopentene reaction has received considerable attention by both synthetic[1,4] and mechanistic organic chemists.[1-4] The mechanism of this reaction has not been established and remains the subject of intense scrutiny with both diradical and concerted mechanisms under consideration.[1-4]

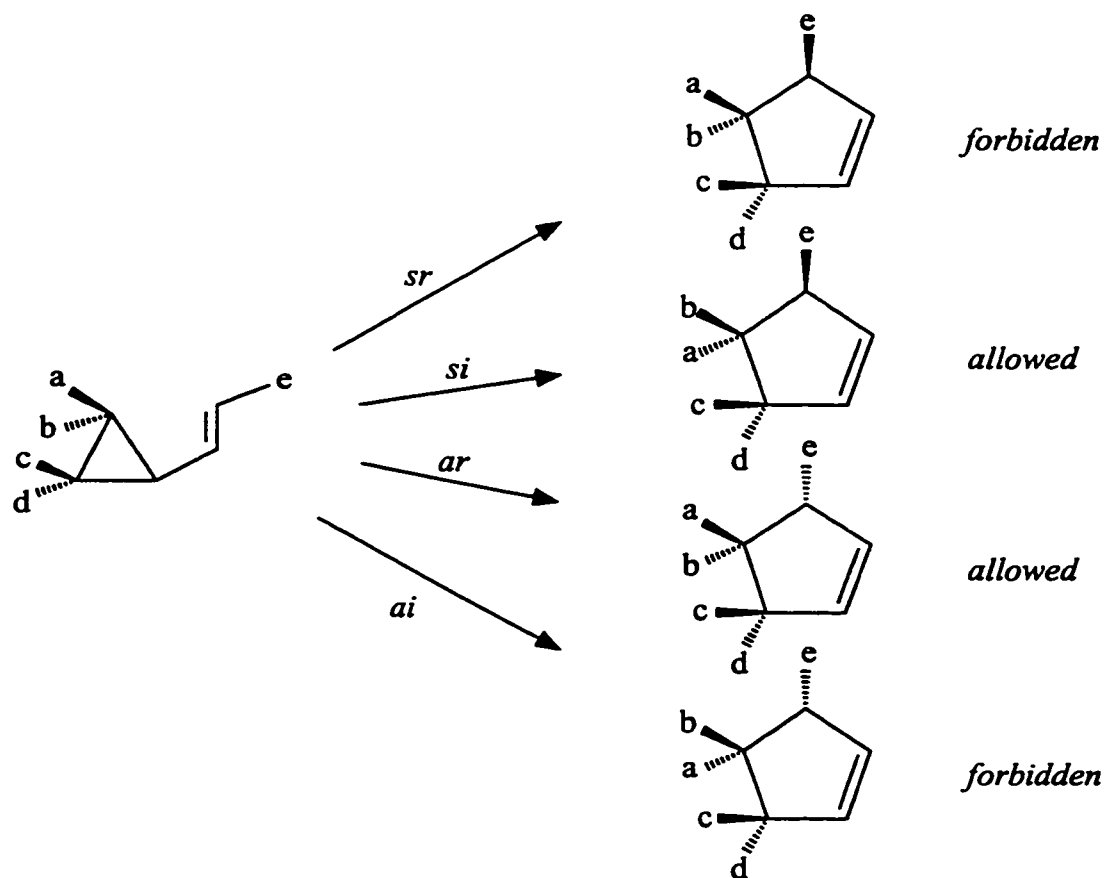


Figure 5.16: Stereochemical outcome of the four pathways for a concerted [1,3]-sigmatropic rearrangement of a vinylcyclopropane.

### 5.1.5 Stereochemical Studies

Information is available about the stereochemical course of ring expansion for some cyclopropyl compounds. This in turn provides information about the mechanism of ring expansion.

Those ring expansions which occur via a ring-opened reactive intermediate

(cation, diradical) would be expected to lose the stereochemical integrity of the starting material. Free rotation in the acyclic intermediate would allow racemization or the preferential formation of the thermodynamically most favoured isomer (eg. a *trans* isomer) from any stereoisomer of the starting material. Racemization has indeed been observed during the ring expansion of a number of cyclopropyl compounds including vinylcyclopropanes,[1-4] cyclopropyl ketones,[15] cyclopropanecarboxaldehydes,[17] and cyclopropanecarboxylic acid esters[12] (Figures 5.17-5.19).

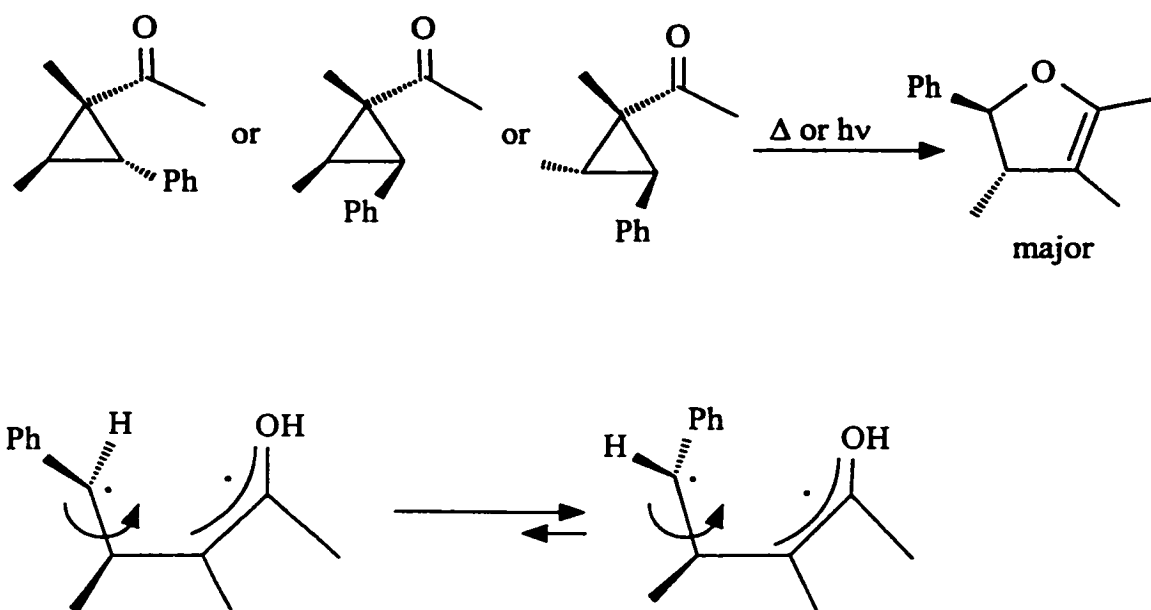


Figure 5.17: The *trans* dihydrofuran isomer predominates during thermal or photochemical isomerization. Free rotation in a biradical intermediate accounts for the observed stereoselectivity.

In the case of ring expansion by double nucleophilic displacement, the stereochemistry of the starting material will be retained. Each nucleophilic displacement will cause inversion of the migrating centre, leading to net retention of the

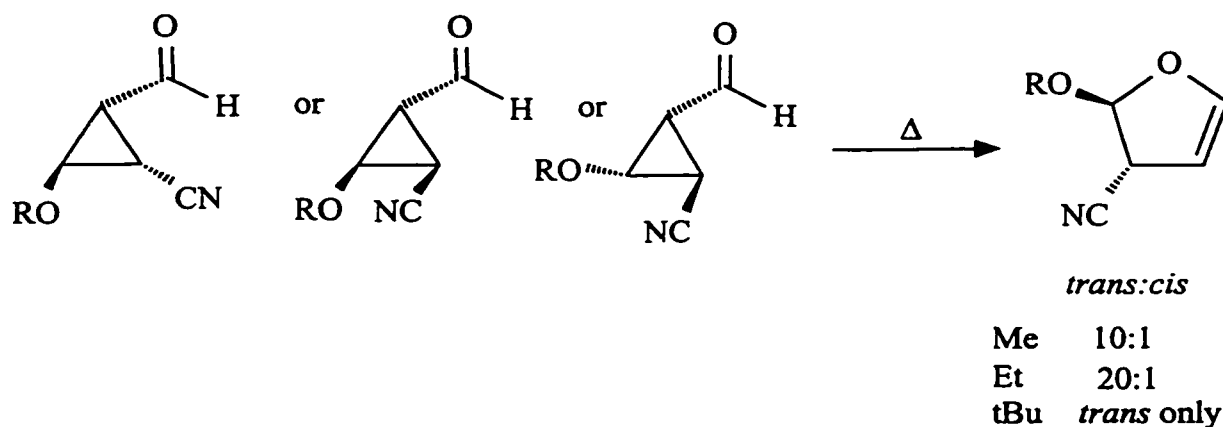


Figure 5.18: Isomerization of 2-alkoxy-3-cyanocyclopropanecarboxaldehydes produces the *trans* product preferentially.

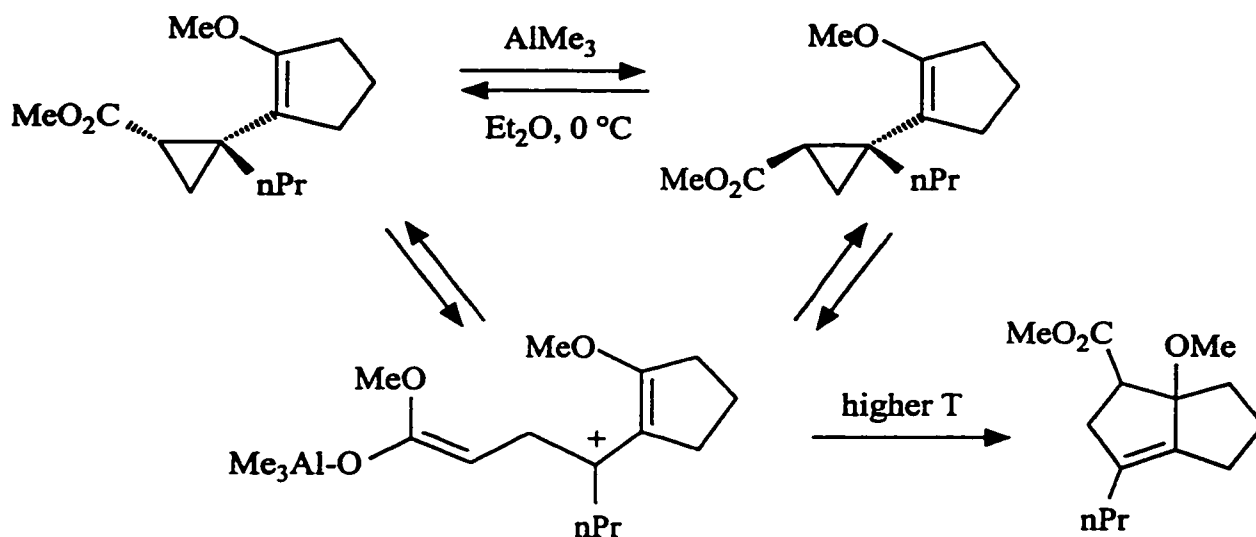


Figure 5.19: The *cis* and *trans* isomers of the methyl cyclopropanecarboxylate equilibrate via an acyclic allylic cation.

stereochemistry at this centre. Complete retention of the stereochemistry has been observed with a variety of cyclopropyl compounds exposed to acids and/or strong nucleophiles.[27-31] Two examples are shown in Figure 5.20. In addition, there are other examples in the literature in which Lewis acid assisted ring expansion of

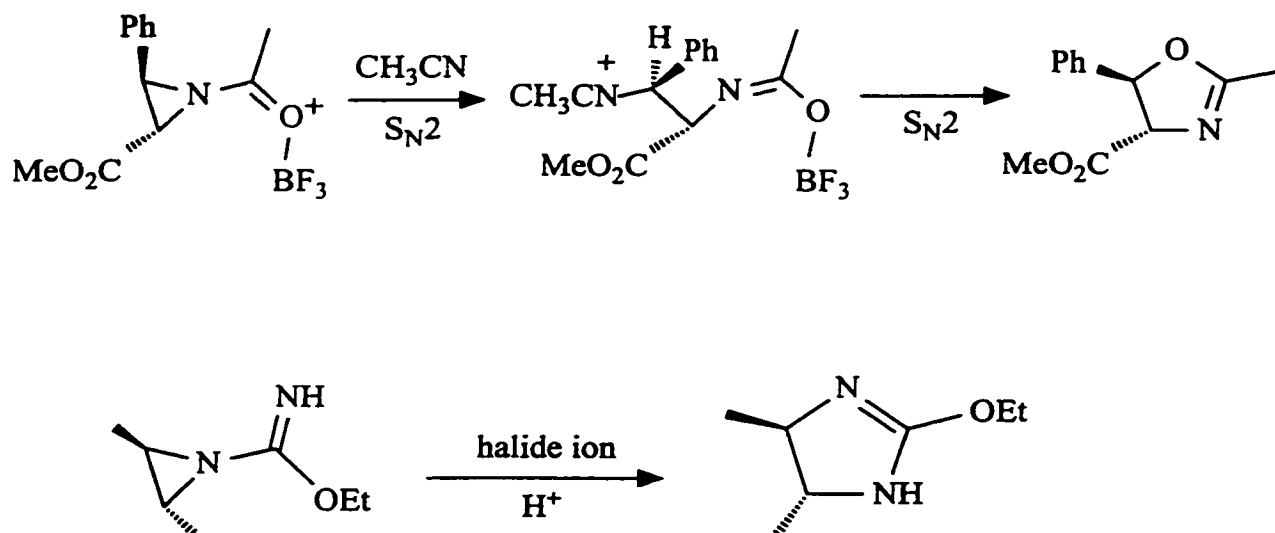


Figure 5.20: Examples of ring expansions in which the stereochemistry of the starting material is retained.

cyclopropyl compounds occurs with complete retention of reactant stereochemistry.[34]

Although the authors were uncertain about the reaction mechanisms, a double nucleophilic displacement would account for the stereospecificity of the rearrangement.

As mentioned earlier, a concerted ring expansion would be governed by orbital symmetry and, as such, it should result in stereoselective reactions of suitably substituted compounds. The *si* and *ar* pathways (Figure 5.16) are allowed by orbital symmetry but the contorted geometry required for an antarafacial process makes the *ar* pathway unlikely.[35] Concerted ring expansion by the *si* pathway should lead to products in which the stereochemistry of the migrating centre has been inverted.

The *sr* pathway, one of the forbidden pathways, is the most geometrically facile of the four pathways, and it involves the least atomic motion. The product stereochemistry from an *sr* pathway would be the same as that from a double nucleophilic displacement,

however, it would be possible to differentiate between the two pathways on the basis of other evidence (dependence on nucleophile concentration,  $\Delta S^\ddagger$ ).

The ring expansion that has received the greatest attention as a possible concerted reaction is the vinylcyclopropane to cyclopentene isomerization.[1-4] Stereochemical analysis of the isomerization is difficult for a number of reasons: 1) synthesis of simple stereolabelled vinylcyclopropanes is challenging, 2) characterization of cyclopentene stereoisomers can be complex, 3) ring expansion is often a minor pathway ( $\leq 5\%$ ), and 4) stereomutations of the starting materials occur, and are often more rapid than isomerization. The mechanistic studies have been the source of considerable debate and have been interpreted to support either a concerted or a diradical mechanism for the ring expansion of vinylcyclopropanes. Recent studies continue to give conflicting conclusions.[2a,2b,3a,3b]

Danheiser and coworkers[4c-4e] have investigated the anion-accelerated ring expansion of vinylcyclopropanes. Vinylcyclopropanes with oxygen or carbon centred anions bound to the 2-position of the cyclopropyl ring undergo facile ring expansion (e.g., at 25 °C or lower) to give cyclopentenols in good yield and with high stereoselectivity. The observed stereoselectivity was ascribed to either a concerted ring expansion or a stepwise pathway involving rapid cyclization of acyclic intermediates before conformational changes occurred.

### 5.1.6 Goals

Ring expansion is known for a many different cyclopropyl compounds and occurs

under a variety of reaction conditions. The mechanism of the reactions in acidic media have been postulated to occur by: 1) ring protonation, 2) an alkyl cation intermediate, 3) double nucleophilic displacement, or 4) a concerted pathway. Analogous mechanisms exist for neutral cyclopropyl compounds.

Investigation of the ring expansion of protonated cyclopropyl ketones is of interest for several reasons. The reaction shares obvious parallels with the ring expansions of more intensively studied systems (vinylcyclopropanes, cyclopropyl ketimines) and any information may be useful to the study of these systems. While ring expansion of many cyclopropyl compounds is reluctant, and is often accompanied by significant amounts of ring opened products, the ring expansion of protonated cyclopropyl ketones occurs at reasonable temperatures ( $\leq 100$  °C) and usually leads to the exclusive formation of the ring expanded products (oxolanylium ions). There is growing interest in the reactions of cyclopropyl compounds for use in synthesis, and as such, information about the mechanism of ring expansion, in particular, the stereochemical course of reaction, may be useful in the rational synthesis of more complex molecules. Finally, systems which allow orbital symmetry rules to be tested continue to be of interest.

With protonated cyclopropyl ketones in strong acids there is evidence for the intermediacy of alkyl cations but only in cases where a stable cation (tertiary, benzylic, etc.) can be formed. The mechanism for more simply substituted cyclopropyl ketones is unclear although reaction via ring protonation seems to be ruled out. For this reason, the work described in this chapter focuses on the ring expansion of simply substituted



cyclopropyl ketones.

One goal of this chapter is to elucidate the mechanism of ring expansion of these simple protonated cyclopropyl ketones. Secondly, changes in the activation barrier with changes in substitution pattern provides a valuable quantitative measure of the carbocation stabilizing ability of the substituents. Towards these ends, a series of cyclopropyl ketones were prepared and the effect of substituents on the kinetics of ring expansion in triflic acid was probed. This knowledge was combined with information found in chapter 4 and the literature to narrow the mechanistic possibilities. The final step of the approach was to prepare and study the ring expansion of stereochemically labelled compounds.

## 5.2 Experimental

The preparation and characterization of the cyclopropyl ketones, protonated cyclopropyl ketones, oxolanylium ions and protonated enones were described in chapter 4.

*Kinetic Measurements* - As described in chapter 2. The constant temperature bath contained refluxing ether (35°C), acetone (56°C), methanol (65°C), t-butanol (82°C); or water (100°C).

## 5.3 Results and Discussion

### 5.3.1 Kinetics of Isomerization

The rates of isomerization of protonated cyclopropyl ketones **26H-42H** to oxolanylium ions **43-60** (Figure 5.21) and protonated enones **61H-63H** (Figure 5.22) were determined by monitoring changes in the  $^1\text{H}$  NMR spectra with heating time. All of the reactions displayed first order (or pseudo first order) kinetics with high correlation coefficients. Typical rate plots are shown in Figure 5.23. The results of the kinetic studies are summarized in Tables 5.1 and 5.2.

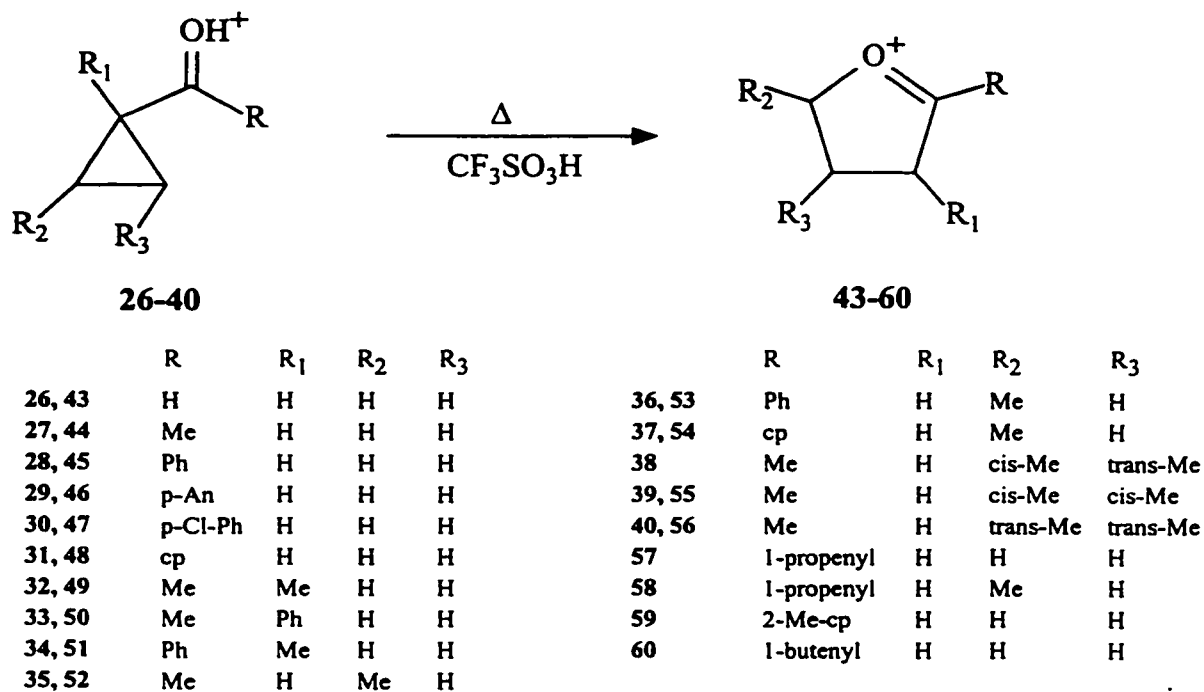


Figure 5.21: Isomerization of protonated cyclopropyl ketones **26-40** in triflic acid leads to oxolanylium ions **43-60**.

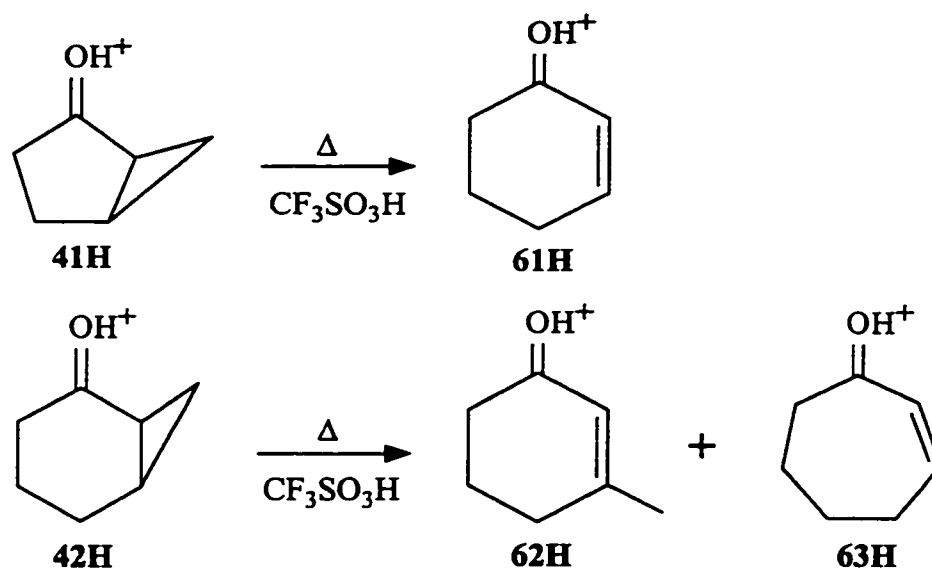


Figure 5.22: Isomerization of protonated bicyclo[n.1.0] ketones **41H** and **42H** to protonated enones **61H-63H**.

The activation barrier for ring expansion of the protonated cyclopropyl ketones is much lower than that required for reaction of neutral cyclopropyl ketones or vinylcyclopropanes. Protonation of the cyclopropyl ketone reduces the bond order of the vicinal cyclopropane bonds which facilitates the bond breaking required for isomerization. It is interesting to note that Dinnocenzo and Conlon [36] have found that the energy barrier for the vinylcyclopropane to cyclopentene reaction is much lower in the presence of electron-transfer agents such as aminium ions. Apparently, the vinylcyclopropyl radical cation formed by electron transfer possesses weakened cyclopropyl bonds (reduced bond order) which facilitates isomerization.

The activation barriers show some interesting trends with changes in the substitution pattern. Replacement of the hydrogen substituent at C1 with either methyl or phenyl (**27H** vs. **32H** vs. **33H**) has essentially no effect on the energy barrier. This is

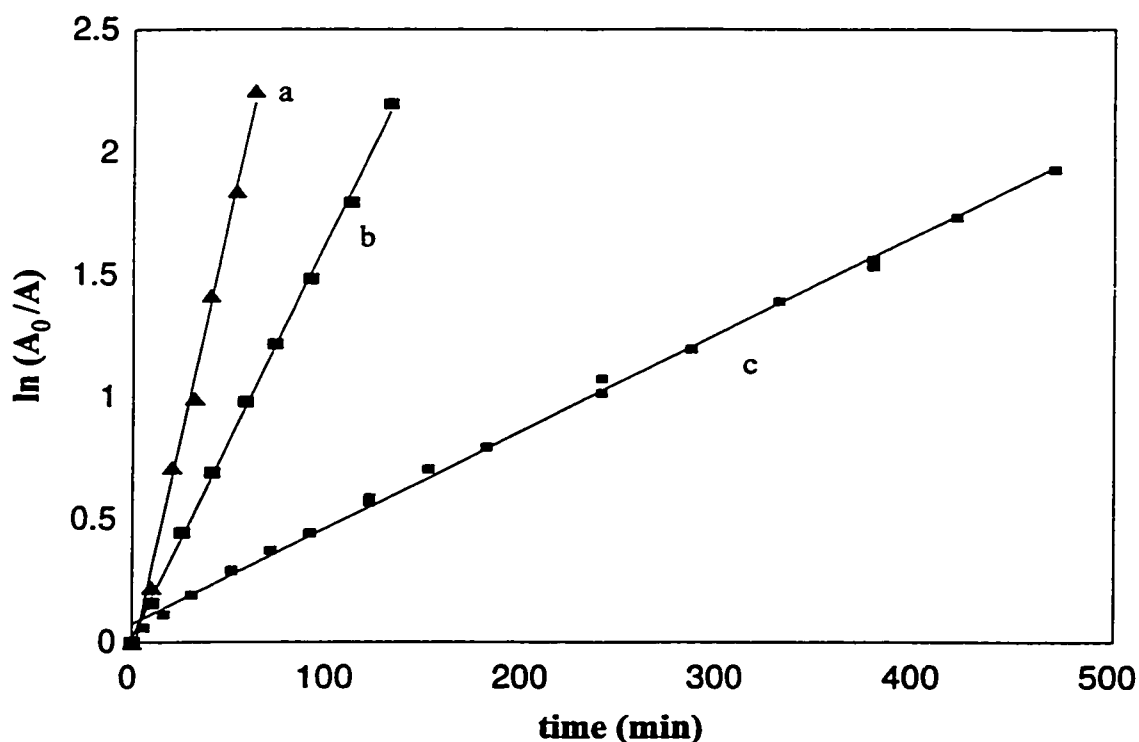


Figure 5.23: First order rate plots for isomerization in triflic acid of : a) protonated cyclopropyl methyl ketone, 27H, at 99.3 °C; b) protonated cis, trans-2,3-dimethylcyclopropyl methyl ketone, 38H, at 65.0 °C; c) protonated 2-methylcyclopropyl phenyl ketone, 36H, at 56.2 °C.

consistent with previous studies[37] of charge delocalization or stabilization of cyclopropyl carbinyl cations including protonated cyclopropyl ketones (see Figure 4.13). Substitution of charge stabilizing groups at C1 would be expected to have little influence on the stability of the starting protonated cyclopropyl ketone. The results in Table 5.1 also show that the substituent plays little or no role in stabilization of the transition state for ring expansion.

Table 5.1. Kinetic results for the isomerization of protonated cyclopropyl ketones to oxolanylium ions.<sup>a</sup>

reaction	T (°C)	10 <sup>5</sup> k (s <sup>-1</sup> )	ΔG <sup>‡</sup> (kcal/mol)	ΔS <sup>‡</sup> (cal/K mol)
<b>26H</b> → <b>43</b> <sup>b</sup>	34.5	6.8 ± 0.2	23.90 ± 0.03	
<b>27H</b> → <b>44</b>	99.3	62 ± 2	27.43 ± 0.04	
	82.0	9.0 ± 0.2	27.41 ± 0.02	-4 ± 2
	64.5	1.50 ± 0.05	27.28 ± 0.03	
<b>28H</b> → <b>45</b>	99.3	66 ± 1	27.38 ± 0.02	
	82.0	4.3 ± 0.4	27.78 ± 0.10	5 ± 10
	64.5	1.04 ± 0.04	27.55 ± 0.04	
<b>29H</b> → <b>46</b>	100	17.8 ± 1.1	28.36 ± 0.06	
<b>30H</b> → <b>47</b>	100	48 ± 2	27.67 ± 0.03	
<b>31H</b> → <b>48</b> <sup>c</sup>	100	≈0.1	≈31	
<b>32H</b> → <b>49</b>	99.3	58 ± 3	27.48 ± 0.06	
<b>33H</b> → <b>50</b>	99.7	70 ± 6	27.38 ± 0.09	
<b>34H</b> → <b>51</b>	100	≥400	≤26.1	
<b>35H</b> → <b>52</b>	56.2	6.44 ± 0.09	25.67 ± 0.01	
	≈35 <sup>d</sup>	≈80 <sup>d</sup>	≈22.4 <sup>d</sup>	
<b>36H</b> → <b>53</b>	56.2	6.60 ± 0.08	25.64 ± 0.01	
<b>37H</b> → <b>54</b> <sup>c</sup>	100	16.8 ± 0.3	28.41 ± 0.02	
<b>38H</b> → <b>55/56</b>	65	27.7 ± 0.3	25.38 ± 0.01	
<b>39H</b> → <b>55</b>	34.6	18.0 ± 0.4	23.31 ± 0.02	
<b>40H</b> → <b>55/56</b>	65	≈20	≈25.6	
<b>54</b> → <b>58</b>	99	1.20 ± 0.02	30.33 ± 0.02	
<b>55</b> → <b>56</b> <sup>e</sup>	100	31 ± 2	27.99 ± 0.05	

a) first order rate constants measured in CF<sub>3</sub>SO<sub>3</sub>H unless otherwise indicated.

b) the initial product of the isomerization of **26H** has only been tentatively identified.

c) more than one product is obtained.

d) **35H/52** as SbCl<sub>6</sub><sup>-</sup> salt in CD<sub>2</sub>Cl<sub>2</sub>.

e) reaction proceeds to a 19:81 equilibrium.

Table 5.2: Kinetic results for the isomerization of protonated bicyclo[n.1.0]alkanones **41H** and **42H**.<sup>a</sup>

reaction	T (°C)	10 <sup>4</sup> k (s <sup>-1</sup> )	ΔG <sup>‡</sup> (kcal/mol)
<b>41H</b> → <b>61H</b>	65.0	1.59 ± 0.05	25.75 ± 0.03
<b>42H</b> → <b>62H/63H</b>	99.3	1.7	28.4

a) first order rate constants measured in CF<sub>3</sub>SO<sub>3</sub>H.

Conversely, replacement of one of the C2 hydrogens with a methyl group leads to a lowering of the activation barrier by approximately 2 kcal/mole in each case: **27H** vs. **35H**; **28H** vs. **36H**; **31H** vs. **37H**. A methyl substituent at C2 will stabilize the reactant. It is clear from the reduced activation barriers that even greater charge is located on C2 in the transition state for rearrangement than is found in the reactant (protonated cyclopropyl ketone).

This effect is even more dramatic when data found in the literature for the isomerization of the 2,2-dimethylcyclopropyl methyl ketone is considered. This compound was studied in both 90% sulfuric acid [7] and in FSO<sub>3</sub>H/SO<sub>2</sub>ClF [10]. A <sup>1</sup>H NMR spectrum taken immediately after protonation in 90% sulfuric acid at 10 °C showed only the oxolanylium ion product.[7] In FSO<sub>3</sub>H/SO<sub>2</sub>ClF, isomerization at -50 °C produced both the oxolanylium ion and protonated 5-methyl-hex-3-en-2-one (Figure 5.24).[10] At higher temperatures (34 °C), the protonated 5-methyl-hex-3-en-2-one cyclized to the oxolanylium ion. The activation barrier (ΔG<sup>‡</sup> = 16.4 kcal/mol) for the ring expansion of protonated 2,2-dimethylcyclopropyl methyl ketone[10] is much lower than that for **27H** or **35H**, consistent with a transition state bearing considerable charge at C2.

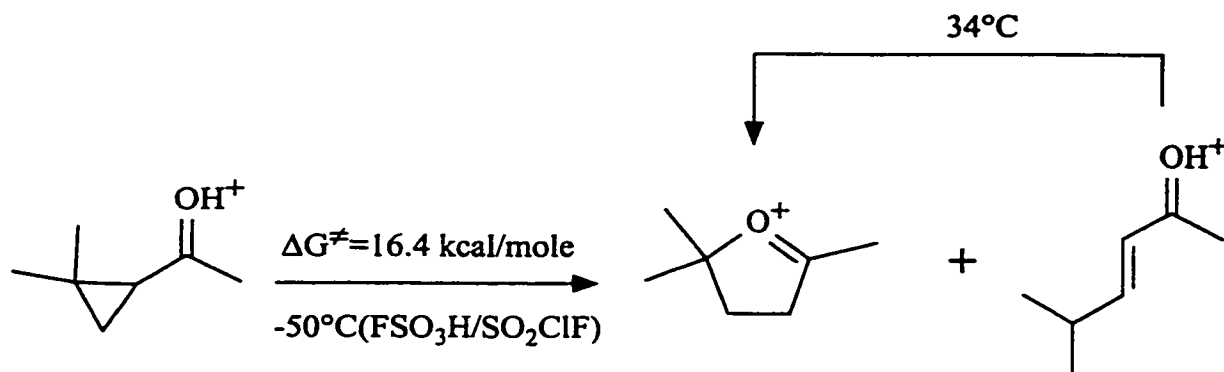


Figure 5.24: Isomerization of protonated 2,2-dimethylcyclopropyl methyl ketone.

Since the reaction is rapid at temperatures well below 0 °C, it was not feasible to study this reaction in triflic acid (mp -30 °C).

Compounds **38-40** also have two methyl groups on the cyclopropyl ring but on different ring positions. The second methyl group might be expected to further stabilize the reactants, but have little effect at the transition states, where charge is localized on C2. Thus, it was anticipated that the activation energy for the isomerizations of the 2,3-dimethyl substituted systems, **38H-40H** would be greater than that for the 2-methyl compound, **35H**. In fact, the activation barriers for the rearrangements of **35H**, **38H** and **40H** were essentially identical while the dimethyl compound **39H** proved to have the least kinetic stability (Table 5.1, Figure 5.25).

With **39H**, the cyclopropyl ring bears three groups on the same side of the ring. There must be considerable steric interactions which likely hamper **39H** from adopting a bisected geometry. Thus, the ground state of **39H** might be expected to be less stable than **35H**. The steric strain present in **39H** may be reduced upon reaching the transition

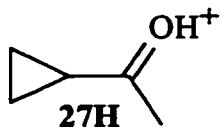
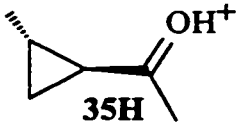
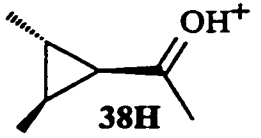
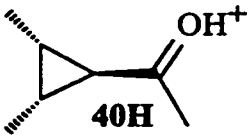
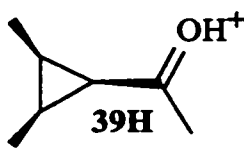
	$\Delta G^\ddagger$ (kcal/mol)	# of cis interactions
	27.4	0
	25.7	0
	25.4	1
	25.6	1
	23.3	3

Figure 5.25: Comparison of the activation energy for ring expansion with the number of steric interactions between groups on the cyclopropyl ring.

state. It appears that this relief of strain more than outweighs any charge stabilization provided by the methyl group to the reactant, and the activation barrier is lower than that for **35H**. For **38H** and **40H** in which two of the three ring substituents are cis to each other, any charge stabilization provided the reactant by the second methyl group must be balanced by an equal and opposite steric interaction which is reduced as the reaction progresses.

Bicyclic ketones **41H** and **42H** are substituted in a manner similar to that of **35H**, with an alkyl substituent on C(O) and an alkyl substituent on one of the  $\beta$ -positions.



Since **41H** and **42H** cannot form oxolanylium ions, it was anticipated that they might isomerize to enones in a reaction with a higher activation barrier. As expected, the [4.1.0]-system isomerizes at a considerably slower rate than **35H**, but the [3.1.0]-system isomerizes at about the same rate as **35H** (see Tables 5.1 and 5.2, and Figure 5.26).

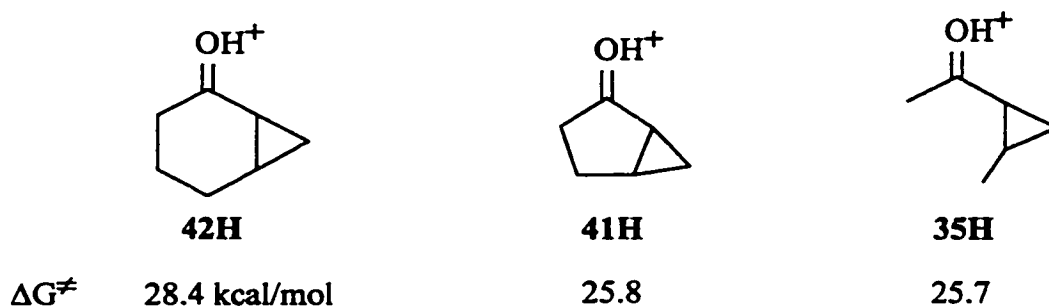


Figure 5.26: Comparison of activation barriers for isomerization of three similarly substituted cyclopropyl ketones in triflic acid.

Simple mechanical models show that the [3.1.0]-system **41H** is quite rigid and that it can not easily achieve a geometry in which the cyclopropyl-ring is bisected by the carbonyl  $\pi$ -system. Thus, **41H** may be destabilized relative to **42H** and **35H**, which would explain the lower activation barrier. Both **42H** and **35H** can achieve a bisected geometry quite easily and should be of similar stability. The difference in activation energy for the reactions of these two compounds reflects a difference in the transition states for the two reactions: ring cleavage vs. ring expansion. In triflic acid, it appears that the transition state for ring opening to an enone lies nearly 3 kcal/mol higher than the transition state for ring expansion to an oxolanylium ion.

A similar effect is observed with the opening of the cyclopropyl ring of the 2-cyclopropyloxolanylium ion **54** to form 2-(1-propenyl)oxolanylium ion **58**. The

activation barrier for this reaction (30.3 kcal/mol) at 100 °C is about 3 kcal/mol higher than the barrier for the ring expansion of a similarly substituted protonated cyclopropyl ketone (i.e. 27.4 kcal/mol for protonated cyclopropyl methyl ketone **27H**).

### 5.3.2 *The Effect of the Substituent at C(O).*

As the bond in the cyclopropyl ring is broken, and the initial product (cyclic or acyclic) of the reaction appears, the positive charge found at C(O) will be greatly reduced (Figure 5.27). As such, the role of the substituent at C(O) in charge delocalization will be minimized in the transition state. Comparison of molecules which differ only in the substitution pattern at C(O) should give a sense of the charge stabilizing abilities of these substituents in the cyclopropylcarbinyl cation reactants (protonated cyclopropyl ketones). If a better electron donor is placed at C(O), the activation barrier should increase because the reactant energy will be lowered while the transition state energy will be relatively unaffected (Figure 5.28). This is the reverse of the situation for solvolyses in which the charge at the site of substitution increases as the transition state is approached, and the rate of reaction is accelerated by better electron donors.

In this thesis the activation barriers for **26H-31H** were found to fall in the order: **26H < 27H = 28H = 30H < 29H < 31H** (Figure 5.29). This gives the relative charge stabilizing order: hydrogen < methyl = phenyl = p-chlorophenyl < p-anisyl < cyclopropyl. The same relative ordering of methyl = phenyl < cyclopropyl is observed for **35H-37H** (Figure 5.29).

Other studies of cyclopropyl ketones in acidic media show that isomerization

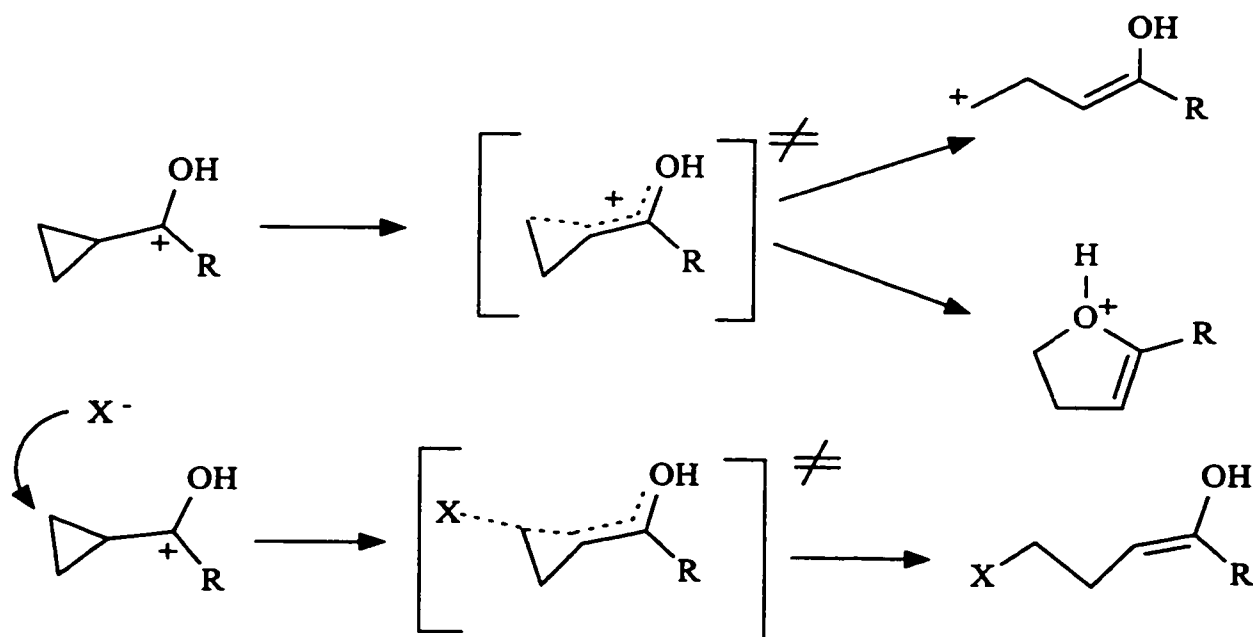


Figure 5.27: During isomerization by concerted, double nucleophilic displacement, or alkyl cation pathways the charge at C(O) is reduced at the transition state.

slows as the C(O) substituent becomes a better electron donor. Pittman and McManus[7] found that the rate for isomerization **27H**, **28H** and **31H** in 90% sulfuric acid fell in the order: **28H**  $\leq$  **27H** < **31H**, and thus support the ranking of methyl  $\approx$  phenyl < cyclopropyl. Nakajima et al[38] found that cyclopropyl ketones substituted at C(O) with trimethylsilyl groups underwent reaction (ring opening or ring expansion) in acidic media ( $\text{TiCl}_4$ ,  $\text{SnCl}_4$ ,  $\text{HCl}$ ,  $\text{BF}_3$ ) at lower temperature than alkyl substituted analogs. Spectral studies of the TMS-substituted cyclopropyl ketones showed reduced electron density at the carbonyl carbon relative to that in the alkyl substituted analogs which indicates that TMS is a poorer charge stabilizing group than an alkyl group. This evidence supports the hypothesis developed above -- the rate of ring expansion will slow as better charge stabilizing groups are substituted at C(O)

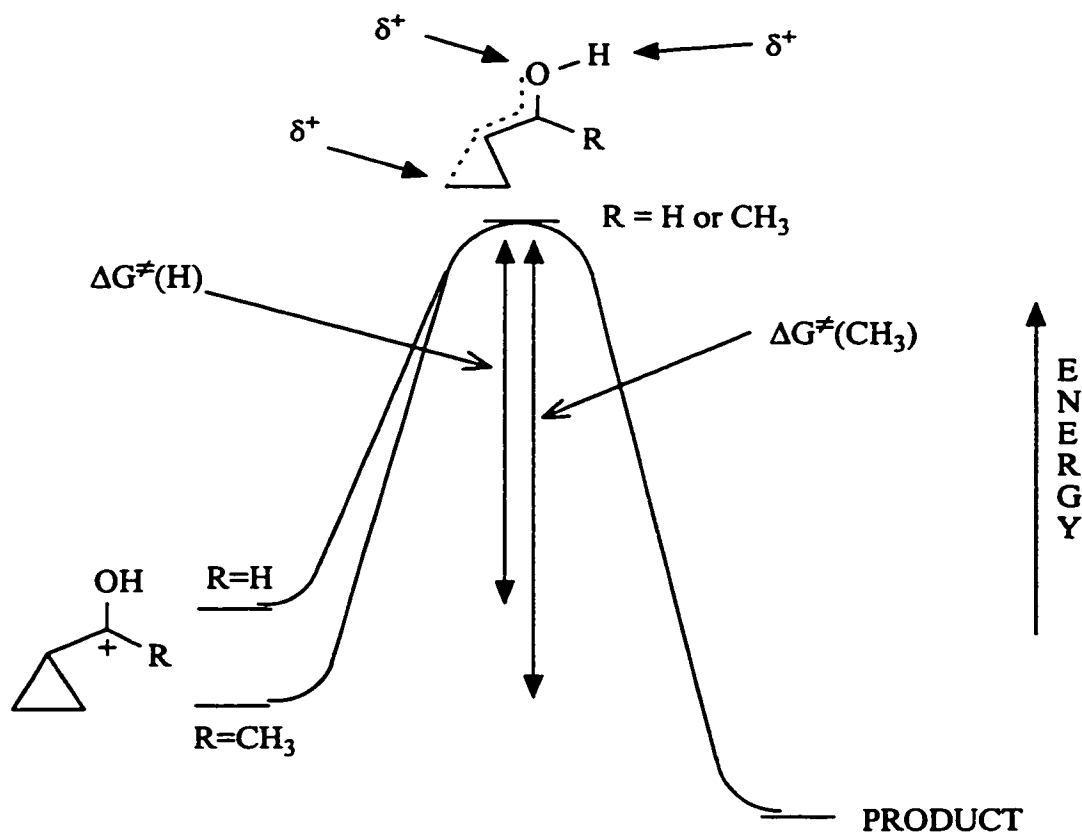


Figure 5.28: Methyl substitution at C(O) should lower the energy of the reactant but have little effect on the transition state energy and thus, the activation barrier should be larger for R = CH<sub>3</sub>.

Rankings of the charge stabilizing abilities of substituents from kinetic studies of solvolytic reactions,[39]  $\text{pK}_{\text{R}^+}$  measurements[40], product studies of electrophilic additions to alkenes[41] and NMR studies [41,42] give the order cyclopropyl > phenyl > methyl > hydrogen. Similarly, the structural studies of Childs et al[43] rank cyclopropyl as better than phenyl as a charge stabilizer.

Farcasiu and Sharma[44] derived the charge stabilizing ability of a number of substituents from the <sup>13</sup>C NMR chemical shift data for 2,6-disubstituted pyrylium ions

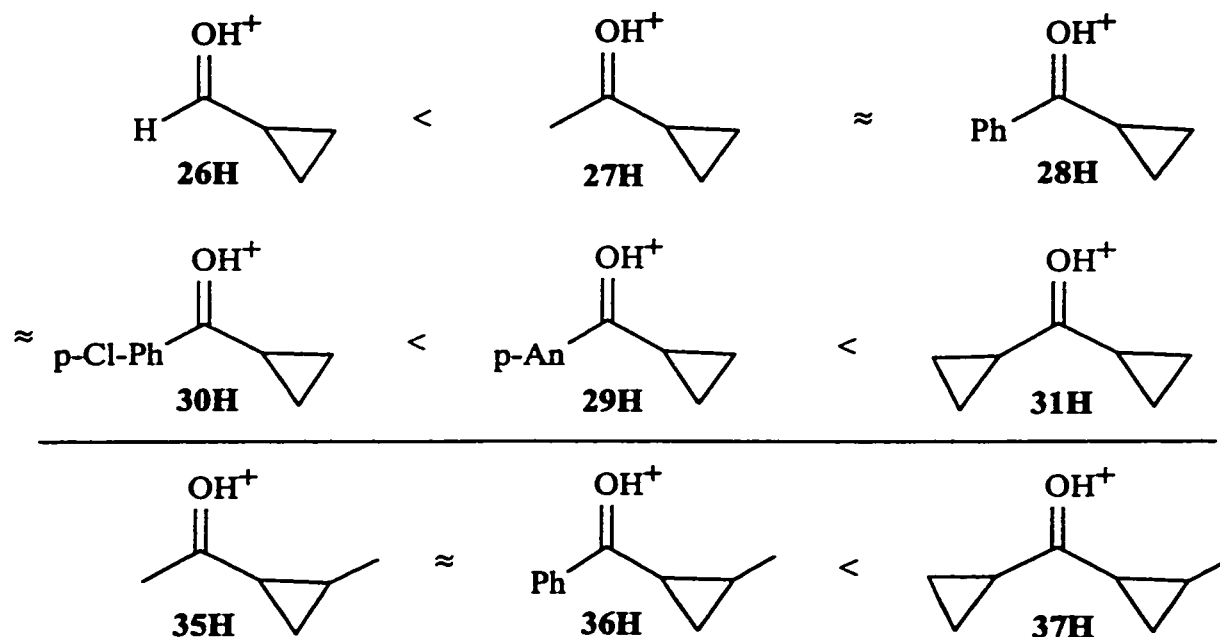


Figure 5.29: The activation barriers for the isomerization of the 26H-31H series and the 35H-37H series reveal the relative charge stabilizing abilities of the substituents at C(O).

which they claim gives a good measure of the charge density in the ring, free of other substituent effects. The charge stabilizing abilities derived from the C4 chemical shift of the pyrylium ions (hydrogen < methyl < p-chlorophenyl < phenyl < cyclopropyl = p-anisyl) shows a similar trend, but not an exact correspondence with the activation barriers for ring expansion measured in this thesis (hydrogen < methyl ≈ phenyl ≈ p-chlorophenyl < p-anisyl < cyclopropyl).

By many measures a phenyl group is a better stabilizing group for a carbocation than is a methyl group, but the equal ranking observed in this work is not without precedent. Larsen, Bouis and Little[45] concluded that a methyl group was a better stabilizing group than phenyl based on heats of protonation measured by themselves and those found in the literature. They could not rationalize this behaviour but argued that it

was not due to steric or solvation effects.

Differences in the nature of the cations, the processes being observed and the media are thought to be responsible for the failure to detect a regular order in the substituent effects.[46] The activation barrier of the ring expansion of protonated cyclopropyl ketones provides another means of determining the charge stabilizing ability of substituents.

### *5.3.3 Isomerization Mechanism(s) Leading to Oxolanylium Ions*

As presented in the Introduction to this chapter, there are several possible mechanisms by which ring expansion may occur and there is evidence in the literature that each of these mechanisms is operative for certain cyclopropyl substrates under certain conditions.

Protonation of the cyclopropyl ring (see Figure 5.1) is not believed to be responsible for the isomerizations. The exclusive cleavage of the C1-C2 cyclopropyl bond observed in this work supports this proposal. Also, there is no evidence that isomerization of the simple protonated cyclopropyl ketones studied in this thesis occurs via an alkyl cation (see Figure 5.5). Alkyl cation intermediates might be expected to undergo 1,2-hydrogen shifts to yield protonated enone. In the reactants that contain aryl rings (**28H-30H**, **34H** and **36H**), tetralone formation might be expected if an alkyl cation existed. However, enones and tetralones are not formed from cyclopropyl ketone substrates **26-40**. (Note: bicyclic ketones **41** and **42** are special cases for which oxolanylium ion formation is impossible.) One possible explanation is that enones are

formed but are unstable to the reaction conditions. However, protonated pent-3-en-2-one and hex-3-en-2-one were unchanged by extended heating in triflic acid at temperatures at which oxolanylium ions are formed from protonated cyclopropyl ketones. Thus, enones would be detected if formed. The complete absence of protonated enones, or tetralones provides strong evidence that alkyl cations and enones are not formed as intermediates during the formation of oxolanylium ions.

Further evidence against the intermediacy of alkyl cations in the ring expansion is provided by the kinetic data. The transition state required for formation of an alkyl cation would be expected to have considerable charge at C2. Thus, methyl substitution at C2 might be expected to lower  $\Delta G^\ddagger$  substantially. The energies of primary and secondary cations in the gas phase are known to be higher than that of a tertiary cation by about 45 and 17 kcal/mol, respectively.[47] In the case of **27**,  $\Delta G^\ddagger$  for ring expansion drops by 2 kcal/mol when one methyl group is introduced at C2 (giving **35**) which shows that the charge increases at C2 during isomerization. While solvation in the condensed phase may attenuate the energy difference between primary, secondary and tertiary cations, the observed decrease in  $\Delta G^\ddagger$  is not large enough to support the formation of an alkyl cation.

The third compound in the series of cyclopropyl ketones which bear zero (**27**), one (**35**) and two methyl groups at C2 has been studied by Childs and co-workers[10] (see Figure 5.24). In  $\text{FSO}_3\text{H}/\text{SO}_2\text{ClF}$ ,  $\Delta G^\ddagger$  for the isomerization of the protonated ketone with two methyl groups at C2 was 9 kcal/mol lower than that observed for **35H** in triflic acid. In addition, one of the initial products of isomerization was a protonated enone. The large decrease in  $\Delta G^\ddagger$  and the formation of an enone indicates that an alkyl cation is

involved in the isomerization of this reactant which can form a tertiary cation.

A similar rate effect, where the first methyl substitution causes a moderate rate acceleration and the second a much larger acceleration, is seen during the ring expansion of cyclopropanedicarboxylic acids in water or aqueous sulfuric acid,[22] and the solvolysis of alkyl halides[48] (Figure 5.30). These are rationalized as being due to a change from an  $S_N2$  (or  $S_N2$ -like) to an  $S_N1$  (or  $S_N1$ -like) mechanism. Similarly, it appears that the cyclopropyl ketone with two methyls at C2 undergoes isomerization by a different mechanism than **27H** and **35H**. Only protonated cyclopropyl ketones capable of forming highly stabilized cations (tertiary, benzylic, allylic, etc.) react via an alkyl cation.

#### *5.3.4 Concerted Ring Expansion or Double Nucleophilic Displacement?*

For simply substituted cyclopropyl ketones the alkyl-cation and ring-protonation mechanisms seem unlikely, however, the other two mechanisms (double nucleophilic displacement, and concerted ring expansion) remain as viable pathways. It should be possible to differentiate the two mechanisms on the basis of: 1) the dependence on nucleophile strength and concentration, 2) the entropy of activation, and 3) the stereochemical outcome of the reaction. If the ring expansion occurs by a double nucleophilic displacement then: 1) the rate should be strongly dependent on nucleophile strength and concentration, 2) the entropy of activation should be large and negative, and 3) the stereochemistry of the migrating centre should be retained. On the other hand, a concerted mechanism should have: 1) little dependence on the strength and concentration of the nucleophile, 2) a small entropy of activation, and 3) inversion of stereochemistry at



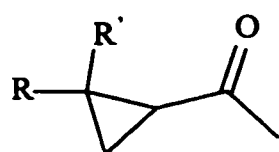
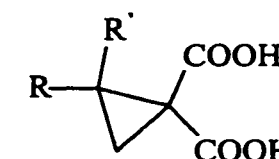
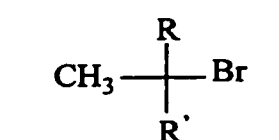
	relative rate (ring expansion in triflic acid)	R=R'=H 1	R=Me; R'=H 18	R=R'=Me 10 <sup>8</sup>
	relative rate (ring expansion in D <sub>2</sub> O)	1	31	80,000
	relative rate (formolysis)	1	26	10 <sup>8</sup>

Figure 5.30: Reactions for which a single methyl-substitution causes a moderate rate acceleration but a second methyl group causes a large rate acceleration. The relative rates of ring expansion of protonated cyclopropyl ketones were calculated at 25 °C by assuming that  $\Delta G^\ddagger$  was temperature independent (i.e.  $\Delta S^\ddagger = 0$ ).

the migrating centre (assuming an *si* pathway).

Pittman and McManus[7] noted that the rate of the cyclopropyl ketone to oxolanylium ion isomerization decreased as the acid strength was increased from 75 to 100% sulfuric acid. This trend is continued upon extension to triflic acid as the rate is 27 times slower in triflic acid than it is in 75% sulfuric acid (see Table 5.3). In fact, a plot of  $\Delta G^\ddagger$  vs.  $H_0$  displays a linear relationship (Figure 5.31). Since the ketones are fully protonated in every solution, this behaviour points to a mechanism in which the concentration and strength of the nucleophile may be important.

During this work, additional indirect evidence of the importance of nucleophile concentration was obtained. A triflate salt of **35H** was prepared by the addition of one

Table 5.3: The effect of acid strength on the rate of the isomerization of 27H to 44.<sup>a</sup>

acid	-H <sub>0</sub> <sup>b</sup>	T (°C)	rel. rate	ΔG <sup>‡</sup> (kcal/mol)
75% H <sub>2</sub> SO <sub>4</sub>	6.7	81	27	25.1
80% H <sub>2</sub> SO <sub>4</sub>	7.5	81	21	25.3
85% H <sub>2</sub> SO <sub>4</sub>	8.3	81	18	25.4
90% H <sub>2</sub> SO <sub>4</sub>	9.0	81	15	25.5
96% H <sub>2</sub> SO <sub>4</sub>	9.9	81	9	25.9
CF <sub>3</sub> SO <sub>3</sub> H	14.1	82	1	27.4

a) data for H<sub>2</sub>SO<sub>4</sub> solutions is from reference [7].

b) H<sub>0</sub> values from C.H. Rochester, "Acidity Functions", Academic Press, New York, 1970, p. 26 except for CF<sub>3</sub>SO<sub>3</sub>H which is from G.A. Olah, G.K.S. Prakash, J. Sommer, "Superacids", Wiley, Toronto, 1985, p. 37.

equivalent of triflic acid to ketone 35 dissolved in dichloromethane. A <sup>1</sup>H NMR spectrum of the oily product in CD<sub>2</sub>Cl<sub>2</sub> revealed that complete isomerization to the oxolanylium ion 52 had occurred. Apparently, the isomerization of the triflate salt of 35H in dichloromethane is rapid at room temperature and much more rapid than in triflic acid.

In a similar fashion, the SbCl<sub>6</sub><sup>-</sup> salt of 35H was prepared, except that a solid precipitated upon mixing of the ketone and acid. This solid was isolated and then dissolved in CD<sub>2</sub>Cl<sub>2</sub> for <sup>1</sup>H NMR analysis. The NMR spectrum revealed that 35H had been formed, however, this ion was found to isomerize to 52 at the temperature of the NMR probe (30 - 35°C). The progress of the isomerization was followed and the rate constant estimated (Table 5.1). The isomerization of the SbCl<sub>6</sub><sup>-</sup> salt of 35H to 52 has an activation barrier more than 3 kcal/mole less than the same reaction in triflic acid.

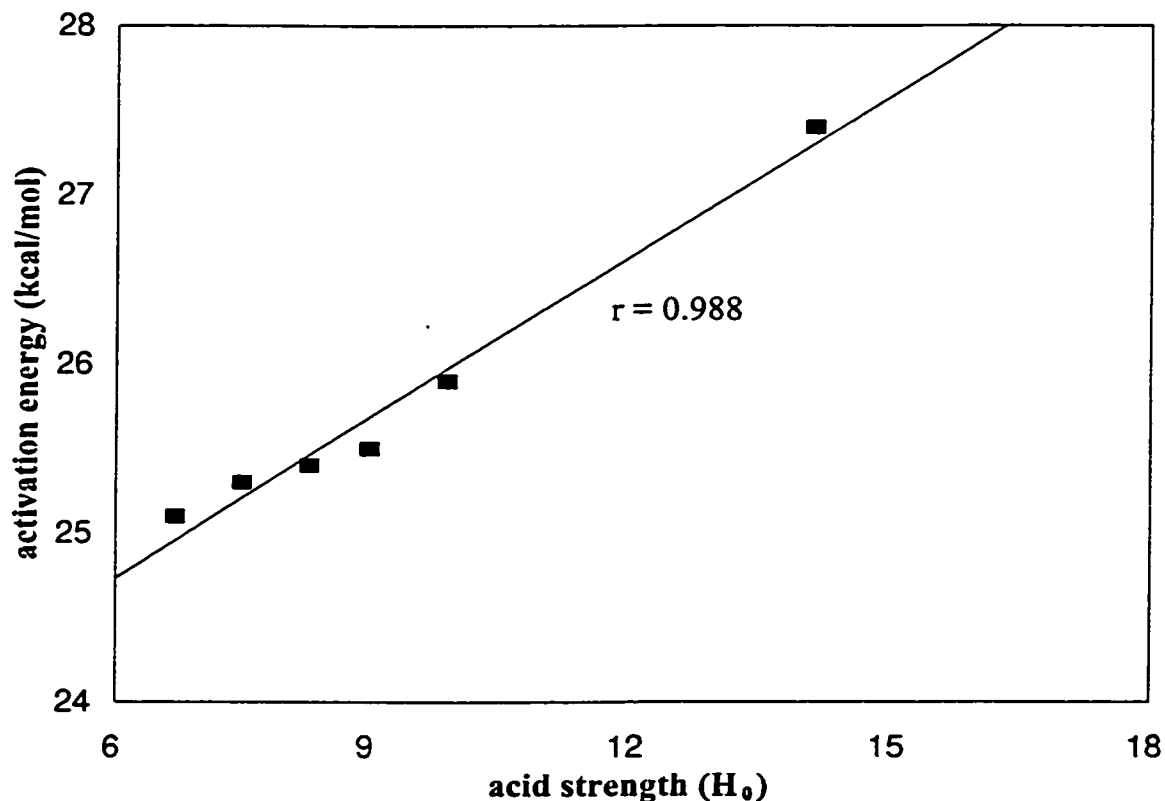


Figure 5.31: Effect of acid strength on the activation barrier for isomerization of protonated cyclopropyl methyl ketone, **27H**, at 81-2 °C.

One possible reason for the accelerated rate of reaction in dichloromethane is that ion pairing or clustering may be occurring. Pairing or clustering would lead to a higher effective concentration of counteranions and these nucleophiles may be held in very close proximity to the cations. In triflic acid, the cation and anion will be better solvated and will be separated by their respective solvent cages. In dichloromethane, the ions may not be as strongly solvated, and thus may exist as tight ion pairs. This might facilitate nucleophilic attack on the cyclopropyl ring of the ions **26H-40H**.

The entropy of activation is known for the ring expansion reactions of some cyclopropyl compounds. The thermal isomerizations of vinylcyclopropanes,[3f,49] azocyclopropanes[18a] and cyclopropyl ketones[15] are believed to be unimolecular reactions, proceeding via biradical intermediates or perhaps a concerted reaction in the case of vinylcyclopropane. The entropy of activation for these reactions is quite small (-5 to 5 cal/K mol) as illustrated in Figure 5.32.

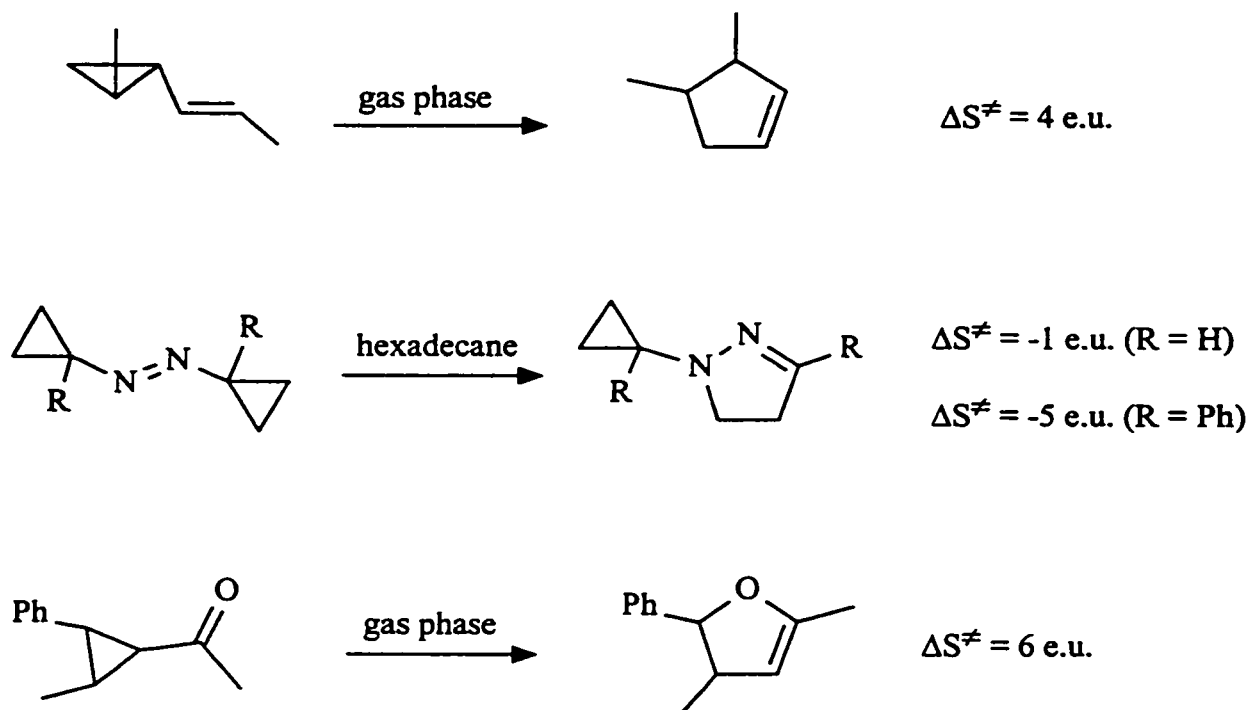


Figure 5.32: Entropies of activation for the thermal ring expansions of several cyclopropyl compounds.

Bus, Steinberg and de Boer[22] investigated the ring expansion of 1,1-cyclopropanedicarboxylic acids in water and aqueous sulfuric acid. The entropy of activation for systems bearing zero or one  $\beta$ -methyl group was  $\Delta S^\ddagger = -21 \text{ cal/K mole}$ . The

$\beta,\beta$ -dimethyl isomer reacted 80,000 times faster than the unsubstituted isomer, and determination of  $\Delta S^\ddagger$  was not possible. They concluded that the unsubstituted and singly substituted compounds reacted via rate-determining attack of water at the  $\beta$ -carbon of the cyclopropyl ring (i.e. ring expansion by a double nucleophilic displacement). For the  $\beta,\beta$ -dimethyl isomer, the rate-determining step was believed to be heterolytic cleavage of the cyclopropyl ring (i.e. an alkyl-cation mechanism). The two reaction pathways are illustrated in Figure 5.33.

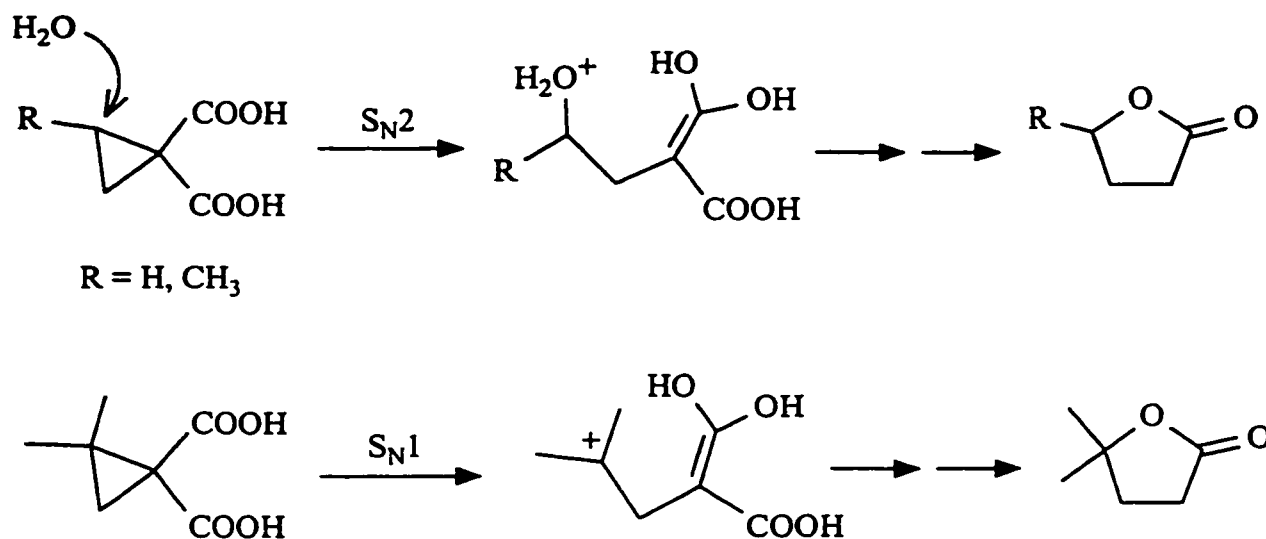


Figure 5.33: Proposed ring-expansion mechanisms for 1,1-cyclopropanedicarboxylic acids with 0, 1 or 2 methyl groups at the  $\beta$ -position in water and aqueous sulfuric acid.

An estimate of the entropy of activation for the rearrangement of **32H** in 80% sulfuric acid can be calculated from the data presented by Pittman and McManus.[7] The rates of reaction determined at 76 and 98 °C, allow the entropy of activation to be estimated as  $\Delta S^\ddagger = -34 \text{ cal/K mol}$ . This value is typical of a reaction involving a

bimolecular transition state.

In distinct contrast, the entropies of activation for **27H** and **28H** in triflic acid are close to zero; -4 and +5 cal/K mol for **27H** and **28H**, respectively (Table 5.1). Values close to zero are expected for a reaction proceeding through a unimolecular transition state. Thus, it appears that in 80% sulfuric acid **32H** is reacting by a double nucleophilic displacement (possibly with  $\text{HSO}_4^-$  as the nucleophile), but a mechanism change occurs when triflic acid is the solvent. A unimolecular (possibly concerted) pathway is active for **27H** and **28H** in triflic acid.

#### *5.3.5 Isomerizations of Stereochemically Labelled Protonated Cyclopropyl Ketones*

To further test for a concerted ring expansion of protonated cyclopropyl ketones, the isomerizations of compounds which had stereochemical labels were investigated. Thus, the dimethyl substituted compounds **38-40** (Figure 5.34) were prepared and the relative stereochemistry of the methyl groups was confirmed as described in Chapter 4. Protonated ketones **38H-40H** yield the cis- and trans-dimethyloxolanylium ions, **55** and **56**, upon heating in triflic acid (Figure 5.34). The ratio of cis- to trans-dimethyloxolanylium ions was determined from the  $^1\text{H}$  NMR spectra (chapter 4), and the results are presented in Table 5.4.

The isomerization of **40H** at 60 °C leads to preferential formation of the cis isomer, however, conclusions regarding the mechanism are made uncertain by the extensive decomposition that accompanies isomerization. The formation of decomposition products is peculiar to this compound and it is not clear why this does not

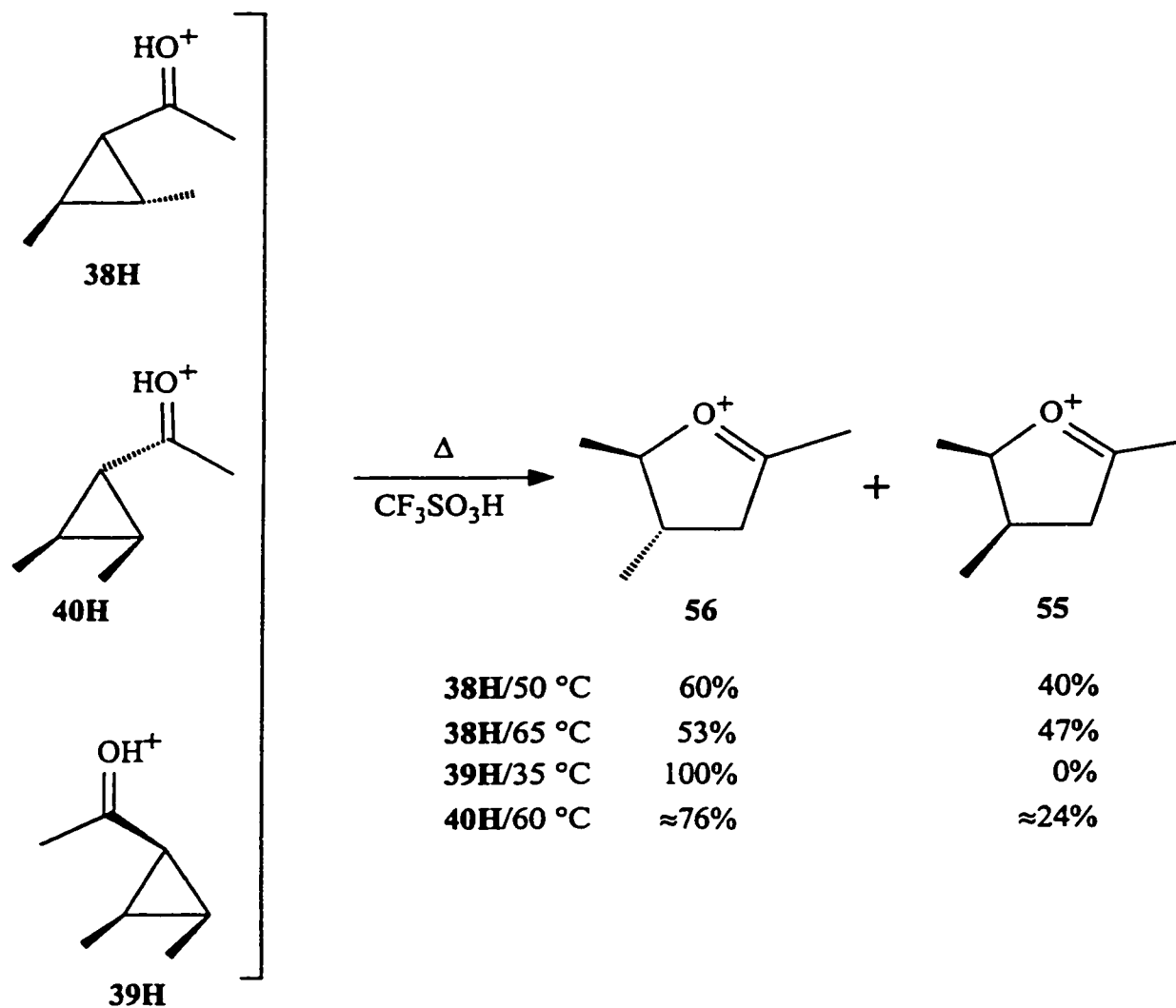


Figure 5.34: Isomerization of protonated 2,3-dimethylcyclopropyl methyl ketones **38H-40H** produces the cis and trans 4,5-dimethyloxolanylium ions **55** and **56**.

occur with closely related starting materials.

With **39H** the exclusive formation of the cis-dimethyl oxolanylium ion, **55**, is not surprising when one considers the geometry required for a concerted reaction. Concerted ring expansion can only occur from the s-cis conformer of the protonated cyclopropyl ketone (Figure 5.35). Placing the carbonyl oxygen close enough to C2 or C3 for bond formation to occur may be rendered impossible because of steric interactions between the

Table 5.4: Ratio of cis- to trans-4,5-dimethyloxolanylium ions produced during the isomerization of the protonated 2,3-dimethylcyclopropyl methyl ketones, **38H-40H**.

reactant	T (°C)	%cis ( <b>55</b> )	%trans ( <b>56</b> )
<b>38H</b>	50	60	40
	65	53	47
<b>39H</b>	35	100	0
<b>40H<sup>a</sup></b>	60	76	24

a) isomerization is accompanied by extensive decomposition.

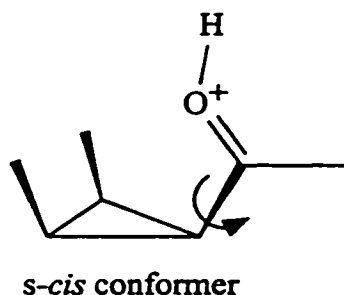


Figure 5.35: The *s-cis* conformer required for concerted ring expansion of **39H** is sterically crowded.

carbonyl and methyl groups. It is clear that another mechanism, perhaps double nucleophilic displacement, is active in this case. The intervention of this mechanism would account for the complete retention of the cis-dimethyl stereochemistry.

Heating a solution of **38H** led to the formation of a 53:47 mixture of **55**:**56** at 65 °C and a 60:40 mixture at 50 °C. Thus, the transition state for reaction favours the *cis* isomer by about 0.2 kcal/mole. The preference for the *cis* isomer, **55**, is further emphasized when one considers that it is the thermodynamically less stable isomer; equilibrium concentrations of **55** and **56** are 19:81 at 100 °C, so the *trans* isomer, **56**, is



1.1 kcal/mole more stable than **55**. The most apparent mechanism which can be used to explain the preferential formation of the less stable *cis* isomer is a concerted reaction governed by orbital symmetry constraints. The mechanism which would lead to the *cis*-dimethyl oxolanylium ion would involve suprafacial migration along the  $\pi$ -system with inversion of the stereochemistry at the migrating centre, the *si* pathway (Figure 5.36). Thus, on the basis of the stereochemical results for **38H**, low  $\Delta S^\ddagger$  values and the effect of substituents on  $\Delta G^\ddagger$ , it can be concluded that ring expansion in triflic acid of the simply substituted protonated cyclopropyl ketones studied in this thesis occurs via a concerted pathway. This conclusion would hold for those cyclopropyl ketones which bear alkyl or aryl substituents at C(O) and one or no alkyl substituents at C2.

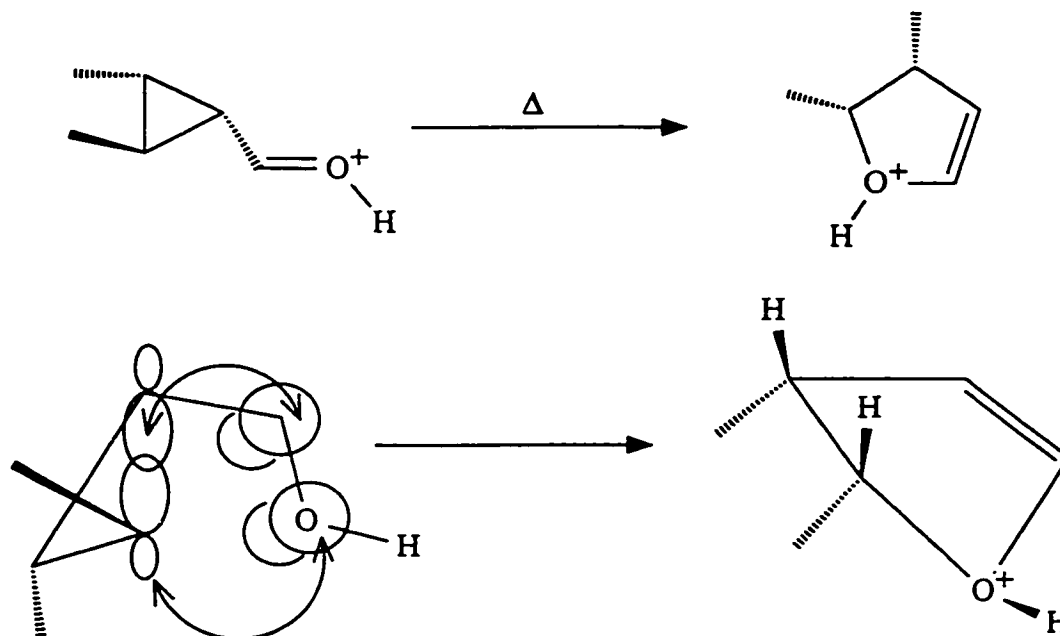


Figure 5.36: Orbital interactions for thermally-allowed *si* pathway for ring expansion of protonated *cis,trans*-2,3-dimethylcyclopropyl methyl ketone.

Inversion at the migrating centre causes the substituent *cis* to the carbonyl group to be rotated into the oxallyl framework in the transition state (Figure 5.37). Migration with inversion may only be possible for centres in which the *cis* substituent is small (eg. hydrogen). In fact, Berson and coworkers found that 1,3-sigmatropic migrations in bicyclo[3.2.0]heptenes showed a 10:1 preference for the allowed *si* pathway when hydrogen was rotated into the allyl system but when this group was methyl the forbidden *sr* pathway was favoured by a similar amount.[33b,50] With 38H migration with inversion may be only be possible for the carbon with the methyl *trans* to the carbonyl group.

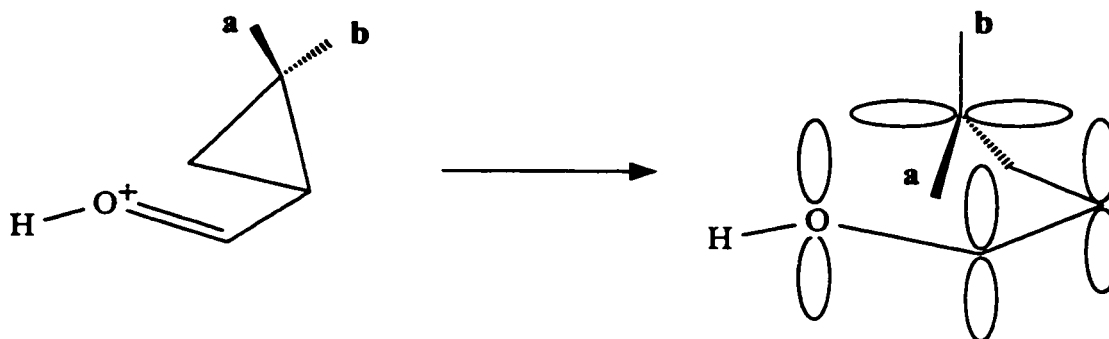


Figure 5.37: Inversion at the migrating centre rotates substituent **a** into the oxallyl framework in the transition state.

It appears that the transition state for the allowed pathway lies only slightly lower than that of the forbidden pathway (and perhaps other pathways) and the relative energies may be inverted easily by other factors such as steric ones. The forbidden *sr* pathway may be the source of the *trans*-4,5-dimethyloxolanylium isomer, **56**. Concerted ring expansion by this pathway, possibly stabilized by interactions with subjacent orbitals (eg. orbitals other than the HOMO and LUMO), may be of lower energy than stepwise

processes.[4c-4e,33b,51,52] The observation of  $\Delta S^\ddagger \approx 0$  indicates that double nucleophilic displacement is not involved in the isomerizations of most protonated cyclopropyl ketones and probably not **38H**.

Concerted reactions might be expected to be more facile for protonated cyclopropyl ketones which are unsubstituted at C2 and C3. Cyclopropyl ketones with small labels (eg. deuterium) at C2 and C3 might show an even greater preference for reaction via a concerted reaction.

In summary, it appears that protonated cyclopropyl ketones isomerize via concerted ring expansion if a weakly nucleophilic acid medium (i.e. triflic or fluorosulfuric acid) and substrates that are not able to form a highly stable carbocation via ring opening are used. Molecules that can form a stable carbocation (i.e. tertiary, allylic, benzylic, alkoxy- or hydroxy-substituted) will likely react via an alkyl cation. Carbocation intermediates may close to an oxolanylium ion, or undergo another reaction such as enone formation. In the presence of suitable nucleophiles, attack at the  $\beta$ -position of the cyclopropyl ring can cause ring opening. The  $\gamma$ -substituted ketone thus formed may be isolable or it may experience ring closure to an oxolanylium ion. Nucleophilic attack is more likely for molecules with one or no substituents at the  $\beta$ -carbon of the cyclopropyl ring. Thus, over a narrow range of acid strengths and substitution patterns it should be possible to observe ring expansion reactions which occur via alkyl cation intermediates, double nucleophilic displacements and concerted reactions. This makes for complicated but fascinating chemistry.

## 5.4 Conclusion

The isomerizations of protonated cyclopropyl ketones to oxolanylium ions in triflic acid are clean reactions displaying first-order kinetics. The rates of isomerization provide information about the mechanism and charge stabilizing ability of substituents. Methyl substitution at C2 increases the rate of reaction indicating a charge increase at C2 during isomerization. As the substituent at C(O) becomes a better electron donor the rate of reaction slows because these substituents provide greater stabilization to the ground state relative to the transition state. The rates of reaction were used to rank the charge stabilizing ability of several substituents as: hydrogen < methyl  $\approx$  phenyl < p-anisyl < cyclopropyl.

In triflic acid the activation barrier for cyclopropyl ring opening to yield enones appears to lie about 3 kcal/mol higher than that for ring expansion.

A good correlation was found between the rate of reaction and the acid strength; the isomerization slows as the acid strength increases. Thus, measurement of the isomerization rate might be used to estimate the strength of acidic media.

In triflic acid the ring expansion of protonated cyclopropyl ketones occurs by a concerted mechanism governed by orbital symmetry constraints. This is based on product analyses, entropies of activation and the stereochemical outcome of the isomerization of **38H**. However, other reaction mechanisms may become operative when the substitution pattern or acidic medium is changed. Compounds capable of forming highly stabilized cations (tertiary, allylic, benzylic, etc.) may react via a ring opened alkyl cation intermediate. When the acid strength of the reaction medium is reduced ring

expansion via a double nucleophilic displacement may become dominant as the nucleophilic strength and concentration will be greater. Each of these mechanisms has a different stereochemical outcome, and by controlling the reaction conditions it may be possible to produce pure (or enriched) stereoisomers. This aspect might be of synthetic utility.

### 5.5 References

1. N.P. Neureiter, *J. Org. Chem.*, **1959**, *24*, 2044; Z. Goldschmidt, B. Crammer, *Chem. Soc. Rev.*, **1988**, *17*, 229; J. Salaun in *The Chemistry of the Cyclopropyl Group*, Z. Rappoport (ed.), Wiley, Toronto, 1987, vol. 1, chpt. 13, p. 809.
2. a) K.N. Houk, M. Nendel, O. Wiest, J.W. Storer, *J. Am. Chem. Soc.*, **1997**, *119*, 10545; b) J.E. Baldwin, S.J. Bonacorsi, *J. Am. Chem. Soc.*, **1996**, *118*, 8258; c) J.E. Baldwin, K.A. Villarica, D.I. Freedberg, F.A.L. Anet, *J. Am. Chem. Soc.*, **1994**, *116*, 10845; d) J. E. Baldwin, N. D. Ghatlia, *J. Am. Chem. Soc.* **1991**, *113*, 6273; e) J.J. Gajewski, M. Warner, *J. Am. Chem. Soc.*, **1984**, *106*, 802; f) W.E. Doering, K. Sachdev, *J. Am. Chem. Soc.*, **1974**, *96*, 1168; g) W.E. Doering, K. Sachdev, *J. Am. Chem. Soc.*, **1975**, *97*, 5512.
3. a) E.R. Davidson, J.J. Gajewski, *J. Am. Chem. Soc.*, **1997**, *119*, 10543; b) J.J. Gajewski, L.P. Olson, M.R. Willcott, *J. Am. Chem. Soc.*, **1996**, *118*, 299; c) J.J. Gajewski, G.C. Paul, *J. Org. Chem.* **1991**, *56*, 1986; d) J.J. Gajewski, L.P. Olsen, *J. Am. Chem. Soc.* **1991**, *113*, 7432; e) J.J. Gajewski, M.P. Squicciarini, *J. Am. Chem. Soc.*, **1989**, *111*, 6717; f) G. D. Andrews, J.E. Baldwin, *J. Am. Chem. Soc.* **1976**, *98*,

- 6705.
4. a) T. Hudlicky, T.M. Kutchan, S.M. Naqvi, *Org. React. (N.Y.)*, **1985**, *33*, 247; b) T. Hudlicky, N.E. Heard, A. Fleming, *J. Org. Chem.*, **1990**, *55*, 2570; c) R.L. Danheiser, C. Martinez-Davila, J.M. Morin, Jr., *J. Org. Chem.*, **1980**, *45*, 1340; d) R.L. Danheiser, C. Martinez-Davila, R.J. Auchus, J.T. Kadonaga, *J. Am. Chem. Soc.*, **1981**, *103*, 2443; e) R.L. Danheiser, J.J. Bronson, K. Okano, *J. Am. Chem. Soc.*, **1985**, *107*, 4579; f) D.F. Harvey, M.F. Brown, *Tetrahed. Lett.*, **1991**, *32*, 2871; g) H.W.L. Davies, B. Hu, *J. Org. Chem.*, **1992**, *57*, 3186.
  5. R.B. Woodward, R. Hoffmann, *The Conservation of Orbital Symmetry*, Academic Press, New York, 1970, p. 114; F.A. Carey, R.J. Sundberg, *Advanced Organic Chemistry*, Plenum Press, New York, 1990, part A, p. 609; T.H. Lowry, K.S. Richardson, *Mechanism and Theory in Organic Chemistry*, Harper & Row, New York, 1981, 2nd edn., p. 764, 869.
  6. a) R.V. Stevens, *Acc. Chem. Res.*, **1977**, *10*, 193; b) R.K. Boeckman, Jr., M.A. Walters, in *Advances in Heterocyclic Natural Product Synthesis*, W.H. Pearson (ed.), JAI Press, Greenwich, Conn., 1990, Vol. 1, p. 1; c) H.U. Reissig in *The Chemistry of the Cyclopropyl Group*, Z. Rappoport (ed.), Wiley, Toronto, 1987, vol. 1, chpt. 8, p. 375; d) T. Hudlicky, J.W. Reed in *Comprehensive Organic Synthesis*, B.M. Trost, I. Fleming (eds.), Pergamon Press, Oxford, 1991, vol. 5, chpt. 8.1, p. 899; e) J.R.Y. Salaun, *Top. Curr. Chem.*, **1988**, *144*, 1.
  7. C.U. Pittman, S.P. McManus, *J. Am. Chem. Soc.*, **1969**, *91*, 5915.
  8. C.J. Collins, *Chem. Rev.*, **1969**, *69*, 543; C.C. Lee, *Prog. Phys. Org. Chem.*, **1970**,

- 7, 129; T.H. Lowry, K.S. Richardson, *Mechanism and Theory in Organic Chemistry*, Harper & Row, New York, 1981, 2nd edn., p. 429; M. Saunders, P. Vogel, E.L. Hagen, J. Rosenfeld, *Acc. Chem. Res.*, **1973**, *6*, 53.
9. N.C. Deno, W.E. Billups, D. LaVietes, P.C. Scholl, S. Schneider, *J. Am. Chem. Soc.*, **1970**, *92*, 3700.
10. R.F. Childs, T. DiClemente, E.F. Lund-Lucas, T.J. Richardson, C.V. Rogerson, *Can. J. Chem.*, **1983**, *61*, 856.
11. W.S. Murphy, S. Wattanasin, *Tetrahed. Lett.*, **1980**, *21*, 1887; W.S. Murphy, S. Wattanasin, *Tetrahed. Lett.*, **1980**, *21*, 3517; W.S. Murphy, S. Wattanasin, *J. Chem. Soc., Perkin Trans. 2*, **1981**, 2920; W.S. Murphy, S. Wattanasin, *J. Chem. Soc., Perkin Trans. 2*, **1982**, 1029; W.S. Murphy, S. Wattanasin, *J. Chem. Soc., Perkin Trans. 2*, **1983**, 817; K. Hantawong, W.S. Murphy, D.K. Boyd, G. Ferguson, M. Parvez, *J. Chem. Soc., Perkin Trans. 2*, **1985**, 1577.
12. D.F. Harvey, M.F. Brown, *Tetrahed. Lett.*, **1991**, *32*, 2871.
13. X. Creary, F. Hudock, M. Keller, J.F. Kerwin, J.P. Dinnocenzo, *J. Org. Chem.*, **1977**, *42*, 409.
14. D.M. Brouwer, J.A. van Doorn, A.A. Kiffen, *Rec. Trav. Chim.*, **1975**, *94*, 198.
15. D.E. McGreer, J.W. McKinley, *Can. J. Chem.*, **1973**, *51*, 1487.
16. E. Lee-Ruff, P. Khazanie, *Can. J. Chem.*, **1975**, *53*, 1708; E. Lee-Ruff, P.G. Khazanie, *Can. J. Chem.*, **1978**, *56*, 803; P.G. Khazanie, E. Lee-Ruff, *Can. J. Chem.*, **1978**, *56*, 808.

17. H. Hiraoka, *Tetrahedron*, **1973**, *29*, 2955.
18. a) P.S. Engel, D.B. Gerth, *J. Am. Chem. Soc.*, **1981**, *103*, 7689; b) J. Bonnekessel, C. Ruchardt, *Chem. Ber.*, **1973**, *106*, 2890.
19. M. Buchert, H.U. Reissig, *Liebigs Ann.*, **1996**, 2007; B. Hofmann, H.-U. Reissig, *Chem. Ber.*, **1994**, *127*, 2327; B. Hofmann, H.-U. Reissig, *Synlett*, **1993**, 27; C. Bruckner, H.U. Reissig, *Liebigs Ann. Chem.*, **1988**, 465; C. Bruckner, B. Suchland, H.U. Reissig, *Liebigs Ann. Chem.*, **1988**, 471; H.U. Reissig, *Top. Curr. Chem.*, **1988**, *144*, 73.
20. S. Danishefsky, *Acc. Chem. Res.*, **1979**, *12*, 66; R.D. Miller, D.R. McKean, *J. Org. Chem.*, **1981**, *46*, 2412.
21. J.B. Cloke, *J. Am. Chem. Soc.*, **1929**, *51*, 1174; R.K. Boeckman, Jr., P.F. Jackson, J.P. Sabatucci, *J. Am. Chem. Soc.*, **1985**, *107*, 2191; R.K. Boeckman, Jr., J.P. Sabatucci, S.W. Goldstein, D.M. Springer, P.F. Jackson, *J. Org. Chem.*, **1986**, *51*, 3742; R.K. Boeckman, Jr., S.W. Goldstein, M.A. Walters, *J. Am. Chem. Soc.*, **1988**, *110*, 8250; H.H. Wasserman, R.P. Dion, *Tetrahed. Lett.*, **1983**, *24*, 3409; H.H. Wasserman, R.P. Dion, *Tetrahed. Lett.*, **1982**, *23*, 1413; P.C. Heidt, S.C. Bergmeier, W.H. Pearson, *Tetrahed. Lett.*, **1990**, *31*, 5441; R.B. Bennett, J.K. Cha, *Tetrahed. Lett.*, **1990**, *31*, 5437.
22. J. Bus, H. Steinberg, T. J. de Boer, *Rec. Trav. Chim.*, **1972**, *91*, 657.
23. S. Oae, *J. Am. Chem. Soc.*, **1956**, *78*, 4030; D.J. Pasto, M.P. Serve, *J. Am. Chem. Soc.*, **1965**, *87*, 1515.



24. H.R. Ward, P.D. Sherman, *J. Am. Chem. Soc.*, **1968**, *90*, 3812; J.P. Bégué, D. Bonnet-Delpon, *Org. Magn. Reson.*, **1980**, *14*, 349.
25. J. Bus, H. Steinberg, T.J. deBoer, *Tetrahed. Lett.*, **1966**, 1979.
26. for the first example of cyclopropylimine ring expansion that does not need acid/nucleophile see P.-L. Wu, W.S. Wang, *J. Org. Chem.*, **1994**, *59*, 622.
27. H.W. Heine in *Mechanisms of Molecular Migrations*, B.S. Thyagarajan (ed.), Wiley, New York, 1971, vol. 3, p. 145.
28. J. Legters, L. Thijs, B. Zwanenburg, *Rec. Trav. Chim.*, **1992**, *111*, 16
29. S.-H. Jung, H. Kohn, *J. Am. Chem. Soc.*, **1985**, *107*, 2931
30. H.W. Heine, D.C. King, L.A. Portland, *J. Org. Chem.*, **1966**, *31*, 2662; H.W. Heine, M. Kaplan, *J. Org. Chem.*, **1967**, *32*, 3069.
31. J.A. Deyrup in *Small Ring Heterocycles*, A. Hassner (ed.), Wiley, New York, 1983, p.1.
32. N. Murai, M. Komatsu, T. Yagii, H. Nishihara, Y. Ohshiro, T. Agawa, *J. Org. Chem.*, **1977**, *42*, 847.
33. a) T.H. Lowry, K.S. Richardson, *Mechanism and Theory in Organic Chemistry*, Harper & Row, New York, 1981, 2nd edn., p. 870; b) J.A. Berson, *Acc. Chem. Res.*, **1972**, *5*, 406.
34. M.E. Alonso, A. Morales, *J. Org. Chem.*, **1980**, *45*, 4530; H.W.L. Davies, B. Hu, *J. Org. Chem.*, **1992**, *57*, 3186. (see also *Tetrahedron*, **1993**, *49*, 1057 and *J. Org. Chem.*, **1990**, *55*, 4975).
35. F.A. Carey, R.J. Sundberg, *Advanced Organic Chemistry*, Plenum Press, New

- York, 1990, part A, p. 612; F. Bernardi, M.A. Robb, H.B. Schlegel, G. Tonachini, *J. Am. Chem. Soc.*, **1984**, *106*, 1198.
36. J.P. Dinnocenzo, D.A. Conlon, *J. Am. Chem. Soc.*, **1988**, *110*, 2324.
37. G.A. Olah, R.J. Spear, P.C. Hiberty, W.J. Hehre, *J. Am. Chem. Soc.*, **1976**, *98*, 7470.
38. T. Nakajima, H. Miyaji, M. Segi, S. Suga, *Chem. Lett.*, **1986**, 181; T. Nakajima, M. Tanabe, K. Ohno, M. Segi, S. Suga, *Chem. Lett.*, **1986**, 177.
39. H.C. Brown, M. Ravindranathan, E.N. Peters, *J. Org. Chem.*, **1977**, *42*, 1073; H.C. Brown, E.N. Peters, *J. Am. Chem. Soc.*, **1977**, *99*, 1712.
40. H.G. Richey, Jr. in *Carbonium Ions*, G.A. Olah, P.v.R. Schleyer (eds.), Wiley, Toronto, 1972, vol. 3, chpt. 25, p. 1201.
41. G.A. Olah, P.W. Westerman, J. Nishimura, *J. Am. Chem. Soc.*, **1974**, *96*, 3548; G.A. Olah, P.W. Westerman, *J. Am. Chem. Soc.*, **1973**, *95*, 7530.
42. G.A. Olah, R.J. Spear, *J. Am. Chem. Soc.*, **1975**, *97*, 1539; G.A. Olah, V.P. Reddy, G. Rasul, G.K.S. Prakash, *J. Org. Chem.*, **1992**, *57*, 1114.
43. R.F. Childs, R. Faggiani, C.J.L. Lock, M. Mahendran, S.D. Zweep, *J. Am. Chem. Soc.*, **1986**, *108*, 1692.
44. D. Farcasiu, S. Sharma, *J. Org. Chem.*, **1991**, *56*, 126.
45. J.W. Larsen, P.A. Bouis, C.A. Riddle, *J. Org. Chem.*, **1980**, *45*, 4969.
46. T.T. Tidwell in *The Chemistry of the Cyclopropyl Group*, Z. Rappoport (ed.), Wiley, Toronto, 1987, vol. 1, chpt. 10, p. 565; E.M. Arnett, T.C. Hofelich, *J. Am. Chem. Soc.*, **1983**, *105*, 2889.

47. J. March, *Advanced Organic Chemistry: Reactions, Mechanisms, and Structure*, 4th ed., Wiley, Toronto, 1992, p. 171; J.C. Schultz, F.A. Houle, J.L. Beauchamp, *J. Am. Chem. Soc.*, **1984**, *106*, 3917.
48. F.A. Carey, R.J. Sundberg, *Advanced Organic Chemistry*, Plenum Press, New York, 1990, part A, p. 294.
49. G.D. Andrews, J.E. Baldwin, *J. Am. Chem. Soc.*, **1976**, *98*, 6705; J.M. Simpson, H.G. Richey Jr., *Tetrahed. Lett.*, **1973**, 2545; C.A. Wellington, *J. Phys. Chem.*, **1962**, *66*, 1671.
50. J.A. Berson, G.L. Nelson, *J. Am. Chem. Soc.*, **1970**, *92*, 1096; J.A. Berson, R.W. Holder, *J. Am. Chem. Soc.*, **1973**, *95*, 2037.
51. J.A. Berson, L. Salem, *J. Am. Chem. Soc.*, **1972**, *94*, 8917.
52. I. Fleming, *Frontier Orbitals and Organic Chemical Reactions*, Wiley, Toronto, 1976, p.228.

## **Chapter 6: Concluding Remarks**

Carbocations play key roles in the reactions of many organic molecules, including those of biological and industrial importance. For example, the biosynthesis of steroids from isoprenyl subunits and the cleavage of polysaccharides by the enzyme lysozyme occur via carbocation intermediates. Nicotinamide adenine dinucleotide (NAD<sup>+</sup>) is a carbocation which is involved in oxidations of biological fuel molecules (e.g., glucose, fatty acids), reactions which likely occur via carbocation intermediates. The chromophore (light absorbing unit) of the visual pigment is a stable iminium carbocation formed from retinal.

Industrial examples that rely on carbocation chemistry include the preparation of polymers (e.g, polyisobutylene), the preparation of alcohols from alkenes, and the refining of hydrocarbons. During catalytic cracking long-chain hydrocarbons are broken down into shorter, often branched, hydrocarbons which are suitable for industrial usage (e.g., fuels, solvents, chemical feedstock). Very small hydrocarbons can be converted into larger, branched chains suitable for gasoline via a process known as alkylation. Isomerization is used to convert straight-chain hydrocarbons into more branched isomers which improve the anti-knock properties of gasoline. All of these processes utilize acidic catalysts and the reactions occur via carbocations.

The course of each of the above reactions is determined by the energies of the

carbocations. Thus, information regarding the energies of carbocations is of fundamental importance. While considerable effort has been expended towards this end, the approaches are often indirect. This thesis describes the first application of differential scanning calorimetry (DSC) to measure the heats of isomerization of carbocations. The heat of isomerization provides the energy difference between isomeric carbocations and reveals the effect of structural changes upon the carbocation energies, information of great value to any scientist interested in understanding or predicting the path of an organic reaction.

In this thesis DSC was used to study three types of carbocation isomerizations which allowed the effect of structural changes, in particular methyl substitution, upon the energies of the carbocations to be quantified. It would be fairly simple to extend the present work to study isomerizations in related or unrelated carbocation systems. In this work, methyl migrations in protonated 4,4-dimethyl substituted cyclopentenone or cyclohexenone were investigated. This could easily be extended to include the migrations of a variety of substituents, and thus provide both the stabilizing effect of the substituents and the migratory aptitudes of the various groups.

The work described in this thesis also provides evidence that the ring expansion of protonated cyclopropyl ketones in triflic acid occurs via a concerted 1,3-migration, a reaction for which there are relatively few examples. While this should spur further investigation of the mechanism of this isomerization, perhaps the greatest potential lies in synthetic applications. It is fairly straightforward to prepare specific stereoisomers of cyclopropyl compounds. With an understanding of conditions under which ring opening

or ring expansion occurs stereoselectively, it should be possible to stereoselectively synthesize a variety of compounds. Tetrahydrofurans, dihydrofurans, cyclopentanones and cyclopentenones could all be produced stereoselectively via the ring expansion (or ring opening) of protonated cyclopropyl ketones. This approach could be extended to related cyclopropyl compounds such as cyclopropyl imines. While the ring expansion of protonated cyclopropyl imines has been utilized synthetically, the potential for stereoselective ring opening or ring expansion has not been recognized and thus has not been exploited.

**Appendix: Crystallographic Data for 40-DNP, the 2,4-Dinitrophenylhydrazone Derivative of trans,trans-2,3-Dimethylcyclopropyl Methyl Ketone (40)**

Table A1: Crystal data and structure refinement for 40-DNP.

Identification code	burkel
Empirical formula	$C_{13}H_{16}N_4O_4$
Formula weight	292.30
Temperature	298(2) K
Wavelength	0.71073 Å
Crystal system	Monoclinic
Space group	$P2_1/c$
Unit cell dimensions	$a = 13.226(2)$ Å $\alpha = 90^\circ$ $b = 6.6710(10)$ Å $\beta = 100.78(2)^\circ$ $c = 16.177(3)$ Å $\gamma = 90^\circ$
Volume, Z	$1402.1(4)$ Å <sup>3</sup> , 4
Density (calculated)	$1.385$ Mg/m <sup>3</sup>
Absorption coefficient	$0.105$ mm <sup>-1</sup>
F(000)	616
Crystal size	0.35 x 0.30 x 0.25 mm
$\theta$ range for data collection	2.74 to $22.57^\circ$
Limiting indices	$-2 \leq h \leq 14$ , $0 \leq k \leq 7$ , $-15 \leq l \leq 15$
Reflections collected	1975
Independent reflections	1801 ( $R_{int} = 0.0136$ )
Absorption correction	None

Table A1 (continued): Crystal data and structure refinement for 40-DNP.

Refinement method	Full-matrix least-squares on $F^2$
Data / restraints / parameters	1801 / 0 / 194
Goodness-of-fit on $F^2$	1.062
Final R indices [ $I > 2\sigma(I)$ ]	R1 = 0.0448, wR2 = 0.1153
R indices (all data)	R1 = 0.0635, wR2 = 0.1308
Extinction coefficient	0.014(7)
Largest diff. peak and hole	0.134 and -0.135 $e\text{\AA}^{-3}$



Table A2: Atomic coordinates ( $\times 10^4$ ) and equivalent isotropic displacement parameters ( $\text{\AA}^2 \times 10^3$ ) for 40-DNP.  $U(\text{eq})$  is defined as one third of the trace of the orthogonalized  $U_{ij}$  tensor.

	x	y	z	$U(\text{eq})$
O(1)	-376 (1)	1641 (4)	7293 (1)	73 (1)
O(2)	1259 (1)	1332 (4)	7555 (1)	82 (1)
O(3)	3348 (1)	2287 (3)	5557 (1)	76 (1)
O(4)	2679 (2)	2386 (3)	4240 (2)	69 (1)
N(1)	461 (2)	1655 (3)	7057 (1)	51 (1)
N(2)	2602 (2)	2344 (3)	4976 (2)	52 (1)
N(3)	-1342 (1)	2384 (3)	5764 (1)	41 (1)
N(4)	-2213 (2)	2442 (3)	5130 (1)	42 (1)
C(1)	-395 (2)	2348 (3)	5572 (1)	34 (1)
C(2)	505 (2)	2053 (3)	6198 (1)	37 (1)
C(3)	1474 (2)	2068 (3)	5992 (2)	40 (1)
C(4)	1577 (2)	2352 (3)	5178 (2)	40 (1)
C(5)	711 (2)	2612 (3)	4540 (2)	42 (1)
C(6)	-243 (2)	2617 (3)	4744 (1)	38 (1)
C(7)	-3064 (2)	2702 (3)	5400 (2)	39 (1)
C(8)	-4027 (2)	2604 (4)	4746 (2)	57 (1)
C(9)	-3119 (2)	3070 (4)	6285 (1)	41 (1)
C(10)	-4099 (2)	3269 (4)	6622 (2)	50 (1)
C(11)	-3463 (2)	1436 (4)	6831 (2)	56 (1)
C(12)	-4181 (2)	4866 (5)	7256 (2)	73 (1)
C(13)	-2847 (3)	1019 (6)	7685 (2)	91 (1)

Table A3: Selected bond lengths (Å) and angles (°) for 40-DNP.

O(1)-N(1)	1.236(2)	O(2)-N(1)	1.221(2)
O(3)-N(2)	1.229(3)	O(4)-N(2)	1.214(3)
N(1)-C(2)	1.427(3)	N(2)-C(4)	1.453(3)
N(3)-C(1)	1.345(3)	N(3)-N(4)	1.393(3)
N(4)-C(7)	1.292(3)	C(1)-C(6)	1.402(3)
C(1)-C(2)	1.425(3)	C(2)-C(3)	1.384(3)
C(3)-C(4)	1.361(3)	C(4)-C(5)	1.402(3)
C(5)-C(6)	1.363(3)	C(7)-C(9)	1.467(3)
C(7)-C(8)	1.497(3)	C(9)-C(10)	1.503(3)
C(9)-C(11)	1.525(3)	C(10)-C(11)	1.487(4)
C(10)-C(12)	1.496(4)	C(11)-C(13)	1.492(4)
O(2)-N(1)-O(1)	120.5(2)	O(2)-N(1)-C(2)	119.2(2)
O(1)-N(1)-C(2)	120.3(2)	O(4)-N(2)-O(3)	123.2(2)
O(4)-N(2)-C(4)	118.3(2)	O(3)-N(2)-C(4)	118.6(2)
C(1)-N(3)-N(4)	120.5(2)	C(7)-N(4)-N(3)	114.1(2)
N(3)-C(1)-C(6)	121.7(2)	N(3)-C(1)-C(2)	121.8(2)
C(6)-C(1)-C(2)	116.5(2)	C(3)-C(2)-C(1)	121.1(2)
C(3)-C(2)-N(1)	116.4(2)	C(1)-C(2)-N(1)	122.5(2)
C(4)-C(3)-C(2)	119.9(2)	C(3)-C(4)-C(5)	120.9(2)
C(3)-C(4)-N(2)	118.9(2)	C(5)-C(4)-N(2)	120.2(2)
C(6)-C(5)-C(4)	119.2(2)	C(5)-C(6)-C(1)	122.4(2)
N(4)-C(7)-C(9)	123.9(2)	N(4)-C(7)-C(8)	115.8(2)
C(9)-C(7)-C(8)	120.4(2)	C(7)-C(9)-C(10)	124.9(2)
C(7)-C(9)-C(11)	121.4(2)	C(10)-C(9)-C(11)	58.8(2)
C(11)-C(10)-C(12)	122.6(2)	C(11)-C(10)-C(9)	61.4(2)
C(12)-C(10)-C(9)	119.3(2)	C(10)-C(11)-C(13)	123.5(3)
C(10)-C(11)-C(9)	59.9(2)	C(13)-C(11)-C(9)	119.9(2)

Symmetry transformations used to generate equivalent atoms:

Table A4: Bond lengths (Å) and angles (°) for 40-DNP.

O(1)-N(1)	1.236(2)	O(2)-N(1)	1.221(2)
O(3)-N(2)	1.229(3)	O(4)-N(2)	1.214(3)
N(1)-C(2)	1.427(3)	N(2)-C(4)	1.453(3)
N(3)-C(1)	1.345(3)	N(3)-N(4)	1.393(3)
N(4)-C(7)	1.292(3)	C(1)-C(6)	1.402(3)
C(1)-C(2)	1.425(3)	C(2)-C(3)	1.384(3)
C(3)-C(4)	1.361(3)	C(4)-C(5)	1.402(3)
C(5)-C(6)	1.363(3)	C(7)-C(9)	1.467(3)
C(7)-C(8)	1.497(3)	C(9)-C(10)	1.503(3)
C(9)-C(11)	1.525(3)	C(10)-C(11)	1.487(4)
C(10)-C(12)	1.496(4)	C(11)-C(13)	1.492(4)
C(3)-H(3A)	0.93	N(3)-H(3B)	0.86
C(5)-H(5A)	0.93	C(6)-H(6A)	0.93
C(8)-H(8A)	0.96	C(8)-H(8B)	0.96
C(8)-H(8C)	0.96	C(9)-H(9A)	0.98
C(10)-H(10A)	0.98	C(11)-H(11A)	0.98
C(12)-H(12A)	0.96	C(12)-H(12B)	0.96
C(12)-H(12C)	0.96	C(13)-H(13A)	0.96
C(13)-H(13B)	0.96	C(13)-H(13C)	0.96
O(2)-N(1)-O(1)	120.5(2)	O(2)-N(1)-C(2)	119.2(2)
O(1)-N(1)-C(2)	120.3(2)	O(4)-N(2)-O(3)	123.2(2)
O(4)-N(2)-C(4)	118.3(2)	O(3)-N(2)-C(4)	118.6(2)
C(1)-N(3)-N(4)	120.5(2)	C(7)-N(4)-N(3)	114.1(2)
N(3)-C(1)-C(6)	121.7(2)	N(3)-C(1)-C(2)	121.8(2)
C(6)-C(1)-C(2)	116.5(2)	C(3)-C(2)-C(1)	121.1(2)
C(3)-C(2)-N(1)	116.4(2)	C(1)-C(2)-N(1)	122.5(2)
C(4)-C(3)-C(2)	119.9(2)	C(3)-C(4)-C(5)	120.9(2)
C(3)-C(4)-N(2)	118.9(2)	C(5)-C(4)-N(2)	120.2(2)
C(6)-C(5)-C(4)	119.2(2)	C(5)-C(6)-C(1)	122.4(2)
N(4)-C(7)-C(9)	123.9(2)	N(4)-C(7)-C(8)	115.8(2)
C(9)-C(7)-C(8)	120.4(2)	C(7)-C(9)-C(10)	124.9(2)
C(7)-C(9)-C(11)	121.4(2)	C(10)-C(9)-C(11)	58.8(2)
C(11)-C(10)-C(12)	122.6(2)	C(11)-C(10)-C(9)	61.4(2)
C(12)-C(10)-C(9)	119.3(2)	C(10)-C(11)-C(13)	123.5(3)
C(10)-C(11)-C(9)	59.9(2)	C(13)-C(11)-C(9)	119.9(2)
C(4)-C(3)-H(3A)	120.05(14)	C(2)-C(3)-H(3A)	120.05(14)
C(1)-N(3)-H(3B)	119.75(12)	N(4)-N(3)-H(3B)	119.75(11)
C(6)-C(5)-H(5A)	120.39(14)	C(4)-C(5)-H(5A)	120.39(14)
C(5)-C(6)-H(6A)	118.81(14)	C(1)-C(6)-H(6A)	118.81(14)
C(7)-C(8)-H(8A)	109.47(14)	C(7)-C(8)-H(8B)	109.47(14)
H(8A)-C(8)-H(8B)	109.5	C(7)-C(8)-H(8C)	109.47(14)
H(8A)-C(8)-H(8C)	109.5	H(8B)-C(8)-H(8C)	109.5

Table A4 (continued): Bond lengths (Å) and angles (°) for 40-DNP.

C(7)-C(9)-H(9A)	113.65(13)	C(10)-C(9)-H(9A)	113.65(13)
C(11)-C(9)-H(9A)	113.65(14)	C(11)-C(10)-H(10A)	114.44(15)
C(12)-C(10)-H(10A)	114.44(14)	C(9)-C(10)-H(10A)	114.44(13)
C(10)-C(11)-H(11A)	114.26(15)	C(13)-C(11)-H(11A)	114.3(2)
C(9)-C(11)-H(11A)	114.26(14)	C(10)-C(12)-H(12A)	109.5(2)
C(10)-C(12)-H(12B)	109.5(2)	H(12A)-C(12)-H(12B)	109.5
C(10)-C(12)-H(12C)	109.47(14)	H(12A)-C(12)-H(12C)	109.5
H(12B)-C(12)-H(12C)	109.5	C(11)-C(13)-H(13A)	109.5(2)
C(11)-C(13)-H(13B)	109.5(2)	H(13A)-C(13)-H(13B)	109.5
C(11)-C(13)-H(13C)	109.5(2)	H(13A)-C(13)-H(13C)	109.5
H(13B)-C(13)-H(13C)	109.5		

---

Symmetry transformations used to generate equivalent atoms:

Table A5: Anisotropic displacement parameters ( $\text{\AA}^2 \times 10^3$ ) for 40-DNP. The anisotropic displacement factor exponent takes the form:

$$-2\pi^2 [(ha^*)^2 U_{11} + \dots + 2hka^*b^*U_{12}]$$

	U <sub>11</sub>	U <sub>22</sub>	U <sub>33</sub>	U <sub>23</sub>	U <sub>13</sub>	U <sub>12</sub>
O(1)	49(1)	124(2)	48(1)	14(1)	12(1)	8(1)
O(2)	52(1)	136(2)	53(1)	21(1)	-3(1)	13(1)
O(3)	38(1)	96(2)	94(2)	-9(1)	8(1)	-7(1)
O(4)	65(1)	73(1)	78(2)	6(1)	38(1)	6(1)
N(1)	42(1)	66(2)	43(1)	5(1)	3(1)	5(1)
N(2)	50(2)	39(1)	69(2)	-4(1)	22(1)	-2(1)
N(3)	36(1)	50(1)	36(1)	1(1)	4(1)	3(1)
N(4)	37(1)	43(1)	42(1)	3(1)	0(1)	1(1)
C(1)	36(1)	26(1)	39(2)	-3(1)	5(1)	0(1)
C(2)	41(1)	33(1)	36(1)	-2(1)	5(1)	-1(1)
C(3)	35(1)	34(1)	50(2)	-4(1)	1(1)	0(1)
C(4)	37(1)	30(1)	54(2)	-6(1)	12(1)	-3(1)
C(5)	53(2)	32(1)	43(2)	-5(1)	14(1)	-2(1)
C(6)	41(1)	29(1)	42(2)	-1(1)	2(1)	1(1)
C(7)	37(1)	34(1)	45(2)	3(1)	5(1)	1(1)
C(8)	43(1)	72(2)	52(2)	-2(1)	0(1)	3(1)
C(9)	35(1)	42(1)	43(2)	1(1)	4(1)	0(1)
C(10)	38(1)	60(2)	53(2)	-4(1)	9(1)	5(1)
C(11)	61(2)	50(2)	60(2)	9(1)	20(1)	4(1)
C(12)	72(2)	77(2)	72(2)	-7(2)	20(2)	22(2)
C(13)	91(2)	120(3)	73(2)	47(2)	38(2)	48(2)

Table A6: Hydrogen coordinates ( $\times 10^4$ ) and isotropic displacement parameters ( $\text{\AA}^2 \times 10^3$ ) for 40-DNP.

	x	y	z	U(eq)
H(3B)	-1409 (1)	2370 (3)	6283 (1)	49
H(3A)	2055 (2)	1884 (3)	6408 (2)	48
H(5A)	787 (2)	2779 (3)	3984 (2)	50
H(6A)	-814 (2)	2806 (3)	4319 (1)	46
H(8A)	-3854 (2)	2311 (26)	4209 (3)	85
H(8B)	-4378 (7)	3869 (9)	4720 (8)	85
H(8C)	-4467 (6)	1569 (18)	4891 (6)	85
H(9A)	-2555 (2)	3899 (4)	6582 (1)	49
H(10A)	-4728 (2)	3064 (4)	6202 (2)	60
H(11A)	-3743 (2)	237 (4)	6521 (2)	67
H(12A)	-4701 (11)	4502 (15)	7569 (9)	110
H(12B)	-4361 (15)	6115 (8)	6972 (2)	110
H(12C)	-3532 (5)	5004 (22)	7633 (8)	110
H(13A)	-3286 (5)	460 (34)	8035 (5)	137
H(13B)	-2550 (15)	2245 (8)	7929 (6)	137
H(13C)	-2309 (12)	84 (29)	7638 (3)	137

Table A7: Observed and calculated structure factors for 40-DNP.

h	k	l	10Fo	10Fc	10s	h	k	l	10Fo	10Fc	10s	h	k	l	10Fo	10Fc	10s	h	k	l	10Fo	10Fc	10s	h	k	l	10Fo	10Fc	10s	h	k	l	10Fo	10Fc	10s
2	4	0	217	215	1	-7	1	1	164	163	2	5	4	1	31	28	7	1	1	2	542	521	2	-9	5	2	32	35	8	2	2	2	32	35	8
4	0	0	102	99	1	-6	1	1	21	26	7	4	4	1	19	6	9	2	2	2	221	230	2	-8	2	2	19	12	10	2	2	2	19	12	10
5	0	0	169	171	2	-5	1	1	22	24	6	6	7	1	13	3	10	2	2	2	196	218	2	-7	3	2	82	85	3	2	2	82	85	3	
6	0	0	88	92	1	-4	1	1	293	293	2	8	8	1	95	91	2	4	4	4	109	109	1	-6	4	4	215	215	2	4	4	215	215	2	
7	0	0	358	365	3	-3	1	1	455	459	2	9	9	1	53	50	2	2	2	2	263	274	2	-5	5	2	12	12	10	4	4	12	12	10	
8	0	0	76	81	2	-2	1	1	85	88	1	10	10	1	139	136	5	5	5	5	79	71	2	-4	6	5	48	45	3	4	4	48	45	3	
10	0	0	185	184	2	-1	1	1	284	292	1	-9	9	1	56	58	2	2	2	2	152	157	2	-3	7	2	63	64	3	2	2	63	64	3	
11	0	0	275	293	3	0	1	1	93	89	1	-10	10	1	128	126	2	2	2	2	55	61	2	-2	8	2	88	91	2	2	2	88	91	2	
12	0	0	449	453	3	0	1	1	84	83	1	-9	9	1	108	104	2	2	2	2	55	55	2	-2	9	2	41	37	2	2	2	41	37	2	
13	0	0	64	68	4	2	1	1	111	106	2	-8	8	1	112	111	2	2	2	2	377	381	3	0	1	0	39	36	3	3	3	39	36	3	
14	0	0	99	97	3	3	2	1	443	438	2	-5	5	1	65	61	3	3	3	3	550	548	4	0	1	0	66	66	3	3	3	66	66	3	
3	3	1	217	224	2	5	4	1	243	239	7	-6	6	1	18	13	10	7	7	7	30	31	9	5	5	5	44	44	5	5	5	44	44	5	
4	4	1	217	224	2	6	7	1	163	173	4	-4	4	1	46	44	5	5	5	5	67	68	4	4	4	4	42	40	5	5	5	42	40	5	
5	5	1	144	132	1	8	8	1	32	33	7	-2	2	1	96	96	2	2	2	2	172	172	2	6	6	6	53	47	4	4	4	53	47	4	
6	6	1	253	257	2	9	9	1	25	31	7	-1	1	1	229	231	2	2	2	2	53	45	4	7	7	7	16	16	9	9	9	16	16	9	
7	7	1	116	119	2	10	11	1	166	175	2	0	0	1	112	113	9	9	9	9	23	16	10	8	8	8	15	15	10	10	10	15	15	10	
9	9	1	84	84	2	11	11	1	14	14	8	1	1	1	15	15	9	9	9	9	12	12	9	9	9	9	24	22	10	10	10	24	22	10	
10	11	1	156	158	2	12	12	1	32	37	8	2	2	2	23	23	3	3	3	3	242	250	2	7	7	7	28	28	9	9	9	28	28	9	
11	11	1	322	328	3	13	13	1	28	20	9	3	3	3	148	152	5	5	5	5	151	144	3	6	6	6	16	16	10	10	10	16	16	10	
12	12	1	369	353	3	-12	12	2	109	109	2	4	4	4	40	43	5	5	5	5	148	146	1	-5	5	5	17	14	10	10	10	17	14	10	
13	13	1	51	45	4	-12	12	2	76	76	3	5	5	5	26	14	9	9	9	9	106	101	1	-4	4	4	25	14	10	10	10	25	14	10	
2	2	3	297	281	2	-10	10	2	189	191	2	7	7	7	43	46	5	5	5	5	403	430	2	-2	2	2	113	115	3	3	3	113	115	3	
4	4	4	433	418	2	-9	9	2	27	25	2	8	8	8	24	24	1	1	1	1	220	224	2	-1	1	1	87	87	3	3	3	87	87	3	
5	5	4	146	144	1	-8	8	1	79	70	2	9	9	9	25	25	2	2	2	2	305	287	2	0	0	0	380	388	3	3	3	380	388	3	
6	6	7	147	141	1	-7	7	2	87	85	2	-7	7	7	66	65	4	4	4	4	433	405	2	6	6	6	129	134	3	3	3	129	134	3	
8	8	9	65	56	2	-6	6	2	172	162	1	-5	5	5	50	49	4	4	4	4	42	37	3	6	6	6	111	115	3	3	3	111	115	3	
9	9	8	121	123	2	-5	5	2	165	159	1	-6	6	6	55	62	4	4	4	4	197	187	2	6	6	6	63	67	3	3	3	63	67	3	
10	10	8	153	151	2	-4	4	2	123	123	1	-4	4	4	34	45	7	7	7	7	102	104	1	6	6	6	83	83	3	3	3	83	83	3	
11	11	8	220	220	2	-3	3	2	213	211	1	-3	3	3	22	14	10	10	10	10	275	275	3	6	6	6	102	103	3	3	3	102	103	3	
12	12	8	270	272	2	-1	1	0	326	311	1	0	0	0	37	40	6	6	6	6	31	35	7	6	6	6	39	24	10	10	10	39	24	10	
13	13	1	32	25	8	0	2	2	826	774	1	1	1	1	23	23	6	6	6	6	62	65	3	-3	3	3	20	20	11	11	11	20	20	11	
1	1	1	18	25	11	2	2	2	93	94	1	1	1	1	219	227	8	8	8	8	25	14	10	2	2	2	41	41	6	6	6	41	41	6	
2	2	3	226	210	2	3	3	3	179	176	2	2	2	2	30	15	8	8	8	8	31	31	11	-2	2	2	20	13	10	10	10	20	13	10	
3	3	3	94	95	1	4	4	4	8	2	2	3	3	3	58	57	4	4	4	4	35	36	7	0	0	0	53	53	3	3	3	53	53	3	
4	4	3	223	225	2	5	5	5	79	73	2	4	4	4	41	34	5	5	5	5	19	23	10	7	7	7	17	5	10	10	10	17	5	10	
5	5	4	170	169	2	6	7	2	63	56	6	5	5	5	16	12	9	9	9	9	97	97	3	5	5	5	22	13	10	10	10	22	13	10	
6	6	7	123	122	2	8	8	2	131	138	2	7	7	7	39	38	6	6	6	6	45	37	5	-14	14	14	38	33	7	7	7	38	33	7	
7	7	8	12	10	9	9	9	9	76	75	3	-3	3	3	30	32	3	3	3	3	120	113	2	-13	13	13	23	18	10	10	10	23	18	10	
8	8	9	12	12	10	10	10	10	151	152	2	-2	2	2	19	22	10	10	10	10	40	31	5	-11	11	11	13	8	8	8	8	8	13	8	8
9	9	10	284	281	2	11	11	2	155	157	2	0	0	0	57	60	3	3	3	3	191	178	3	-10	10	10	36	29	9	9	9	36	29	9	
10	10	11	292	288	2	12	12	2	155	157	2	0	0	0	57	60	3	3	3	3	442	433	4	-9	9	9	12	12	10	10	10	12	12	10	
11	11	12	67	59	4	-12	12	2	60	60	2	-1	1	1	16	19	10	10	10	10	42	37	3	-8	8	8	16	15	10	10	10	16	15	10	
12	12	0	808	773	3	-11	11	3	111	112	2	2	2	2	21	19	10	10	10	10	197	200	2	7	7	7	328	325	2	2	2	328	325	2	
13	13	1	187	173	3	-10	10	3	142	145	2	-14	14	14	16	18	10	10	10	10	11	5	8	-5	5	5	54	55	5	5	5	54	55	5	
2	2	4	170	167	2	-9	9	2	83	78	2	-13	13	13	131	133	2	2	2	2	99	96	1	-4	4	4	292	294	2	2	2	292	294	2	
4	4	4	52	51	3	-8	8	3	94	89	2	-12	12	12	121	124	2	2	2	2	275	264	4	-3	3	3	449	467	2	2	2	449	467	2	
5	5	4	85	82	2	-7	7	2	16	11	1	-11	11	11	69	65	3	3	3	3	160	156	1	-2	2	2	211	223	2	2	2	211	223	2	
6	6	4	20	20	1	-6	6	3	12	11	1	-10	10	10	90	81	2	2	2	2	129	124	1	0	0	0	171	186	2	2	2	171	186	2	
7	7	4	42	45	5	-5	5	5	22	18	4	-9	9	9	58	66	3	3	3	3	131	127	1	0	0	0	30	25	2	2	2	30	25	2	
8	8	4	94	97	2	-4	4	3	36	34	7	-8	8	8	19	17	8	8	8	8	143	138	1	1	1	1	346	333	2	2	2	346	333	2	
9	9	4	17	15	10	-3	3	3	30	36	5	-6	6	6	184	185	2	2	2	2	200	188	2	2	2	72	72	1	1	1	72	72	1		
10																																			

Table A7 (continued): Observed and calculated structure factors for 40-DNP.

h	k	l	10Fo	10Fc	10s	h	k	l	10Fo	10Fc	10s	h	k	l	10Fo	10Fc	10s	h	k	l	10Fo	10Fc	10s	h	k	l	10Fo	10Fc	10s
7			77	72	2	-1	7	3	23	32	10	-7	3	4	18	10	9	-2	1	5	79	83	2	-9	5	5	21	19	10
9			113	112	2	0	7	3	19	18	6	-6	3	4	540	532	3	-1	1	5	157	165	2	-8	5	5	52	52	4
8			77	75	2	1	7	3	61	66	4	-5	3	4	54	54	3	0	1	5	40	37	2	-8	5	5	41	46	4
10			37	41	6	-14	0	4	50	41	5	-3	4	4	221	216	2	1	1	5	132	132	2	-7	5	5	50	54	5
11			36	24	7	-13	0	4	107	104	4	-4	4	4	61	54	4	1	1	5	40	42	5	-6	5	5	50	98	2
12			130	134	2	-12	0	4	22	22	10	-2	4	4	23	15	7	3	3	5	26	17	5	-4	4	4	50	49	4
11			32	27	8	-11	0	4	146	148	2	-3	4	4	65	58	4	4	4	5	162	165	5	-3	4	4	43	33	4
-10			25	30	10	-10	0	4	130	129	2	0	3	4	186	191	2	5	5	5	160	159	2	-2	2	2	109	110	2
-9			102	102	2	-9	0	4	21	22	2	2	3	4	42	44	3	6	6	5	146	153	2	-1	1	1	52	48	4
-8			95	92	10	-8	0	4	10	10	9	2	3	4	159	155	1	1	1	5	34	40	6	0	0	0	64	67	2
-7			249	246	2	-6	0	4	165	182	9	5	3	4	133	130	8	8	8	5	55	55	4	1	1	1	37	29	5
-6			27	13	2	-5	0	4	13	3	8	4	4	4	165	154	2	9	9	1	24	27	9	2	2	2	34	26	6
-5			64	64	8	-4	0	4	341	364	2	6	6	4	68	67	3	7	7	5	62	61	4	4	4	4	75	77	3
-4			60	66	8	-3	0	4	147	152	2	7	7	4	29	22	4	4	4	10	20	19	10	7	7	10	82	90	9
-3			392	395	2	-2	0	4	636	655	2	8	8	4	51	55	4	4	4	5	35	36	6	6	6	6	14	14	4
-2			60	64	2	-1	0	4	731	767	2	9	9	4	201	204	4	4	4	10	49	44	2	-7	7	7	33	39	7
-1			392	395	2	0	0	4	203	205	2	10	10	4	51	60	4	4	4	-12	39	35	6	6	6	6	33	39	7
0			43	49	3	1	0	4	327	344	2	-11	11	4	201	204	2	2	2	-12	49	44	2	-8	8	8	35	35	10
1			70	67	3	2	0	4	667	693	2	11	11	4	210	216	2	9	9	-10	60	58	4	-6	6	6	21	22	7
2			397	388	3	3	0	4	343	337	2	-11	11	4	30	27	9	9	9	-9	40	24	5	-5	5	5	30	30	9
3			17	11	7	4	0	4	596	609	3	-10	10	4	59	51	4	4	4	-8	69	68	3	-4	4	4	27	26	9
4			187	175	5	5	0	4	611	616	3	-9	9	4	26	17	4	4	4	-7	225	224	2	-5	5	5	61	62	9
5			103	92	6	6	0	4	256	268	2	-8	8	4	26	5	9	9	9	-6	17	23	9	-3	3	3	23	23	4
6			35	31	5	7	0	4	33	29	5	-7	7	4	22	11	10	10	10	-5	198	200	2	-2	2	2	29	30	8
7			89	85	9	8	0	4	131	138	2	-6	6	4	12	17	9	9	9	-4	16	18	8	-1	1	1	29	27	8
8			13	18	9	9	0	4	47	45	4	-5	5	4	76	74	3	3	3	-3	102	96	6	0	0	0	58	58	3
9			15	10	10	10	0	4	108	106	2	-4	4	4	46	45	4	4	4	-2	44	52	3	1	1	1	16	16	10
10			78	76	9	11	0	4	30	38	9	-3	3	4	73	86	2	2	2	-1	247	253	2	0	0	0	14	14	10
11			73	70	10	12	0	4	76	77	3	-2	2	4	181	186	2	2	2	0	470	482	13	0	0	0	20	20	10
12			54	56	10	13	0	4	186	185	2	-1	1	4	261	260	2	2	2	2	80	102	13	-1	1	1	35	35	9
11			81	80	10	-14	0	4	52	52	5	0	4	4	203	200	1	1	1	2	90	69	1	-1	1	1	19	17	10
-10			12	12	10	-13	0	4	46	33	4	1	4	4	63	65	3	3	3	3	14	6	7	0	0	0	21	22	10
-9			29	25	10	-12	0	4	53	51	4	2	4	4	25	11	2	2	2	4	112	77	1	-1	1	1	207	210	10
-8			67	65	10	-11	0	4	17	4	10	3	4	4	26	23	8	8	8	5	77	74	2	-1	2	2	166	175	3
-7			26	16	9	-10	0	4	212	219	2	4	4	4	219	211	2	2	2	6	56	59	9	-10	10	10	70	70	9
-6			101	95	8	-9	0	4	90	95	2	5	5	4	88	78	2	2	2	7	91	92	3	-9	9	9	118	121	9
-5			99	96	8	-7	0	4	310	297	2	8	8	4	58	45	3	3	3	9	48	45	5	-8	8	8	92	91	2
-4			93	99	2	-6	0	4	1013	967	2	7	7	4	37	42	6	6	6	10	17	19	10	-7	7	7	200	202	2
-3			26	26	4	-5	0	4	228	229	2	9	9	4	27	25	5	5	5	11	66	66	4	-6	6	6	214	210	2
-2			44	39	4	-4	0	4	228	238	2	10	10	4	47	38	9	9	9	12	18	15	11	-5	5	5	201	220	2
-1			125	119	2	-3	0	4	362	365	2	-10	10	4	39	42	6	6	6	-12	16	17	10	-4	4	4	120	134	1
0			43	39	2	-2	0	4	436	475	2	-9	9	4	17	18	11	11	11	-11	47	43	5	-3	3	3	107	100	1
1			100	95	2	-1	0	4	11	2	7	-8	8	4	31	36	8	8	8	-10	58	60	4	-2	2	2	568	575	2
2			16	26	9	0	0	4	96	104	3	-7	7	4	22	19	10	10	10	9	59	59	4	1	1	1	537	569	2
3			206	191	2	1	0	4	86	83	3	-6	6	4	202	206	2	2	2	8	248	250	2	0	0	0	341	357	2
4			114	113	2	2	0	4	405	387	2	-5	5	4	57	60	4	4	4	-6	111	104	2	1	1	1	469	458	2
5			86	76	2	3	0	4	313	317	2	-4	4	4	86	86	3	3	3	-5	104	99	2	2	2	2	229	223	2
6			29	23	7	4	0	4	290	296	2	-3	3	4	75	76	3	3	3	-4	234	225	2	3	3	3	171	171	2
7			36	29	6	5	0	4	636	617	2	-2	2	4	85	84	3	3	3	-3	90	92	2	4	4	4	268	252	2
8			13	9	4	6	0	4	18	11	8	0	4	4	68	73	3	3	3	-2	59	60	3	5	5	5	578	579	1
9			78	77	3	7	0	4	31	26	6	-1	1	4	156	160	3	3	3	-1	158	167	2	6	6	6	38	49	4
10			17	20	3	8	0	4	40	40	5	2	2	4	19	15	4	4	4	0	79	77	2	7	7	7	194	199	2
11			23	21	10	9	0	4	141	138	2	1	1	4	55	58	9	9	9	0	105	108	1	8	8	8	55	58	4
12			17	17	10	10	0	4	111	120	2	0	4	4	15	11	3	3	3	1	26	35	9	9	9	9	56	53	4
11			105	114	7	-15	0	4	189	190	2	1	1	4	77	77	3	3	3	10	31	34	10	0	0	0	94	109	3
10			36	35	2	-13	0	4	30	47	9	0	4	4	54	53	4	4	4	276	258	2	11	11	11	37	46	7	
9			72	68	2	-12	0	4	136	131	2	0	4	4	60	61	3	3	3	-12	62	61	2	12	12	12	80	84	3
8			43	34	10	-11	0	4	40	39	10	1	1	4	33	32	8	8	8	-13	210	210	2	13	13	13	28	29	9
7			22	30	10	-10	0	4	20	22	10	2	2	4	32	32	9	9	9	-11	117	115	2	11	11	11	73	70	9
6			38	37	6	-9	0	4	36	34	6	3	3	4	28	28	9	9	9	-10	58	58	3	10	10	10	81	80	6
5			32	33	4	-8	0	4	12	8	4	4	4	4	23	26	10	10	10	-9	54	54	4	9	9	9	31	38	6
4			176	171	2	-7	0	4	14	9	8																		



Table A7 (continued): Observed and calculated structure factors for 40-DNP.

h	k	l	10Fo	10Fc	10s	h	k	l	10Fo	10Fc	10s	h	k	l	10Fo	10Fc	10s	h	k	l	10Fo	10Fc	10s	h	k	l	10Fo	10Fc	10s	h	k	l	10Fo	10Fc	10s
9	0	0	16	4	10	-1	0	1	25	16	10	-3	4	7	12	10	9	9	1	88	200	210	2	-1	0	6	34	30	7	6	7	34	30	7	
9	0	1	31	28	10	0	1	17	11	17	10	4	4	4	48	50	44	10	10	11	88	81	78	3	0	6	39	12	6	19	12	7			
9	0	2	42	40	10	0	2	55	11	55	10	-1	1	4	114	117	22	10	11	11	88	37	23	7	0	6	36	12	7	19	12	7			
9	0	3	179	177	10	0	3	22	3	22	10	0	0	4	22	21	22	10	-13	2	88	117	122	2	2	2	57	54	4	4	4	4			
9	0	4	94	88	10	0	4	43	4	48	10	0	0	4	24	38	88	10	-12	2	88	88	97	3	3	3	76	77	3	3	3	3			
9	0	5	66	63	10	0	5	131	5	135	10	0	0	4	76	70	22	10	-11	2	88	19	24	10	10	10	21	10	10	10	10	10			
9	0	6	41	46	10	0	6	123	6	122	10	0	0	4	125	124	10	10	-10	2	88	17	6	10	-13	1	17	10	10	10	10	10			
9	0	7	428	446	10	0	7	30	7	24	10	0	0	4	58	61	33	10	-9	2	88	168	157	2	2	2	58	51	4	4	4	4			
9	0	8	349	346	10	0	8	23	8	21	10	0	0	4	18	15	9	10	-8	2	88	111	113	2	-10	1	17	12	10	10	10	10			
9	0	9	35	29	10	0	9	62	9	69	10	0	0	4	15	17	9	10	-11	2	88	21	25	9	-9	9	57	58	4	4	4	4			
9	1	0	221	204	10	1	0	13	10	6	10	0	0	4	28	21	8	10	-10	2	88	42	42	4	-8	8	67	64	4	4	4	4			
9	1	1	215	207	10	1	1	21	11	26	10	0	0	4	56	49	4	10	-9	2	88	39	42	4	-7	7	70	88	3	3	3	3			
9	1	2	82	89	10	1	2	91	12	89	10	0	0	4	19	13	10	10	-8	2	88	125	127	2	-6	6	87	85	2	2	2	2			
9	1	3	311	287	10	1	3	96	13	102	10	0	0	4	42	43	8	10	-7	2	88	179	183	2	-5	5	72	68	2	2	2	2			
9	1	4	394	372	10	1	4	31	14	33	10	0	0	4	62	63	6	10	-6	2	88	41	41	2	-4	4	51	51	2	2	2	2			
9	1	5	106	101	10	1	5	157	15	160	10	0	0	4	83	86	4	10	-5	2	88	17	24	8	-3	3	52	52	2	2	2	2			
9	1	6	19	19	10	1	6	258	16	260	10	0	0	4	20	20	2	10	-4	2	88	61	63	1	-2	2	106	112	2	2	2	2			
9	1	7	94	88	10	1	7	128	17	129	10	0	0	4	19	19	2	10	-3	2	88	57	53	1	-1	1	237	242	2	2	2	2			
9	1	8	66	63	10	1	8	228	18	231	10	0	0	4	71	76	2	10	-2	2	88	95	99	2	0	0	14	3	2	2	2	2			
9	1	9	179	177	10	1	9	37	19	41	10	0	0	4	36	32	7	10	-1	2	88	139	132	2	0	0	67	65	2	2	2	2			
9	2	0	42	40	10	2	0	52	20	52	10	0	0	4	18	18	10	10	0	2	88	142	141	2	2	2	86	87	2	2	2	2			
9	2	1	179	177	10	2	1	15	21	16	10	0	0	4	52	55	5	10	-1	2	88	223	211	2	2	2	15	24	2	2	2	2			
9	2	2	66	63	10	2	2	66	22	72	10	0	0	4	38	34	5	10	0	2	88	12	1	9	4	4	64	68	2	2	2	2			
9	2	3	41	46	10	2	3	130	23	130	10	0	0	4	36	34	6	10	-1	2	88	112	112	2	-10	1	53	59	2	2	2	2			
9	2	4	428	446	10	2	4	107	24	116	10	0	0	4	26	31	9	10	-1	2	88	17	6	10	-7	7	19	19	2	2	2	2			
9	2	5	349	346	10	2	5	16	25	16	10	0	0	4	31	33	4	10	-1	2	88	20	27	10	-12	1	44	43	2	2	2	2			
9	2	6	35	29	10	2	6	34	26	20	10	0	0	4	19	19	10	10	-1	2	88	19	16	10	-10	1	33	33	2	2	2	2			
9	2	7	82	89	10	2	7	48	27	54	10	0	0	4	48	48	5	10	-1	2	88	34	34	10	-12	1	47	52	2	2	2	2			
9	2	8	311	287	10	2	8	66	28	67	10	0	0	4	19	19	10	10	-1	2	88	39	39	10	-11	1	69	69	2	2	2	2			
9	2	9	394	372	10	2	9	26	29	34	10	0	0	4	35	33	5	10	-1	2	88	263	256	2	-10	1	78	75	2	2	2	2			
9	3	0	106	101	10	3	0	81	30	82	10	0	0	4	25	25	10	10	-1	2	88	51	63	2	-9	9	32	40	2	2	2	2			
9	3	1	19	19	10	3	1	83	31	83	10	0	0	4	19	19	10	10	-1	2	88	68	62	2	-8	8	78	74	2	2	2	2			
9	3	2	94	88	10	3	2	83	32	83	10	0	0	4	37	34	6	10	-1	2	88	119	120	2	-7	7	14	23	2	2	2	2			
9	3	3	428	446	10	3	3	83	33	83	10	0	0	4	33	36	7	10	-1	2	88	62	65	2	-6	6	16	8	2	2	2	2			
9	3	4	349	346	10	3	4	95	34	97	10	0	0	4	37	37	6	10	-1	2	88	314	307	2	-5	5	71	79	2	2	2	2			
9	3	5	35	29	10	3	5	170	35	170	10	0	0	4	46	45	4	10	-1	2	88	85	79	2	-4	4	49	54	2	2	2	2			
9	3	6	82	89	10	3	6	46	36	41	10	0	0	4	40	47	4	10	-1	2	88	51	43	2	-3	3	21	33	2	2	2	2			
9	3	7	311	287	10	3	7	42	37	41	10	0	0	4	24	24	7	10	-1	2	88	137	131	2	-2	2	28	28	2	2	2	2			
9	3	8	394	372	10	3	8	42	38	46	10	0	0	4	42	46	3	10	-1	2	88	54	55	2	-1	1	15	19	2	2	2	2			
9	3	9	106	101	10	3	9	228	39	235	10	0	0	4	147	143	2	10	0	2	88	83	75	2	0	0	155	154	2	2	2	2			
9	4	0	19	19	10	4	0	132	40	129	10	0	0	4	143	139	2	10	0	2	88	18	18	10	0	0	150	142	2	2	2	2			
9	4	1	94	88	10	4	1	135	41	129	10	0	0	4	199	190	2	10	0	2	88	19	9	2	0	0	55	62	2	2	2	2			
9	4	2	428	446	10	4	2	15	42	15	10	0	0	4	113	123	2	10	0	2	88	74	79	2	0	0	25	25	2	2	2	2			
9	4	3	349	346	10	4	3	228	43	213	10	0	0	4	98	107	2	10	0	2	88	103	104	2	0	0	76	80	2	2	2	2			
9	4	4	35	29	10	4	4	50	44	46	10	0	0	4	44	46	3	10	0	2	88	13	2	2	0	0	63	73	2	2	2	2			
9	4	5	82	89	10	4	5	34	45	35	10	0	0	4	31	29	4	10	0	2	88	67	58	2	0	0	19	28	2	2	2	2			
9	4	6	311	287	10	4	6	66	46	66	10	0	0	4	127	121	1	10	0	2	88	145	144	2	-1	1	103	98	2	2	2	2			
9	4	7	394	372	10	4	7	113	47	108	10	0	0	4	58	59	2	10	0	2	88	91	97	2	-10	1	27	18	2	2	2	2			
9	4	8	106	101	10	4	8	23	48	23	10	0	0	4	20	25	7	10	0	2	88	36	33	2	-10	1	139	137	2	2	2	2			
9	4	9	19	19	10	4	9	27	49	27	10	0	0	4	151	162	1	10	0	2	88	111	108	2	-7	7	113	104	2	2	2	2			
9	5	0	94	88	10	5	0	21	50	21	10	0	0	4	193	182	1	10	0	2	88	22	16	2	-6	6	219	228	2	2	2	2			
9	5	1	428	446	10	5	1	77	51	70	10	0	0	4	133	134	1	10	0	2	88	33	33	10	-6	6	21	21	2	2	2	2			
9	5	2	349	346	10	5	2	116	52	116	10	0	0	4	397	405	1	10	0	2	88	121	128	2	-5	5	53	60	2	2	2	2			
9	5	3	35	29	10	5	3	13	53	13	10	0	0	4	230	229	1	10	0	2	88	17	25	2	-4	4	47	40	2	2	2	2			
9	5																																		

Table A7 (continued): Observed and calculated structure factors for 40-DNP.

h	k	l	10Fo	10Fc	10s	h	k	l	10Fo	10Fc	10s	h	k	l	10Fo	10Fc	10s	h	k	l	10Fo	10Fc	10s	h	k	l	10Fo	10Fc	10s
6	4	9	17	19	10	9	2	10	92	96	3	5	2	11	116	124	2	-11	2	12	87	78	3	4	2	13	122	121	2
7	4	9	22	22	10	-11	3	10	39	37	6	6	2	11	16	17	10	-10	2	12	45	52	5	4	2	13	122	121	2
8	4	9	24	24	11	-10	3	10	21	19	10	6	2	11	45	45	5	-10	2	12	134	130	5	4	2	13	122	121	2
5	5	9	25	33	10	-9	3	10	134	139	2	8	8	11	27	27	9	-9	3	10	458	443	3	4	2	13	122	121	2
5	5	9	70	70	10	-8	3	10	214	203	2	-10	8	11	26	22	10	-7	3	10	207	200	2	4	2	13	122	121	2
5	5	9	21	7	10	-8	3	10	51	47	5	-9	8	11	96	79	3	-7	3	10	86	82	3	4	2	13	122	121	2
4	4	9	43	53	6	-6	3	10	62	67	3	-8	8	11	144	143	2	-5	3	10	103	103	2	4	2	13	122	121	2
4	4	9	39	40	6	-5	3	10	90	92	2	-7	3	10	105	102	2	-4	3	10	53	63	4	4	2	13	122	121	2
3	3	9	39	34	6	-4	3	10	77	79	3	-6	3	10	53	56	4	-3	3	10	58	64	3	3	3	13	122	121	2
2	2	9	101	110	2	-3	3	10	14	2	10	-5	3	10	105	102	2	-2	3	10	20	24	10	4	2	13	122	121	2
0	0	9	84	90	2	-2	3	10	287	290	3	-4	3	10	56	56	4	-1	3	10	16	19	10	3	3	13	122	121	2
1	1	9	17	8	2	-1	3	10	113	113	3	-3	3	10	22	22	5	0	3	10	46	48	3	3	3	13	122	121	2
2	2	9	30	26	8	0	3	10	57	57	5	-2	3	10	51	56	4	1	3	10	129	122	2	3	3	13	122	121	2
3	3	9	30	27	8	0	3	10	15	2	9	-2	3	10	31	32	4	2	3	10	260	262	3	3	3	13	122	121	2
4	4	9	27	31	8	0	3	10	145	136	2	0	3	10	66	67	4	4	3	10	341	340	3	3	3	13	122	121	2
4	4	9	13	11	9	2	3	10	38	31	2	1	3	10	50	48	4	4	3	10	85	79	3	3	3	13	122	121	2
4	4	9	23	8	11	4	3	10	100	101	2	4	3	10	239	229	2	5	3	10	52	55	4	4	3	13	122	121	2
3	3	9	32	33	8	4	3	10	85	87	2	4	3	10	31	26	6	6	3	10	50	46	4	4	3	13	122	121	2
3	3	9	44	48	8	4	3	10	38	46	6	4	3	10	129	129	2	7	3	10	20	20	3	4	3	13	122	121	2
0	0	9	16	10	10	8	3	10	18	16	10	9	3	10	145	138	2	9	3	10	14	11	10	4	3	13	122	121	2
0	0	9	20	5	10	8	3	10	51	50	5	9	3	10	13	13	10	10	3	10	23	31	10	4	3	13	122	121	2
1	1	9	46	46	5	-10	3	10	13	4	4	-9	3	10	67	58	3	-9	3	10	123	113	2	4	3	13	122	121	2
1	1	9	10	5	5	-9	3	10	127	125	2	7	3	10	114	113	3	-8	3	10	20	25	11	4	3	13	122	121	2
1	1	9	75	73	3	-12	4	10	275	269	2	4	4	10	74	69	4	-6	4	10	31	36	8	4	3	13	122	121	2
1	1	9	13	3	3	-11	4	10	108	105	2	4	4	10	59	55	5	-5	4	10	31	35	8	4	3	13	122	121	2
1	1	9	243	239	2	-10	4	10	40	44	6	-6	4	10	46	40	5	-4	4	10	42	40	5	5	3	13	122	121	2
0	0	9	109	110	2	-9	4	10	48	60	6	-5	4	10	27	27	9	-3	4	10	40	40	2	10	3	13	122	121	2
0	0	9	346	349	2	-8	4	10	17	9	10	-4	4	10	82	80	3	-2	4	10	42	46	6	6	3	13	122	121	2
0	0	9	97	99	2	-7	4	10	76	82	3	-3	4	10	25	25	9	-1	4	10	45	41	5	5	3	13	122	121	2
0	0	9	47	48	4	-6	4	10	27	30	9	-2	4	10	39	39	10	0	4	10	42	43	5	5	3	13	122	121	2
0	0	9	145	149	4	-5	4	10	19	19	10	-1	4	10	91	91	10	1	4	10	45	41	5	5	3	13	122	121	2
0	0	9	131	133	2	-4	4	10	12	12	5	0	4	10	26	26	3	2	4	10	221	213	2	10	3	13	122	121	2
0	0	9	87	91	2	-3	4	10	12	11	5	0	4	10	91	91	3	3	4	10	253	245	2	10	3	13	122	121	2
0	0	9	50	61	2	-2	4	10	247	233	2	4	4	10	110	108	2	4	4	10	28	24	4	10	3	13	122	121	2
0	0	9	171	172	1	-1	4	10	260	249	1	4	4	10	52	46	10	4	4	10	17	17	4	10	3	13	122	121	2
0	0	9	95	106	1	4	4	10	18	14	10	4	4	10	75	68	4	4	4	10	51	52	4	4	3	13	122	121	2
0	0	9	77	76	2	5	4	10	33	33	7	6	4	10	35	35	7	6	4	10	85	81	3	3	3	13	122	121	2
0	0	9	138	146	2	6	4	10	37	42	6	7	4	10	32	24	8	7	4	10	29	28	3	3	3	13	122	121	2
0	0	9	277	281	2	6	4	10	15	23	10	8	4	10	40	26	8	8	4	10	29	28	3	3	3	13	122	121	2
0	0	9	143	142	2	5	4	10	52	49	10	6	4	10	24	24	6	6	4	10	77	77	6	6	3	13	122	121	2
0	0	9	105	103	4	-5	4	10	19	12	10	-4	4	10	14	8	11	-4	4	10	13	13	3	3	3	13	122	121	2
0	0	9	55	55	4	-4	4	10	19	16	10	-3	4	10	28	25	9	-3	4	10	77	77	2	3	3	13	122	121	2
0	0	9	12	7	9	-3	4	10	11	4	11	-2	4	10	25	25	10	-2	4	10	68	73	3	3	3	13	122	121	2
0	0	9	108	113	2	-2	4	10	111	118	2	0	4	10	58	63	4	4	4	10	71	72	3	3	3	13	122	121	2
0	0	9	145	151	2	-1	4	10	115	125	2	0	4	10	63	64	4	4	4	10	21	27	3	3	3	13	122	121	2
1	1	9	27	20	10	0	4	10	13	2	10	-12	4	10	133	132	6	-12	4	10	92	94	3	3	3	13	122	121	2
1	1	9	23	16	10	0	4	10	38	50	6	-11	4	10	44	44	5	-11	4	10	182	169	2	3	3	13	122	121	2
1	1	9	165	169	2	4	4	10	77	73	3	4	4	10	27	27	2	4	4	10	27	15	2	5	3	13	122	121	2
1	1	9	485	472	2	-12	4	10	19	12	10	-10	4	10	34	35	7	-10	4	10	16	16	5	5	3	13	122	121	2
1	1	9	148	150	2	-11	4	10	19	15	10	-9	4	10	155	155	2	-9	4	10	46	49	2	5	3	13	122	121	2
1	1	9	17	12	10	-11	4	10	27	1	9	-8	4	10	683	661	4	-8	4	10	27	23	7	9	3	13	122	121	2
1	1	9	267	264	2	-10	4	10	11	0	9	-7	4	10	250	247	2	-7	4	10	19	19	5	5	3	13	122	121	2
1	1	9	203	200	2	-9	4	10	14	25	10	-6	4	10	52	38	4	-6	4	10	32	34	7	5	3	13	122	121	2
1	1	9	23	18	8	-8	4	10	42	36	6	-5	4	10	143	151	2	-5	4	10	19	19	5	5	3	13	122	121	2
1	1	9	176	170	8	-7	4	10	141	150	2	-4	4	10	86	80	2	-4	4	10	44	20	9	5	3	13	122	121	2
1	1	9	21	28	8	-6	4	10	19	24	2	-3	4	10	41	39	4	-3	4	10	27	27	9	5	3	13	122	121	2
1	1	9	55	54	8	-5	4	10	15	13	9	-2	4	10	23	16	9	-2	4	10	21	32	7	7	3	13	122	121	2
1	1	9	147	151	8	-4	4	10	19	17	10	-1	4	10	34	26	9	-1	4	10	25	25	10	7	3	13	122	121	2
2	2	9	101	101	2	-3	4	10	14	17	9	0	4	10	15	0	9	0	4	10	83	76	3	3	3	13	122	121	2
2	2																												

Table A7 (continued): Observed and calculated structure factors for 40-DNP.

h	k	l	10Fo	10Fc	10s	h	k	l	10Fo	10Fc	10s	h	k	l	10Fo	10Fc	10s	h	k	l	10Fo	10Fc	10s	h	k	l	10Fo	10Fc	10s																																																																																																																																																																																																																								
3	3	14	180	174	2	-7	1	15	37	29	6	2	1	15	55	52	4	-2	2	15	32	43	8	-3	3	15	13	11	9	-5	4	14	18	4	10	-6	1	15	33	28	7	3	1	15	14	10	10	-1	2	15	24	9	9	-2	3	15	18	5	11	-4	4	14	21	20	10	-5	1	15	13	0	10	4	1	15	19	15	10	0	2	15	24	28	5	-1	3	15	29	25	9	-3	4	14	45	45	5	-4	1	15	28	28	8	-8	2	15	15	1	10	1	2	15	14	2	10	0	3	15	30	35	5	-2	4	14	21	14	10	-3	1	15	22	8	10	-7	2	15	32	31	8	2	2	15	21	27	10	1	3	15	47	44	5	-1	4	14	21	21	10	-2	1	15	55	51	4	-6	2	15	43	40	5	3	2	15	49	26	5	0	4	14	20	21	10	-1	1	15	22	24	10	-5	2	15	27	26	9	-6	3	15	12	15	9	-9	1	15	19	17	6	0	1	15	50	49	3	-4	2	15	27	27	9	-5	3	15	21	27	10	-8	1	15	15	10	10	1	1	15	21	2	10	-3	2	15	27	20	9	-4	3	15	23	25	10

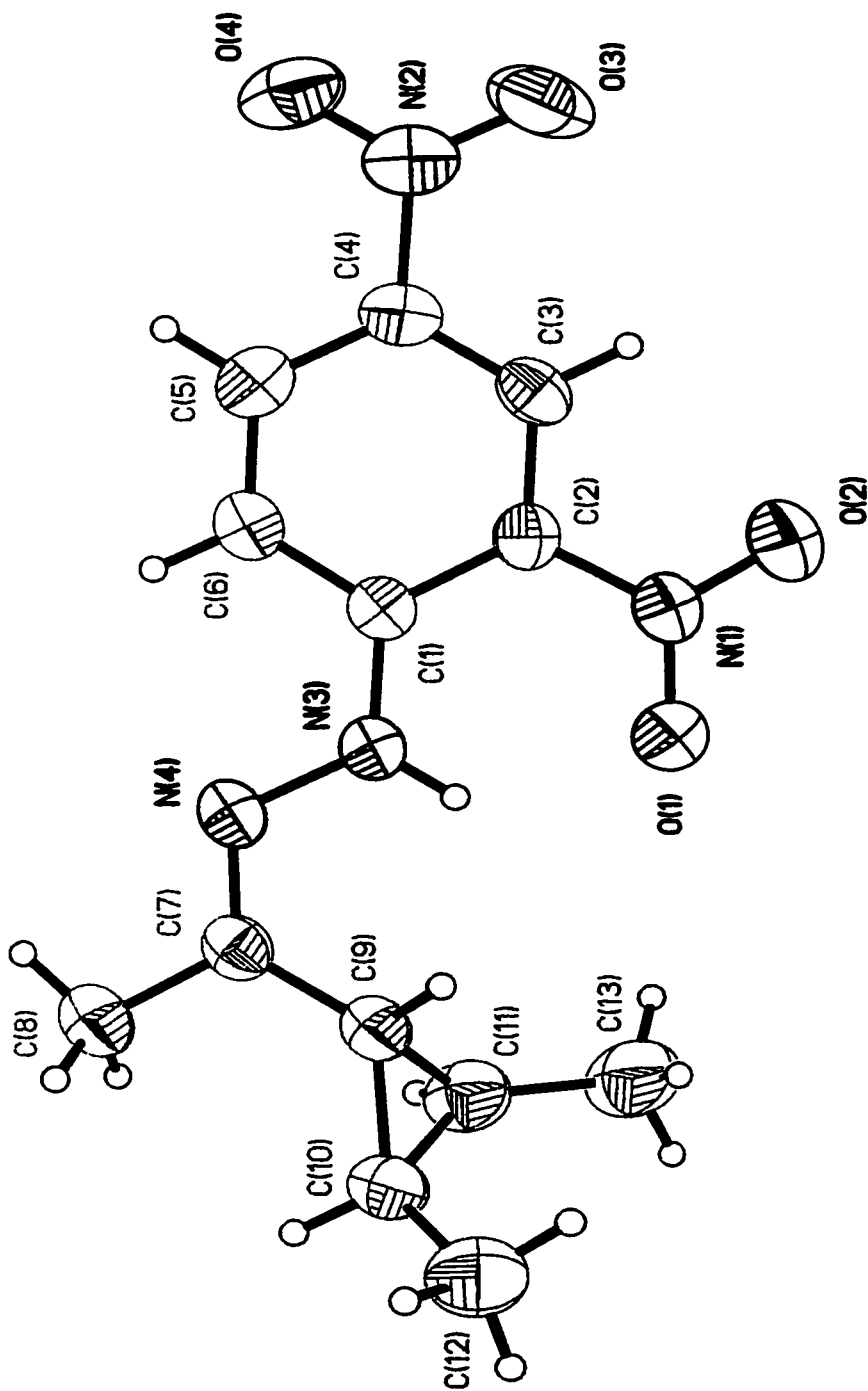


Figure A1: Crystal structure of 40-DNP, the 2,4-dinitrophenylhydrazone derivative of *trans,trans*-2,3-dimethyl cyclopropyl methyl ketone.

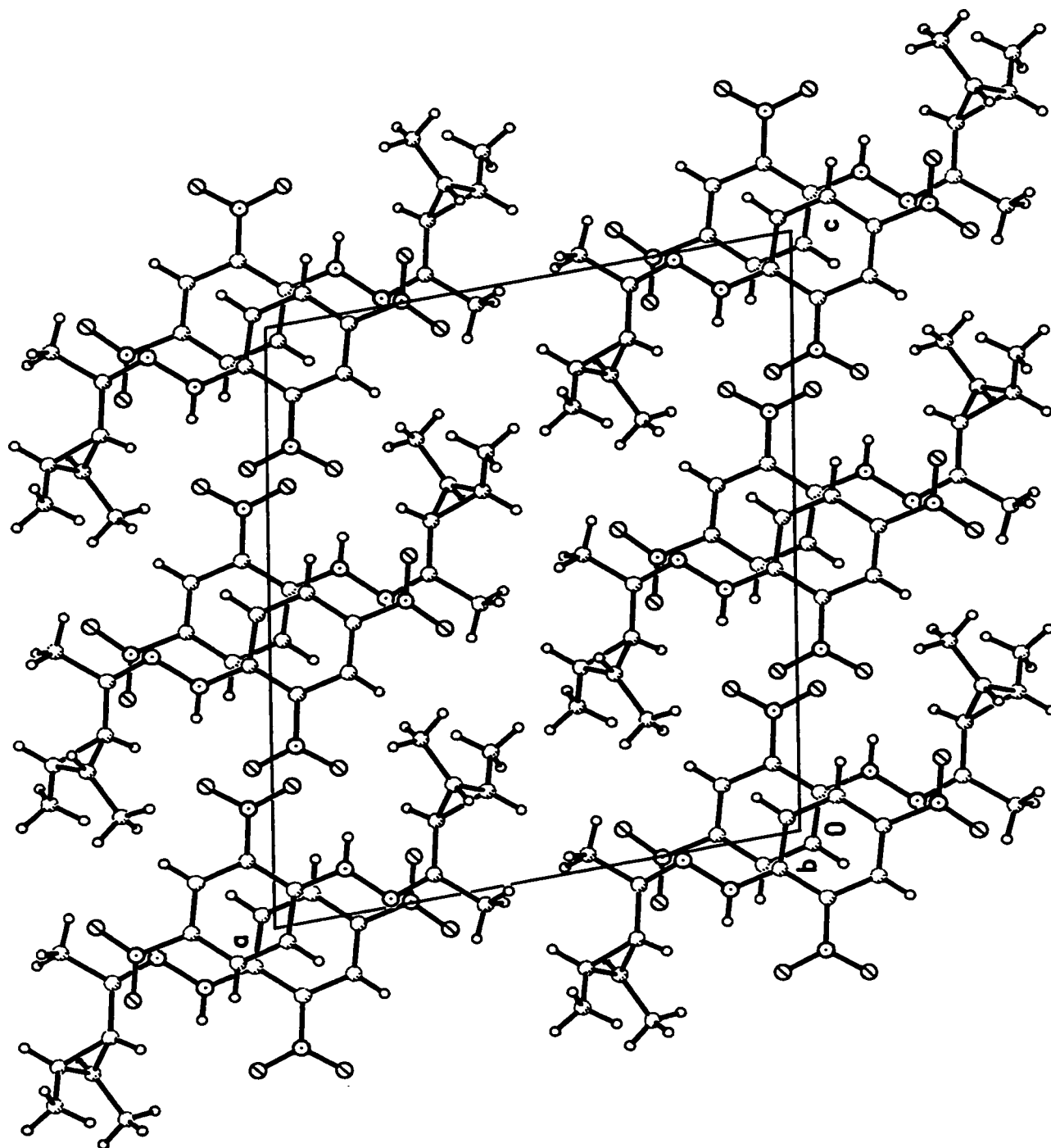


Figure A2: Unit cell for crystal of 40-DNP.